



Dynamic Asset Allocation - Identifying Regime Shifts in Financial Time Series to Build Robust Portfolios

Nystrup, Peter

Publication date:
2018

Document Version
Publisher's PDF, also known as Version of record

[Link back to DTU Orbit](#)

Citation (APA):

Nystrup, P. (2018). *Dynamic Asset Allocation - Identifying Regime Shifts in Financial Time Series to Build Robust Portfolios*. DTU Compute. DTU Compute PHD-2017, Vol.. 465

General rights

Copyright and moral rights for the publications made accessible in the public portal are retained by the authors and/or other copyright owners and it is a condition of accessing publications that users recognise and abide by the legal requirements associated with these rights.

- Users may download and print one copy of any publication from the public portal for the purpose of private study or research.
- You may not further distribute the material or use it for any profit-making activity or commercial gain
- You may freely distribute the URL identifying the publication in the public portal

If you believe that this document breaches copyright please contact us providing details, and we will remove access to the work immediately and investigate your claim.

Ph.D. Thesis
Doctor of Philosophy

DTU Compute
Department of Applied Mathematics and Computer Science

Dynamic Asset Allocation

Identifying Regime Shifts in Financial Time Series to Build
Robust Portfolios

Peter Nystrup

Kongens Lyngby
November 2017



Technical University of Denmark
Department of Applied Mathematics and Computer Science
Richard Petersens Plads, Building 324
2800 Kongens Lyngby, Denmark
Phone +45 4525 3031
compute@compute.dtu.dk
www.compute.dtu.dk

Short Contents

Short Contents	i
Abstract	iii
Resumé	v
Preface	vii
Acknowledgments	ix
Publications	xi
Acronyms	xiii
Contents	xv
1 Introduction	1
2 Contribution	9
3 Conclusion	23
References	27
A Stylized facts of financial time series and hidden Markov models in continuous time	37
B Long memory of financial time series and hidden Markov models with time-varying parameters	59
C Regime-based versus static asset allocation: Letting the data speak	85

D Dynamic allocation or diversification: A regime-based approach to multiple assets	99
E Detecting change points in VIX and S&P 500: A new approach to dynamic asset allocation	119
F Greedy Gaussian segmentation of multivariate time series	141
G Dynamic portfolio optimization across hidden market regimes	173
H Multi-period trading via convex optimization	203
I Multi-period portfolio selection with drawdown control	263

Abstract

Long-term investors can often bear the risk of outsized market movements or tail events more easily than the average investor; for bearing this risk, they hope to earn significant excess returns. Rebalancing periodically to a fixed benchmark allocation, however, is not the way to do this. In the presence of time-varying investment opportunities, portfolio weights should be adjusted as new information arrives to take advantage of favorable regimes and reduce potential drawdowns. This thesis contributes to a better understanding of financial markets' behavior in the form of a model-based framework for dynamic asset allocation.

Regime-switching models can match financial markets' tendency to change their behavior abruptly and the phenomenon that the new behavior often persists for several periods after a change. Regime shifts lead to time-varying parameters and, in addition, the parameters within the regimes and the transition probabilities change over time. Using recursive and adaptive estimation techniques to capture this, we are able to better reproduce the volatility persistence that dynamic asset allocation benefits from. With this approach it is sufficient to distinguish between two regimes in stock returns in order for it to be profitable to change asset allocation based solely on the inferred regimes, both in a single- and multi-asset universe.

We advocate the use of model predictive control for translating forecasts into a dynamic strategy and controlling drawdowns by solving a multi-period optimization problem. We implement this based on forecasts from a multivariate hidden Markov model with time-varying parameters. Our results show that a substantial amount of value can be added by adjusting the asset allocation to the current market conditions, rather than rebalancing periodically to a static benchmark. By proposing a practical approach to drawdown control, we demonstrate the theoretical link to dynamic asset allocation and the importance of identifying and acting on regime shifts in order to limit losses and build robust portfolios.

Keywords: Risk management; Regime switching; Adaptive estimation; Forecasting; Model predictive control; Portfolio optimization; Drawdown control.

Resumé

Langsigtede investorer kan ofte bære risikoen for store markedsudsving eller ekstreme hændelser bedre end den gennemsnitlige investor. Som kompenstation for at påtage sig denne risiko håber de at opnå betydelige merafkast. Periodewis rebalancering til en statisk benchmark-allokering er imidlertid ikke måden at opnå dette. Ved tilstedeværelse af tidsvarierende investeringsmuligheder bør porteføljevægtene tilpasses, efterhånden som ny information bliver tilgængelig, for at drage fordel af gunstige regimer og reducere potentielle tab. Denne afhandling bidrager til en bedre forståelse af finansielle markeders opførsel i form af et modelbaseret fundament for dynamisk aktivallokering.

Regimeskiftmodeller kan genskabe finansielle markeders tendens til pludseligt at skifte opførsel og det fænomen, at den nye opførsel ofte varer ved længe efter et skift. Regimeskift fører til tidsvarierende parametre, men også parametrene inden for regimerne og overgangssandsynlighederne ændrer sig over tid. Ved at bruge rekursive og adaptive estimationsmetoder til at fange dette er vi i stand til bedre at genskabe den volatilitetspersistens, som dynamisk aktivallokering udnytter. Med denne tilgang er det tilstrækkeligt at skelne mellem to regimer i aktieafkast, før end det er profitabelt at ændre aktivallokering udelukkende baseret på de udledte regimer i universer bestående af et enkelt eller flere aktiver.

Vi advokerer for brugen af modelprædiktiv regulering til at omsætte forudsigelser til en dynamisk strategi og kontrollere tab gennem løsning af et flerperiode optimeringsproblem. Vi implementerer dette baseret på forudsigelser fra en skjult Markov model med tidsvarierende parametre. Vores resultater viser, at betydelig værdi kan tilføres ved at tilpasse aktivallokeringen til de nuværende markedsforhold frem for at rebalance periodewis til et statisk benchmark. Ved at foreslå en praktisk tilgang til tabskontrol demonstrerer vi den teoretiske forbindelse til dynamisk aktivallokering og vigtigheden af at identificere og agere på regimeskift for at begrænse tab og bygge robuste porteføljer.

Nøgleord: Risikostyring; Regimeskift; Adaptiv estimation; Forudsigelse; Modelprædiktiv regulering; Porteføljeoptimering; Tabskontrol.

Preface

This thesis was prepared in the Department of Applied Mathematics and Computer Science at Technical University of Denmark in partial fulfillment of the requirements for the degree of Doctor of Philosophy (Ph.D.) in Engineering. It consists of a collection of nine papers written during the course of my Ph.D. study.

The research study was carried out in collaboration with Danish pension fund Sampension and Lund University in Sweden, with support from Innovation Fund Denmark under Grant No. 4135-00077B. As part of the study, I spent the summer of 2016 as a visiting student researcher in the Department of Electrical Engineering at Stanford University in California.

In addition to a handful of visits to Stanford, the financial support from Sampension and Innovation Fund Denmark has allowed me to participate in conferences and seminars in London, Frankfurt, Rennes, Aarhus, Paris, New York, Austin, Cairns, and Brussels.

This thesis deals with different aspects of mathematical modeling of the stylized behavior of financial returns using regime-switching models with the aim of developing a model-based framework for dynamic asset allocation. The idea for the study emanated from my Master's thesis (Nystrup 2014), which established the potential for model-driven, regime-based asset allocation. In continuation of this work we initially focused on adaptive estimation of regime-switching models. Before pursuing with a multi-period optimization approach based on model predictive control, demonstrating the connection between dynamic asset allocation and drawdown control, we tested strategies where the asset allocation was fully determined by the identified market regime.

Copenhagen, November 2017

Peter Nystrup

Acknowledgments

My first acknowledgment is to my academic supervisors, Professor Henrik Madsen from Technical University of Denmark and Professor Erik Lindström from Lund University, for many interesting discussions over the years. Henrik has a great ability to combine theoretical insight with a hands-on approach to mathematical modeling, forecasting, and control. His vast experience makes him able to draw parallels to previous applications in many different areas. Erik has played an important role with his enthusiasm and knowledge of quantitative finance. He has always made time to provide feedback and to research new ideas that could contribute to the study.

I want to thank my two industrial supervisors, Head of Investment Analysis Bo William Hansen and Chief Investment Officer Henrik Olejasz Larsen, along with the rest of my colleagues from Sampension, for their contribution. Bo and Henrik have shown a lot of interest in my work since the beginning of my Master's thesis and have encouraged me to continue working on the topic of dynamic asset allocation. I have benefitted from their background in economics and practical experience with financial markets and asset allocation. This study would not have been possible without the strong support from Bo and Henrik.

I also want to thank Professor Stephen Boyd and his research group at Stanford University for their collaboration. Stephen challenged me from the first day we met to view *everything* as an optimization problem. He has a great ability to translate a profound mathematical understanding into practical solutions to pertinent problems. Thanks to Stephen, my visits to Stanford have been very rewarding.

I am grateful to my parents and my fiancée Jenn for their love and support and extensive help with proofreading. Thank you also to the anonymous reviewers at various journals and conference participants, whose comments and suggestions have led to improvements of the individual publications. Finally, the financial support from Sampension and Innovation Fund Denmark is gratefully acknowledged.

x

Publications

Paper A

Nystrup, P., H. Madsen, and E. Lindström. “Stylised facts of financial time series and hidden Markov models in continuous time.” *Quantitative Finance*, vol. 15, no. 9 (2015b), pp. 1531–1541.

Paper B

Nystrup, P., H. Madsen, and E. Lindström. “Long memory of financial time series and hidden Markov models with time-varying parameters.” *Journal of Forecasting*, vol. 36, no. 8 (2017b), pp. 989–1002.

Paper C

Nystrup, P., B. W. Hansen, H. Madsen, and E. Lindström. “Regime-based versus static asset allocation: Letting the data speak.” *Journal of Portfolio Management*, vol. 42, no. 1 (2015a), pp. 103–109.

Paper D

Nystrup, P., B. W. Hansen, H. O. Larsen, H. Madsen, and E. Lindström. “Dynamic allocation or diversification: A regime-based approach to multiple assets.” *Journal of Portfolio Management*, vol. 44, no. 2 (2017a), pp. 62–73.

Paper E

Nystrup, P., B. W. Hansen, H. Madsen, and E. Lindström. “Detecting change points in VIX and S&P 500: A new approach to dynamic asset allocation.” *Journal of Asset Management*, vol. 17, no. 5 (2016), pp. 361–374.

Paper F

Hallac, D., P. Nystrup, and S. Boyd. “Greedy Gaussian segmentation of multivariate time series.” *Advances in Data Analysis and Classification* (2018), p. forthcoming.

Paper G

Nystrup, P., H. Madsen, and E. Lindström. “Dynamic portfolio optimization across hidden market regimes.” *Quantitative Finance*, vol. 18, no. 1 (2018b), pp. 83–95.

Paper H

Boyd, S., E. Busseti, S. Diamond, R. N. Kahn, K. Koh, P. Nystrup, and J. Speth. “Multi-period trading via convex optimization.” *Foundations and Trends in Optimization*, vol. 3, no. 1 (2017), pp. 1–76.

Paper I

Nystrup, P., S. Boyd, E. Lindström, and H. Madsen. “Multi-period portfolio selection with drawdown control.” *Annals of Operations Research* (2018a), p. forthcoming.

Acronyms

ACF	Autocorrelation function
AIC	Akaike's information criterion
AR	Annualized return
AT	Annual turnover
BIC	Bayesian information criterion
CPPI	Constant-proportion portfolio insurance
CR	Calmar ratio
CTHMM	Continuous-time hidden Markov model
DAA	Dynamic asset allocation
DM	Developed market
EM	Emerging market
EM	Expectation–maximization
ETF	Exchange-traded fund
EWMA	Exponentially-weighted moving average
FM	Fixed mix
GARCH	Generalized autoregressive conditional heteroskedasticity
GAS	Generalized autoregressive score
GGS	Greedy Gaussian segmentation
HMM	Hidden Markov model

HSMM	Hidden semi-Markov model
IR	Information ratio
LASSO	Least absolute shrinkage and selection operator
LLO	Leveraged long-only
LO	Long only
LS	Long–short
MDD	Maximum drawdown
ML	Maximum likelihood
MLE	Maximum-likelihood estimate
MPC	Model predictive control
MPO	Multi-period optimization
NLP	Natural language processing
OBPI	Option-based portfolio insurance
RBA	Regime-based asset allocation
SAA	Strategic asset allocation
SD	Standard deviation
SGM	Segmented Gaussian model
SPO	Single-period optimization
SR	Sharpe ratio
TAA	Tactical asset allocation
VIX	Chicago Board Options Exchange's Volatility Index

Contents

Short Contents	i
Abstract	iii
Resumé	v
Preface	vii
Acknowledgments	ix
Publications	xi
Acronyms	xiii
Contents	xv
1 Introduction	1
1.1 Regime shifts	2
1.2 Stylized facts of financial returns	3
1.3 Time-varying parameters	5
1.4 Dynamic portfolio optimization	5
1.5 Research questions	7
1.6 Thesis outline	8
2 Contribution	9
2.A Stylized facts of financial time series and hidden Markov models in continuous time	9
2.B Long memory of financial time series and hidden Markov models with time-varying parameters	10
2.C Regime-based versus static asset allocation: Letting the data speak	12
2.D Dynamic allocation or diversification: A regime-based approach to multiple assets	13

2.E Detecting change points in VIX and S&P 500: A new approach to dynamic asset allocation	14
2.F Greedy Gaussian segmentation of multivariate time series	16
2.G Dynamic portfolio optimization across hidden market regimes	17
2.H Multi-period trading via convex optimization	18
2.I Multi-period portfolio selection with drawdown control	19
3 Conclusion	23
3.1 Commercial perspectives	25
3.2 Future work	26
References	27
A Stylized facts of financial time series and hidden Markov models in continuous time	37
1 Introduction	39
2 Hidden Markov models in discrete time	41
3 Hidden Markov models in continuous time	43
4 Data	46
5 Empirical results	47
6 Conclusion	52
References	53
A Parameter estimates	55
B FTSE results	57
B Long memory of financial time series and hidden Markov models with time-varying parameters	59
1 Introduction	61
2 The hidden Markov model	63
3 Long memory and regime switching	65
4 Adaptive parameter estimation	67
5 Data	69
6 Results	72
7 Conclusion	80
References	81
C Regime-based versus static asset allocation: Letting the data speak	85
1 Introduction	87
2 Letting the data speak	88
3 The hidden Markov model	90
4 Empirical results	92
5 Summary and discussion	95
References	95

D Dynamic allocation or diversification: A regime-based approach to multiple assets	99
1 Introduction	101
2 Asset universe	103
3 The hidden Markov model	107
4 State inference	109
5 Empirical results	110
6 Conclusion	116
References	116
E Detecting change points in VIX and S&P 500: A new approach to dynamic asset allocation	119
1 Introduction	121
2 VIX and S&P 500	123
3 Change-point detection	125
4 Empirical results	128
5 Summary and discussion	137
References	138
F Greedy Gaussian segmentation of multivariate time series	141
1 Introduction	143
2 Problem setup	146
3 Greedy Gaussian segmentation	150
4 Validation and parameter selection	152
5 Variations and extensions	153
6 Experiments	155
7 Summary	166
References	166
G Dynamic portfolio optimization across hidden market regimes	173
1 Introduction	175
2 The hidden Markov model	177
3 Dynamic portfolio optimization	182
4 Empirical results	187
5 Conclusion	197
References	198
H Multi-period trading via convex optimization	203
1 Introduction	205
2 The model	208
3 Metrics	218
4 Single-period optimization	220
5 Multi-period optimization	237
6 Implementation	243

7	Examples	245
	References	256
I	Multi-period portfolio selection with drawdown control	263
1	Introduction	265
2	Multi-period portfolio selection	267
3	Data model	275
4	Empirical results	280
5	Conclusion	292
	References	293

CHAPTER 1

Introduction

Asset allocation is the most important determinant of portfolio performance (Brinson et al. 1986, Ibbotson and Kaplan 2000). In the presence of time-varying investment opportunities, portfolio weights should be adjusted as new information arrives (Bansal et al. 2004). Traditional strategic approaches rather seek to develop robust, static portfolios that optimize efficiency across a range of scenarios (Sheikh and Sun 2012). Strategic asset allocation (SAA) is long term in nature and based on long-term views of asset class performance (Dahlquist and Harvey 2001, Campbell and Viceira 2002). Even if the SAA is reconsidered on an annual basis, it is unlikely to change significantly, as long as the purpose remains “all-weather” efficiency.

The purpose of dynamic asset allocation (DAA) is to take advantage of favorable regimes and reduce potential drawdowns during adverse regimes. DAA is, by definition, more restricted than SAA in terms of the size of the investment opportunity set, because it is difficult to invest dynamically in illiquid assets such as private real estate, private equity, infrastructure, etc. This is worth mentioning, given that illiquid alternatives have become a larger part of institutional investors’ portfolios in recent years. Strategic investors, such as pension funds, that invest with a long time horizon typically face constraints on the size of possible deviations from their benchmark allocation; even so, they can still benefit from reacting to significant regime shifts (Kritzman et al. 2012).

The 2008 financial crisis clearly showed that diversification is not sufficient to avoid large drawdowns. Diversification fails, when needed the most, because correlations between risky assets tend to strengthen during times of crisis (see, e.g., Pedersen 2009, Ibragimov et al. 2011). Large drawdowns challenge investors’

financial and psychological tolerance and lead to fund redemption and firing of portfolio managers. By engaging in DAA it is possible to generate protection against drawdowns. In fact, portfolio insurance can be regarded as the most general form of DAA, as argued by Goltz et al. (2008).¹

DAA can be profitable even if markets are efficient. A market is said to be efficient if prices in the market fully reflect all available information. When this condition is satisfied, market participants cannot earn a riskless profit on the basis of available information—in other words, there are no arbitrage opportunities (Fama 1970, Pedersen 2015). Trends can be present in efficient markets if the equilibrium expected return changes over time. The existence of a business cycle, where the expected rate of return on capital changes over time, is one example. When the business cycle is not a deterministic phenomenon, asset prices need not follow a random walk with a constant or deterministic trend (Levich 2001).

This first chapter introduces the concept of DAA and a distinction between rule- and optimization-based approaches. This includes the stylized facts that are exploited and the significance of time-varying parameters. The purpose is to motivate the importance of identifying and acting on regime shifts in order to limit losses and build robust portfolios. At the end of the chapter, a list of research questions is posed and the remainder of the thesis is outlined.

1.1 Regime shifts

Regime shifts, some of which can be recurring (recessions versus expansions) and some of which can be permanent (structural breaks), are prevalent across a wide range of financial markets and in the behavior of many macro variables (Ang and Timmermann 2012). Observed regimes in financial markets are related to the phases of the business cycle (Campbell 1999, Cochrane 2005). The link is complex and difficult to exploit for investment purposes, due to the low frequency and large lag in the availability of data related to the business cycle.

In this thesis, the focus is on readily available market data, instead of attempting to establish the link to the business cycle. If financial markets are efficient, the outlook for the economy should be reflected in asset prices to the extent that it can be predicted (Siegel 1991). Interestingly, most studies on DAA consider monthly rather than daily returns. A monthly data frequency might make sense for SAA, but not when studying DAA. Even if it is not the expectation to trade every day, the option should be there. In an optimization-based framework there are more efficient ways to reduce turnover than lowering the data frequency.

¹It is known from Merton's (1973) replicating argument interpretation of the Black and Scholes (1973) formula that nonlinear payoffs based on an underlying asset can be replicated by dynamic trading in the underlying asset and a risk-free asset.

Ang and Bekaert (2002) were among the first to consider the impact of regime shifts on asset allocation. They showed that regime-based asset allocation (RBAA) can add value over rebalancing to static weights and reduce drawdowns. Numerous studies have followed, including Ang and Bekaert (2004), Bauer et al. (2004), Ammann and Verhofen (2006), Guidolin and Timmermann (2007, 2008), Bulla et al. (2011), Guidolin and Ria (2011), Kritzman et al. (2012), Bae et al. (2014). Only Kritzman et al. (2012) forecasted regimes in important drivers of asset returns rather than identifying regimes directly in asset returns based on a model with a fixed number of recurring regimes. The majority have considered dynamic allocation to stocks in combination with bonds and/or a risk-free asset, often involving larger changes in allocation than most investors are willing to or allowed to implement. The focus on stocks is natural, since portfolio risk is typically dominated by stock market risk (see, e.g., Goyal et al. 2015, Bass et al. 2017). In a multi-asset setting, however, it is essential whether regime shifts occur synchronously across asset classes.

It is important to emphasize that regime shifts are an abstraction. Abrupt, seemingly discontinuous changes can occur in systems with no switches (Preis and Stanley 2010); for example, complex systems subject to reinforcing feedback (Gărleanu and Pedersen 2007). Models with a fixed number of recurring regimes, as discussed in the next sections, is only one out of many possible ways to model or capture abrupt changes; for example, adaptive estimation can be used to track variations in (the parameters of) a system (see, e.g., Gustafsson 2000), change-point detection can be used to identify significant changes (see, e.g., Ross et al. 2011), or stochastic differential equations can be used to model nonlinear variability at multiple levels (see, e.g., Lindström et al. 2015).

1.2 Stylized facts of financial returns

The hidden Markov model (HMM) is a popular choice for inferring the state of financial markets. In an HMM, the distribution that generates an observation depends on the state of an unobserved Markov chain (Cappé et al. 2005, Frühwirth-Schnatter 2006, Zucchini and MacDonald 2009).² It is a black-box model, but the inferred states can often be linked to phases of the business cycle (Guidolin and Timmermann 2007, Ang and Timmermann 2012). The possibility of interpreting the states combined with the model's ability to reproduce stylized facts of financial returns is part of the reason why it has become increasingly popular.

Rydén et al. (1998) showed the ability of the HMM to reproduce most of the stylized facts of daily return series introduced by Granger and Ding (1995a,b). The one stylized fact that could not be reproduced by an HMM was the positive, significant, and slowly decaying autocorrelation function (ACF) of absolute and

²See paper A for an introduction to hidden Markov models.

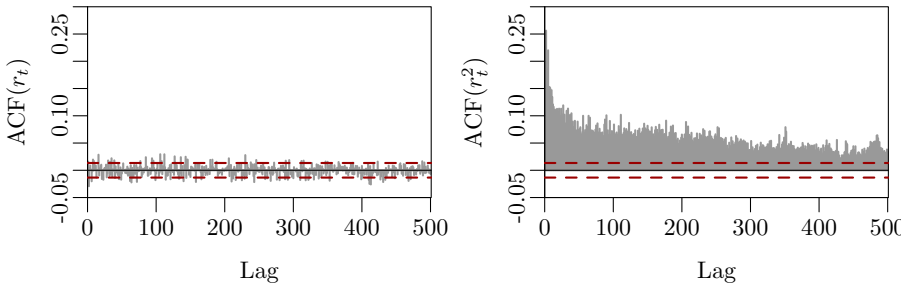


Figure 1.1: Autocorrelation functions for daily log-returns of the S&P 500 index and their squared values from 1928 to 2016. The dashed lines are the boundaries of approximate 95% confidence intervals under the null hypothesis of independence (Madsen 2008).

squared daily returns, which is of great importance, for example, in financial risk management.

First noted by Mandelbrot (1963), the volatility of asset prices forms clusters, as large price movements tend to be followed by large price movements and vice versa. Daily returns do not have the long-memory property themselves, only their absolute and squared values do, as it can be seen from figure 1.1. Malmsten and Teräsvirta (2010) argued that the very slow decay rate of autocorrelations should not be considered a stylized fact, since the decay rate in shorter subseries, on average, is substantially faster and roughly exponential.

In order to improve its ability to reproduce the long memory, subsequent papers have extended the Gaussian HMM studied by Rydén et al. (1998). Bulla and Bulla (2006) considered hidden semi-Markov models (HSMMs) with other sojourn-time distributions than the memoryless geometric distribution and Bulla (2011) considered HMMs with other conditional distributions than the Gaussian distribution. The types of sojourn-time and conditional distributions are highly dependent on the number of regimes. For example, Langrock and Zucchini (2011) showed how an HMM can be structured to fit any sojourn-time distribution with arbitrary precision by mapping multiple latent states to the same output state.

Guidolin (2011a,b) found in his review of the literature on applications of Markov-switching models in empirical finance that roughly half the studies selected this model based on economic motivations rather than statistical reasoning. Further, half the studies did not consider it a possibility that the number of regimes could exceed two, and there was an overweight of studies based on Gaussian mixtures in which the underlying Markov chain was assumed to be time homogeneous.

1.3 Time-varying parameters

Regime shifts in the data-generating process lead to time-varying parameters, but the parameters within the regimes and the transition probabilities also change over time. It is hardly realistic that the parameters of the conditional distributions can only jump with constant probability between a fixed number of constant values. Rydén et al. (1998) found that the parameters as well as the optimal number of states have changed considerably over time. Additionally, Bulla (2011) found that the optimal choice of conditional distributions has changed over time.

Attempts to capture this dynamic with a stationary model result in very complex models with lots of parameters that need to be estimated (see, e.g., Calvet and Fisher 2004, Song 2014, Augustyniak et al. 2016). A better alternative to a complex stationary model is to take into account the development of the parameters in the underlying model. This is crucial in order to minimize the difference between in- and out-of-sample forecasting performance (Dacco and Satchell 1999).

The time variation can be either parameter or observation driven. In parameter-driven models, the parameters are stochastic processes with their own source of error. A model for the parameter changes in the form of a hierarchical model can include exogenous explanatory variables (see, e.g., Ang and Bekaert 2004). Alternatively, the time variation can be observation driven based on the gradient of the likelihood function—i.e., the score function. This estimation approach was an important part of my Master’s thesis (Nystrup 2014).

Recursive and adaptive techniques for estimating models with time-varying parameters are well known in the engineering literature (see, e.g., Ljung and Söderström 1983). Although there exist earlier examples of applications to econometric models (e.g., Madsen et al. 1999), these techniques have attracted renewed attention in the econometrics literature following the paper by Creal et al. (2013). Several recursive and adaptive estimation techniques have been proposed specifically for HMMs (see Khreich et al. 2012, and references therein). Without increasing the number of parameters it is possible to reproduce much more complex dynamics by allowing for them to be time varying. The time variation has a significant impact on the optimal choice of sojourn-time and conditional distributions. Although the regimes are not really recurring when the parameters are allowed to change within the regimes, the number of regimes remains a determining factor.

1.4 Dynamic portfolio optimization

DAA aims to benefit from volatility persistence, since risk-adjusted returns, on average, are substantially lower during turbulent periods, irrespective of the

source of turbulence (Kritzman and Li 2010, Moreira and Muir 2017). The negative correlation between volatility and returns is sometimes explained by changes in attitudes toward risk; because high-volatility regimes are associated with increased risk aversion and reduced risk capacity, a high-volatility environment is likely to be accompanied by falling asset prices.³

DAA can be divided into rule- and optimization-based approaches, respectively. Examples of heuristic, rule-based approaches include scaling the proportion of stocks inversely proportionally to forecasted, realized, or unexpected volatility and switching between risky and risk-free assets based on whether the volatility is above or below a threshold (see, e.g., Zakamulin 2014, Moreira and Muir 2017). RBAA is a subcategory of rule-based approaches, where the asset allocation depends on the inferred regime.

Fornaciari and Grillenzoni (2017) proposed to estimate the parameters of the model and the decision rule simultaneously and recursively based on a profitability criteria. Optimizing the parameters of the decision rule, however, does not guarantee that the decision rule is optimal for the problem at hand. Testing many different specifications in order to find a decision rule with good performance increases the risk of inferior performance out of sample. Further, it can be argued that a static decision rule is hardly optimal if the underlying model used for regime inference is time varying.

DAA is a multi-period problem, yet it is often approximated by a sequence of myopic, single-period optimizations, which makes it impossible to properly account for the consequences of trading, constraints, time-varying forecasts, etc. Following Mossin (1968), Samuelson (1969), and Merton (1969), the literature on multi-period portfolio selection is predominantly based on dynamic programming, which properly takes into account the idea of recourse and updated information available as a sequence of trades is chosen (see Gărleanu and Pedersen 2013, and references therein). Unfortunately, actually carrying out dynamic programming for trade selection is impractical, except for some very special or small cases, due to the curse of dimensionality (Bellman 1956, Boyd et al. 2014).

Herzog et al. (2007) and Boyd et al. (2014) proposed to solve the stochastic control problem of DAA using model predictive control (MPC). The idea is to control a portfolio based on forecasts of asset returns and relevant parameters. Every day a decision is made whether or not to change the current portfolio allocation, knowing that the decision will be reconsidered the next day with new input. Possible benefits from changing allocation are traded off against risks and costs.

MPC constitutes a promising alternative to the static decision rules that dominate the literature on RBAA following Ang and Bekaert (2002). It offers an

³Increased risk aversion (a behavioral explanation) and reduced risk capacity (an institutional explanation) are difficult to distinguish in data. Both effects have support (e.g., Cohn et al. 2015, Brunnermeier and Pedersen 2009).

optimal implementation conditional on the choice of hyperparameters, which all have a clear interpretation as transaction costs, holding costs, etc. Further, there are computational advantages to using MPC in cases when forecasts are updated every time a new observation becomes available, since the optimal control actions are reconsidered anyway. If asset returns are forecasted using a regime model, significant allocation changes will still occur in response to regime shifts.

MPC is a mathematically tractable approach to multi-period portfolio optimization. For this approach to be useful in practical applications, it is crucial that the problem can be quickly solved. It does not matter whether it has a closed-form solution. Similarly, it should be easy to handle all costs and constraints that are practically important in portfolio management. Following Markowitz (1952), the goal is to find an optimal tradeoff between risk and return, where risk can be variance, maximum drawdown, or something else. It is essential that the risk function measures the risk that the investor is concerned with and that its minimization is feasible, not what kind of utility function justifies it or what assumptions are implicitly made about the return distribution (Markowitz 2014).

The mean-variance criterion is the most commonly used in portfolio selection (Kolm et al. 2014). Unlike this quadratic measure, alternatives exist that only penalize down-side risk; popular choices are value-at-risk and conditional value-at-risk focused on a small fraction of the worst possible outcomes (see, e.g., Rockafellar and Uryasev 2000, Bertsimas et al. 2004). However, risk measures based on a narrow part of the distribution are more susceptible to forecast uncertainty, causing portfolios resulting from their minimization to be less robust (Lim et al. 2011, Downing et al. 2015). A better alternative for investors concerned with tail risk is drawdown control, which, unlike tail-risk minimization, prevents a portfolio from losing more than a given limit.

1.5 Research questions

1. Previous studies have achieved a better reproduction of financial returns' stylized behavior by considering other sojourn-time and conditional distributions than the Gaussian HMM. Can this be explained by the parameters changing over time, and is it possible to achieve a better reproduction by taking this into account?
2. How many regimes are needed, and are they recurring?
3. Can the returns from other asset classes/risk factors be described by a multivariate regime-switching model?
4. Previous studies on RBAA have obtained significantly better results in sample than out of sample. Is it possible to increase the robustness by

basing a dynamic strategy on a model with time-varying parameters in order to obtain similarly good result out of sample?

5. Is it profitable to change asset allocation based solely on identified regimes?
6. How do model predictions optimally translate into a DAA strategy?
7. In continuation of the previous question, what role do transaction and holding costs play?
8. Is it possible to realize higher risk-adjusted returns by including other asset classes than stocks and cash?

In this study, we use R for statistical modeling and forecasting (R Core Team 2017). For optimization, we use Python and the library CVXPY (Diamond and Boyd 2016).

1.6 Thesis outline

This thesis consists of a collection of nine papers written during the course of my Ph.D. study. Each paper is included as a separate appendix: paper A through paper I. Before that, in the next chapter, I will go through each paper individually and summarize its main findings and contribution in order to emphasize the common thread through the study. Chapter 3 concludes the study by providing answers to the research questions posed in section 1.5.

CHAPTER 2

Contribution

In this chapter, I will go through each paper individually and summarize its main findings and contribution. I will describe the process that led to each paper, including some of the work that did not get included in the final version. In addition, I will discuss possibilities for future work. The chapter assumes that an introduction to the different topics and the existing literature has already been given, thus, it is highly recommended to read chapter 1 before delving into this chapter.

Research, and publication of research results in particular, is a highly nonlinear process. The papers are, therefore, not arranged in chronological order based on when the work was done or the time of publication. Rather, I have arranged them in order to emphasize the common thread in the work.

2.A Stylized facts of financial time series and hidden Markov models in continuous time

Published in Quantitative Finance

Subsequent papers have extended the Gaussian HMM studied by Rydén et al. (1998) in order to improve its ability to reproduce the slow decay of the autocorrelation function that is characteristic for long series of squared and absolute daily returns. Paper A contributes to this literature by proposing a continuous-time formulation as a flexible alternative to the dominating discrete-time models.

A major limitation of discrete-time HMMs and HSMMs is the quadratic increase in the number of parameters with the number of states. This limitation does

not apply to continuous-time HMMs, as it can reasonably be assumed that the only possible transitions in an infinitesimally short time interval are to the neighboring states. This assumption leads to a linear rather than quadratic increase in the number of parameters with the number of states and, consequently, a significant reduction in the number of parameters for higher-order models.

We find that the possibility to increase the number of states leads to a better fit to both the distributional and temporal properties of daily log-returns of the S&P 500 and FTSE indices from 1993 to 2013. Specifically, we find that a continuous-time HMM with four states provides a better fit to the autocorrelation function of the squared returns than discrete-time, two- and three-state HMMs and HSMMs with conditional Gaussian and t distributions (see, e.g., figure 4 on page 48). This is also the case when restraining the impact of outliers in order to reduce the amount of noise in the empirical autocorrelation function (see, e.g., figure 7 on page 50).

In the paper, we emphasize the possibility of approximating any positive-valued sojourn-time distribution with arbitrary precision by introducing dummy states that are indistinguishable from one or more of the original states.⁴ We, however, do not find any indication that the memoryless property of the sojourn-time distribution is inconsistent with the long-memory property of the squared returns. There are other advantages of a continuous-time formulation that we do not explore in the paper; most importantly the possibility to incorporate temporal inhomogeneity without a dramatic increase in the number of parameters and the flexibility to use data that is not (assumed to be) equidistantly sampled.

2.B Long memory of financial time series and hidden Markov models with time-varying parameters

Published in the Journal of Forecasting

Paper B contributes to the same strand of literature proposing extensions to the Gaussian HMM in order to improve its ability to reproduce the long memory of volatility. As an alternative to increasing the model complexity, for example by adding more states or considering other sojourn-time or conditional distributions, we propose a recursive maximum-likelihood estimation approach that allows for the parameters of the estimated model to be time varying. Adaptivity in time is achieved with exponential forgetting of past observations. It is implicitly assumed that the time scales of the regime changes and the variations of the model parameters are separable.

This fundamentally different approach was an important part of my Master's thesis (Nystrup 2014). The time variation is observation driven based on the score function of the predictive likelihood function. A disadvantage of HMMs

⁴This is also possible in discrete time, as shown by Langrock and Zucchini (2011).

is that the score function must consider all previous observations and cannot reasonably be approximated by the score function of the latest observation, as it is often done for other models (Khreich et al. 2012). This leads to a significant increase in computational complexity.

We find that the parameters of the estimated models vary significantly over time (see, e.g., figure 5 on page 76), in agreement with the findings by Rydén et al. (1998) and Bulla (2011). By taking this variation into account, we show that a Gaussian HMM with only two states is able to reproduce the long memory of squared daily returns of the S&P 500 index from 1928 to 2014 (figure 6 on page 77). Rydén et al. (1998) considered this stylized fact to be the most difficult fact to reproduce with an HMM. The adaptively-estimated model provides a particularly good fit to the autocorrelation function of the squared daily returns when the impact of exceptional observations is reduced.

Fast adaptation to parameter changes leads to improved one-step density forecasts. The choice of memory length affects the parameter estimates and can be viewed as a tradeoff between bias and variance. A shorter memory yields a faster adaptation to changes but a more noisy estimate, as fewer observations are used for the estimation. We find that by using exponential forgetting, the effective memory length can be reduced compared to when using a sliding-window approach. Exponential forgetting is also more meaningful, because it assigns most weight to the most recent observations and, at the same time, does not exclude observations from the estimation from one time step to the next. It can be seen as a continuous mixture of sliding windows of different lengths.

A two-state HMM with a t -distribution in the high-variance state has the highest predictive log-likelihood (see table 8 on page 79). When leaving out the 20 observations that make the most negative contributions to the log-likelihood, however, the adaptively-estimated Gaussian HMM outperforms the other models and estimation approaches considered. This is less than 0.1% of the total number of observations. Thus, while the t -distribution is a better fit to the most exceptional observations, the adaptively-estimated Gaussian HMM provides the best one-step-ahead density forecasts for the remainder of the sample. We show that the forecasting performance can be further improved using local smoothing to forecast the parameter variations. The largest improvement is obtained for the 20 observations that are most difficult to forecast.

The adaptively-estimated HMM combines abrupt regime changes with smooth variations in the underlying parameters. We have spent some time looking into variable forgetting (Fortescue et al. 1981, Uosaki et al. 1996, Cooper and Worden 2000), which is a natural extension of the fixed-parameter forgetting approach proposed in this paper. The idea is to reduce the memory following a decay in forecasting accuracy in order to quickly adapt the model parameters to a new setting. On the contrary, if the forecasting error is small, then the memory is increased in order to get stable estimates. The method of Fortescue et al. (1981)

is not directly applicable to a regime-switching model, because of the need to distinguish between parameter changes caused by a regime change and parameter changes in the underlying model—that is, the forecasting performance naturally changes whenever the regime changes.

We have also contemplated the possibility of formulating a model for the parameter changes in the form of a hierarchical model, possibly including relevant exogenous variables (see, e.g., Ang and Bekaert 2004). The proposed method for estimating the time variation of the parameters is an important step toward the identification of a hierarchical model structure. Another possibility for future work is to further develop the proposed estimation approach and compare it to approaches that have been proposed in areas other than finance (see Khreich et al. 2012, and references therein); for example, it would be interesting to explore the impact of adding a regularization term to the likelihood objective as a means of introducing prior information (see, e.g., Johansen 1997, Pinson and Madsen 2012).

2.C Regime-based versus static asset allocation: Letting the data speak

Published in The Journal of Portfolio Management

Paper C presents an application of the recursive, adaptive estimation approach and the model from the previous paper to regime-based asset allocation. We focus on the Gaussian HMM with two regimes for several reasons: first, because we know from the previous paper that this model is able to reproduce the long memory of volatility; second, because increasing the number of regimes makes it more difficult to distinguish between them out of sample; and third, because more regimes lead to more transitions between regimes and, consequently, higher portfolio turnover and transaction costs.

The adaptive estimation approach is a new contribution to the literature on RBAA. Previously, Bulla et al. (2011) were the only ones to apply an HMM with time-varying parameters to asset allocation, but they used a simple sliding-window estimation approach. The adaptive, online approach ensures robustness in order to prevent large differences between in- and out-of-sample performance, as observed in some previous studies. Instead of the median filter used by Bulla et al. (2011), we apply a filter based on the inferred probability to decode the hidden market regimes.

We identify regimes in daily returns of a global stock index and, based on this, allocate the entire portfolio between the stock index in the low-volatility regime and a global government bond index in the high-volatility regime. We do this over a 20-year period from 1994 to 2013 and assume a one-day delay in the implementation of allocation changes. The identified regimes seem intuitive

when looking at the log-returns at the bottom of figure 4 on page 93, although the result is different from what would be expected if the regimes were based on a business cycle indicator.

The performance of the RBAA strategy is good compared to that of a static portfolio with the same average asset allocation, but the difference is mainly due to the financial crisis in 2008. The break-even transaction cost is more than 200 basis points per one-way transaction. In other words, a simple switching rule based on the identified regimes alone is profitable. A long–short strategy based on the stock index is not as successful.

2.D Dynamic allocation or diversification: A regime-based approach to multiple assets

Published in The Journal of Portfolio Management

Paper D is an extension of the approach from the previous paper to a multi-asset portfolio. The potential benefit from taking large positions in a few assets at a time comes at the cost of reduced diversification. In order to analyze this tradeoff, we compare the performance of RBAA to a static benchmark in a more comprehensive asset universe, because the potential for diversification is limited by the size of the asset universe. This analysis is the main contribution of the paper.

The market indices included in the study are carefully chosen to mimic the major liquid asset classes typically considered by an institutional investor. These include developed market (DM) and emerging market (EM) stocks and high-yield bonds, listed DM real estate, gold, oil, corporate bonds, inflation-linked bonds, and government bonds. The data period is 1997 through 2015.

We first considered deriving and modeling a few central risk factors in order to reduce the complexity of the modeling task and develop a scalable approach—not to uncover a hidden potential for diversification (see Cocoma et al. 2017). We analyzed the correlation structure and its principal components and did not find any stationary structure. Both the eigenvalues and eigenvectors change over time, and the changes are larger than what can be explained by measurement noise (Fenn et al. 2011, Allez and Bouchaud 2012).

Instead, we define risk-on and risk-off portfolios based on the asset class' correlation with DM stocks. We choose the benchmark allocation to mimic a 60/40 long-only SAA portfolio of an institutional investor. This is a much simpler approach than carrying out an actual portfolio optimization, which should increase its robustness. We use the same model and estimation approach as in the previous paper (which originates from paper B) to switch between the risk-on and risk-off portfolios based on regimes in the daily returns of DM stocks.

A second contribution of the paper is to introduce a new way of decoding hidden market regimes that is based on Narasimhan et al. (2006). The essence of the algorithm is that the initial state becomes increasingly certain as more observations are included in the sequence and the latency increases. It accumulates evidence online until the certainty estimate reaches a threshold, after which the identified initial state is outputted and the algorithm proceeds to estimate the next state in the sequence. Despite being very intuitive, the algorithm has never been applied in studies of RBAA.

We find that the annualized standard deviation is minimized when half of the portfolio is allocated to the RBAA strategy, and the risk-adjusted return is maximized when the allocation to RBAA reaches 80% (see figure 6 on page 112). Compared to the 60/40 SAA portfolio, the RBAA portfolios have higher risk-adjusted returns and suffer much smaller maximum drawdowns. Compared to the median-filter approach used by Bulla et al. (2011), the online decoding approach leads to a higher risk-adjusted return and a lower turnover.

2.E Detecting change points in VIX and S&P 500: A new approach to dynamic asset allocation

Published in the Journal of Asset Management

The starting point for paper E is a belief that a fixed number of recurring regimes is too simplistic a model to represent the dynamics of financial returns, albeit the regimes are not really recurring when the underlying parameters change over time. Its contribution is to propose a new approach to DAA that is based on detection of change points without fitting a model with a fixed number of regimes to the data, without estimating any parameters, and without assuming a specific distribution of the data.

Most traditional approaches to change detection assume that the distributional form of the data is known before and after a change with only the parameters being unknown (see, e.g., Page 1954, Roberts 1959, Siegmund and Venkatraman 1995, Gustafsson 2000). However, this assumption rarely holds in sequential applications. Typically, there is no prior knowledge of the true distribution or assumptions made about the distribution may be incorrect; for example, assuming the data is Gaussian will cause occasional large values to be interpreted as change points, even though they should more correctly be classified as extreme values (Ross 2013).

We apply the nonparametric (distribution-free) change-detection approach of Ross et al. (2011), which does not assume that anything is known about the distribution of the data before monitoring begins. We examine whether to test for location, scale or more general distributional changes and whether changes in Chicago Board Options Exchange's Volatility Index (VIX) or change points

detected in daily returns of the S&P 500 index from 1990 to 2015 provide the most profitable signal.

We consider the VIX because of its forward-looking nature. It essentially offers a market-determined, forward-looking estimate of one-month stock market volatility and is regarded as an indicator of market stress (Whaley 2000). It imbeds many properties of other macroeconomic and financial uncertainty measures, as shown by Racicot and Théoret (2016). Moreover, there is a significantly negative relationship between changes in the VIX and contemporaneous returns of the S&P 500 index, as depicted in figure 1 on page 123.

When a change point is detected, the only knowledge of the new regime is the observations encountered between the change point and the time of detection. Unlike the previous two papers, where the asset allocation was determined by the inferred regime, there is no natural strategy for changing allocation when a change point is detected. We find that simple switching strategies perform better than strategies where the allocation to the stock index is a linear function of the estimated volatility, despite the fact that the volatility assumes many different levels in the detected regimes.

The best performing strategy is a switching strategy that is fully invested in the S&P 500 index in the low-volatility state and cash in the high-volatility state, based on detected changes in the scale parameter of log-returns of the VIX. This strategy outperforms both the S&P 500 index and a static portfolio with the same average allocation to the stock index both in terms of realized and risk-adjusted return, and it has a significantly lower tail risk (see figure 12 on page 136). Due to the assumption of zero interest on cash positions, there is no other source of performance than the index. We show that a similar risk-adjusted return can be obtained by selling short-term VIX futures instead of buying the S&P 500 index in the low-volatility state.

It is left for future research to generalize the nonparametric change-detection approach of Ross et al. (2011) to a multivariate setting. Change detection is a compelling alternative to a regime-switching model, because it makes fewer assumptions about the data. It captures the same abrupt regime changes, but provides a more flexible representation of the dynamics of financial returns. The disadvantage is that there is no prior knowledge of the new dynamics when a change point is detected. After a change point, when important allocation decisions are made based on forecasts of future dynamics, this is done based on very limited information.

2.F Greedy Gaussian segmentation of multivariate time series

To appear in Advances in Data Analysis and Classification

Before discussing its contribution, I will describe the work that led to paper F. We began by adapting the ℓ_1 trend filtering method proposed by Kim et al. (2009) to produce estimates that are piecewise constant, making it suited to analyzing time series that are subject to level shifts. A regularization parameter was used to control the tradeoff between smoothness (or number of changes) of the estimated level and size of the residuals, somewhat similar to the average run length in change detection (see, e.g., Gustafsson 2000). It can be thought of as an optimization-based approach to change detection and time series segmentation. We tested this on daily log-returns of the S&P 500 and their squared values and experimented with using iterated reweighting to improve the results (Candès et al. 2008). We found that there was much more information in the volatility than in the returns themselves, in agreement with the finding in the previous paper.

Kim et al. (2009) described how the basic ℓ_1 trend (level) estimation method can be generalized to handle multivariate time series data by using the sum of the ℓ_2 norms of the second (first) differences as the measure of smoothness. Compared to estimating levels separately in each time series, this formulation couples together changes in the levels of individual entries at the same time index, so the level component found tends to show simultaneous changes.⁵ The multivariate time series could be simultaneous returns of the FTSE and S&P 500 indices or returns of the S&P 500 and their squared values.

A difficulty with this method is scaling the relative importance of changes in mean and volatility or one time series relative to another; however, this is exactly what the Gaussian density does. Further, by assuming a multivariate Gaussian distribution, we can benefit from information in the correlation structure when identifying regimes (Müninx et al. 2012, Chetalova et al. 2015). Similar to the ℓ_1 and ℓ_2 trend filtering problems, Gaussian segmentation is a convex optimization problem, yet there is no available software that can solve it.

We formulate this as a covariance-regularized maximum-likelihood problem, which can be reduced to a combinatorial optimization problem of searching over the possible breakpoints. This problem is in general difficult to solve globally. The contribution of paper F is to propose an efficient heuristic method that approximately solves it, and always yields a locally optimal choice, in the sense that no change of any one breakpoint improves the objective. Our implementation is made available in a Python software package.⁶

⁵The idea behind this penalty is used in the group lasso (Yuan and Lin 2006).

⁶Available at <https://github.com/cvxgrp/GGS>.

We illustrate the approach with four different examples. First, we do a small example with daily log-returns from 1997 to 2015 for a stock, bond, and oil price index, where we plot the means, variances, and correlations in figure 4 on page 159. This is a great alternative to using a sliding window to illustrate the dynamics. Second, we emphasize the scalability of our method by considering a larger example with the 309 companies in the S&P 500 index that have been publicly listed for the entire 19-year period from before. Our method is quite efficient and easily scales to problems with vectors of dimension over 1,000 and time series of arbitrary length. Third, we look at an example from the field of natural language processing to illustrate how our method can be applied to a different type of dataset. Our method correctly identifies both the breakpoint locations and the general topic of each segment in data obtained by concatenating the introductions from five different Wikipedia articles (see figure 9 on page 164). Fourth, we show that our method is more robust than a left-to-right HMM using a synthetic example where observations are generated from a known sequence of segments.

2.G Dynamic portfolio optimization across hidden market regimes

Published in Quantitative Finance

Paper G contributes to the literature on dynamic asset allocation by combining forecasts from an HMM with a multi-period optimization approach to asset allocation based on model predictive control. It is a promising alternative to the static decision rules that dominate the literature, including paper C and paper D (see also Ang and Bekaert 2004, Guidolin and Timmermann 2007, Bulla et al. 2011, Kritzman et al. 2012). Fornaciari and Grillenzoni (2017) proposed to dynamically optimize the parameters of the decision rule, but this led to problems with overfitting and poor performance. MPC, on the other hand, offers an optimal implementation, conditional on the choice of hyperparameters, which all have a clear interpretation as transaction costs, holding costs, etc.

The benefit of MPC for multi-period portfolio optimization was proposed by Herzog et al. (2007), Meindl and Primbs (2008), and Boyd et al. (2014). The idea is to control a portfolio based on forecasts of asset returns and relevant parameters. Every day a decision is made whether or not to change the current portfolio allocation, knowing that the decision will be reconsidered the next day with new input. Possible benefits from changing allocation are traded off against risks and costs. A sequence of trades is planned, but only the first one is executed. There are computational advantages to using MPC in cases when estimates of future return statistics are updated every time a new observation becomes available, since the optimal control actions are reconsidered anyway.

The implementation is based on forecasts from the same HMM with time-varying parameters estimated using the recursive, adaptive approach that was presented in paper B and applied in paper C and paper D. It is the first time that we use this model for forecasting returns and not just distinguishing between market regimes. Although change detection, trend filtering, and Gaussian segmentation are great tools for analysis, we find them to be less useful for forecasting.

We test this on various major stock market indices, one at a time, using daily data from 1984 to 2015. Cash positions are assumed to be risk-free and yield zero interest; hence, the only source of performance is the stock indices. The MPC approach realizes a higher risk-adjusted return than a buy-and-hold investment in five out of six indices—regardless of whether risk is measured by standard deviation or maximum drawdown—and has a higher annualized return than the underlying index in four out of six cases, cf. table 10 on page 197. We experiment with the impact of an additional ℓ_1 trading penalty and find that it increases the robustness of the approach.

2.H Multi-period trading via convex optimization

Published in Foundations and Trends in Optimization

Paper H presents a continuation of the MPC idea from Boyd et al. (2014) that was utilized in the previous paper. We consider a basic model of multi-period trading, which can be used to evaluate the performance of a trading strategy. We describe a framework for single-period optimization, where the trades in each period are found by solving a convex optimization problem that trades off expected return, risk, transaction and holding cost. We then describe a multi-period version of the trading method, where optimization is used to plan a sequence of trades, with only the first one executed, using estimates of future quantities that are unknown when the trades are chosen.

Our contribution is to describe the single- and multi-period methods in one simple framework, giving a careful description of the development and the approximations made, and discussing how convex optimization can be used in multi-period trading. The methods can be thought of as good ways to exploit forecasts, no matter how they are made. It is a better alternative to the more or less ad-hoc trading strategies that are sometimes used to evaluate new return-prediction models.

Our focus is not on theoretical issues, but on practical ones that arise in multi-period trading. The advantages of a multi-period approach include the ability to properly model transaction and holding costs and take into account differences in short- and long-term forecasts. We develop a basic dynamic model of trading that describes how a portfolio and associated cash account change over time, due to trading, investment gains, and various costs associated with trading and holding portfolios. We present realistic models of transaction and holding

costs along with examples of many different constraints that arise in practical investment management and can easily be included.

The optimization-based trading methods we describe are practical and reliable when the problems to be solved are convex (Boyd and Vandenberghe 2004). Vast increases in computing power have changed how optimization can be used in investing. In particular, it is now possible to quickly run full-blown, multi-period optimizations and search over hyperparameters in backtests. Real-world single-period convex problems with thousands of assets can be solved using generic algorithms in well under a second, which is critical for evaluating a proposed algorithm with historical or simulated data, for many values of the parameters in the method.

At the end of the paper we discuss computation times as well as possibilities for speedup for a few examples based on daily data for the constituents of the S&P 500 index from 2012 through 2016. The examples illustrate the usefulness of the approach and the potential for exploiting the power of convex optimization in multi-period trading and portfolio optimization.

Having established a well-functioning framework for utilizing and assessing the value of multi-step forecasts, it is left for future research to develop these. Many of the ideas and methods described in the paper are implemented in a companion open-source Python package.⁷ Hopefully this will be useful in future research—in academia as well as in industry—when evaluating the performance of return-prediction models.

2.I Multi-period portfolio selection with drawdown control

To appear in Annals of Operations Research

Paper I implements a specific case of the methods from the previous paper, with an additional mode that controls for drawdown by adjusting the risk aversion based on realized drawdown. By proposing a practical approach to drawdown control, we provide evidence of the theoretical link between dynamic asset allocation and drawdown control. We disprove the common conception that mean-variance optimization cannot be consistent with a focus on controlling tail risk.

We demonstrate the approach using data from 1999 through 2016 for the same ten indices that we considered in paper D.⁸ These indices are chosen to mimic the major liquid asset classes typically considered by an institutional investor. Compared to paper G, it is an extension from one to ten assets. In connection with paper D, we attempted to derive and model central risk factors without success, so this time we focus on a multivariate model of all ten indices.

⁷ Available at <https://github.com/cvxgrp/cvxportfolio>.

⁸The only difference is that the LBMA Gold Price is substituted for the S&P GSCI Gold index.

We contemplated an approach similar to Fortescue et al. (1981) with a memory length that is adjusted based on forecasting accuracy, as an alternative to using regime shifts to capture abrupt parameter changes. This would overcome the issue with distinguishing between parameter changes caused by a regime shift and parameter changes in the underlying model. Taking this idea one step further, the memory could depend on portfolio performance rather than forecasting accuracy, as in closed-loop control (Bertsekas 1995). A disadvantage is that the forecasts become constant, in the absence of a model describing the dynamics. Although the approach is conceptually intriguing, we found that it does not compete with a regime-switching model.

We instead base our implementation on forecasts from a multivariate hidden Markov model with time-varying parameters. We estimate the model using the online, adaptive version of the expectation–maximization algorithm proposed by Stenger et al. (2001). Contrary to the recursive, adaptive estimation approach from paper B, where it is necessary to consider past observations when evaluating the score function, the algorithm of Stenger et al. (2001) is truly online. It is much faster and easily scales to higher dimensions (Khreich et al. 2012). We find that two regimes is sufficient, after testing models with two, three, and four regimes.

The usual issues when estimating a high-dimensional covariance matrix also arise in the context of HMMs, causing unstable estimates of the transition matrix and of the hidden states. In fact, the problem is even more pronounced, as some regimes are seldom visited, leaving a very small sample for estimating the covariance matrix. When we fit a multivariate HMM to all indices at once using in-sample training data, the state sequence has low persistence and frequent switches, leading to excessive portfolio turnover and poor results. In addition to applying a Stein-type shrinkage estimator to the estimated covariance matrix in each regime, as proposed by Fiecas et al. (2017), we find that it is necessary to estimate the state sequence based solely on two stock indices. We still estimate the mean vector and covariance matrix in each state based on all the indices. This approach is inspired by paper D and supported by the finding of meaningful common breakpoints across stocks, bonds, and oil in paper F. In addition to regularizing the estimated covariance matrices, we find that it is necessary to include transaction and holding costs and constraints in order to regularize the portfolio optimization problem and reduce the risk due to estimation error.

Our testing shows that, even if they knew the future returns when choosing their benchmark, investors who insist on rebalancing to a static, diversified benchmark portfolio could not have outperformed the dynamic approach net of transaction costs over the 18-year test period in terms of risk-adjusted return. This is regardless of whether risk is measured by standard deviation or maximum drawdown (figure 7 on page 290). The dynamic approach also outperforms an equally-weighted portfolio and a fixed-mix portfolio with the same average allocation. The outperformance happens continually over the 18-year period

(figure 6 on page 288). The combination of leverage and drawdown control is particularly successful, as it is possible to increase the excess return by several hundred basis points without suffering a larger maximum drawdown (figure 8(b) on page 291).

In summary, the MPC approach to multi-period portfolio optimization combined with the proposed approach to drawdown control is practical, efficient, and leads to impressive results. In addition to improving the multi-period forecasts, it would be interesting in future research to compare the deterministic MPC approach with stochastic MPC based on scenarios. The starting point for the comparison could be the multivariate HMM proposed in this paper. By generating scenarios, rather than summarizing the forecast distribution by its first two moments at every time step, it is possible to account for both the interdependence structure of prediction errors and the predictive distributions (Pinson et al. 2009). The entire forecast distribution could also be taken into account by using stochastic programming (see, e.g., Ali et al. 2015).

CHAPTER 3

Conclusion

Long-term investors can often bear the risk of outsized market movements or tail events more easily than the average investor; for bearing this risk, they hope to earn significant excess returns. Our results show that rebalancing periodically to a fixed benchmark allocation is not the way to do this. Regime shifts that present a big challenge to traditional, static approaches to asset allocation pose a large potential for dynamic approaches. A substantial amount of value can be added by adjusting the asset allocation to the current market conditions, rather than rebalancing periodically to a static benchmark.

Regime shifts lead to time-varying parameters and, in addition, we found that the parameters within the regimes and the transition probabilities change over time. By taking this into account, we were able to better reproduce the long memory of squared daily returns that DAA benefits from. When applying an adaptive estimation approach to allow for time-varying parameters, we found that a two-state Gaussian HMM was able to reproduce this long memory. There was no need for other sojourn-time or conditional distributions. The time variation was observation driven based on the gradient of the likelihood function. Furthermore, fast adaptation to parameter changes led to improved one-step density forecasts.

We showed that by using a continuous-time formulation it is possible to increase the number of states with a linear rather than quadratic increase in the number of parameters and thereby obtain a better fit to the distributional and temporal properties of daily returns. Meanwhile, when allowing for time-varying parameters, two regimes were sufficient, though the time-varying behavior meant that the regimes were not actually recurring.

We found that it is profitable to change asset allocation based solely on regimes identified in stock returns. This included changing allocation between stocks and bonds and switching between predefined risk-on and risk-off portfolios to sustain a level of diversification. In both cases, a regime-based approach led to higher risk-adjusted returns and a lower maximum drawdown compared to a static portfolio. It was not a problem to obtain good results out of sample when using the two-state Gaussian HMM with time-varying parameters for regime inference.

The nonrecurring regimes led us to consider alternatives to the application of HMMs to identify regime shifts, such as nonparametric change detection and trend filtering. We even developed a greedy algorithm for segmenting multivariate Gaussian time series, applicable to everything from text data to high-dimensional return series. Using this algorithm we were able to benefit from information in the correlation structure when identifying regimes in past returns. Although change detection, trend filtering, and Gaussian segmentation are great tools for analysis, we found them to be less useful for forecasting.

Expanding the univariate HMM to a multivariate model was a challenging task. In order to reduce the complexity of the modeling task, we considered deriving and modeling central risk factors, but when we analyzed the correlation structure and its principal components, we did not find any stationary structure. We switched from the gradient-based estimation approach to an online version of the expectation–maximization algorithm that is significantly faster and easily scalable to high dimensions.

The usual issues when estimating a high-dimensional covariance matrix based on a limited number of observations also arose in the context of HMMs, causing unstable estimates of the transition matrix and of the hidden states. If the returns were perfectly Gaussian, then increasing the dimension should enhance the regime inference, since more information is available. As the multivariate Gaussian distribution was only an approximation, increasing the dimension introduced more outliers and led to a state sequence with low persistence and frequent switches, resulting in excessive portfolio turnover and poor results. We obtained better results by estimating the state sequence based solely on two stock indices, while still estimating the mean vector and covariance matrix in each state based on all the indices.

We showed how forecasts can be optimally translated into a DAA strategy using MPC. By taking advantage of powerful computers combined with advances in convex optimization, we developed a framework based on MPC that makes it feasible to solve multi-period portfolio optimization problems with large numbers of assets and search over hyperparameters in backtests. This was a significant breakthrough compared to analytical solutions based on dynamic programming that are infeasible in most practical applications due to the curse of dimensionality. We found that transaction and holding costs play an important role in

terms of regularizing the optimization problem and reducing the risk due to estimation error.

By allowing for investment in a portfolio of assets rather than only stocks and cash, it was possible to achieve a higher risk-adjusted return and a more steady outperformance over time relative to a fixed-weight benchmark. We implemented the MPC approach based on forecasts from the multivariate HMM with time-varying parameters. Our testing showed that, even if they knew the future returns when choosing their benchmark, investors who insisted on rebalancing to a static, diversified benchmark portfolio could not have outperformed the dynamic approach net of transaction costs in terms of risk-adjusted return. This was regardless of whether risk was measured by standard deviation or maximum drawdown.

We showed how an optimization approach based on MPC can be used to control drawdowns, with little or no loss of mean–variance efficiency, by adjusting the risk aversion based on realized drawdown. DAA, even without drawdown control, led to a significantly lower maximum drawdown compared to a fixed-weight portfolio, regardless of whether the approach was rule or optimization based. The combination of leverage and drawdown control was particularly successful, as it was possible to increase the excess return by several hundred basis points without suffering a larger maximum drawdown.

3.1 Commercial perspectives

DAA is a highly relevant topic, since the majority of assets, for example in pension funds, are still being managed using primarily static benchmarks. Institutional investors are increasingly looking to incorporate some element of dynamic decision-making within portfolios, both for return enhancement and as a risk-management tool. The two financial crises during the 2000s have exposed the weaknesses of a static asset allocation and contributed to the rising interest in dynamic and regime-based approaches. The recency of events means that large amounts of data containing turbulent periods are available for backtesting.

Avoiding large drawdowns is valuable in itself—even for investors with a *very* long investment horizon—and, in addition, provides an opportunity for taking more risk at other, more favorable times, without increasing the overall risk. Hence, better risk management can be directly converted into higher (risk-adjusted) returns.

This study underpins the demand for dynamic approaches with better possibility for adjusting risk and asset allocation over time, in order to benefit from time-varying risk premia by continually allocating investments toward the best risk–return tradeoff, concurrently with developments in the business cycle and financial markets. It contributes to a better understanding of financial markets’ behavior in the form of a model-based framework for DAA.

The commercial value of the study extends beyond the specific methods that have been developed. The demonstration of the advantages of DAA and its connection to drawdown control should give rise to a fundamental reform of the approach to asset allocation. This could potentially contribute to better risk management within financial institutions.

3.2 Future work

Having established a well-functioning framework for assessing the value of multi-period forecasts, it is left for future research to develop these. There is potential for further developing recursive and adaptive estimation techniques for regime-switching models, for example by exploring the impact of adding a regularization term reflecting prior information to the likelihood objective. One possible way to obtain a better description of the time-varying behavior of the parameters could be to allow different forgetting factors for each parameter or consider more advanced state-, time-, or data-dependent forgetting. Another way could be to formulate a model for the parameter changes in the form of a hierarchical model, possibly including exogenous explanatory variables. This could be a hierarchical stochastic-differential-equation model with continuous rather than discrete regime shifts, where the parameters themselves are stochastic processes.

Although we did not have success with risk-factor-based forecasting, this approach still has appealing properties in terms of scalability. If the main importance is to distinguish between risk-on and risk-off regimes, as our results suggest, it may suffice to consider stock returns. Conversely, it is worth exploring in more detail whether information from other asset classes, correlations (within and between asset classes), economic variables, interest rates, or other possible indicators can be included to improve regime inference.

Given the promising results of the MPC approach to portfolio optimization and drawdown control, it is worth further developing this approach and considering integrating estimation and control. For example, the forgetting parameter used in estimation could be adjusted based on forecasting accuracy or even portfolio performance. As an alternative to allocation at asset-class level, the MPC approach could be utilized for dynamic allocation to risk premia, such as value and momentum, or various quantitative strategies.

Stochastic MPC is another open route for future research. Instead of replacing all future, unknown quantities by their forecasted values, in order to turn the stochastic control problem into a deterministic optimization problem, scenarios could be generated to represent the uncertainty in the forecasts. Alternatively, the entire distribution could be taken into account by using stochastic programming. It is not a given, however, that the increase in computational complexity would be offset by better results.

References

- Ali, A., J. Z. Kolter, S. Diamond, and S. Boyd. “Disciplined convex stochastic programming: A new framework for stochastic optimization.” In *Proceedings of the 31st Conference on Uncertainty in Artificial Intelligence* (2015), pp. 62–71.
- Allez, R. and J. P. Bouchaud. “Eigenvector dynamics: General theory and some applications.” *Physical Review E*, vol. 86, no. 4 (2012), p. 046202.
- Ammann, M. and M. Verhofen. “The effect of market regimes on style allocation.” *Financial Markets and Portfolio Management*, vol. 20, no. 3 (2006), pp. 309–337.
- Ang, A. and G. Bekaert. “International asset allocation with regime shifts.” *Review of Financial Studies*, vol. 15, no. 4 (2002), pp. 1137–1187.
- Ang, A. and G. Bekaert. “How regimes affect asset allocation.” *Financial Analysts Journal*, vol. 60, no. 2 (2004), pp. 86–99.
- Ang, A. and A. Timmermann. “Regime changes and financial markets.” *Annual Review of Financial Economics*, vol. 4, no. 1 (2012), pp. 313–337.
- Augustyniak, M., L. Bauwens, and A. Dufays. “A new approach to volatility modeling: the high-dimensional Markov model.” Tech. Rep. 2016042, Université catholique de Louvain (2016).
- Bae, G. I., W. C. Kim, and J. M. Mulvey. “Dynamic asset allocation for varied financial markets under regime switching framework.” *European Journal of Operational Research*, vol. 234, no. 2 (2014), pp. 450–458.

- Bansal, R., M. Dahlquist, and C. R. Harvey. "Dynamic trading strategies and portfolio choice." Working Paper 10820, National Bureau of Economic Research (2004).
- Bass, R., S. Gladstone, and A. Ang. "Total portfolio factor, not just asset, allocation." *Journal of Portfolio Management*, vol. 43, no. 5 (2017), pp. 38–53.
- Bauer, R., R. Haerden, and R. Molenaar. "Asset allocation in stable and unstable times." *Journal of Investing*, vol. 13, no. 3 (2004), pp. 72–80.
- Bellman, R. E. "Dynamic programming and Lagrange multipliers." *Proceedings of the National Academy of Sciences*, vol. 42, no. 10 (1956), pp. 767–769.
- Bertsekas, D. P. *Dynamic Programming and Optimal Control*. Athena Scientific: Belmont (1995).
- Bertsimas, D., G. J. Lauprete, and A. Samarov. "Shortfall as a risk measure: properties, optimization and applications." *Journal of Economic Dynamics & Control*, vol. 28, no. 7 (2004), pp. 1353–1381.
- Black, F. and M. Scholes. "The pricing of options and corporate liabilities." *Journal of Political Economy*, vol. 81, no. 3 (1973), pp. 637–654.
- Boyd, S., M. T. Mueller, B. O'Donoghue, and Y. Wang. "Performance bounds and suboptimal policies for multi-period investment." *Foundations and Trends in Optimization*, vol. 1, no. 1 (2014), pp. 1–72.
- Boyd, S. and L. Vandenberghe. *Convex Optimization*. Cambridge University Press: New York (2004).
- Brinson, G. P., L. R. Hood, and G. L. Beebower. "Determinants of portfolio performance." *Financial Analysts Journal*, vol. 42, no. 4 (1986), pp. 39–44.
- Brunnermeier, M. K. and L. H. Pedersen. "Market liquidity and funding liquidity." *Review of Financial studies*, vol. 22, no. 6 (2009), pp. 2201–2238.
- Bulla, J. "Hidden Markov models with t components. Increased persistence and other aspects." *Quantitative Finance*, vol. 11, no. 3 (2011), pp. 459–475.
- Bulla, J. and I. Bulla. "Stylized facts of financial time series and hidden semi-Markov models." *Computational Statistics & Data Analysis*, vol. 51, no. 4 (2006), pp. 2192–2209.
- Bulla, J., S. Mergner, I. Bulla, A. Sesboüé, and C. Chesneau. "Markov-switching asset allocation: Do profitable strategies exist?" *Journal of Asset Management*, vol. 12, no. 5 (2011), pp. 310–321.

- Calvet, L. E. and A. J. Fisher. “How to forecast long-run volatility: Regime switching and the estimation of multifractal processes.” *Journal of Financial Econometrics*, vol. 2, no. 1 (2004), pp. 49–83.
- Campbell, J. Y. “Asset prices, consumption, and the business cycle.” In *Handbook of Macroeconomics*, edited by J. B. Taylor and M. Woodford, vol. 1C, chap. 19. Elsevier: Amsterdam (1999), pp. 1231–1303.
- Campbell, J. Y. and L. M. Viceira. *Strategic Asset Allocation: Portfolio Choice for Long-Term Investors*. Oxford University Press: New York (2002).
- Candès, E. J., M. B. Wakin, and S. Boyd. “Enhancing sparsity by reweighted ℓ_1 minimization.” *Journal of Fourier Analysis and Applications*, vol. 14, no. 5–6 (2008), pp. 877–905.
- Cappé, O., E. Moulines, and T. Rydén. *Inference in Hidden Markov Models*. Springer: New York (2005).
- Chetalova, D., R. Schäfer, and T. Guhr. “Zooming into market states.” *Journal of Statistical Mechanics: Theory and Experiment*, vol. 2015, no. 1 (2015), p. P01029.
- Cochrane, J. H. “Financial markets and the real economy.” *Foundations and Trends in Finance*, vol. 1, no. 1 (2005), pp. 1–101.
- Cocoma, P., M. Czasonis, M. Kritzman, and D. Turkington. “Facts about factors.” *Journal of Portfolio Management*, vol. 43, no. 5 (2017), pp. 55–65.
- Cohn, A., J. Engelmann, E. Fehr, and M. A. Maréchal. “Evidence for counter-cyclical risk aversion: an experiment with financial professionals.” *American Economic Review*, vol. 105, no. 2 (2015), pp. 860–885.
- Cooper, J. E. and K. Worden. “On-line physical parameter estimation with adaptive forgetting factors.” *Mechanical Systems and Signal Processing*, vol. 14, no. 5 (2000), pp. 705–730.
- Creal, D., S. J. Koopman, and A. Lucas. “Generalized autoregressive score models with applications.” *Journal of Applied Econometrics*, vol. 28, no. 5 (2013), pp. 777–795.
- Dacco, R. and S. Satchell. “Why do regime-switching models forecast so badly?” *Journal of Forecasting*, vol. 18, no. 1 (1999), pp. 1–16.
- Dahlquist, M. and C. R. Harvey. “Global tactical asset allocation.” *Emerging Markets Quarterly*, vol. 5, no. 1 (2001), pp. 6–14.
- Diamond, S. and S. Boyd. “CVXPY: A Python-embedded modeling language for convex optimization.” *Journal of Machine Learning Research*, vol. 17, no. 83 (2016), pp. 1–5.

- Downing, C., A. Madhavan, A. Ulitsky, and A. Singh. "Portfolio construction and tail risk." *Journal of Portfolio Management*, vol. 42, no. 1 (2015), pp. 85–102.
- Fama, E. F. "Efficient capital markets: A review of theory and empirical work." *Journal of Finance*, vol. 25, no. 2 (1970), pp. 383–417.
- Fenn, D. J., M. A. Porter, S. Williams, M. McDonald, N. F. Johnson, and N. S. Jones. "Temporal evolution of financial-market correlations." *Physical Review E*, vol. 84, no. 2 (2011), p. 026109.
- Fiecas, M., J. Franke, R. von Sachs, and J. T. Kamgaing. "Shrinkage estimation for multivariate hidden Markov models." *Journal of the American Statistical Association*, vol. 112, no. 517 (2017), pp. 424–435.
- Fornaciari, M. and C. Grillenzoni. "Evaluation of on-line trading systems: Markov-switching vs time-varying parameter models." *Decision Support Systems*, vol. 93 (2017), pp. 51–61.
- Fortescue, T. R., L. S. Kershenbaum, and B. E. Ydstie. "Implementation of self-tuning regulators with variable forgetting factors." *Automatica*, vol. 17, no. 6 (1981), pp. 831–835.
- Frühwirth-Schnatter, S. *Finite Mixture and Markov Switching Models*. Springer: New York (2006).
- Gârleanu, N. and L. H. Pedersen. "Liquidity and risk management." *American Economic Review*, vol. 97, no. 2 (2007), pp. 193–197.
- Gârleanu, N. and L. H. Pedersen. "Dynamic trading with predictable returns and transaction costs." *Journal of Finance*, vol. 68, no. 6 (2013), pp. 2309–2340.
- Goltz, F., L. Martellini, and K. D. Simsek. "Optimal static allocation decisions in the presence of portfolio insurance." *Journal of Investment Management*, vol. 6, no. 2 (2008), pp. 37–56.
- Goyal, A., A. Ilmanen, and D. Kabiller. "Bad habits and good practices." *Journal of Portfolio Management*, vol. 41, no. 4 (2015), pp. 97–107.
- Granger, C. W. J. and Z. Ding. "Some properties of absolute return: An alternative measure of risk." *Annales D'Economie Et Statistique*, vol. 40 (1995a), pp. 67–92.
- Granger, C. W. J. and Z. Ding. "Stylized facts on the temporal and distributional properties of daily data from speculative markets." Unpublished paper, Department of Economics, University of California, San Diego (1995b).

- Guidolin, M. “Markov switching in portfolio choice and asset pricing models: A survey.” In *Missing Data Methods: Time-Series Methods and Applications*, edited by D. M. Drukker, vol. 27b of *Advances in Econometrics*. Emerald Group Publishing: Bingley (2011a), pp. 87–178.
- Guidolin, M. “Markov switching models in empirical finance.” In *Missing Data Methods: Time-Series Methods and Applications*, edited by D. M. Drukker, vol. 27b of *Advances in Econometrics*. Emerald Group Publishing: Bingley (2011b), pp. 1–86.
- Guidolin, M. and F. Ria. “Regime shifts in mean–variance efficient frontiers: Some international evidence.” *Journal of Asset Management*, vol. 12, no. 5 (2011), pp. 322–349.
- Guidolin, M. and A. Timmermann. “Asset allocation under multivariate regime switching.” *Journal of Economic Dynamics and Control*, vol. 31, no. 11 (2007), pp. 3503–3544.
- Guidolin, M. and A. Timmermann. “International asset allocation under regime switching, skew, and kurtosis preferences.” *Review of Financial Studies*, vol. 21, no. 2 (2008), pp. 855–901.
- Gustafsson, F. *Adaptive Filtering and Change Detection*. Wiley: West Sussex (2000).
- Herzog, F., G. Dondi, and H. P. Geering. “Stochastic model predictive control and portfolio optimization.” *International Journal of Theoretical and Applied Finance*, vol. 10, no. 2 (2007), pp. 203–233.
- Ibbotson, R. G. and P. D. Kaplan. “Does asset allocation policy explain 40, 90, or 100 percent of performance?” *Financial Analysts Journal*, vol. 56, no. 1 (2000), pp. 26–33.
- Ibragimov, R., D. Jaffee, and J. Walden. “Diversification disasters.” *Journal of Financial Economics*, vol. 99, no. 2 (2011), pp. 333–348.
- Johansen, T. A. “On Tikhonov regularization, bias and variance in nonlinear system identification.” *Automatica*, vol. 33, no. 3 (1997), pp. 441–446.
- Khreich, W., E. Granger, A. Miri, and R. Sabourin. “A survey of techniques for incremental learning of HMM parameters.” *Information Sciences*, vol. 197 (2012), pp. 105–130.
- Kim, S. J., K. Koh, S. Boyd, and D. Gorinevsky. “ ℓ_1 trend filtering.” *SIAM Review*, vol. 51, no. 2 (2009), pp. 339–360.
- Kolm, P., R. Tütüncü, and F. Fabozzi. “60 years of portfolio optimization: Practical challenges and current trends.” *European Journal of Operational Research*, vol. 234, no. 2 (2014), pp. 356–371.

- Kritzman, M. and Y. Li. "Skulls, financial turbulence, and risk management." *Financial Analysts Journal*, vol. 66, no. 5 (2010), pp. 30–41.
- Kritzman, M., S. Page, and D. Turkington. "Regime shifts: Implications for dynamic strategies." *Financial Analysts Journal*, vol. 68, no. 3 (2012), pp. 22–39.
- Langrock, R. and W. Zucchini. "Hidden Markov models with arbitrary state dwell-time distributions." *Computational Statistics & Data Analysis*, vol. 55, no. 1 (2011), pp. 715–724.
- Levich, R. M. *International Financial Markets: Prices and Policies*. McGraw-Hill: New York, 2nd ed. (2001).
- Lim, A. E., J. G. Shanthikumar, and G. Y. Vahn. "Conditional value-at-risk in portfolio optimization: Coherent but fragile." *Operations Research Letters*, vol. 39, no. 3 (2011), pp. 163–171.
- Lindström, E., H. Madsen, and J. N. Nielsen. *Statistics for Finance*. Chapman & Hall: London (2015).
- Ljung, L. and T. Söderström. *Theory and Practice of Recursive Identification*. MIT Press: Cambridge (1983).
- Madsen, H. *Time Series Analysis*. Chapman & Hall: London (2008).
- Madsen, H., J. N. Nielsen, E. Lindström, M. Baadsgaard, and J. Holst. "Statistics in finance." Lund University (1999). Lecture notes.
- Malmsten, H. and T. Teräsvirta. "Stylized facts of financial time series and three popular models of volatility." *European Journal of Pure and Applied Mathematics*, vol. 3, no. 3 (2010), pp. 443–477.
- Mandelbrot, B. "The variation of certain speculative prices." *Journal of Business*, vol. 36, no. 4 (1963), pp. 394–419.
- Markowitz, H. "Portfolio selection." *Journal of Finance*, vol. 7, no. 1 (1952), pp. 77–91.
- Markowitz, H. "Mean–variance approximations to expected utility." *European Journal of Operational Research*, vol. 234, no. 2 (2014), pp. 346–355.
- Meindl, P. J. and J. A. Primbs. "Dynamic hedging of single and multi-dimensional options with transaction costs: a generalized utility maximization approach." *Quantitative Finance*, vol. 8, no. 3 (2008), pp. 299–312.
- Merton, R. C. "Lifetime portfolio selection under uncertainty: The continuous-time case." *Review of Economics and Statistics*, vol. 51, no. 3 (1969), pp. 247–257.

- Merton, R. C. “Theory of rational option pricing.” *Bell Journal of Economics and Management Science*, vol. 4, no. 1 (1973), pp. 141–183.
- Moreira, A. and T. Muir. “Volatility-managed portfolios.” *Journal of Finance*, vol. 72, no. 4 (2017), pp. 1611–1644.
- Mossin, J. “Optimal multiperiod portfolio policies.” *Journal of Business*, vol. 41, no. 2 (1968), pp. 215–229.
- Münnix, M. C., T. Shimada, R. Schaefer, F. Leyvraz, T. H. Seligman, T. Guhr, and H. E. Stanley. “Identifying states of a financial market.” *Scientific Reports*, vol. 2, no. 1 (2012), p. 644.
- Narasimhan, M., P. Viola, and M. Shilman. “Online decoding of Markov models under latency constraints.” In *Proceedings of the 23rd International Conference on Machine Learning* (2006), pp. 657–664.
- Nystrup, P. *Regime-Based Asset Allocation: Do Profitable Strategies Exist?* Master’s thesis, Technical University of Denmark (2014).
- Page, E. S. “Continuous inspection schemes.” *Biometrika*, vol. 41, no. 1–2 (1954), pp. 100–115.
- Pedersen, L. H. “When everyone runs for the exit.” *International Journal of Central Banking*, vol. 5, no. 4 (2009), pp. 177–199.
- Pedersen, L. H. *Efficiently inefficient: how smart money invests and market prices are determined*. Princeton University Press: Princeton (2015).
- Pinson, P. and H. Madsen. “Adaptive modelling and forecasting of offshore wind power fluctuations with Markov-switching autoregressive models.” *Journal of Forecasting*, vol. 31, no. 4 (2012), pp. 281–313.
- Pinson, P., H. Madsen, H. A. Nielsen, G. Papaefthymiou, and B. Klöckl. “From probabilistic forecasts to statistical scenarios of short-term wind power production.” *Wind Energy*, vol. 12, no. 1 (2009), pp. 51–62.
- Preis, T. and H. E. Stanley. “Switching phenomena in a system with no switches.” *Journal of Statistical Physics*, vol. 438, no. 1–3 (2010), pp. 431–446.
- R Core Team. *R: A Language and Environment for Statistical Computing*. R Foundation for Statistical Computing, Vienna, Austria (2017). URL <https://www.R-project.org/>.
- Racicot, F. É. and R. Théoret. “Macroeconomic shocks, forward-looking dynamics, and the behavior of hedge funds.” *Journal of Banking & Finance*, vol. 62 (2016), pp. 41–61.

- Roberts, S. W. "Control chart tests based on geometric moving averages." *Technometrics*, vol. 1, no. 3 (1959), pp. 239–250.
- Rockafellar, R. T. and S. Uryasev. "Optimization of conditional value-at-risk." *Journal of Risk*, vol. 2, no. 3 (2000), pp. 21–42.
- Ross, G. J. "Modelling financial volatility in the presence of abrupt changes." *Physica A: Statistical Mechanics and its Applications*, vol. 392, no. 2 (2013), pp. 350–360.
- Ross, G. J., D. K. Tasoulis, and N. M. Adams. "Nonparametric monitoring of data streams for changes in location and scale." *Technometrics*, vol. 53, no. 4 (2011), pp. 379–389.
- Rydén, T., T. Teräsvirta, and S. Åsbrink. "Stylized facts of daily return series and the hidden Markov model." *Journal of Applied Econometrics*, vol. 13, no. 3 (1998), pp. 217–244.
- Samuelson, P. A. "Lifetime portfolio selection by dynamic stochastic programming." *Review of Economics and Statistics*, vol. 51, no. 3 (1969), pp. 239–246.
- Sheikh, A. Z. and J. Sun. "Regime change: Implications of macroeconomic shifts on asset class and portfolio performance." *Journal of Investing*, vol. 21, no. 3 (2012), pp. 36–54.
- Siegel, J. J. "Does it pay stock investors to forecast the business cycle?" *Journal of Portfolio Management*, vol. 18, no. 1 (1991), pp. 27–34.
- Siegmund, D. and E. S. Venkatraman. "Using the generalized likelihood ratio statistic for sequential detection of a change-point." *Annals of Statistics*, vol. 23, no. 1 (1995), pp. 255–271.
- Song, Y. "Modelling regime switching and structural breaks with an infinite hidden Markov model." *Journal of Applied Econometrics*, vol. 29, no. 5 (2014), pp. 825–842.
- Stenger, B., V. Ramesh, N. Paragios, F. Coetze, and J. M. Buhmann. "Topology free hidden Markov models: Application to background modeling." In *Proceedings of the Eighth IEEE International Conference on Computer Vision*, vol. 1 (2001), pp. 294–301.
- Uosaki, K., M. Yotsuya, and T. Hatanaka. "Adaptive identification of non-stationary systems with multiple forgetting factors." In *Proceedings of the 35th IEEE Conference on Decision and Control* (1996), pp. 851–856.
- Whaley, R. E. "The investor fear gauge." *Journal of Portfolio Management*, vol. 26, no. 3 (2000), pp. 12–17.

- Yuan, M. and Y. Lin. “Model selection and estimation in regression with grouped variables.” *Journal of the Royal Statistical Society. Series B (Methodological)*, vol. 68, no. 1 (2006), pp. 49–67.
- Zakamulin, V. “Dynamic asset allocation strategies based on unexpected volatility.” *Journal of Alternative Investments*, vol. 16, no. 4 (2014), pp. 37–50.
- Zucchini, W. and I. L. MacDonald. *Hidden Markov Models for Time Series: An Introduction Using R*. Chapman & Hall: London, 2nd ed. (2009).

PAPER A

Originally published in *Quantitative Finance*

Stylized facts of financial time series and hidden Markov models in continuous time

Peter Nystrup, Henrik Madsen, and Erik Lindström

Abstract

Hidden Markov models are often applied in quantitative finance to capture the stylized facts of financial returns. They are usually discrete-time models and the number of states rarely exceeds two because of the quadratic increase in the number of parameters with the number of states. This paper presents an extension to continuous time where it is possible to increase the number of states with a linear rather than quadratic growth in the number of parameters. The possibility of increasing the number of states leads to a better fit to both the distributional and temporal properties of daily returns.

Keywords: Hidden Markov models; Continuous time; Daily returns; Leptokurtosis; Volatility clustering; Long memory.

1 Introduction

The normal distribution is well-known as being a poor fit to most financial returns. Mixtures of normal distributions provide a much better fit as they are able to reproduce both the skewness and leptokurtosis often observed (Cont 2001). Markov switching mixture models, also referred to as hidden Markov models (HMMs), are a natural extension in order to also capture the temporal properties of financial returns. In an HMM, the distribution that generates an observation depends on the state of an underlying and unobserved Markov chain.

The ability of an HMM to reproduce most of the stylized facts of daily return series introduced by Granger and Ding (1995b,a) was illustrated by Rydén et al. (1998). They found that the one stylized fact that cannot be reproduced by an HMM is the slow decay of the autocorrelation function (ACF) of squared daily returns, which is of great importance, for instance, in financial risk management.

According to Bulla and Bulla (2006), the lack of flexibility of an HMM to model this temporal higher-order dependence can be explained by the implicit assumption of geometrically distributed sojourn times in the hidden states. Silvestrov and Stenberg (2004), among others, argued that the memoryless property of the

geometric distribution is inadequate from an empirical perspective, although it is consistent with the no-arbitrage principle.

Bulla and Bulla (2006) considered hidden semi-Markov models (HSMMs) in which the sojourn-time distribution is modeled explicitly for each hidden state so that the Markov property is transferred to the imbedded first-order Markov chain. They showed that HSMMs with negative binomial sojourn-time distributions are able to reproduce most of the stylized facts comparably well, and often better, than the HMM. Specifically, they found HSMMs to reproduce the long-memory property of squared daily returns much better than HMMs. They, however, did not consider the complicated problem of selecting the most appropriate sojourn-time distributions, and, following the approach by Rydén et al. (1998), they only considered models with two hidden states.

Bulla (2011) later showed that HMMs with t -distributed components reproduce most of the stylized facts as well or better than the Gaussian HMM, at the same time as increasing the persistence of the visited states and the robustness to outliers. Bulla (2011) also found that models with three states provided a better fit than models with two states.

Many different stylized facts have been established for financial returns. See, for example, Granger and Ding (1995b,a), Granger et al. (2000), Cont (2001), Malmsten and Teräsvirta (2010). This paper focuses on the stylized facts relating to the long memory of the ACF and examines the importance of the number of hidden states on the ability to fit the slowly decaying ACF of squared daily returns. An extension of HMMs to continuous time is presented as a flexible alternative to the discrete-time models.

Two hidden states are found to be too few to reproduce the slowly decaying ACF as well as the observed skewness and leptokurtosis. A major limitation of discrete-time HMMs and HSMMs is the quadratic increase in the number of parameters with the number of states. This limitation does not apply to HMMs in continuous time, as it can reasonably be assumed that the only possible transitions in an infinitesimally short time interval are to the neighboring states.

This assumption leads to a linear rather than quadratic growth in the number of parameters with the number of states, and consequently, a significant reduction in the number of parameters for higher-order models. With the added flexibility, the number of states can be considered a parameter that needs to be estimated.¹ In addition, it is possible to incorporate temporal inhomogeneity without a dramatic increase in the number of parameters using a continuous-time formulation.

Section 2 gives an introduction to the main theory relating to HMMs and HSMMs. Section 3 introduces HMMs where the underlying Markov chain is

¹See Cappé et al. (2005) for a perspective on order estimation.

a continuous-time Markov chain. Section 4 contains a description of the data analyzed. The empirical results are reported in section 5 and section 6 concludes. All parameter estimates can be found in appendix A. The results of the analysis of the FTSE 100 index can be found in appendix B.

2 Hidden Markov models in discrete time

In a hidden Markov model, the probability distribution that generates an observation depends on the state of an underlying and unobserved Markov process. HMMs are a particular kind of dependent mixture and are therefore also referred to as Markov switching mixture models.

A sequence of discrete random variables $\{S_t : t \in \mathbb{N}\}$ is said to be a Markov chain if, for all $t \in \mathbb{N}$, it satisfies the Markov property:

$$\Pr(S_{t+1} | S_t, \dots, S_1) = \Pr(S_{t+1} | S_t). \quad (1)$$

The conditional probabilities $\Pr(S_{u+t} = j | S_u = i) = \gamma_{ij}(t)$ are called transition probabilities. The Markov chain is said to be homogeneous if the transition probabilities are independent of u , otherwise inhomogeneous.

A Markov chain with transition probability matrix $\boldsymbol{\Gamma}(t) = \{\gamma_{ij}(t)\}$ has stationary distribution $\boldsymbol{\pi}$ if $\boldsymbol{\pi}\boldsymbol{\Gamma} = \boldsymbol{\pi}$ and $\boldsymbol{\pi}\mathbf{1} = 1$. The Markov chain is termed stationary if $\boldsymbol{\pi} = \boldsymbol{\delta}$, where $\boldsymbol{\delta}$ is the initial distribution, that is $\delta_i = \Pr(S_1 = i)$.

If the Markov chain $\{S_t\}$ has m states, then $\{X_t : t \in \mathbb{N}\}$ is called an m -state HMM. With $\mathbf{X}^{(t)}$ and $\mathbf{S}^{(t)}$ representing the sequence of values from time 1 to time t , the simplest model of this kind can be summarized by

$$\Pr(S_t | \mathbf{S}^{(t-1)}) = \Pr(S_t | S_{t-1}), \quad t = 2, 3, \dots, \quad (2a)$$

$$\Pr(X_t | \mathbf{X}^{(t-1)}, \mathbf{S}^{(t)}) = \Pr(X_t | S_t), \quad t \in \mathbb{N}. \quad (2b)$$

When the current state S_t is known, the distribution of X_t depends only on S_t . This causes the autocorrelation of X_t to be strongly dependent on the persistence of S_t .

A specific observation can usually arise from more than one state as the support of the conditional distributions overlaps. Therefore, the unobserved state process $\{S_t\}$ is not directly observable through the observation process $\{X_t\}$, but can only be estimated.

As an example, consider the two-state model with Gaussian conditional distributions:

$$X_t = \mu_{S_t} + \varepsilon_{S_t}, \quad \varepsilon_{S_t} \sim N(0, \sigma_{S_t}^2),$$

where

$$\mu_{S_t} = \begin{cases} \mu_1, & \text{if } S_t = 1, \\ \mu_2, & \text{if } S_t = 2, \end{cases} \quad \sigma_{S_t}^2 = \begin{cases} \sigma_1^2, & \text{if } S_t = 1, \\ \sigma_2^2, & \text{if } S_t = 2, \end{cases} \quad \text{and } \boldsymbol{\Gamma} = \begin{bmatrix} 1 - \gamma_{12} & \gamma_{12} \\ \gamma_{21} & 1 - \gamma_{21} \end{bmatrix}.$$

For this model, the value of the autocorrelation function at lag k is

$$\rho_{X_t}(k|\theta) = \frac{\pi_1(1-\pi_1)(\mu_1-\mu_2)^2}{\sigma^2} \lambda^k,$$

and the autocorrelation function for the squared process is

$$\rho_{X_t^2}(k|\theta) = \frac{\pi_1(1-\pi_1)(\mu_1^2 - \mu_2^2 + \sigma_1^2 - \sigma_2^2)^2}{E[X_t^4|\theta] - E[X_t^2|\theta]^2} \lambda^k,$$

when θ denotes the model parameters, $\sigma^2 = \text{Var}[X_t|\theta]$ is the unconditional variance, and $\lambda = \gamma_{11} + \gamma_{22} - 1$ is the second largest eigenvalue of $\boldsymbol{\Gamma}$ (Frühwirth-Schnatter 2006). It is evident from these expressions, as noted by Rydén et al. (1998), that HMMs can only reproduce an exponentially-decaying autocorrelation structure.

The ACF of the first-order process becomes zero if the means are equal, whereas persistence in the squared process can be induced either by a difference in the mean values, as for a mixed effects model, or by a difference in the variances across the states. In both cases, the persistence increases with the combined persistence of the states as measured by λ (Ang and Timmermann 2012).

The parameters of an HMM are usually estimated using the maximum-likelihood method. Under the assumption that successive observations are independent, the likelihood is given by

$$L_T(\theta) = \Pr\left(\mathbf{X}^{(T)} = \mathbf{x}^{(T)} \mid \theta\right) = \delta \mathbf{P}(x_1) \boldsymbol{\Gamma} \mathbf{P}(x_2) \cdots \boldsymbol{\Gamma} \mathbf{P}(x_T) \mathbf{1}, \quad (3)$$

where $\mathbf{P}(x)$ is a diagonal matrix with the state-dependent conditional densities $p_i(x) = \Pr(X_t = x | S_t = i)$, $i \in \{1, 2, \dots, m\}$, as entries. The conditional distribution of X_t may be either discrete or continuous, univariate or multivariate. In mixtures of continuous distributions, the likelihood can be unbounded in the vicinity of certain parameter combinations.²

The likelihood function of an HMM is in general a complicated function of the parameters with several local maxima. The two most popular approaches to maximizing the likelihood are direct numerical maximization and the Baum–Welch algorithm, a special case of the expectation–maximization (EM) algorithm (Cappé et al. 2005, Zucchini and MacDonald 2009). All discrete-time

²If the conditional distribution is normal, then the likelihood can be made arbitrarily large by setting the mean equal to one of the observations and letting the conditional variance tend to zero (Frühwirth-Schnatter 2006).

models are estimated using the R-package `hsmm` due to Bulla et al. (2010) that implements the EM algorithm in the version presented by Guédon (2003).

In an HMM, the sojourn times are implicitly assumed to be geometrically distributed:

$$\Pr(\text{'staying } t \text{ time steps in state } i') = \gamma_{ii}^{t-1} (1 - \gamma_{ii}). \quad (4)$$

The geometric distribution is memoryless, implying that the time until the next transition out of the current state is independent of the time spent in the state.

Hidden semi-Markov models

If the assumption of geometrically distributed sojourn times is unsuitable, then hidden semi-Markov models can be applied. HMMs and HSMMs differ only in the way that the state process is defined. In an HSMM, the sojourn-time distribution is modeled explicitly for each state i :

$$d_i(u) = \Pr(S_{t+u+1} \neq i, S_{t+u-v} = i, v = 0, \dots, u-2 | S_{t+1} = i, S_t \neq i) \quad (5)$$

and the transition probabilities are defined as

$$\gamma_{ij} = \Pr(S_{t+1} = j | S_{t+1} \neq i, S_t = i) \quad (6)$$

for each $i \neq j$ with $\gamma_{ii} = 0$ and $\sum_j \gamma_{ij} = 1$.

The conditional independence assumption for the observation process is similar to a simple HMM, but the semi-Markov chain associated with an HSMM does not have the Markov property at each time t . This property is transferred to the imbedded, first-order Markov chain—that is, the sequence of visited states (Bulla and Bulla 2006). In other words, the future states are only conditionally independent of the past states when the process changes state.

3 Hidden Markov models in continuous time

In a continuous-time Markov chain, transitions can occur at any time rather than at discrete and equidistant time points. There is no smallest time step and the quantities of interest are the transition probabilities

$$p_{ij}(\Delta t) = \Pr(S(t + \Delta t) = j | S(t) = i) \quad (7)$$

as $\Delta t \rightarrow 0$. Clearly, $p_{ij}(0) = 0$ for different states i and j , and it can be shown that under certain regularity conditions

$$\lim_{t \rightarrow 0} \mathbf{P}(t) = \mathbf{I}. \quad (8)$$

Assuming that $p_{ij}(\Delta t)$ is differentiable at 0, the transition rates are defined as

$$\begin{aligned} p'_{ij}(0) &= \lim_{\Delta t \rightarrow 0} \frac{p_{ij}(\Delta t) - p_{ij}(0)}{\Delta t} \\ &= \lim_{\Delta t \rightarrow 0} \frac{\Pr(S(t + \Delta t) = j | S(t) = i)}{\Delta t} \\ &= q_{ij} \end{aligned} \quad (9)$$

with the additional definition $q_{ii} = q_i = -\sum_{j \neq i} q_{ij}$. The transition intensity matrix $\mathbf{Q} = \{q_{ij}\}$ has nonnegative off-diagonal elements q_{ij} , nonpositive diagonal elements q_i , and all rows sum to zero.

The stationary distribution $\boldsymbol{\pi}$, if it exists, is found by solving the system of equations

$$\begin{cases} \boldsymbol{\pi} \mathbf{Q} = \mathbf{0} \\ \boldsymbol{\pi} \mathbf{1} = 1. \end{cases} \quad (10)$$

If it has a strictly positive solution (all elements in $\boldsymbol{\pi}$ are strictly positive), then the stationary distribution exists and is independent of the initial distribution.

The matrix of transition probabilities $\mathbf{P}(t) = \{p_{ij}(t)\}$ can be found as the solution to Kolmogorov's differential equation

$$\frac{d\mathbf{P}(t)}{dt} = \mathbf{P}(t) \mathbf{Q} \quad (11)$$

with the initial condition $\mathbf{P}(0) = \mathbf{I}$. The solution being

$$\mathbf{P}(t) = e^{\mathbf{Q}t} \mathbf{P}(0) = e^{\mathbf{Q}t}. \quad (12)$$

When the process enters state i , it remains there according to an exponential distribution with parameter $-q_i > 0$ before it instantly jumps to another state $j \neq i$ with probability $-q_{ij}/q_i$. A continuous-time Markov chain is fully characterized by its initial distribution $\boldsymbol{\delta}$ and the transition intensity matrix \mathbf{Q} .

It follows that the transition intensity matrix \mathbf{Q} can in principle be found by taking the logarithm of the one-step transition probability matrix

$$\mathbf{P}(t) = e^{\mathbf{Q}t} \Rightarrow \mathbf{Q} = \log \mathbf{P}(1). \quad (13)$$

Computing the logarithm of a matrix with many elements that are close to zero or zero is not a trivial operation. Instead, an intuitive estimate of the transition rate q_i can be based on the discrete transition probability γ_{ii} as

$$\tilde{q}_i = -\log \hat{\gamma}_{ii}. \quad (14)$$

This estimate does not take into account that the process might change from a given state and back within the sampling interval. Thus, this simple estimate

will underestimate q_i , but the error will be small for $q_i \ll 1$ (Madsen et al. 1985).

The exponential distribution is memoryless just like its discrete analogue, the geometric distribution. By introducing dummy states that are indistinguishable from one or more of the original states, it is possible to allow for nonexponentially-distributed sojourn times (see, e.g., Madsen et al. 1985, Iversen et al. 2013). The sojourn-time distribution will then be a mixture of exponential distributions, which is a phase-type distribution, and the Markov property will be transferred to the imbedded Markov chain, as for the HSMM. Phase-type distributions can be used to approximate any positive-valued distribution with arbitrary precision (see Nielsen 2013, for details). Similarly, Langrock and Zucchini (2011) showed how a discrete-time HMM can be structured to fit any sojourn-time distribution with arbitrary precision.

It is often convenient to assume that in a short time interval Δt , the only possible transitions are to the neighboring states:

$$\left. \begin{aligned} p_{ij} &= o(\Delta t), \quad |i - j| \geq 2, \\ p_{ii}(\Delta t) &= 1 - q_i \Delta t + o(\Delta t), \\ p_{i,i-1}(\Delta t) &= w_i q_i \Delta t + o(\Delta t), \\ p_{i,i+1}(\Delta t) &= (1 - w_i) q_i \Delta t + o(\Delta t), \\ i &\in \{1, 2, \dots, m\}, \end{aligned} \right\} \quad (15)$$

where $\lim_{\Delta t \rightarrow 0} \frac{o(\Delta t)}{\Delta t} = 0$. The notation includes transitions from state 1 to m and reverse with the definition that state 0 = state m and state $(m + 1)$ = state 1.

It should be noted that, even though, the process cannot go straight from state i to state $i + 2$ without going through state $i + 1$, there is no limit to how fast a transition from state i to state $i + 2$ can occur.

Under this assumption, the matrix of transition intensities has the structure

$$\mathbf{Q} = \begin{bmatrix} -q_1 & (1 - w_1) q_1 & 0 & \cdots & 0 & w_1 q_1 \\ w_2 q_2 & -q_2 & (1 - w_2) q_2 & \cdots & 0 & 0 \\ \vdots & \vdots & \vdots & \ddots & \vdots & \vdots \\ (1 - w_m) q_m & 0 & 0 & \cdots & w_m q_m & q_m \end{bmatrix}. \quad (16)$$

The number of parameters increases linearly with the number of states. Thus, a continuous-time Markov chain yields a parameter reduction over its discrete-time analogue if the number of states exceeds three. The higher the number of states, the larger the reduction. In addition, it is possible to incorporate

inhomogeneity without a dramatic increase in the number of parameters using splines, harmonic functions, or similar.³

Another advantage of a continuous-time formulation is the flexibility to use data with any sampling interval as the data is not assumed to be equidistantly sampled. In a discrete-time model, weekends and bank holidays are ignored so that the trading days are aggregated, meaning that Friday is followed by Monday in a normal week. Using a continuous-time model, it is possible to model the sampling times and thereby recognize that there is a longer time span between Friday and Monday. The so-called weekend effect in returns have been studied empirically for decades (see, e.g., French 1980, Rogalski 1984, Asai and McAleer 2007). There are two main effects, first that returns are higher on Fridays and lower on Mondays than on other days and secondly that the variance is larger on Fridays and lower on Mondays. There are several plausible explanations for this, but all of them are more complicated to model than just treating Saturdays and Sundays as missing observations. Below, the observations are assumed to be equidistantly sampled in order to facilitate a comparison to the discrete-time models using model selection criteria.

The continuous-time hidden Markov models (CTHMMs) are estimated using the R-package `msm` due to Jackson (2011) that is based on direct numerical maximization of the likelihood function.

4 Data

The data analyzed is daily log-returns of the S&P 500 and the FTSE 100 total return index covering the period from 23 July 1993 to 22 July 2013. The log-returns are calculated using $r_t = \log(P_t) - \log(P_{t-1})$, where P_t is the closing price of the index on day t and \log is the natural logarithm. The focus will be on the log-returns of the S&P 500 index as the analysis of the FTSE 100 index showed similar results. The results of the analysis of the FTSE returns can be found in appendix B.

The 5,040 log-returns of the S&P 500 index are shown in figure 1. The volatility is seen to form clusters as large price movements tend to be followed by large price movements and vice versa. Volatility clustering is a consequence of the persistence of the ACF of the squared returns (Cont 2001).

The first four moments of the daily log-returns are shown in table 2 together with approximate 95% confidence intervals based on bootstrapping 500,000 series of length 5,040 from the log-returns with replacement. The confidence intervals for the mean and skewness are very wide, whereas the estimates of the standard deviation and kurtosis are more certain. The distribution is left skew and

³See Iversen et al. (2013) for an example of the use of splines to reduce the number of parameters in an inhomogeneous Markov model.

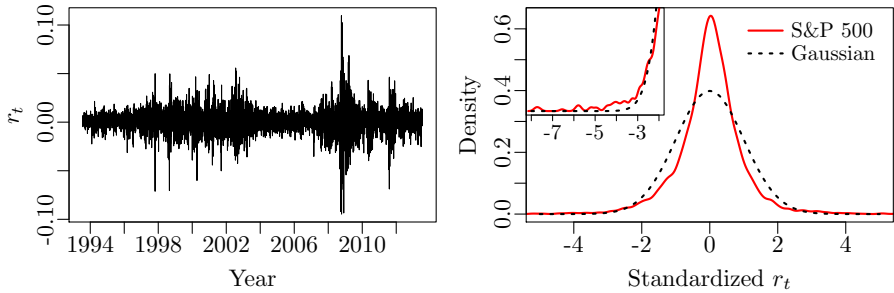


Figure 1: Daily log-returns of the S&P 500 total return index and a kernel estimate of the density of the standardized daily log-returns together with the density function for the standard normal distribution.

Mean	Std. deviation	Skewness	Kurtosis	<i>JB</i>
0.00034 [0.00001; 0.00068]	0.0121 [0.0116; 0.0127]	-0.24 [-0.75; 0.30]	11.3 [8.5; 14.1]	14372 [6356; 25803]

Table 2: First four moments of the S&P 500 log-returns and the Jarque–Bera test statistic together with bootstrapped 95% confidence intervals.

leptokurtic with an excess kurtosis of 8.3 compared to the normal distribution. The Jarque–Bera test statistic⁴ rejects the normal distribution at a 0.1% level of significance.

The excess kurtosis is evident from the plot of the density function in figure 1. There is too much mass centered right around the mean and in the tails compared to the normal distribution. There are 81 observations that deviate more than three standard deviations from the mean compared to an expectation of 14 if the returns were normally distributed.

Figure 3 shows the ACF of the absolute returns raised to different positive powers. It is a stylized fact that autocorrelations of positive powers of absolute returns are highest at power one. This is called the Taylor effect. The results generally agree with the Taylor effect although the effect is not clear-cut at the lowest lags.

5 Empirical results

The empirical autocorrelation function of the squared log-returns is shown in figure 4 together with ACFs of simulated squared returns from the fitted models.

⁴The Jarque–Bera test statistic is defined as $JB = T \left(\frac{\text{Skewness}^2}{6} + \frac{(\text{Kurtosis}-3)^2}{24} \right)$, where T is the number of observations.

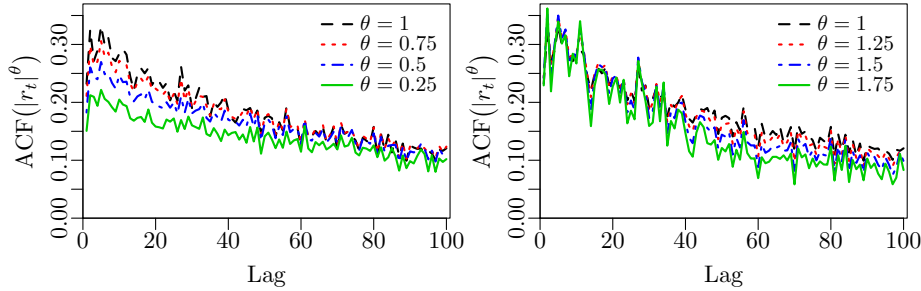


Figure 3: The empirical autocorrelation function of the absolute log-returns of the S&P 500 total return index raised to different positive powers.

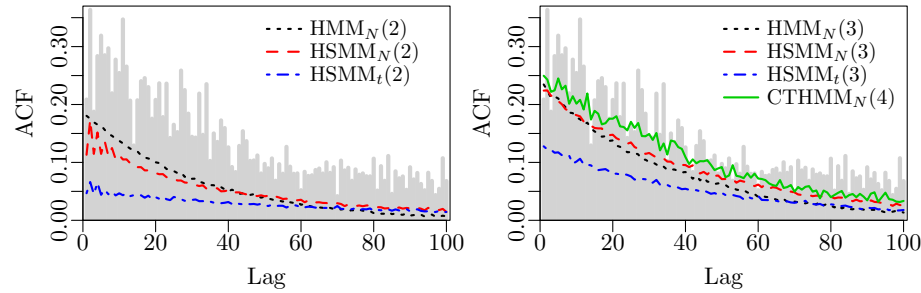


Figure 4: Empirical autocorrelation function of the squared log-returns at lag 1–100 together with simulated autocorrelation functions for the fitted models.

Of the two-state models, the HMM with normal conditional distributions is seen to be the best fit at the lowest lags, whereas the HSMM with normal conditional distributions is the best fit from lag 40 and upwards. The HSMM with t components is seen to be very persistent, but at too low of a level and it provides a poor fit overall.

As the HSMM with normal conditional distributions provides the best fit at the highest lags, this is also the model that best reproduces the stylized fact relating to the persistence of the ACF. This is true when looking at two-state models, as concluded by Bulla and Bulla (2006), but a much better fit can be obtained by increasing the number of states to three.

The HSMM with normal conditional distributions is also a better fit than the HMM when looking at the three-state models in figure 4, as the ACF for the HMM decays too fast. The ACF for the HSMM with conditional t distributions is again at too low of a level.

The fit of a CTHMM with three states with normal conditional distributions is similar to that of the three-state HMM. This appears from the mean squared

	Original data		Outlier-corrected data	
	MSE $\times 10^3$	WMSE $\times 10^3$	MSE $\times 10^3$	WMSE $\times 10^3$
HMM _N (2)	7.9	4.6	13.1	9.7
HSMM _N (2)	9.1	3.6	14.0	8.0
HSMM _t (2)	15.7	4.6	15.1	6.5
HMM _N (3)	4.4	3.2	6.1	6.7
HSMM _N (3)	3.3	2.0	4.1	4.2
HSMM _t (3)	9.2	3.4	5.1	4.0
CTHMM _N (3)	4.2	3.2	6.1	6.5
HMM _N (4)	4.0	2.2	3.4	3.3
HSMM _N (4)	2.4	1.0	1.8	2.0
HSMM _t (4)	3.4	1.1	1.4	1.2
CTHMM _N (4)	1.9	1.3	1.3	1.6

Table 5: Mean squared error and weighted mean squared error of the autocorrelation function of the squared returns and the outlier-corrected squared returns for the fitted models.

error and the weighted mean squared error of the ACF of the squared returns for the fitted models in table 5. The weighted mean squared error reweights the error at lag k by $0.95^{(100-k)}$ to increase the influence of higher-order lags following the approach by Bulla and Bulla (2006).

A CTHMM with four states with normal conditional distributions is seen to provide a better fit to the ACF of the squared returns than the three-state HSMM with normal conditional distributions. This observation is supported by the computed mean squared errors and weighted mean squared errors.

The first four moments of the log-returns are shown in table 6 together with the estimated moments for the fitted models based on 500,000 Monte Carlo simulations. Two states with normal conditional distributions are not enough to adequately capture the excess kurtosis of the log-returns. The two-state model with conditional t distributions is able to reproduce the excess kurtosis, but this model was not a good fit to the ACF.

The three-state models all provide a reasonable fit to the empirical moments. The kurtosis is still a little too low, with the exception of the HSMM with t components. The four-state models all provide a good fit to the empirical moments.

5.1 Correcting for outliers

Figure 7 shows the empirical ACF of the squared outlier-corrected log-returns together with the ACFs of the squared outlier-corrected simulated log-returns

Model	Mean	Std. dev.	Skewness	Kurtosis
r_t	0.00034 [0.00001; 0.00068]	0.0121 [0.0116; 0.0127]	-0.24 [-0.75; 0.30]	11.3 [8.5; 14.1]
HMM _N (2)	0.00034	0.0122	-0.17	5.6
HSMM _N (2)	0.00035	0.0121	-0.24	6.5
HSMM _t (2)	0.00042	0.0122	-0.14	12.0
HMM _N (3)	0.00036	0.0120	-0.18	8.2
HSMM _N (3)	0.00032	0.0121	-0.26	8.4
HSMM _t (3)	0.00037	0.0123	-0.19	14.0
CTHMM _N (3)	0.00025	0.0120	-0.20	8.7
HMM _N (4)	0.00033	0.0122	-0.34	10.3
HSMM _N (4)	0.00033	0.0122	-0.30	10.5
HSMM _t (4)	0.00035	0.0125	-0.33	11.5
CTHMM _N (4)	0.00037	0.0124	-0.30	10.7

Table 6: First four moments of the log-returns together with bootstrapped 95% confidence intervals and simulated moments for the fitted models.

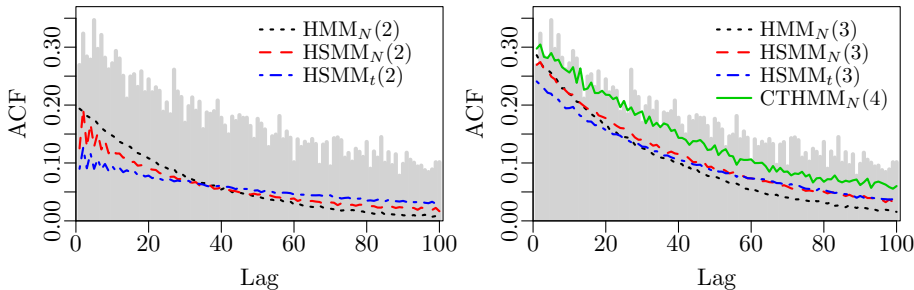


Figure 7: Empirical autocorrelation function of the squared outlier-corrected log-returns at lag 1–100 together with autocorrelation functions of the squared outlier-corrected simulated log-returns for the fitted models.

for the fitted models. Following the approach by Granger and Ding (1995a), values outside the interval $\bar{r}_t \pm 4\hat{\sigma}$ are set equal to the nearest boundary.

Restraining the impact of outliers reduces the amount of noise in the empirical ACF significantly. The noise reduction reveals a weekly variation that could suggest the need for an inhomogeneous, yet continuous, Markov model. The flexibility of a continuous-time model would be necessary to incorporate inhomogeneity without a dramatic increase in the number of parameters.

The conclusions regarding the fit of the different models to the empirical ACF are still valid when looking at the outlier-corrected returns. The outperformance of the HSMMs relative to the HMMs at the high lags is even more apparent

Model	No. of parameters	Log-lik	AIC	BIC
HMM _N (2)	7	15984	-31954	-31908
HSMM _N (2)	9	16062	-32107	-32048
HSMM _t (2)	11	16137	-32251	-32180
HMM _N (3)	14	16214	-32400	-32309
HSMM _N (3)	17	16227	-32419	-32308
HSMM _t (3)	20	16245	-32449	-32319
CTHMM _N (3)	13	16209	-32391	-32306
HMM _N (4)	23	16262	-32478	-32328
HSMM _N (4)	27	16273	-32492	-32316
HSMM _t (4)	31	16284	-32505	-32303
CTHMM _N (4)	19	16256	-32474	-32350

Table 8: Model selection based on the Akaike information criterion and the Bayesian information criterion.

when looking at the outlier-corrected data. What is also more apparent is the outperformance of the four-state CTHMM with normal conditional distributions relative to the three-state HSMMs. The ACF for the four-state CTHMM still decays too fast from lag 40 and onwards, but it clearly provides a better fit than the HSMMs with a similar number of parameters.

5.2 Model selection

Model selection involves both the choice of an appropriate number of states and the choice between competing state-dependent distributions. Likelihood-ratio tests cannot be applied to models with different numbers of states as these are not hierarchically nested. Instead, penalized likelihood criteria can be used to select the model that is estimated to be closest to the 'true' model, as suggested by Zucchini and MacDonald (2009). A disadvantage is that model selection criteria provide no information about the confidence in the selected model relative to others.

A four-state HSMM fits the data as well as the four-state CTHMM with normal conditional distributions, but it has 8 or 12 more parameters (see table 8). Therefore, the four-state CTHMM is preferred to both the three and the four-state HSMMs according to the Bayesian information criterion⁵. Akaike's information criterion⁶ selects the four-state HSMM with t components as it puts less emphasis on the number of parameters. However, various simulation studies have shown that AIC tends to select models with too many states (Bacci et al. 2014).

⁵The Bayesian information criterion is defined as $BIC = -2 \log L + p \log T$, where T is the number of observations and p is the number of parameters.

⁶The Akaike information criterion is defined as $AIC = -2 \log L + 2p$.

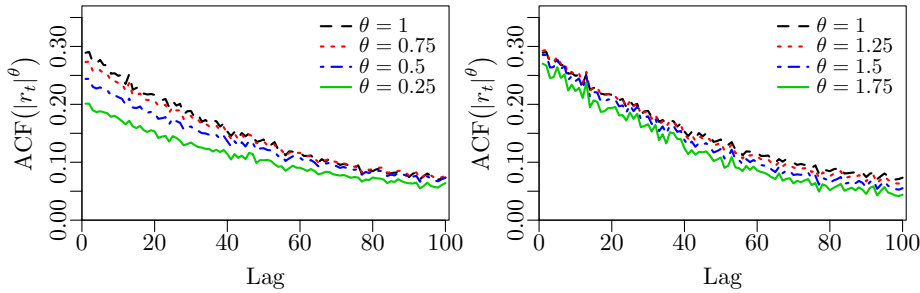


Figure 9: Autocorrelation function of the absolute value of 500,000 returns simulated from the estimated four-state CTHMM raised to different positive powers.

The parameter estimates are more uncertain the higher the number of states because of the quadratic increase in the number of parameters for the discrete-time models. Rydén et al. (1998) investigated HMMs with two and three states and found that the three-state models were “less similar to each other” and that “the estimation results seemed heavily dependent on outlying observations”. That was also the reason why Bulla and Bulla (2006) only considered HSMMs with two-states. There is a strong preference for models with fewer parameters as a four-state HSMM with over 30 parameters is likely to be overfitting the data.

It is problematic to fit a five-state CTHMM to the log-returns. The likelihood function appears to be highly multimodal and it is easy to find several local maxima by using different starting values. This indicates that the model is overfitting the data. It was not possible to find a five-state CTHMM with a lower BIC-value than the four-state CTHMM.

The ability of the four-state CTHMM to capture the Taylor effect is illustrated in figure 9. The ACF of the absolute value of 500,000 simulated returns raised to different positive powers is seen to be highest at power one.

6 Conclusion

HSMMs were found to be better at reproducing the slowly decaying ACF of squared daily returns of the S&P 500 and the FTSE 100 total return index than HMMs when looking at two and three-state models in agreement with the finding by Bulla and Bulla (2006). A much better fit to the slowly decaying ACF and the empirical moments was obtained by increasing the number of hidden states from two to three.

An extension to continuous time was presented and it was shown that a CTHMM with four states provides a better fit than the discrete-time models with three

states with a similar number of parameters and, even more so, after restraining the impact of outliers. There was no indication that the memoryless property of the sojourn-time distribution is inconsistent with the long-memory property of the squared returns.

Different models were preferred by the different selection criteria, but the four-state CTHMM with normal conditional distributions was selected by the Bayesian information criterion that was believed to be the most reliable. Finally, it was argued that the four-state CTHMM is preferred to the four-state HSMMs due to the significantly lower number of parameters resulting from the continuous-time formulation that makes the model less likely to be overfitting the data.

References

- Ang, A. and A. Timmermann. “Regime changes and financial markets.” *Annual Review of Financial Economics*, vol. 4, no. 1 (2012), pp. 313–337.
- Asai, M. and M. McAleer. “Non-trading day effects in asymmetric conditional and stochastic volatility models.” *Econometrics Journal*, vol. 10, no. 1 (2007), pp. 113–123.
- Bacci, S., S. Pandolfi, and F. Pennoni. “A comparison of some criteria for states selection in the latent Markov model for longitudinal data.” *Advances in Data Analysis and Classification*, vol. 8, no. 2 (2014), pp. 125–145.
- Bulla, J. “Hidden Markov models with t components. Increased persistence and other aspects.” *Quantitative Finance*, vol. 11, no. 3 (2011), pp. 459–475.
- Bulla, J. and I. Bulla. “Stylized facts of financial time series and hidden semi-Markov models.” *Computational Statistics & Data Analysis*, vol. 51, no. 4 (2006), pp. 2192–2209.
- Bulla, J., I. Bulla, and O. Nenadić. “hsmm—an R package for analyzing hidden semi-Markov models.” *Computational Statistics & Data Analysis*, vol. 54, no. 3 (2010), pp. 611–619.
- Cappé, O., E. Moulines, and T. Rydén. *Inference in Hidden Markov Models*. Springer: New York (2005).
- Cont, R. “Empirical properties of asset returns: stylized facts and statistical issues.” *Quantitative Finance*, vol. 1, no. 2 (2001), pp. 223–236.
- French, K. R. “Stock returns and the weekend effect.” *Journal of Financial Economics*, vol. 8, no. 1 (1980), pp. 55–69.
- Frühwirth-Schnatter, S. *Finite Mixture and Markov Switching Models*. Springer: New York (2006).

- Granger, C. W. J. and Z. Ding. "Some properties of absolute return: An alternative measure of risk." *Annales D'Economie Et Statistique*, vol. 40 (1995a), pp. 67–92.
- Granger, C. W. J. and Z. Ding. "Stylized facts on the temporal and distributional properties of daily data from speculative markets." Unpublished paper, Department of Economics, University of California, San Diego (1995b).
- Granger, C. W. J., S. Spear, and Z. Ding. "Stylized facts on the temporal and distributional properties of absolute returns: An update." In *Proceedings of the Hong Kong International Workshop on Statistics in Finance*. Imperial College Press: London (2000), pp. 97–120.
- Guédon, Y. "Estimating hidden semi-Markov chains from discrete sequences." *Journal of Computational and Graphical Statistics*, vol. 12, no. 3 (2003), pp. 604–639.
- Iversen, E. B., J. K. Møller, J. M. Morales, and H. Madsen. "Inhomogeneous Markov models for describing driving patterns." IMM-Technical Report-2013 02, Technical University of Denmark (2013).
- Jackson, C. H. "Multi-state models for panel data: The msm package for R." *Journal of Statistical Software*, vol. 38, no. 8 (2011), pp. 1–29.
- Langrock, R. and W. Zucchini. "Hidden Markov models with arbitrary state dwell-time distributions." *Computational Statistics & Data Analysis*, vol. 55, no. 1 (2011), pp. 715–724.
- Madsen, H., H. Spliid, and P. Thyregod. "Markov models in discrete and continuous time for hourly observations of cloud cover." *Journal of Climate and Applied Meteorology*, vol. 24, no. 7 (1985), pp. 629–639.
- Malmsten, H. and T. Teräsvirta. "Stylized facts of financial time series and three popular models of volatility." *European Journal of Pure and Applied Mathematics*, vol. 3, no. 3 (2010), pp. 443–477.
- Nielsen, B. F. *Matrix Analytic Methods in Applied Probability with a View towards Engineering Applications*. Doctoral thesis, Technical University of Denmark (2013).
- Rogalski, R. J. "New findings regarding day-of-the-week returns over trading and non-trading periods: A note." *Journal of Finance*, vol. 39, no. 5 (1984), pp. 1603–1614.
- Rydén, T., T. Teräsvirta, and S. Åsbrink. "Stylized facts of daily return series and the hidden Markov model." *Journal of Applied Econometrics*, vol. 13, no. 3 (1998), pp. 217–244.

Silvestrov, D. and F. Stenberg. “A pricing process with stochastic volatility controlled by a semi-Markov process.” *Communications in Statistics-Theory and Methods*, vol. 33, no. 3 (2004), pp. 591–608.

Zucchini, W. and I. L. MacDonald. *Hidden Markov Models for Time Series: An Introduction Using R*. Chapman & Hall: London, 2nd ed. (2009).

A Parameter estimates

m	Γ			$\mu \times 10^4$	$\sigma^2 \times 10^4$	δ
2	0.990	0.010		8.3	0.52	1.0
		(0.002)		(1.1)	(0.01)	(0.2)
	0.021	0.979		-6.9	3.47	0.0
		(0.004)		(4.9)	(0.14)	
3	0.982	0.018	0.000	10.1	0.32	1.0
		(0.004)	(0.001)	(1.3)	(0.01)	(0.1)
	0.015	0.978	0.006	0.5	1.28	0.0
	(0.003)		(0.002)	(2.5)	(0.04)	(0.1)
4	0.000	0.030	0.970	-12.4	7.08	0.0
	(0.003)	(0.010)		(12.8)	(0.50)	
	0.979	0.021	0.000	10.8	0.29	1.0
	(0.005)	(0.006)	(0.00)	(1.5)	(0.01)	(0.2)
4	0.020	0.970	0.009	3.3	0.96	0.0
	(0.005)		(0.003)	(0.001)	(0.05)	(0.2)
	0.000	0.017	0.976	-2.9	2.39	0.0
	(0.000)	(0.006)		(5.7)	(0.14)	(0.1)
	0.000	0.000	0.049	-29.9	12.16	0.0
	(0.000)	(0.002)	(0.026)	(31.2)	(1.73)	

Table 10: Parameter estimates for the fitted m -state HMMs with normal conditional distributions together with bootstrapped standard errors based on 250 simulations of the model.

m	Γ		$1 - p$	$r \times 10$	$\mu \times 10^4$	$\sigma^2 \times 10^4$	δ
2	0	1		0.994 (0.002)	0.4 (0.1)	9.0 (1.3)	0.48 (0.01)
	1	0		0.975 (0.010)	0.5 (0.2)	-10.8 (5.7)	4.00 (0.18)
	0	1.000 (0.000)	0.000	0.993 (0.003)	0.3 (0.1)	10.5 (1.3)	0.31 (0.01)
3	0.972 (0.013)	0	0.028	0.945 (0.037)	1.7 (1.7)	-1.0 (3.0)	1.51 (0.07)
	0.000 (0.000)	1.000 (0.000)	0	0.983 (0.052)	5.5 (33.0)	-14.3 (12.7)	7.26 (0.54)
	0 (0.022)	1.000 (0.020)	0.000	0.985 (0.006)	0.5 (0.5)	11.6 (1.4)	0.25 (0.01)
4	0.970 (0.022)	0	0.022 (0.020)	0.965 (0.024)	1.0 (0.7)	2.1 (2.8)	1.05 (0.06)
	0.000 (0.000)	0.675 (0.161)	0	0.325 (0.124)	31.2 (124.8)	-2.4 (5.2)	2.38 (0.17)
	0.000 (0.000)	0.000 (0.000)	1.000 (0.000)	0	0.977 (0.098)	-30.6 (68.9)	11.81 (2.26)

Table 11: Parameter estimates for the fitted m -state HSMMs with normal conditional distributions together with bootstrapped standard errors based on 250 simulations of the model. p and r are the parameters of the negative binomial sojourn-time distribution.

m	Γ		$1 - p$	$r \times 10$	$\mu \times 10^4$	$\sigma^2 \times 10^4$	t	δ
2	0	1		0.997 (0.002)	0.2 (0.1)	9.5 (1.2)	0.34 (0.02)	7.2 (1.2)
	1	0		0.984 (0.008)	0.5 (0.2)	-6.0 (4.8)	2.10 (0.17)	5.6 (1.0)
	0 (0.042)	1.000 (0.009)	0.000	0.990 (0.009)	7.4 (7.8)	10.5 (1.1)	0.25 (0.01)	6.7 (1.4)
3	0.630 (0.144)	0	0.370	0.979 (0.047)	10.5 (22.2)	1.3 (2.7)	1.16 (0.07)	22.4 (467.9)
	0.000 (0.045)	1.000 (0.055)	0	0.983 (0.055)	5.2 (28.5)	-12.2 (13.1)	4.96 (0.75)	7.2 (7.4)
	0 (0.000)	1.000 (0.000)	0.000	0.987 (0.013)	8.9 (10.2)	10.6 (1.4)	0.23 (0.01)	6.8 (1.5)
4	0.610 (0.103)	0	0.296 (0.106)	0.957 (0.052)	18.6 (34.2)	4.1 (2.2)	0.86 (0.05)	24.8 (16.4)
	0.000 (0.000)	0.724 (0.148)	0	0.276 (0.115)	34.3 (115.9)	-1.9 (5.2)	2.22 (0.16)	49.0 (98.2)
	0.000 (0.000)	0.000 (0.000)	1.000 (0.110)	0	0.981 (61.9)	3.9 (31.6)	-29.3 (2.44)	13.8 (11968)

Table 12: Parameter estimates for the fitted m -state HSMMs with Student t conditional distributions together with bootstrapped standard errors based on 250 simulations of the model. p and r are the parameters of the negative binomial sojourn-time distribution and t is the degrees of freedom for the conditional t distributions.

m	\mathbf{Q}			$\mu \times 10^4$	$\sigma^2 \times 10^4$	δ
3	-0.014 (0.003)	0.014 (0.003)	0 (0.003)	0 0.020	10.6 (1.4) 0.8 (2.5)	0.32 (0.01) 1.29 (0.03)
	0 0.048 (0.019)	-0.020 0 (0.003)	0.020 -0.068	0 0.020	0.8 0.8	0.0 0.0
	0.005 (0.003)	0.019 (0.003)	0 (0.003)	-0.024 -0.024	-14.6 (12.1)	7.12 (0.26)
	-0.018 (0.005)	0.017 (0.005)	0 (0.002)	0.001 0.005	11.1 (1.6) 3.6 (2.6)	0.29 (0.01) 0.95 (0.03)
	0.015 (0.004)	-0.020 0 (0.003)	0.005 -0.015	0 0.005	-3.2 (5.2)	0.0 0.0
	0.005 (0.005)	0 (0.013)	0.029 (0.013)	-0.034 -0.034	-29.2 (25.9)	12.29 (0.82)

Table 13: Parameter estimates for the fitted m -state CTHMMs with normal conditional distributions together with approximate standard errors based on the Hessian. The three-state model has a dummy state as the second and the third state are indistinguishable. No standard errors are given for the initial distributions as the Hessian is unreliable for this purpose.

B FTSE results

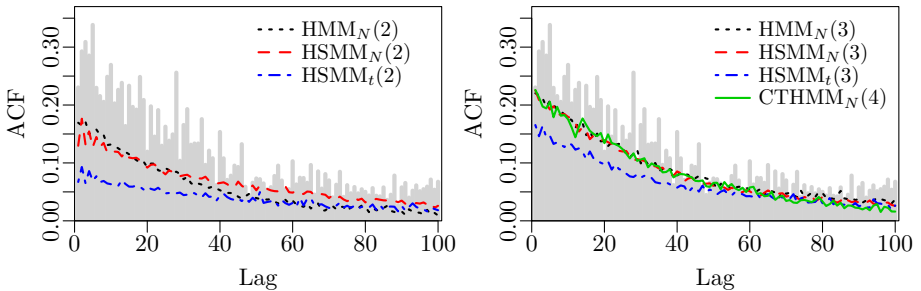


Figure 14: Empirical autocorrelation function of the squared FTSE 100 log-returns at lag 1–100 together with simulated autocorrelation functions for the fitted models.

Model	Mean	Std. dev.	Skewness	Kurtosis
r_t	0.00031 [-0.00002; 0.00063]	0.0118 [0.0113; 0.0123]	-0.16 [-0.56; 0.24]	8.9 [7.0; 10.9]
HMM _N (2)	0.00026	0.0119	-0.16	5.4
HSMM _N (2)	0.00032	0.0115	-0.18	6.0
HSMM _t (2)	0.00038	0.0116	-0.19	8.5
HMM _N (3)	0.00028	0.0116	-0.21	7.2
HSMM _N (3)	0.00026	0.0118	-0.23	7.1
HSMM _t (3)	0.00037	0.0118	-0.15	9.1
CTHMM _N (4)	0.00026	0.0123	-0.33	8.0

Table 15: First four moments of the FTSE 100 log-returns together with bootstrapped 95% confidence intervals and simulated moments for the fitted models.

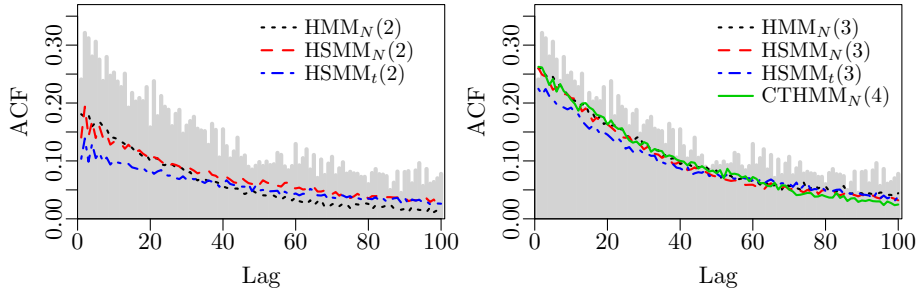


Figure 16: Empirical autocorrelation function of the squared outlier-corrected FTSE 100 log-returns at lag 1–100 together with autocorrelation functions of the squared outlier-corrected simulated log-returns for the fitted models.

Model	No. of parameters	Log-lik	AIC	BIC
HMM _N (2)	7	16054	-32093	-32047
HSMM _N (2)	9	16093	-32167	-32108
HSMM _t (2)	11	16125	-32227	-32156
HMM _N (3)	14	16220	-32413	-32321
HSMM _N (3)	17	16224	-32414	-32303
HSMM _t (3)	20	16235	-32429	-32299
CTHMM _N (4)	19	16252	-32466	-32342

Table 17: Model selection based on the Akaike information criterion and the Bayesian information criterion.

PAPER **B**

Originally published in the *Journal of Forecasting*

Long memory of financial time series and hidden Markov models with time-varying parameters

Peter Nystrup, Henrik Madsen, and Erik Lindström

Abstract

Hidden Markov models are often used to model daily returns and to infer the hidden state of financial markets. Previous studies have found that the estimated models change over time, but the implications of the time-varying behavior have not been thoroughly examined. This paper presents an adaptive estimation approach that allows for the parameters of the estimated models to be time varying. It is shown that a two-state Gaussian hidden Markov model with time-varying parameters is able to reproduce the long memory of squared daily returns that was previously believed to be the most difficult fact to reproduce with a hidden Markov model. Capturing the time-varying behavior of the parameters also leads to improved one-step density forecasts. Finally, it is shown that the forecasting performance of the estimated models can be further improved using local smoothing to forecast the parameter variations.

Keywords: Hidden Markov models; Daily returns; Long memory; Adaptive estimation; Time-varying parameters.

1 Introduction

Many different stylized facts have been established for financial returns (see, e.g., Granger and Ding 1995a,b, Granger et al. 2000, Cont 2001, Malmsten and Teräsvirta 2010). Rydén et al. (1998) showed the ability of a hidden Markov model (HMM) to reproduce most of the stylized facts of daily return series introduced by Granger and Ding (1995a,b). In an HMM, the distribution that generates an observation depends on the state of an unobserved Markov chain. Rydén et al. (1998) found that the one stylized fact that could not be reproduced by an HMM was the slow decay of the autocorrelation function (ACF) of squared and absolute daily returns, which is of great importance in financial risk management. The daily returns do not have the long-memory property themselves, only their squared and absolute values do. Rydén et al. (1998) considered this stylized fact to be the most difficult to reproduce with an HMM.

According to Bulla and Bulla (2006), the lack of flexibility of an HMM to model this temporal higher-order dependence can be explained by the implicit assumption of geometrically distributed sojourn times in the hidden states. This led them to consider hidden semi-Markov models (HSMMs) in which the sojourn-time distribution is modeled explicitly for each hidden state so that the Markov property is transferred to the imbedded first-order Markov chain. They found that an HSMM with negative-binomially distributed sojourn times was better than the HMM at reproducing the long-memory property of squared daily returns.

Bulla (2011) later showed that HMMs with t -distributed components reproduce most of the stylized facts as well or better than the Gaussian HMM at the same time as increasing the persistence of the visited states and the robustness to outliers. Bulla (2011) also found that models with three states provide a better fit than models with two states. In Nystrup et al. (2015b), an extension to continuous time was presented and it was shown that a continuous-time Gaussian HMM with four states provides a better fit than discrete-time models with three states with a similar number of parameters.

The data analyzed in this paper is daily returns of the S&P 500 stock index from 1928 to 2014. It is the same time series that was studied in the majority of the above-mentioned studies, just extended through the end of 2014. Granger and Ding (1995a) divided the full sample into ten subsamples of 1,700 observations, corresponding to a little less than seven years, as they believed it was likely that with such a long time span there could have been structural shifts in the data-generating process. Using the same approach, Rydén et al. (1998) and Bulla (2011) found that the estimated HMMs, including the number of states and the type of conditional distributions, changed considerably between the subsamples.

HMMs are popular for inferring the hidden state of financial markets and several studies have shown the profitability of dynamic asset allocation strategies based on this class of models (see, e.g., Bulla et al. 2011, Nystrup et al. 2015a). The profitability of those strategies is directly related to the persistence of the volatility. Therefore, it is relevant to explore in depth the importance of the time-varying behavior for the models' ability to reproduce the long memory and forecast future returns. Failure to account for the time-varying behavior of the estimated models is likely part of the reason why regime-switching models often get outperformed by a simple random walk model when used for out-of-sample forecasting, as discussed by Dacco and Satchell (1999).

In this paper, an adaptive estimation approach that allows for the parameters of the estimated models to be changing over time is presented as an alternative to fixed-length forgetting. After all, it is unlikely that the parameters change after exactly 1,700 observations. The time variation is observation driven based on the score function of the predictive likelihood function, which is related to the generalized autoregressive score (GAS) model of Creal et al. (2013).

In agreement with the findings by Rydén et al. (1998) and Bulla (2011), the parameters of the estimated models are found to vary significantly throughout the data period. As a consequence of the time-varying transition probabilities, the sojourn-time distribution is not the memoryless geometric distribution. A two-state Gaussian HMM with time-varying parameters is shown to reproduce the long memory of the squared daily returns. Faster adaption to the parameter changes improves both the fit to the ACF of the squared returns and the one-step density forecasts. Using local smoothing to forecast the parameter variations, it is possible to further improve the density forecasts. Finally, the need for a third state or a conditional t -distribution in the high-variance state to capture the full extent of excess kurtosis is discussed in light of the nonstationary behavior of the estimated models.

Section 2 gives an introduction to the HMM. Section 3 discusses the relation between long memory and regime switching. In section 4, a method for adaptive parameter estimation is outlined. Section 5 contains a description of the data. The results are presented in section 6 and section 7 concludes.

2 The hidden Markov model

In a hidden Markov model, the probability distribution that generates an observation depends on the state of an underlying and unobserved Markov process. An HMM is a particular kind of dependent mixture and is therefore also referred to as a Markov-switching mixture model. General references to the subject include Cappé et al. (2005), Frühwirth-Schnatter (2006), and Zucchini and MacDonald (2009).

A sequence of discrete random variables $\{S_t : t \in \mathbb{N}\}$ is said to be a first-order Markov chain if, for all $t \in \mathbb{N}$, it satisfies the Markov property:

$$\Pr(S_{t+1} | S_t, \dots, S_1) = \Pr(S_{t+1} | S_t). \quad (1)$$

The conditional probabilities $\Pr(S_{u+t} = j | S_u = i) = \gamma_{ij}(t)$ are called transition probabilities. The Markov chain is said to be homogeneous if the transition probabilities are independent of u , and inhomogeneous otherwise.

If the Markov chain $\{S_t\}$ has m states, then the bivariate stochastic process $\{(S_t, X_t)\}$ is called an m -state HMM. With $\mathbf{S}^{(t)}$ and $\mathbf{X}^{(t)}$ representing the values from time 1 to time t , the simplest model of this kind can be summarized by

$$\Pr(S_t | \mathbf{S}^{(t-1)}) = \Pr(S_t | S_{t-1}), \quad t = 2, 3, \dots, \quad (2a)$$

$$\Pr(X_t | \mathbf{X}^{(t-1)}, \mathbf{S}^{(t)}) = \Pr(X_t | S_t), \quad t \in \mathbb{N}. \quad (2b)$$

Hence, when the current state S_t is known, the distribution of X_t depends only on S_t . This causes the autocorrelation of $\{X_t\}$ to be strongly dependent on the persistence of $\{S_t\}$.

An HMM is a state-space model with finite state space, where (2a) is the state equation and (2b) is the observation equation. A specific observation can usually arise from more than one state as the support of the conditional distributions overlaps. Therefore, the unobserved state process $\{S_t\}$ is not directly observable through the observation process $\{X_t\}$, but can only be estimated.

As an example, consider the two-state model with Gaussian conditional densities:

$$X_t = \mu_{S_t} + \varepsilon_{S_t}, \quad \varepsilon_{S_t} \sim N(0, \sigma_{S_t}^2),$$

where

$$\begin{aligned}\mu_{S_t} &= \begin{cases} \mu_1, & \text{if } S_t = 1, \\ \mu_2, & \text{if } S_t = 2, \end{cases} \\ \sigma_{S_t}^2 &= \begin{cases} \sigma_1^2, & \text{if } S_t = 1, \\ \sigma_2^2, & \text{if } S_t = 2, \end{cases}\end{aligned}$$

and

$$\boldsymbol{\Gamma} = \begin{bmatrix} 1 - \gamma_{12} & \gamma_{12} \\ \gamma_{21} & 1 - \gamma_{21} \end{bmatrix}.$$

For this model, the value of the autocorrelation function at lag k is

$$\rho_{X_t}(k|\theta) = \frac{\pi_1(1-\pi_1)(\mu_1 - \mu_2)^2}{\sigma^2} \lambda^k \quad (3)$$

and the autocorrelation function for the squared process is

$$\rho_{X_t^2}(k|\theta) = \frac{\pi_1(1-\pi_1)(\mu_1^2 - \mu_2^2 + \sigma_1^2 - \sigma_2^2)^2}{E[X_t^4|\theta] - E[X_t^2|\theta]^2} \lambda^k, \quad (4)$$

where π_1 is the stationary probability of state one and $\lambda = \gamma_{11} + \gamma_{22} - 1$ is the second largest eigenvalue of $\boldsymbol{\Gamma}$ (Frühwirth-Schnatter 2006).¹ It is evident from these expressions, as noted by Rydén et al. (1998), that an HMM with constant parameters can only reproduce an exponentially-decaying autocorrelation structure. The ACF of the first-order process becomes zero if the mean values are equal whereas persistence in the squared process can be induced either by a difference in the means or by a difference in the variances. In both cases the persistence increases with the combined persistence of the states as measured by λ .

¹The other eigenvalue of $\boldsymbol{\Gamma}$ is $\lambda = 1$.

The sojourn times are implicitly assumed to be geometrically distributed:

$$\Pr(\text{'staying } t \text{ time steps in state } i) = \gamma_{ii}^{t-1} (1 - \gamma_{ii}). \quad (5)$$

The geometric distribution is memoryless, implying that the time until the next transition out of the current state is independent of the time spent in the state.

Langrock and Zucchini (2011) showed how an HMM can be structured to fit any sojourn-time distribution with arbitrary precision by mapping multiple latent states to the same output state. The distribution of sojourn times is then a mixture of geometric distributions, which is a phase-type distribution, and the Markov property is transferred to the imbedded Markov chain as in an HSMM.² Phase-type distributions can be used to approximate any positive-valued distribution with arbitrary precision (Nielsen 2013). Similarly, time-varying transition probabilities will lead to nongeometrically distributed sojourn times. Thus, an estimation approach that allows the transition probabilities to be changing over time has the flexibility to fit sojourn-time distributions other than the geometric.

3 Long memory and regime switching

Granger and Teräsvirta (1999) and Gourieroux and Jasiak (2001) showed how simple nonlinear time series models with infrequent regime switching can generate a long-memory effect in the autocorrelation function. Around the same time, Diebold and Inoue (2001) showed analytically how stochastic regime switching is easily confused with long memory. They specifically showed that under the assumption that the persistence of the states converges to one as a function of the sample size, the variances of partial sums of a Markov-switching process will match those of a fractionally integrated process. This led Baek et al. (2014) to question the relevance of the HMM for long memory as they found common estimators of the long-memory parameter to be extremely biased when applied to data generated by the Markov-switching model of Diebold and Inoue (2001). Baek et al. (2014) argued that the HMM should be viewed as a short-memory model with some long-memory features rather than a long-memory model.

Gourieroux and Jasiak (2001) emphasized that the distinction between a short-memory model with long-memory features and a long-memory model has important practical implications, for example, when the model is used for making predictions. If a fractional model is retained, the predictions should be based on a long history of the observed series. If, on the other hand, a short-memory

²In an HSMM, the sojourn-time distribution is modeled explicitly for each state. The conditional independence assumption for the observation process is similar to a simple HMM, but the Markov property is transferred to the imbedded first-order Markov chain—that is, the sequence of visited states (Bulla and Bulla 2006).

(regime-switching) model with long-memory features is selected, then the predictions should be based on only the most recent observations.

Several studies have documented how structural changes in the unconditional variance can cause long-range dependence in the volatility and integrated generalized autoregressive conditional heteroskedasticity (GARCH) effects (see, e.g., Mikosch and Stărică 2004, and references therein). The GARCH model of Engle (1982) and Bollerslev (1986) has been extended in various ways since its introduction in an effort to capture long-range dependencies in economic time series (see, e.g., Baillie et al. 1996, Bauwens et al. 2014). Stărică and Granger (2005) identified intervals of homogeneity where the nonstationary behavior of the S&P 500 series can be approximated by a stationary model. They found that the most appropriate is a simple model with no linear dependence but with significant changes in the mean and variance of the time series. On the intervals of homogeneity, the data is approximately a white noise process. Their results indicate the time-varying unconditional variance as the main source of nonstationarity in the S&P 500 series.

Calvet and Fisher (2004) showed that a multifrequency regime-switching model is able to generate substantial outliers and capture both the low-frequency regime shifts that cause abrupt volatility changes and the smooth autoregressive volatility transitions at mid-range frequencies without including GARCH components or heavy-tailed conditional distributions. The multifrequency regime-switching model reproduces the long memory of the volatility by having a component with a duration of the same order as the sample size. With two possible values for the volatility the number of states increases at the rate 2^f , where f is the number of switching frequencies. Thus there are over 1,000 states when $f = 10$.

It was already known that a Markov chain with a countably-infinite state space can have the long-memory property (see Granger and Teräsvirta 1999, and references therein). The model proposed in this paper is much simpler and, consequently, less likely to be overfitted out of sample or in an on-line application like adaptive forecasting. The model is a simple Gaussian HMM with parameters that are time varying in a nonparametric way. This approach, in principle, allows for an infinite number of states, but the number of parameters that has to be estimated remains unchanged compared to an HMM with constant parameters. The time variation is observation driven based on the score function of the predictive model density. This is similar to the GAS model of Creal et al. (2013), but the time variation is not limited to the transition probabilities as in the study by Bazzi et al. (2017).

4 Adaptive parameter estimation

The parameters of an HMM are often estimated using the maximum-likelihood (ML) method. The likelihood function of an HMM is, in general, a complicated function of the parameters with several local maxima and in mixtures of continuous distributions the likelihood can be unbounded in the vicinity of certain parameter combinations.³ The two most popular approaches to maximizing the likelihood are direct numerical maximization and the Baum–Welch algorithm, a special case of the expectation–maximization (EM) algorithm (Baum et al. 1970, Dempster et al. 1977).

When maximizing the likelihood, every observation is usually assumed to be of equal importance no matter how long the sample period is. This approach works well when the sample period is short and the underlying process does not change over time. The time-varying behavior of the parameters documented in previous studies (Rydén et al. 1998, Bulla 2011), however, calls for an adaptive approach that assigns more weight to the most recent observations while keeping in mind past patterns at a reduced confidence.

As pointed out by Cappé et al. (2005), it is possible to evaluate derivatives of the likelihood function with respect to the parameters for virtually any model that the EM algorithm can be applied to. This is, for example, true when the standard (Cramer-type) regularity conditions for the ML estimator hold because the maximizing quantities in the M-step are derived based on the derivatives of the likelihood function. As a consequence, instead of resorting to a specific algorithm such as the EM algorithm, the likelihood can be maximized using gradient-based optimization methods. Lystig and Hughes (2002) described an algorithm for exact computation of the score vector and the observed information matrix in HMMs that can be performed in a single pass through the data. The algorithm was derived from the forward–backward algorithm.

The reason for exploring gradient-based methods is the flexibility to make the estimator recursive and adaptive.⁴ The estimation of the parameters through a maximization of the conditional log-likelihood function can be done recursively using the estimator

$$\hat{\theta}_t = \arg \max_{\theta} \sum_{n=1}^t w_n \log \Pr \left(X_n \mid \mathbf{X}^{(n-1)}, \theta \right) = \arg \max_{\theta} \tilde{\ell}_t(\theta) \quad (6)$$

with $w_n = 1$. The recursive estimator can be made adaptive by introducing a different weighting. A popular choice is to use exponential weights $w_n = \lambda^{t-n}$,

³If, for example, the conditional distribution is Gaussian then the likelihood can be made arbitrarily large by setting the mean equal to one of the observations and letting the conditional variance tend to zero (Frühwirth-Schnatter 2006).

⁴See Khreich et al. (2012) for a survey of techniques for incremental learning of HMM parameters.

where $0 < \lambda < 1$ is the forgetting factor (Madsen 2008). The speed of adaption is then determined by the effective memory length

$$N_{\text{eff}} = \frac{1}{1 - \lambda}. \quad (7)$$

Maximizing the second-order Taylor expansion of $\tilde{\ell}_t(\theta)$ around $\hat{\theta}_{t-1}$ with respect to θ and defining the solution as the estimator $\hat{\theta}_t$ leads to

$$\hat{\theta}_t = \hat{\theta}_{t-1} - \left[\nabla_{\theta\theta} \tilde{\ell}_t(\hat{\theta}_{t-1}) \right]^{-1} \nabla_{\theta} \tilde{\ell}_t(\hat{\theta}_{t-1}). \quad (8)$$

This is equivalent to a specific case of the GAS model of Creal et al. (2013). Using the estimator (8) it is possible to reach quadratic convergence whereas the GAS model in general converges only linearly (see Cappé et al. 2005).

For HMMs, the score function must consider the previous observations and cannot reasonably be approximated by the score function of the latest observation, as it is often done for other models (Khreich et al. 2012). In order to compute the weighted score function the algorithm of Lystig and Hughes (2002) has to be run for each iteration and the contribution of each observation has to be weighted. Experimentation suggests that with an effective memory length of 250 observations, it is necessary to compute the contribution of the last 2,500 observations to get a satisfactory approximation of the weighted score function. This leads to a significant increase in computational complexity.

Approximating the Hessian by

$$\begin{aligned} \nabla_{\theta\theta} \tilde{\ell}_t(\hat{\theta}_{t-1}) &= \nabla_{\theta\theta} \sum_{n=1}^t \lambda^{t-n} \log \Pr(X_n \mid \mathbf{X}^{(n-1)}, \hat{\theta}_{t-1}) \\ &= \sum_{n=1}^t \lambda^{t-n} \nabla_{\theta\theta} \log \Pr(X_n \mid \mathbf{X}^{(n-1)}, \hat{\theta}_{t-1}) \\ &\approx \sum_{n=1}^t \lambda^{t-n} (-I_t(\hat{\theta}_{t-1})) \\ &= \frac{1 - \lambda^t}{1 - \lambda} (-I_t(\hat{\theta}_{t-1})), \end{aligned} \quad (9)$$

leads to the recursive, adaptive estimator

$$\hat{\theta}_t \approx \hat{\theta}_{t-1} + \frac{A}{\min(t, N_{\text{eff}})} \left[I_t(\hat{\theta}_{t-1}) \right]^{-1} \nabla_{\theta} \tilde{\ell}_t(\hat{\theta}_{t-1}), \quad (10)$$

where the tuning constant A can be adjusted to increase or decrease the speed of convergence without changing the effective memory length. In order to improve

for clarity, the fraction $\frac{1-\lambda}{1-\lambda^t}$ was replaced by $\frac{1}{\min(t, N_{\text{eff}})}$, where N_{eff} is the effective memory length (7). The two fractions share the property that they decrease toward a constant when t increases. It is necessary to apply a transformation to all constrained parameters for the estimator (10) to converge. Further, in order to avoid very large initial steps, it is often advisable to start the estimation at a $t_0 > 0$.

The Fisher information can be updated recursively using the identity $E[\nabla_{\theta\theta}\ell_t] = -E[\nabla_{\theta}\ell_t \nabla_{\theta}\ell_t']$:

$$\begin{aligned} I_t(\hat{\theta}) &= -\frac{1}{t} \sum_{n=1}^t \nabla_{\theta}\ell_n(\hat{\theta}) \nabla_{\theta}\ell_n(\hat{\theta})' \\ &= -\frac{t-1}{t} \frac{1}{t-1} \left\{ \sum_{n=1}^{t-1} \nabla_{\theta}\ell_n(\hat{\theta}) \nabla_{\theta}\ell_n(\hat{\theta})' \right. \\ &\quad \left. + \nabla_{\theta} \log \Pr(X_t | \mathbf{X}^{(t-1)}, \hat{\theta}) \nabla_{\theta} \log \Pr(X_t | \mathbf{X}^{(t-1)}, \hat{\theta})' \right\} \quad (11) \\ &= I_{t-1}(\hat{\theta}) + \frac{1}{t} \left[\nabla_{\theta} \log \Pr(X_t | \mathbf{X}^{(t-1)}, \hat{\theta}) \right. \\ &\quad \left. \cdot \nabla_{\theta} \log \Pr(X_t | \mathbf{X}^{(t-1)}, \hat{\theta})' - I_{t-1}(\hat{\theta}) \right]. \end{aligned}$$

Further, the matrix inversion lemma is applicable, since the estimator (10) only makes use of the inverse of the Fisher information. The diagonal elements of the inverse of the Fisher information provide uncertainties of the parameter estimates as a by-product of the algorithm.⁵

5 Data

The data analyzed is 21,851 daily log-returns of the S&P 500 index covering the period from 1928 to 2014.⁶ The log-returns are calculated using $r_t = \log(P_t) - \log(P_{t-1})$, where P_t is the closing price of the index on day t and \log is the natural logarithm. It is evident from the plot of the log-returns shown in figure 1 that the data includes a larger number of exceptional observations. The Global Financial Crisis of 2007–2008 does not stand out when compared to the Great

⁵If some of the parameters are on or near the boundary of their parameter space, which is often the case in HMMs, the use of the Hessian to compute standard errors is unreliable. Moreover, the conditions for asymptotic normality of the ML estimator are often violated, thus making confidence intervals based on the computed standard errors unreliable. In those cases confidence intervals based on the profile likelihood function or bootstrapping provide a better approximation.

⁶The definition of the index was changed twice during the period. In 1957, the S&P 90 was expanded to 500 stocks and became the S&P 500 index. The 500 stocks contained exactly 425 industrials, 25 railroads, and 50 utility firms. This requirement was relaxed in 1988.

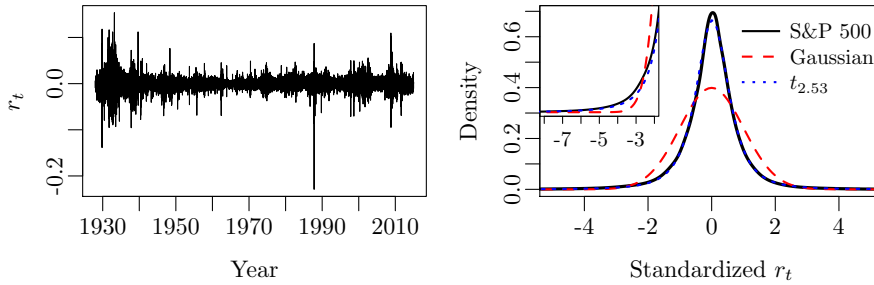


Figure 1: Daily log-returns of the S&P 500 index and the density of the standardized daily log-returns together with the density function for the standard normal distribution and a t -distribution.

Depression of 1929–1933 and the period around Black Monday in October 1987. The tendency for the volatility to form clusters as large price movements are followed by large price movements and vice versa is a stylized fact (see, e.g., Cont 2001, Lindström et al. 2015).

The excess kurtosis is evident from the plot of the density function shown in figure 1. There is too much mass centered right around the mean and in the tails compared to the normal distribution. The t -distribution with 2.53 degrees of freedom is a much better fit to the unconditional distribution of the log-returns. There are 169 observations that deviate more than four standard deviations from the mean compared to an expectation of 1.4 observations if the returns were normally distributed. The most extreme being the -22.9% log-return on Black Monday which deviates more than 19 standard deviations from the sample mean.

In figure 2, the sample autocorrelation function of the squared log-returns is shown together with the ACF of the squared, outlier-corrected log-returns (the two top panels). The dashed lines are the upper boundary of an approximate 95% confidence interval under the null hypothesis of independence (Madsen 2008). To analyze the impact of outliers, values outside the interval $\bar{r}_t \pm 4\hat{\sigma}$, where \bar{r}_t and $\hat{\sigma}$ are the estimated sample mean and standard deviation, are set equal to the nearest boundary following the approach by Granger and Ding (1995a). According to Granger et al. (2000), the choice of four standard deviations was arbitrary, but experimentation suggested that the results were not substantially altered if the value was changed somewhat. The long memory of the squared returns is evident from both plots although the large number of exceptional observations greatly reduces the magnitude of the ACF of the unadjusted squared returns (see Chan 1995).

The persistence of the ACF of the squared returns is, to some extent, a consequence of the volatility clustering seen in figure 1, but the significantly positive

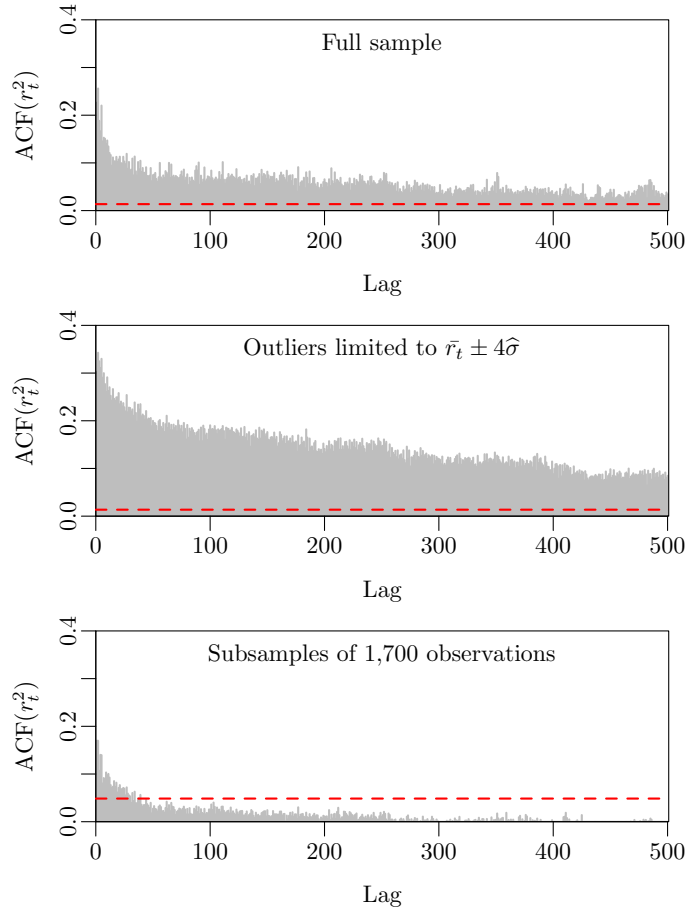


Figure 2: The top panel shows the autocorrelation function of the squared log-returns at lag 1–500. The middle panel shows the autocorrelation function of the squared, outlier-corrected log-returns. The bottom panel shows the average autocorrelation of the squared log-returns for subsamples of 1,700 observations.

level at lags well over 100 is more likely caused by the data-generating process being nonstationary. This is supported by the third panel of figure 2, which shows the average autocorrelation of the squared returns for 12 subsamples of 1,700 observations. The decay of the autocorrelations in the subseries is, on average, substantially faster than in the full series and roughly exponential, as concluded by Malmsten and Teräsvirta (2010). Stărică and Granger (2005) reached the same conclusion based on scaling the absolute log-returns with the time-varying unconditional variance.

6 Results

Rather than dividing the full sample into subsamples of 1,700 observations, as done by Granger and Ding (1995a), Rydén et al. (1998), and Bulla (2011), the parameters of a two-state HMM with conditional normal distributions are estimated using a rolling window of 1,700 trading days. By using a rolling window it is possible to get an idea of the evolution of the model parameters over time. The result is shown in figure 3, where the dashed lines are the maximum-likelihood estimate (MLE) for the full sample and the gray areas are bootstrapped 95% confidence intervals based on re-estimating the model to 1,000 simulated series of 1,700 observations.

It is evident that the parameters are far from constant as noted by Rydén et al. (1998) and Bulla (2011). The variation of the variances and the transition probabilities far exceeds the likely range of variation as indicated by the 95% confidence intervals. This implies that the sojourn-time distribution is not memoryless. The first ten years after World War II, in particular, stand out as the probability of staying in the same state was extraordinarily low. The impact of the extreme returns in 1987 on the parameters of the high-variance state also stands out. One of the drawbacks of using fixed-length forgetting appears from the estimated variance in the second state; the variance spikes on Black Monday in 1987 and does not return to its pre-1987 level until 1,700 days later, thus making the length of the rolling window evident from the figure.

The substantial variation of the parameters could indicate that the regime-switching model is unsuitable for the S&P 500 series, but its ability to reproduce the stylized facts suggests otherwise (see Rydén et al. 1998, Bulla 2011, Nystrup et al. 2015b). It could also be an indication that the model is misspecified, i.e., that it has too few states or a wrong kind of conditional distributions. Rydén et al. (1998) found that in some periods there was a need for a third so-called outlier state with a low unconditional probability. Adding a third state, however, does not lead to smaller variations which suggests that the need for a third state was a consequence of the lack of adaption of the parameters. The addition of a conditional t -distribution in the high-variance state, on the other hand, dampens the variations as shown in figure 4. The parameters are still not constant, but the variations are smaller especially around 1987. It is only

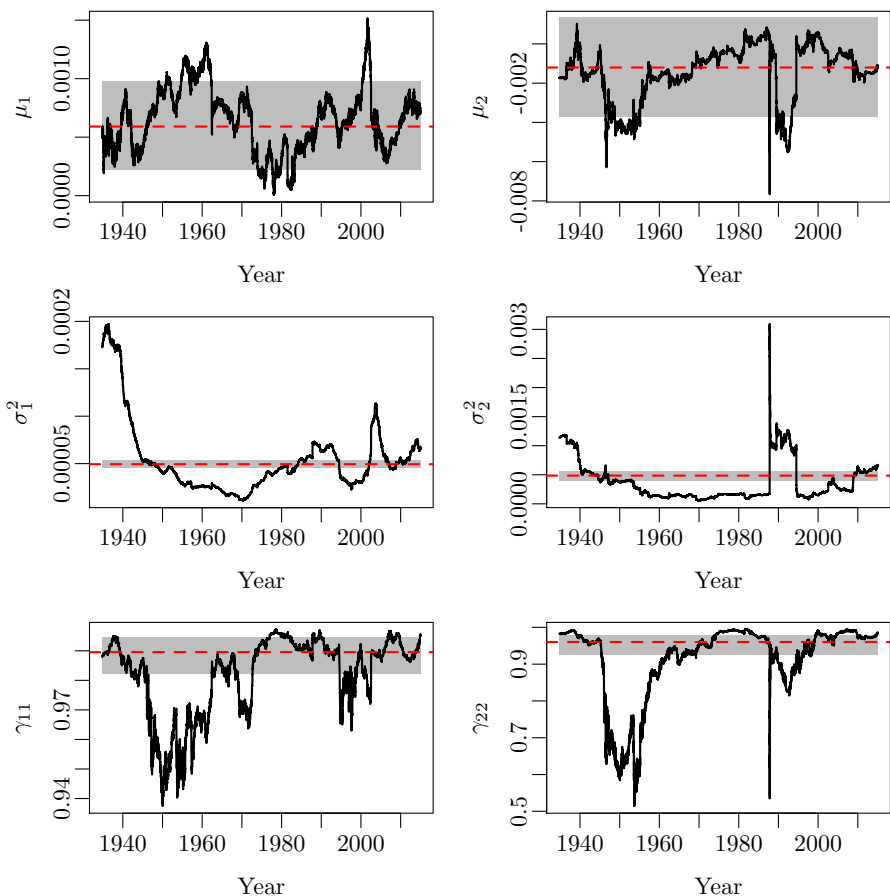


Figure 3: Parameters of a two-state Gaussian HMM estimated using a rolling window of 1,700 trading days. The dashed lines are the MLE for the full series and the gray areas are bootstrapped 95% confidence intervals.

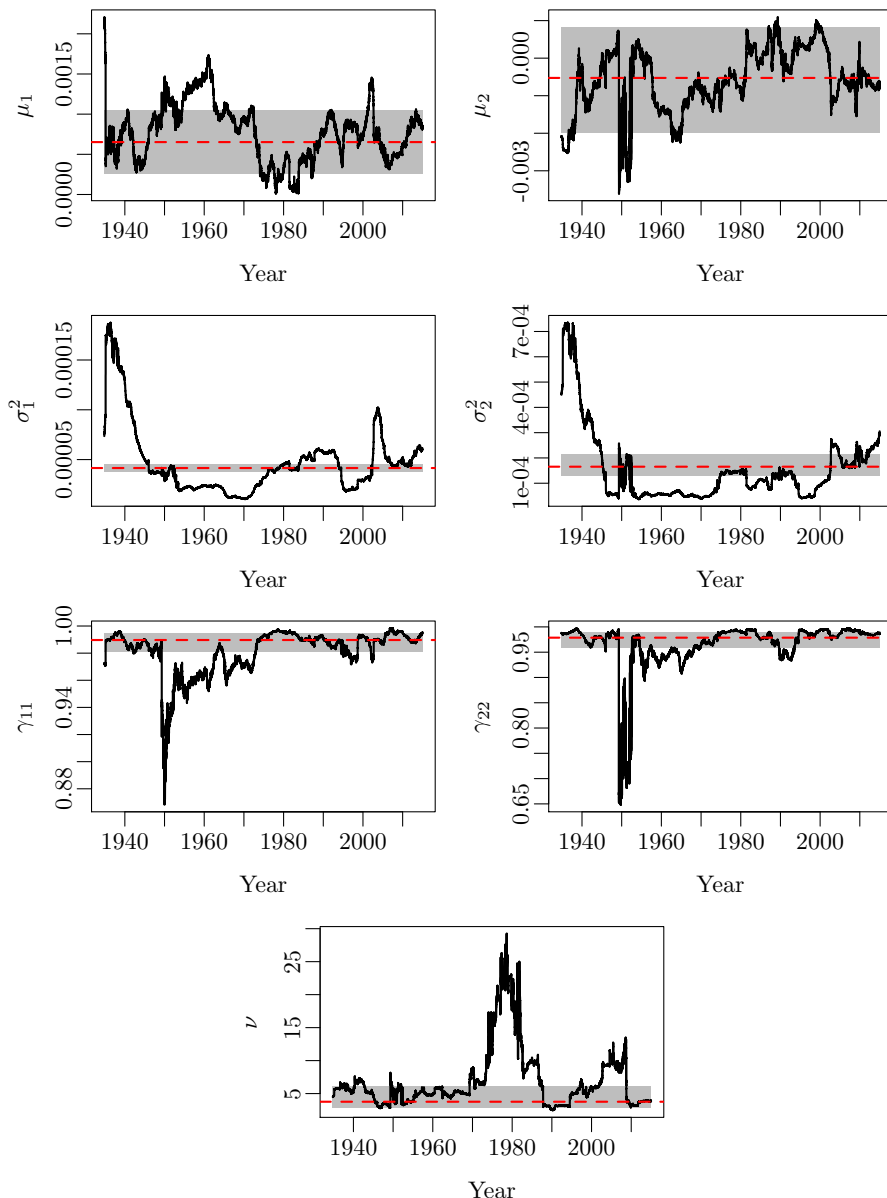


Figure 4: Parameters of a two-state HMM with a conditional t -distribution in the high-variance state estimated using a rolling window of 1,700 trading days. The dashed lines are the MLE for the full series and the gray areas are bootstrapped 95% confidence intervals.

the degrees of freedom of the t -distribution that change dramatically from a maximum of 29 in 1978 to a minimum of 2.5 in 1990.

The choice of window length affects the parameter estimates and can be viewed as a tradeoff between bias and variance. A shorter window yields a faster adaption to changes but a more noisy estimate as fewer observations are used for the estimation. The large fluctuations in the parameter values could be a result of the window length being too short, but the parameter values do not stabilize even if the window length is increased to 2,500 days. Instead, there is a strong incentive to reduce the window length to secure a faster adaption to the nonstationary behavior of the data-generating process. If the window length is reduced to 1,000 days, then the degrees of freedom of the t -distribution exceed 100 throughout a large part of the period, meaning that the distribution in the high-variance state is effectively normal. This suggests that the t -distribution, to some extent, is a compensation for too slow an adaption of the parameters.

It cannot be ruled out that adding a couple hundred more states or switching frequencies, as proposed by Calvet and Fisher (2004), would stabilize the parameters, but it would also make the model more likely to be overfitting out of sample and impossible to use for state inference. Given the nonstationary behavior of the data-generating process, it is reasonable to assume that a model with nonconstant parameters is needed.

Figure 5 shows the parameters of the two-state HMM with conditional normal distributions estimated using the adaptive estimation approach outlined in section 4 with an effective memory length $N_{\text{eff}} = 250$.⁷ The dashed lines show the MLE for the full series and the gray areas are approximate 95% confidence intervals based on the profile likelihood functions. The width of the confidence intervals is seen to spike whenever there are large movements in the parameter estimates.

Compared to figure 3, the variations are larger as a result of the shorter memory length. Using exponential forgetting, the effective memory length can be reduced compared to when using fixed-length forgetting without increasing the sensitivity to noise to an undesirable level. Exponential forgetting is also more meaningful as it assigns most weight to the newest observations and, at the same time, observations are not excluded from the estimation from one day to the next. This leads to smoother parameter estimates. The optimal memory length depends on the intended application and is not necessarily constant over time; however, 250 days is close to being the minimum length that offers a reasonable tradeoff between speed of adaption and sensitivity to noise.

⁷The estimation was started at $t_0 = 250$ in order to avoid very large initial steps with the tuning constant $A = 1.25$. Numerical optimization of the weighted likelihood function was used to find initial values for the parameters and the Hessian.

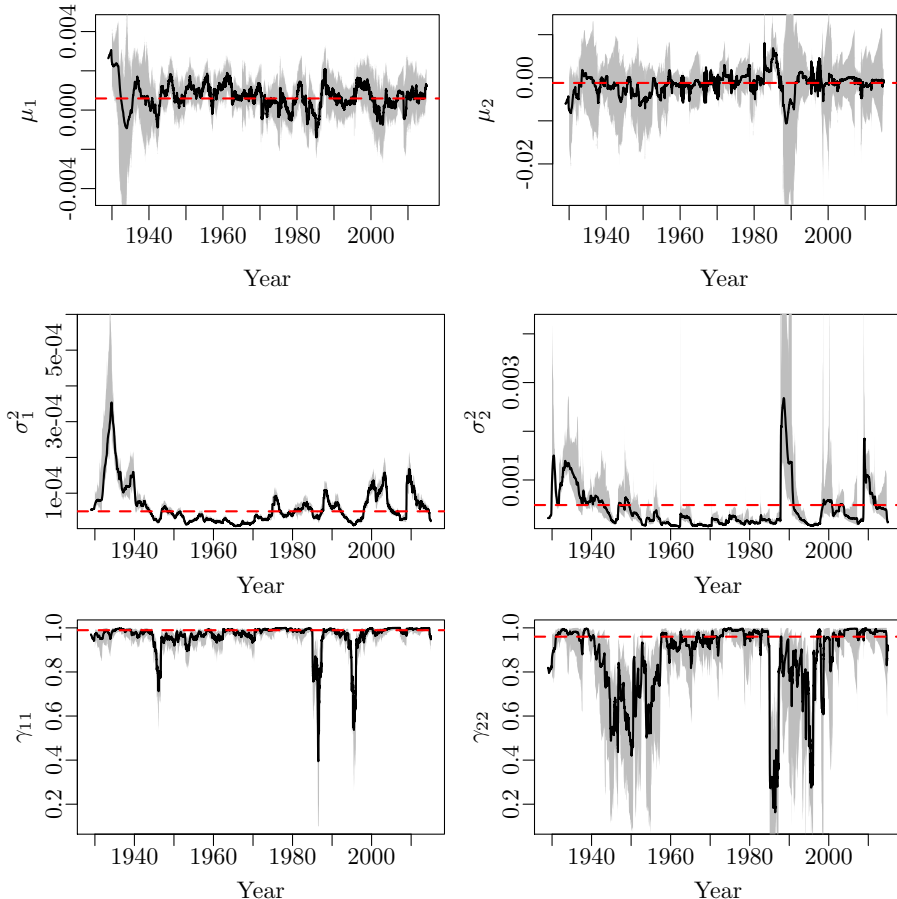


Figure 5: Parameters of a two-state Gaussian HMM estimated adaptively using an effective memory length $N_{\text{eff}} = 250$. The dashed lines are the MLE for the full series and the gray areas are approximate 95% confidence intervals based on the profile likelihood functions.

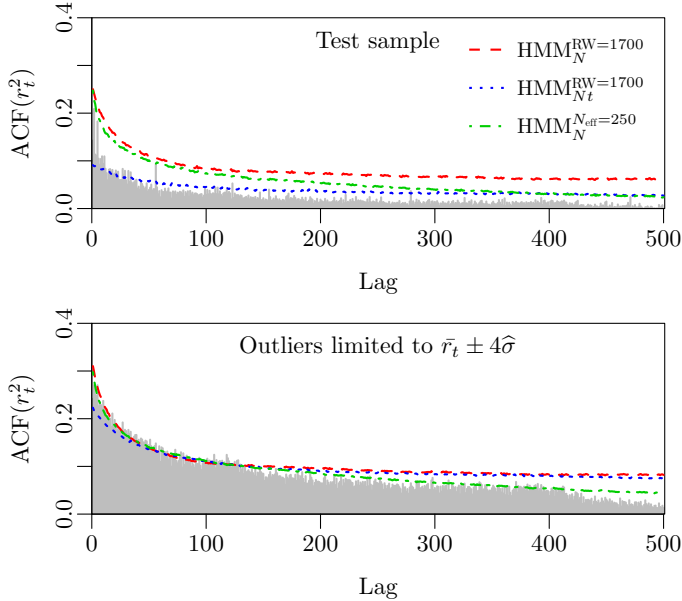


Figure 6: The top panel shows the autocorrelation function of the squared log-returns at lag 1–500 together with the average autocorrelation of squared log-returns simulated using the different estimated models. The test sample does not include the first 1,700 observations. In the bottom panel the impact of outliers is limited to four standard deviations.

6.1 Reproducing the long memory

The top panel of figure 6 shows the ACF of the squared log-returns together with the average autocorrelation of squared log-returns based on 100 datasets simulated using the estimated parameters shown in figure 3–5. The test sample does not include the first 1,700 observations in order to facilitate a comparison with the models estimated using a rolling window. The later starting point causes the ACF to be significantly lower than in figure 2, supporting the hypothesis that the long memory is caused by nonstationarity.

The autocorrelation of the simulated data is, on average, higher than the sample autocorrelation for all three models. The adaptively-estimated Gaussian HMM ($\text{HMM}_N^{N_{\text{eff}}=250}$) appears to have the right shape, but it is the HMM with a conditional t -distribution ($\text{HMM}_{Nt}^{\text{RW}=1700}$) that provides the best fit to the ACF. The fact that the ACFs of the squared log-returns of the Gaussian HMMs exceed that of the data is an indication that the tails of the Gaussian models are too short compared to the empirical distribution.

When constraining the impact of outliers to $\bar{r}_t \pm 4\hat{\sigma}$, as done in the second panel

Model	Test sample		Outlier-corrected	
	$MSE_{1:250} \times 10^3$	$MSE_{251:500} \times 10^3$	$MSE_{1:250} \times 10^3$	$MSE_{251:500} \times 10^3$
HMM _N ^{RW=1700}	3.85	2.99	0.36	1.84
HMM _{Nt} ^{RW=1700}	0.39	0.47	0.32	1.48
HMM _N ^{$N_{\text{eff}}=250$}	2.28	0.62	0.17	0.27

Table 7: Mean squared error for the ACF of the squared log-returns and the outlier-corrected, squared log-returns at lag 1–250 and 251–500 for the estimated models.

of figure 6, the level of autocorrelation in the simulated data is similar to the empirical data. The adaptively-estimated Gaussian HMM provides a good fit to the sample ACF of the squared, outlier-corrected log-returns, while the ACFs of the two models that were estimated using a rolling window are too persistent. The difference in the fit to the ACF of the squared, outlier-corrected log-returns is largest at the highest lags. This observation is supported by the computed mean squared errors for lag 1–250 and 251–500 summarized in table 7. The result when using a threshold of eight instead of four standard deviations is very similar and therefore not shown. With this (equally arbitrary) threshold the model that includes a t -distribution becomes a worse fit at the lowest lags while the adaptively-estimated Gaussian HMM still provides the best fit.

6.2 Comparing one-step density forecasts

Table 8 compares the predictive log-likelihood of the different two-state models for the full test sample and when leaving out the 20 most negative contributions to the log-likelihood. This is to separate the impact of the most exceptional observations, similar to the approach used for the ACF. The 20 observations are not the ones furthest away from the sample mean and they are also not the same for all the models, but there is a large overlap. As HMMs are often used for day-to-day state identification in an on-line setting, the focus is on one-step forecasts.

For the full test sample, which does not include the first 1,700 observations, the HMM with a t -distribution in the high-variance state has the highest predictive log-likelihood. When leaving out the 20 observations that make the most negative contributions to the log-likelihood, the adaptively-estimated Gaussian HMM outperforms all the other models. This is less than 0.1% of the total number of observations. In fact, the adaptively-estimated Gaussian HMM outperforms the other models when removing only the observation from Black Monday. Thus, while the t -distribution is a better fit to the most exceptional observations, the adaptively-estimated Gaussian HMM provides the best one-step-ahead density forecasts for the remainder of the sample.

The predictive log-likelihood of both the Gaussian and the combined Gaussian- t model increases when using a rolling rather than expanding window for the esti-

Model	Predictive log-likelihood	
	Full test sample	Leaving out 20 observations
HMM _N ^{expanding}	66,962	67,093
HMM _{Nt} ^{expanding}	67,319	67,386
HMM _N ^{RW=1700}	67,391	67,739
HMM _{Nt} ^{RW=1700}	67,757	67,860
HMM _N ^{N_{eff}=250}	67,678	68,034

Table 8: Predictive log-likelihood of the different two-state models for the full test sample and when leaving out the 20 observations with the most negative contributions.

mation. This is not surprising given the nonstationarity of the data-generating process and it clearly shows the need to consider nonstationary models. The difference when leaving out the 20 most negative contributions to the predictive log-likelihood is small when using an expanding window because the tails become very heavy in order to compensate for the lack of adaption of the model parameters. This leads to a poor average predictive performance.

Based on the results shown in table 8, it is natural to wonder whether the performance of the combined Gaussian-*t* model could be improved by reducing the effective memory length using the adaptive estimation method. This has been attempted, but the advantage of a conditional *t*-distribution disappears when the memory length is reduced and the degrees of freedom increase. The added uncertainty of the degrees of freedom parameter, which is very sensitive to outliers, leads to more noisy estimates of the mean and scale parameters and a lower predictive likelihood when the memory length is reduced.

To summarize, a shorter memory length of the parameters leads to a good fit to the sample ACF of the squared log-returns when constraining the impact of outliers. A shorter memory also improves the one-step density forecasts with the adaptively-estimated Gaussian HMM being the overall best when leaving out the 20 observations that were most difficult to forecast. Even when the memory length of the parameters is reduced considerably, however, conditional normal distributions provide a poor fit to those very exceptional observations.

6.3 Improving density forecasts with local smoothing

Given that a faster adaption of the parameters leads to improved density forecasts, it should be possible to further improve the density forecasts by improving the parameter forecasts. Recall that the adaptively-estimated parameters are found as solutions to (6) for distinct values of *t*. The observations up to and including time *t* are used when estimating θ_t , which is then used for making inference about X_{t+1} . In other words, the parameters are assumed to stay constant from time *t* to time *t* + 1.

Model	Predictive log-likelihood	
	Full test sample	Leaving out 20 observations
HMM _N ^{RW=1700}	67,408	67,742
HMM _{Nt} ^{RW=1700}	67,771	67,872
HMM _N ^{N_{eff}=250}	67,723	68,058

Table 9: Predictive log-likelihood of the estimated models when using cubic smoothing splines to forecast the parameters.

If the effective memory length is sufficiently short, the approximation of θ_t as a constant vector near t is good. However, this would imply that a relatively low number of observations is used to estimate θ_t , resulting in a noisy estimate. On the contrary, a large bias may occur if the effective memory is long. Joensen et al. (2000) showed that if the parameter variations are smooth, then locally to t the elements of θ_t are better approximated by local polynomials than local constants.

The parameter variations displayed in figure 5 appear to be smooth, especially the variations in the conditional variances. The idea of Joensen et al. (2000) is implemented with more flexible cubic smoothing splines rather than polynomials. Table 9 summarizes the predictive log-likelihood of the two-state models when using cubic smoothing splines to forecast the parameters.

By fitting a cubic smoothing spline to the last nine parameter estimates and then using the fitted spline to forecast the parameters at the next time step, it is possible to increase the predictive log-likelihood of the adaptively-estimated Gaussian HMM from 67,678 to 67,723 for the full test sample. When leaving out the 20 most negative contributions, the predictive log-likelihood is improved from 68,034 to 68,058. Thus, the largest improvement is obtained for the 20 observations that are most difficult to forecast. For the two models that were estimated using a rolling window the improvement in forecasting performance is smaller. This is not surprising given that the parameter variations appeared less smooth when using a rolling window for the estimation.

Modeling the driving forces behind the variations is beyond the scope of this paper, but the improvement in forecasting performance that can be obtained by using simple smoothing splines to forecast the parameters suggests there is great potential for a hierarchical model.

7 Conclusion

By applying an adaptive estimation method that allowed for observation-driven time variation of the parameters it was possible to reproduce the long memory that is characteristic for long series of squared daily returns with a two-state Gaussian hidden Markov model. The transition probabilities were found to be

time varying, implying that the sojourn-time distribution was not the memoryless geometric distribution.

The adaptive estimation approach meant that the effective memory length could be reduced compared to when using fixed-length forgetting, thereby allowing a faster adaption to changes and a better reproduction of the current parameter values. This led to an improved fit to the autocorrelation function of the squared log-returns and better one-step density forecasts. A third state or a conditional t -distribution in the high-variance state may be necessary to capture the full extent of excess kurtosis in a few periods, but the long memory that is needed to justify a third state or a conditional t -distribution with long tails is not consistent with the fast adaption of the parameters that led to the best fit to the long memory of the squared log-returns and the best one-step density forecasts with the exception of the most extreme observations.

The presented results emphasize the importance of taking into account the non-stationary behavior of the data-generating process. The longer the data period, the more important this is. The outlined adaptive estimation method can be applied to other models than regime-switching models and for other purposes than density forecasting. Within financial risk management, for example, possible applications include value-at-risk estimation and dynamic asset allocation based on out-of-sample state identification.

A better description of the time-varying behavior of the parameters is an open route for future work that can be pursued in various ways. One way would be to allow different forgetting factors for each parameter or consider more advanced state-, time-, or data-dependent forgetting. Another way would be to formulate a model for the parameter changes in the form of a hierarchical model possibly including relevant exogenous variables. The proposed method for estimating the time variation of the parameters is an important step toward the identification of a hierarchical model structure.

References

- Baek, C., N. Fortuna, and V. Pipiras. “Can Markov switching model generate long memory?” *Economics Letters*, vol. 124, no. 1 (2014), pp. 117–121.
- Baillie, R. T., T. Bollerslev, and H. O. Mikkelsen. “Fractionally integrated generalized autoregressive conditional heteroskedasticity.” *Journal of Econometrics*, vol. 74, no. 1 (1996), pp. 3–30.
- Baum, L. E., T. Petrie, G. Soules, and N. Weiss. “A maximization technique occurring in the statistical analysis of probabilistic functions of Markov chains.” *Annals of Mathematical Statistics*, vol. 41, no. 1 (1970), pp. 164–171.

- Bauwens, L., A. Dufays, and J. V. Rombouts. "Marginal likelihood for Markov-switching and change-point GARCH models." *Journal of Econometrics*, vol. 178, no. 3 (2014), pp. 508–522.
- Bazzi, M., F. Blasques, S. J. Koopman, and A. Lucas. "Time varying transition probabilities for Markov regime switching models." *Journal of Time Series Analysis*, vol. 38, no. 3 (2017), pp. 458–478.
- Bollerslev, T. "Generalized autoregressive conditional heteroskedasticity." *Journal of Econometrics*, vol. 31, no. 3 (1986), pp. 307–327.
- Bulla, J. "Hidden Markov models with t components. Increased persistence and other aspects." *Quantitative Finance*, vol. 11, no. 3 (2011), pp. 459–475.
- Bulla, J. and I. Bulla. "Stylized facts of financial time series and hidden semi-Markov models." *Computational Statistics & Data Analysis*, vol. 51, no. 4 (2006), pp. 2192–2209.
- Bulla, J., S. Mergner, I. Bulla, A. Sesboüé, and C. Chesneau. "Markov-switching asset allocation: Do profitable strategies exist?" *Journal of Asset Management*, vol. 12, no. 5 (2011), pp. 310–321.
- Calvet, L. E. and A. J. Fisher. "How to forecast long-run volatility: Regime switching and the estimation of multifractal processes." *Journal of Financial Econometrics*, vol. 2, no. 1 (2004), pp. 49–83.
- Cappé, O., E. Moulines, and T. Rydén. *Inference in Hidden Markov Models*. Springer: New York (2005).
- Chan, W. S. "Understanding the effect of time series outliers on sample autocorrelations." *Test*, vol. 4, no. 1 (1995), pp. 179–186.
- Cont, R. "Empirical properties of asset returns: stylized facts and statistical issues." *Quantitative Finance*, vol. 1, no. 2 (2001), pp. 223–236.
- Creal, D., S. J. Koopman, and A. Lucas. "Generalized autoregressive score models with applications." *Journal of Applied Econometrics*, vol. 28, no. 5 (2013), pp. 777–795.
- Dacco, R. and S. Satchell. "Why do regime-switching models forecast so badly?" *Journal of Forecasting*, vol. 18, no. 1 (1999), pp. 1–16.
- Dempster, A. P., N. M. Laird, and D. B. Rubin. "Maximum likelihood from incomplete data via the EM algorithm." *Journal of the Royal Statistical Society. Series B (Methodological)*, vol. 39, no. 1 (1977), pp. 1–38.
- Diebold, F. X. and A. Inoue. "Long memory and regime switching." *Journal of Econometrics*, vol. 105, no. 1 (2001), pp. 131–159.

- Engle, R. F. "Autoregressive conditional heteroscedasticity with estimates of the variance of United Kingdom inflation." *Econometrica*, vol. 50, no. 4 (1982), pp. 987–1007.
- Frühwirth-Schnatter, S. *Finite Mixture and Markov Switching Models*. Springer: New York (2006).
- Gouriéroux, C. and J. Jasiak. "Memory and infrequent breaks." *Economics Letters*, vol. 70, no. 1 (2001), pp. 29–41.
- Granger, C. W. J. and Z. Ding. "Some properties of absolute return: An alternative measure of risk." *Annales D'Economie Et Statistique*, vol. 40 (1995a), pp. 67–92.
- Granger, C. W. J. and Z. Ding. "Stylized facts on the temporal and distributional properties of daily data from speculative markets." Unpublished paper, Department of Economics, University of California, San Diego (1995b).
- Granger, C. W. J., S. Spear, and Z. Ding. "Stylized facts on the temporal and distributional properties of absolute returns: An update." In *Proceedings of the Hong Kong International Workshop on Statistics in Finance*. Imperial College Press: London (2000), pp. 97–120.
- Granger, C. W. J. and T. Teräsvirta. "A simple nonlinear time series model with misleading linear properties." *Economics Letters*, vol. 62, no. 2 (1999), pp. 161–165.
- Joensen, A., H. Madsen, H. A. Nielsen, and T. S. Nielsen. "Tracking time-varying parameters with local regression." *Automatica*, vol. 36, no. 8 (2000), pp. 1199–1204.
- Khreich, W., E. Granger, A. Miri, and R. Sabourin. "A survey of techniques for incremental learning of HMM parameters." *Information Sciences*, vol. 197 (2012), pp. 105–130.
- Langrock, R. and W. Zucchini. "Hidden Markov models with arbitrary state dwell-time distributions." *Computational Statistics & Data Analysis*, vol. 55, no. 1 (2011), pp. 715–724.
- Lindström, E., H. Madsen, and J. N. Nielsen. *Statistics for Finance*. Chapman & Hall: London (2015).
- Lystig, T. C. and J. P. Hughes. "Exact computation of the observed information matrix for hidden Markov models." *Journal of Computational and Graphical Statistics*, vol. 11, no. 3 (2002), pp. 678–689.
- Madsen, H. *Time Series Analysis*. Chapman & Hall: London (2008).

- Malmsten, H. and T. Teräsvirta. “Stylized facts of financial time series and three popular models of volatility.” *European Journal of Pure and Applied Mathematics*, vol. 3, no. 3 (2010), pp. 443–477.
- Mikosch, T. and C. Stărică. “Nonstationarities in financial time series, the long-range dependence, and the IGARCH effects.” *Review of Economics and Statistics*, vol. 86, no. 1 (2004), pp. 378–390.
- Nielsen, B. F. *Matrix Analytic Methods in Applied Probability with a View towards Engineering Applications*. Doctoral thesis, Technical University of Denmark (2013).
- Nystrup, P., B. W. Hansen, H. Madsen, and E. Lindström. “Regime-based versus static asset allocation: Letting the data speak.” *Journal of Portfolio Management*, vol. 42, no. 1 (2015a), pp. 103–109.
- Nystrup, P., H. Madsen, and E. Lindström. “Stylised facts of financial time series and hidden Markov models in continuous time.” *Quantitative Finance*, vol. 15, no. 9 (2015b), pp. 1531–1541.
- Rydén, T., T. Teräsvirta, and S. Åsbrink. “Stylized facts of daily return series and the hidden Markov model.” *Journal of Applied Econometrics*, vol. 13, no. 3 (1998), pp. 217–244.
- Stărică, C. and C. W. J. Granger. “Nonstationarities in stock returns.” *Review of Economics and Statistics*, vol. 87, no. 3 (2005), pp. 503–522.
- Zucchini, W. and I. L. MacDonald. *Hidden Markov Models for Time Series: An Introduction Using R*. Chapman & Hall: London, 2nd ed. (2009).

PAPER C

Originally published in *The Journal of Portfolio Management*

Regime-based versus static asset allocation: *Letting the data speak*

Peter Nystrup, Bo William Hansen, Henrik Madsen,
and Erik Lindström

Abstract

Regime shifts present a big challenge to traditional strategic asset allocation. This paper investigates whether regime-based asset allocation can effectively respond to changes in financial regimes at the portfolio level in an effort to provide better long-term results when compared to more static approaches. The regime-based approach is centered around a regime-switching model with time-varying parameters that can match the tendency of financial markets to change their behavior abruptly and the phenomenon that the new behavior often persists for several periods after a change. In an asset universe consisting of a global stock index and a global government bond index, it is shown that, even without any level of forecasting skill, it may not be optimal to hold a static portfolio.

Keywords: Dynamic asset allocation; Regime shifts; Hidden Markov models; Time-varying parameters; Daily returns; Volatility clustering.

1 Introduction

The behavior of financial markets changes abruptly. Although some changes may be transitory, the new behavior often persists for several periods after a change. The mean, volatility, and correlation patterns in stock returns, for example, changed dramatically at the start of, and continued through the global financial crisis of 2007–2008. Similar regime changes, some of which can be recurring (recessions versus expansions) and some of which can be permanent (structural breaks), are prevalent across a wide range of financial markets and in the behavior of many macro variables (Ang and Timmermann 2012).

Observed regimes in financial markets are related to the phases of the business cycle (see, e.g., Campbell 1999, Cochrane 2005). The link is complex and difficult to exploit for investment purposes due to the large lag in the availability of business cycle related data. Our intention is to let the data speak by focusing

on readily available market data instead of attempting to establish the link to the business cycle.

Regime changes present a big challenge to traditional strategic asset allocation (SAA). In the presence of time-varying investment opportunities, portfolio weights should be adjusted as new information arrives. Traditional SAA approaches seek to develop static “all-weather” portfolios that optimize efficiency across a range of economic scenarios. However, if economic conditions are persistent and strongly linked to asset class performance, then a dynamic strategy should add value over static weights (Sheikh and Sun 2012). The purpose of a regime-based strategy is to take advantage of favorable economic regimes as well as withstand adverse economic regimes and reduce potential drawdowns.

Regime-based investing is distinct from tactical asset allocation (TAA). While the latter is shorter term, higher frequency (i.e., weekly or monthly), and driven primarily by valuation considerations, regime-based investing targets a longer time horizon (i.e., a year or more) and is driven by changing economic fundamentals. A regime-based approach has the flexibility to adapt to changing economic conditions within a benchmark-based investment policy which can involve more than one rebalancing within a year. It straddles a middle ground between strategic and tactical (Sheikh and Sun 2012).

2 Letting the data speak

This paper examines whether regime-based asset allocation (RBAA) can effectively respond to financial regimes in an effort to provide better long-term results when compared to static approaches. Dopfel (2010) showed the potential outperformance of a RBAA strategy assuming complete information about the prevailing regime and future regime shifts is available. Dopfel (2010), however, concluded that an investor who does not possess exceptional forecasting skill is better off holding a static portfolio that is hedged against the uncertainty associated with regime shifts.

This conclusion contrasts the large amount of studies that have documented the profitability of dynamic asset allocation (DAA) strategies based on regime-switching models (see, e.g., Ang and Bekaert 2002, 2004, Guidolin and Timmermann 2007, Bulla et al. 2011, Kritzman et al. 2012). The profitability should be accepted with caution as not all the studies account for transaction costs when comparing the performance of dynamic and static strategies. This is important as frequent rebalancing can offset the potential excess return of a dynamic strategy. Furthermore, the in-sample performance generally exceeds the out-of-sample performance—if the strategies are at all tested out-of-sample.

Inspired by the apparent profitability of regime-switching strategies this paper challenges the conclusion made by Dopfel (2010) by letting the data speak. In an investment universe consisting of a global stock index (MSCI ACWI)¹ and a global government bond index (JPM GBI)², the performance of a RBAA strategy is compared to a strategy based on rebalancing to static weights. The development of the two indices over the 20-year data period is depicted in figure 1.

The intention is to identify regimes in the stock returns using a regime-switching model and let the asset allocation depend on the identified regime. The focus on modeling the stock returns is natural as portfolio risk is typically dominated by stock market risk. In addition, the stock markets generally lead the economy (Siegel 1991). The goal is not to predict regime shifts or future market movements but to identify when a regime shift has occurred and then benefit from the persistence of equilibrium returns and volatilities. The regime-switching process can be interpreted as a momentum process when it is more likely to continue in the same state rather than transition to another state (Ang and Bekaert 2002).

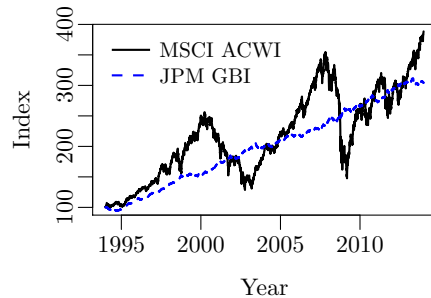


Figure 1: Investment universe.

¹The MSCI All Country World Index, denominated in USD, captures large and mid cap representation across 23 Developed Market and 21 Emerging Market countries. The difference compared to the more well-known MSCI World Index is the weight on EM countries. The data prior to 1999, where the total return index began, has been reconstructed based on the price index by adding the average daily net dividend return over the period from 1999 to 2013 of 0.007% to the price returns.

²The global J.P. Morgan Government Bond Index measures the performance across 13 developed fixed income bond markets hedged to USD. The constituents are selected from all government bonds, excluding floating rate notes, perpetuities, bonds targeted at the domestic market for tax purposes, and bonds with less than one year to maturity. The index had a modified duration of 6.8 at the end of 2013.

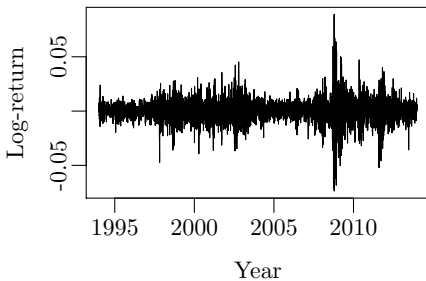


Figure 2: Volatility clustering in the daily log-returns.

to discuss the profitability of a RBAA approach.

3 The hidden Markov model

Imagine knowing a person's heart rate. While the person is sleeping, a low average heart rate with low volatility is observed. When the person wakes up, there is a sudden rise in the average level of the heart rate and its volatility. Without actually seeing the person, it can reasonably be concluded whether he or she is awake or sleeping, that is which state he or she is in.

The heart rate of a financial market is its returns. The use of hidden Markov models (HMMs) to infer the state of financial markets has gained popularity over the last decade. The HMM is a black-box model, but the inferred states can often be linked to phases of the business cycle (see, e.g., Guidolin and Timmermann 2007). The possibility of interpreting the states combined with the model's ability to reproduce stylized facts of financial returns is part of the reason why the HMM has become increasingly popular.

In a hidden Markov model, the probability distribution that generates an observation depends on the state of an unobserved Markov chain. A sequence of discrete random variables $\{X_t : t \in \mathbb{N}\}$ is said to be a first-order Markov chain if, for all $t \in \mathbb{N}$, it satisfies the Markov property:

$$\Pr(X_{t+1} | X_t, \dots, X_1) = \Pr(X_{t+1} | X_t). \quad (1)$$

The conditional probabilities $\Pr(X_{t+1} = j | X_t = i) = \gamma_{ij}$ are called transition probabilities.

³The log-returns are calculated using $r_t = \log(P_t) - \log(P_{t-1})$, where P_t is the closing price of the index on day t and \log is the natural logarithm.

⁴A quantitative manifestation of this fact is that while returns themselves are uncorrelated, absolute and squared returns display a positive, significant and slowly decaying autocorrelation function.

Figure 2 shows the daily log-returns of the stock index.³ The volatility forms clusters as large price movements tend to be followed by large price movements and vice versa, as noted by Mandelbrot (1963).⁴ The RBAA strategy aims to exploit this persistence of the volatility as risk-adjusted returns, on average, are substantially lower during turbulent periods, irrespective of the source of turbulence, as shown by Kritzman and Li (2010). The purpose is not to outline the *optimal* strategy but rather

As an example, consider the two-state model with Gaussian conditional distributions:

$$Y_t | X_t \sim N(\mu_{X_t}, \sigma_{X_t}^2),$$

where

$$\mu_{X_t} = \begin{cases} \mu_1, & \text{if } X_t = 1, \\ \mu_2, & \text{if } X_t = 2, \end{cases} \quad \sigma_{X_t}^2 = \begin{cases} \sigma_1^2, & \text{if } X_t = 1, \\ \sigma_2^2, & \text{if } X_t = 2, \end{cases} \quad \text{and } \boldsymbol{\Gamma} = \begin{bmatrix} 1 - \gamma_{12} & \gamma_{12} \\ \gamma_{21} & 1 - \gamma_{21} \end{bmatrix}.$$

When the current state X_t is known, the distribution of Y_t depends only on X_t .

The sojourn times are implicitly assumed to be geometrically distributed:

$$\Pr(\text{'staying } t \text{ time steps in state } i) = \gamma_{ii}^{t-1} (1 - \gamma_{ii}). \quad (2)$$

The geometric distribution is memoryless, implying that the time until the next transition out of the current state is independent of the time spent in the state.

HMMs can match financial markets' tendency to change their behavior abruptly and the phenomenon that the new behavior often persists for several periods after a change. They are well suited to capture the stylized behavior of many financial series including volatility clustering and leptokurtosis, as shown by Rydén et al. (1998). Subsequent papers have extended the classical Gaussian HMM by considering other sojourn-time distributions than the memoryless geometric distribution (Bulla and Bulla 2006), other conditional distributions than the Gaussian distribution (Bulla 2011), and a continuous-time formulation as an alternative to the dominating discrete-time models (Nystrup et al. 2015b). In ? it was found that the need to consider other sojourn-time distributions and other conditional distributions can be eliminated by adapting to the time-varying behavior of the data process.

The parameters of an HMM are usually estimated using the maximum-likelihood method. Every observation is assumed to be of equal importance no matter how long the sample period is. This approach works well when the sample period is short and the underlying process does not change over time. The time-varying behavior of the parameters documented in previous studies (Rydén et al. 1998, Bulla 2011, Nystrup et al. 2017b) calls for an adaptive approach that assigns more weight to the most recent observations while keeping in mind the past patterns at a reduced confidence.

In Nystrup et al. (2017b), an adaptive estimation approach based on weighting the observations with exponentially-decreasing weights, in other words using exponential forgetting, was outlined. The same approach will be pursued in this article. The regime-switching model is still a two-state HMM with Gaussian conditional distributions, but one that adapts to the time-varying behavior of the underlying process in an effort to produce more robust state estimates.

Index/Strategy	AR	SD	SR	MDD
Bond index (JPM GBI)	0.060	0.03	1.90	0.05
Stock index (MSCI ACWI)	0.069	0.18	0.38	0.58
Static Portfolio	0.064	0.09	0.72	0.32
Stocks–Bonds	0.114	0.09	1.23	0.13
Long–Short	0.096	0.18	0.52	0.44

Table 3: Performance of the indices and the strategies from 1996–2014.

4 Empirical results

The testing is done one day at a time in a live-sample setting to make it as realistic as possible. The model is fitted to the first t observations assigning most weight to the most recent observations. Based on the estimated parameters the probability that on day t the market was in the high and low-volatility state, respectively, are calculated along with the predicted state probabilities for day $t+1$. As the states are highly persistent ($\gamma_{ii} \gg 0.5$), the state that is predicted to be most likely on day $t+1$ will be the same that was identified to be most likely on day t . If the state that is predicted to be most likely on day $t+1$ is different from the state that the asset allocation on day t is based on and the confidence in the prediction is above 95%⁵, then the allocation is changed based on the closing price at day $t+1$, i.e., there is assumed to be a one-day delay in the implementation. Otherwise the asset allocation remains unchanged. The log-return on day $t+1$ is then included in the sample, the model is re-estimated, and the state probabilities are calculated based on the new parameters. This procedure is repeated sequentially by including the observations, one at a time, from 1 January 1996 all the way through the sample.⁶

The performance of two regime-based strategies (Stocks–Bonds and Long–Short) is compared to the performance of the two indices and a static portfolio with a fixed allocation of 49% to stocks in table 3. The first strategy is fully invested in the stock index in the low-volatility state and the bond index in the high-volatility state. The average allocation to the stock index over the period was 49%. The second strategy is long the stock index in the low-volatility state and short the stock index in the high-volatility state. Figure 4 shows the development of the strategies and the indices. In the shaded periods the allocation was based on being in the high-volatility state.

The identified regimes seem intuitive when looking at the log-returns at the bottom of figure 4. There have been a total of 16 regime changes over the

⁵If the confidence threshold is changed to 85% or 90% there will be more regime changes, but the results will only change somewhat. For a given level of transaction costs there exists an optimal threshold that balances the cost of rebalancing with the cost of not reacting to regime shifts or delaying the reaction.

⁶The log-returns from the two years prior to 1996 are used for initialization.

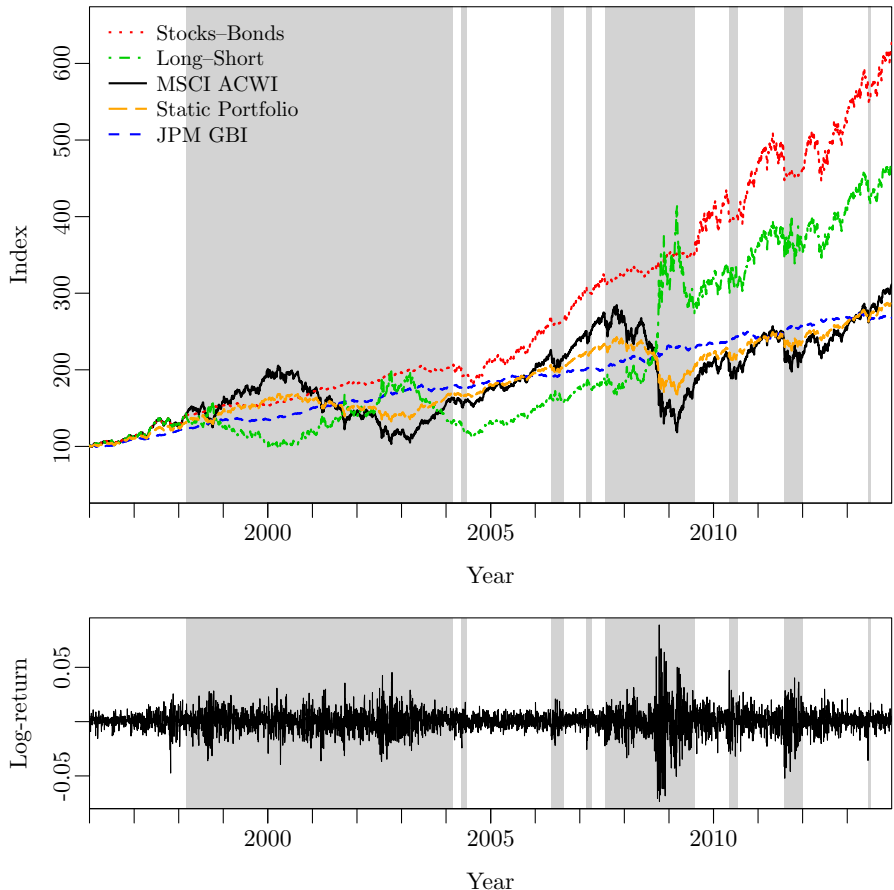


Figure 4: Development of the strategies and indices across the inferred regimes.

18-year period. The length of the identified regimes varies considerably from a few weeks up to six years. This is different from what would be expected if the regimes were based on a business cycle indicator. There appears to be large differences in the level of volatility within the six-year high-volatility regime beginning in 1998 that includes both the build-up and the burst of the dot-com bubble. This suggests that the market states were less persistent around this time.

The bond index has realized the highest Sharpe ratio (SR) with an annualized return (AR) of 6.0% and an adjusted annualized standard deviation (SD) of only 3%. The reported SDs have been adjusted for autocorrelation using the proce-

Index/Strategy	AR	SD	SR	MDD
Bond index (JPM GBI)	0.058	0.03	1.89	0.05
Stock index (MSCI ACWI)	0.111	0.17	0.66	0.50
Static Portfolio	0.084	0.08	1.04	0.21
Stocks–Bonds	0.115	0.09	1.22	0.13
Long–Short	0.063	0.17	0.38	0.44

Table 5: Performance of the indices and the strategies when excluding year 2008.

dure outlined by Kinlaw et al. (2015).⁷ The data period has been characterized by falling interest rates and low inflation leading to a strong performance for bonds. It is unlikely that the environment for bonds will be as favorable going forward.

The Stocks–Bonds strategy has realized the second highest SR of 1.23. The annualized SD is the same as for the static portfolio (that has the same average exposure to the stock index), but the realized return is higher as long as transaction costs do not exceed 239 basis points per one-way transaction. This is when ignoring the costs associated with rebalancing to static weights, thus the break-even transaction cost is higher than 239 basis points. In addition, the maximum drawdown⁸ (MDD) for the Stocks–Bonds strategy is much smaller when compared to the static strategy.

The Long–Short strategy has been less profitable, but it still outperforms the stock index when transaction costs are less than 130 basis points per one-way transaction. The outperformance essentially happened during the financial crisis in 2008. The Long–Short strategy has a lower tail risk compared to the stock index, but the risk of the strategy underperforming the index going forward seems to be real.

This observation is confirmed in table 5, where the performance of the indices and the regime-based strategies are summarized, when excluding year 2008 from the sample. Although it still has a lower tail risk compared to the stock index, the Long–Short strategy then underperforms the stock index. The performance of the bond index and the Stocks–Bonds strategy barely change, whereas the AR and SR of the stock index and the static portfolio increase. The average allocation to the stock index when excluding year 2008 was 52%, which equals the fixed allocation to stocks in the static portfolio in table 5. The realized return of the Stocks–Bonds strategy still exceeds that of the static portfolio as long as transaction costs do not exceed 140 basis points per one-way transaction.

⁷The adjustment for autocorrelation leads to slightly higher standard deviations and correspondingly lower Sharpe ratios. The adjustment is not important to the conclusions drawn as the indices and strategies all displayed fairly similar, low amounts of autocorrelation.

⁸The maximum drawdown is the largest relative decline from a historical peak in the index value.

5 Summary and discussion

Our results indicate that it does not require any level of forecasting skill for a RBAA strategy to be more profitable than a static strategy. The testing was done one day at a time in a live-sample setting to make it as realistic as possible. Our approach was based on identifying regimes in market returns using a regime-switching model with time-varying parameters. As the parameters are updated every day the same approach should work in other time periods as well. The results are robust as they are based on available market data with no assumptions about equilibrium returns, volatilities, or correlations. Additionally, it might be possible to improve the performance by including economic variables, interest rates, investor sentiment surveys, or other possible indicators.

The outperformance of the strategy that switched between stocks and bonds appeared to be most reliable as it did not just happen during one year, as was the case with the Long–Short strategy. Although the break-even transaction cost was more than 239 basis points (140 basis points when excluding year 2008), the strategies will only remain profitable if the persistence of the market states remains high. Volatility clustering is not a new phenomenon, but it can occur at different levels of market persistence.

The tested strategies may be based on larger changes in allocation than most investors are willing to and/or allowed to implement. Suppose your benchmark is a 50–50 allocation to stocks and bonds and that you are allowed to vary it between a 60–40 and a 40–60 allocation. For the Stocks–Bonds strategy, this is equivalent to allocating 80% of the portfolio to a static 50–50 portfolio and the remaining 20% to the regime-based strategy. The excess return that can be obtained is then 20% of the excess return that could be obtained by allocating the entire portfolio to the regime-based strategy.

Our results have important implications for portfolio managers with a medium to long-term investment horizon. Even without any level of forecasting skill it may not be optimal to hold a static portfolio. With some level of forecasting skill the potential outperformance of a RBAA strategy could be substantial. It is definitely worth considering a more dynamic approach to asset allocation if not only to reduce the tail risk.

References

- Ang, A. and G. Bekaert. “International asset allocation with regime shifts.” *Review of Financial Studies*, vol. 15, no. 4 (2002), pp. 1137–1187.
- Ang, A. and G. Bekaert. “How regimes affect asset allocation.” *Financial Analysts Journal*, vol. 60, no. 2 (2004), pp. 86–99.

- Ang, A. and A. Timmermann. "Regime changes and financial markets." *Annual Review of Financial Economics*, vol. 4, no. 1 (2012), pp. 313–337.
- Bulla, J. "Hidden Markov models with t components. Increased persistence and other aspects." *Quantitative Finance*, vol. 11, no. 3 (2011), pp. 459–475.
- Bulla, J. and I. Bulla. "Stylized facts of financial time series and hidden semi-Markov models." *Computational Statistics & Data Analysis*, vol. 51, no. 4 (2006), pp. 2192–2209.
- Bulla, J., S. Mergner, I. Bulla, A. Sesboüé, and C. Chesneau. "Markov-switching asset allocation: Do profitable strategies exist?" *Journal of Asset Management*, vol. 12, no. 5 (2011), pp. 310–321.
- Campbell, J. Y. "Asset prices, consumption, and the business cycle." In *Handbook of Macroeconomics*, edited by J. B. Taylor and M. Woodford, vol. 1C, chap. 19. Elsevier: Amsterdam (1999), pp. 1231–1303.
- Cochrane, J. H. "Financial markets and the real economy." *Foundations and Trends in Finance*, vol. 1, no. 1 (2005), pp. 1–101.
- Dopfel, F. E. "Designing the new policy portfolio: A smart, but humble approach." *Journal of Portfolio Management*, vol. 37, no. 1 (2010), p. 43.
- Guidolin, M. and A. Timmermann. "Asset allocation under multivariate regime switching." *Journal of Economic Dynamics and Control*, vol. 31, no. 11 (2007), pp. 3503–3544.
- Kinlaw, W., M. Kritzman, and D. Turkington. "The divergence of high- and low-frequency estimation: Implications for performance measurement." *Journal of Portfolio Management*, vol. 41, no. 3 (2015), pp. 14–21.
- Kritzman, M. and Y. Li. "Skulls, financial turbulence, and risk management." *Financial Analysts Journal*, vol. 66, no. 5 (2010), pp. 30–41.
- Kritzman, M., S. Page, and D. Turkington. "Regime shifts: Implications for dynamic strategies." *Financial Analysts Journal*, vol. 68, no. 3 (2012), pp. 22–39.
- Mandelbrot, B. "The variation of certain speculative prices." *Journal of Business*, vol. 36, no. 4 (1963), pp. 394–419.
- Nystrup, P., H. Madsen, and E. Lindström. "Stylised facts of financial time series and hidden Markov models in continuous time." *Quantitative Finance*, vol. 15, no. 9 (2015b), pp. 1531–1541.
- Nystrup, P., H. Madsen, and E. Lindström. "Long memory of financial time series and hidden Markov models with time-varying parameters." *Journal of Forecasting*, vol. 36, no. 8 (2017b), pp. 989–1002.

Rydén, T., T. Teräsvirta, and S. Åsbrink. "Stylized facts of daily return series and the hidden Markov model." *Journal of Applied Econometrics*, vol. 13, no. 3 (1998), pp. 217–244.

Sheikh, A. Z. and J. Sun. "Regime change: Implications of macroeconomic shifts on asset class and portfolio performance." *Journal of Investing*, vol. 21, no. 3 (2012), pp. 36–54.

Siegel, J. J. "Does it pay stock investors to forecast the business cycle?" *Journal of Portfolio Management*, vol. 18, no. 1 (1991), pp. 27–34.

PAPER D

Originally published in *The Journal of Portfolio Management*

Dynamic allocation or diversification: *A regime-based approach to multiple assets*

Peter Nystrup, Bo William Hansen, Henrik Olejasz Larsen,
Henrik Madsen, and Erik Lindström

Abstract

This article investigates whether regime-based asset allocation can effectively respond to changes in financial regimes at the portfolio level in an effort to provide better long-term results when compared to a static 60/40 benchmark. The potential benefit from taking large positions in a few assets at a time comes at the cost of reduced diversification. This tradeoff is analyzed in a multi-asset universe with great potential for static diversification. The regime-based approach is centered around a regime-switching model with time-varying parameters that can match financial markets' behavior, and a new, more intuitive way of inferring the hidden market regimes. The empirical results show that regime-based asset allocation is profitable, even when compared to a diversified benchmark portfolio. The results are robust, as they are based on available market data with no assumptions about forecasting skills.

Keywords: Dynamic asset allocation; Regime shifts; Hidden Markov model; Time-varying parameters; Daily returns; Volatility clustering.

1 Introduction

Regime changes present a big challenge to traditional strategic asset allocation (SAA) approaches seeking to develop static “all-weather” portfolios that optimize efficiency across a range of economic scenarios. If economic conditions are persistent and strongly linked to asset class performance, then a dynamic strategy should add value over rebalancing to static weights, as argued by Sheikh and Sun (2012).

Within the last 15 years, a large number of studies have examined the profitability of regime-based asset allocation (RBAA). RBAA is distinct from tactical asset allocation, which relies on forecasting, in that it is based on reacting to observed changes in market conditions. The purpose of RBAA is not to predict regime changes or future market movements, but to identify when a regime

change has occurred and then benefit from the persistence of equilibrium returns, volatilities, and correlations to take advantage of favorable regimes and reduce potential drawdowns.

The hidden Markov model (HMM) is a popular choice for inferring the state of financial markets. Ang and Bekaert (2002, 2004), Guidolin and Timmermann (2007), Bulla et al. (2011), Kritzman et al. (2012), and Nystrup et al. (2015a) have all found RBAA approaches based on HMMs to be profitable. Ang and Bekaert (2002, 2004) and Guidolin and Timmermann (2007), however, did not account for transaction costs, which is important because frequent rebalancing can offset a dynamic strategy's potential excess return.

All of the aforementioned studies considered dynamic allocation to stocks in combination with bonds and/or a risk-free asset, often involving larger changes in allocation than most investors are willing to or allowed to implement. The potential benefit from taking large positions in a few assets at a time comes at the cost of reduced diversification. The benefits of diversification include lower downside risk and higher risk-adjusted returns. In order to analyze this tradeoff, the performance of RBAA has to be compared to a static benchmark using a more comprehensive asset universe, because the potential for diversification is limited by the size of the asset universe.

Dynamic asset allocation is, by definition, more restricted than SAA in terms of the size of the investment opportunity set, since it is difficult to invest dynamically in illiquid assets such as private real estate, private equity, infrastructure, timber, etc. This is worth mentioning, given that illiquid alternatives have become a larger part of institutional investors' portfolios in recent years. Although restricted to the universe of liquid assets, there are more opportunities than just stocks and government bonds.

Regime-based approaches are very popular, *inter alia*, because of the link to the phases of the business cycle. As argued in Nystrup et al. (2015a), the link is complex and difficult to exploit for investment purposes due to the large lag in the availability of data related to the business cycle. Therefore, in this article, the focus will be on readily available market data, instead of attempting to establish the link to the business cycle.

The underlying two-state HMM with time-varying parameters is the same as in Nystrup et al. (2015a). However, this study includes more asset classes, and a new, more intuitive way of inferring the hidden market states based on an online version of the Viterbi algorithm is introduced.¹ It is examined whether RBAA can effectively respond to financial regimes in an effort to provide better long-term results when compared to a diversified, fixed-weight benchmark, with emphasis on the tradeoff between dynamic allocation and diversification.

¹An online algorithm processes its input observation-by-observation in a sequential fashion, without having the entire input sequence available from the start.

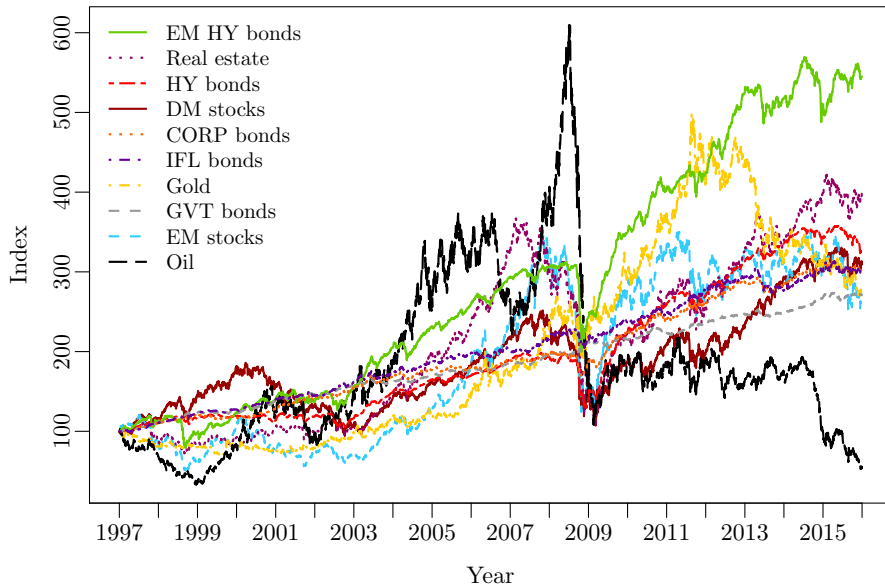


Figure 1: Development of the ten indices over the 19-year data period. The legends are sorted according to the index values at the end of 2015.

2 Asset universe

The asset universe considered in this paper consists of developed (DM) and emerging market (EM) stocks, listed real estate, DM and EM high-yield bonds, gold, oil, corporate bonds, inflation-linked bonds, and government bonds.² All indices measure the total net return in USD with a total of 4,944 daily closing prices per index covering the period from 1997 through 2015.

Figure 1 shows the development of the ten indices over the 19-year data period. It is evident that there are large differences in the asset classes' behavior, which is why diversification works over the long run. The Global Financial Crisis of 2007–2008 stands out, in that respect, as the majority of the indices suffered large losses in this period.

Table 2 summarizes the annualized return, standard deviation, Sharpe ratio, and maximum drawdown³ of the indices. To ensure that the performance comparison

²The ten indices are MSCI World, MSCI Emerging Markets, FTSE EPRA/NAREIT Developed Real Estate, BofA Merrill Lynch U.S. High Yield, Barclays Emerging Markets High Yield, S&P GSCI Crude Oil (funded futures roll), S&P GSCI Gold (funded futures roll), Barclays U.S. Aggregate Corporate Bonds, Barclays World Inflation-Linked Bonds (hedged to USD), and J.P. Morgan Global Government Bonds (hedged to USD).

³The maximum drawdown is the largest relative decline from a historical peak in the index

Index	Annualized return	Standard deviation	Sharpe ratio	Maximum drawdown
1. MSCI World (stocks)	0.061	0.18	0.34	0.57
2. MSCI EM (stocks)	0.052	0.29	0.18	0.65
3. FTSE/EPRA REIT (real estate)	0.075	0.22	0.34	0.72
4. High-Yield Bonds (credit)	0.064	0.12	0.56	0.35
5. EM High-Yield Bonds (credit)	0.093	0.12	0.75	0.36
6. S&P GSCI Crude Oil WTI (commodity)	-0.032	0.43	-0.07	0.91
7. S&P GSCI Gold (commodity)	0.054	0.16	0.34	0.46
8. Corporate Bonds Inv Grade (fixed income)	0.060	0.06	1.07	0.16
9. Inflation-Linked Bonds (fixed income)	0.059	0.04	1.40	0.10
10. JPM Global GBI (fixed income)	0.054	0.03	1.75	0.05

Table 2: Performance of the ten indices over the 19-year data period.

is not distorted by autocorrelation in the daily returns, the reported standard deviations have been adjusted for autocorrelation using the procedure outlined by Kinlaw et al. (2015).⁴ The differences in performance are substantial. Out of the ten indices, the oil price index has been both at the lowest and highest value during the 19-year period. It is the only index that has had a negative return. The EM high-yield bond index finished at the highest value, while the fixed income indices realized the highest Sharpe ratios and, at the same time, suffered the smallest drawdowns. Fixed income benefited from falling interest rates over the considered period.

The differences in Sharpe ratios are too large for a diversified portfolio to be able to outperform a portfolio with an overweight of fixed income. There should not be a strong preference, *ex ante*, for portfolios that overweight fixed income, since the environment for bonds is unlikely to remain as favorable in the coming years. It is, therefore, important to ensure that portfolios have the same average allocation to fixed income before comparing their performance. Alternatively, the mean values of the indices could be adjusted so that they all have the same Sharpe ratio.

Figure 3 shows the correlations between the ten indices estimated from the daily returns over the 19-year data period. The indices are divided into two groups based on whether they are positively or negatively correlated with DM stocks. Gold stands out as having a very low correlation with the other assets. Investment-grade corporate bonds could have been labeled as credit rather than fixed income, but the index appears to be strongly correlated with inflation-linked bonds and government bonds. High-yield bonds, on the other hand, are more strongly correlated with stocks than government bonds.

value.

⁴The adjustment leads to the reported standard deviations being higher than had they been annualized under the assumption of independence, as most of the indices display positive autocorrelation. The adjustment had a large impact on the standard deviation of the high-yield bond index that went from 0.04 to 0.12.

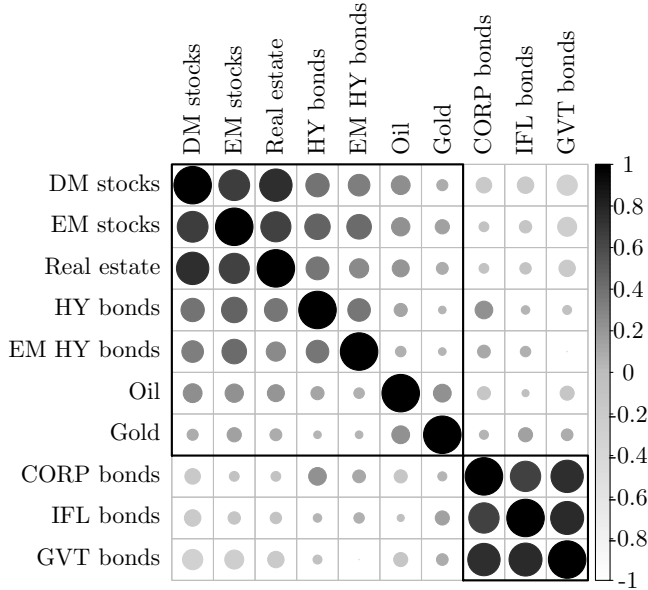


Figure 3: Correlations between the ten indices over the 19-year data period. The size of each circle illustrates the absolute value and the shading indicates the numerical value of the correlation. The indices are divided into two groups based on their correlation with DM stocks.

2.1 Volatility regimes

The regime detection will focus on the log-returns of the MSCI World index, because portfolio risk is typically dominated by stock market risk (see, e.g., Goyal et al. 2015). In addition, the stock markets generally lead the economy (Siegel 1991). Figure 4 shows the log-returns of the MSCI World index.⁵ The volatility forms clusters, as large price movements tend to be followed by large price movements and vice versa, as noted by Mandelbrot (1963).⁶

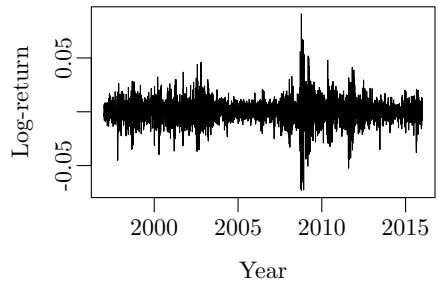


Figure 4: Volatility clustering in the log-returns of the MSCI World index.

⁵The log-returns are calculated using $r_t = \log(P_t) - \log(P_{t-1})$, where P_t is the closing price of the index on day t and \log is the natural logarithm.

⁶A quantitative manifestation of this fact is that while returns themselves are uncorrelated, absolute and squared returns display a positive, significant, and slowly decaying autocorrelation

RBAA aims to exploit this persistence of the volatility, since risk-adjusted returns, on average, are substantially lower during turbulent periods, irrespective of the source of turbulence, as shown by Kritzman and Li (2010). The negative correlation between volatility and returns is sometimes explained by changes in attitudes toward risk; because high-volatility regimes are associated with increased risk aversion and reduced risk capacity, a high-volatility environment is likely to be accompanied by falling asset prices.⁷

The intention is to identify high- and low-volatility regimes in the stock returns using a regime-switching model and let the asset allocation depend on the identified regime. The purpose is not to outline the *optimal* strategy, but rather to discuss the potential profitability of RBAA in a comprehensive asset universe. It appeared from figure 1 that the turning points are not exactly the same for all asset classes, however, it is left for future research to show whether the results presented in this article can be improved by including information from the other asset classes in the regime-detection process.

2.2 A 60/40 benchmark

The first column in table 5 outlines the weight of the indices in a 60/40 portfolio. The weight of stocks, real estate, credit, and commodities sum to 60%, and the weight of corporate, inflation-linked, and government bonds sum to 40%. This portfolio will serve as a benchmark, though the results are not sensitive to the specific choice of benchmark allocation.⁸ The weights have not been optimized, but are chosen to mimic a 60/40 long-only SAA portfolio of an institutional investor, in order to make the study as realistic as possible.⁹ The allocation to high-yield bonds is considered part of the 60% allocation to stocks, because they are more strongly correlated with stocks than government bonds, confer figure 3.

In table 5, the ten indices' weights in the risk-on and risk-off RBAA portfolios are compared to their weights in the 60/40 benchmark portfolio when a fraction $p = 0.5$ of the portfolio is allocated to the RBAA strategy. Risk-on means that in low-volatility regimes the weight of the risky assets (everything that is

function.

⁷Increased risk aversion (a behavioral explanation) and reduced risk capacity (an institutional explanation) are difficult to distinguish in data. Both effects have support (e.g., Cohn et al. 2015, Brunnermeier and Pedersen 2009).

⁸Another possible benchmark portfolio is the $1/N$ portfolio that assigns equal weight to all assets. This agnostic portfolio has in many cases proved to be a difficult benchmark to beat (see DeMiguel et al. 2009b), but it has realized a slightly lower Sharpe ratio than the proposed SAA portfolio over the considered period.

⁹The proposed benchmark allocation is within the range of variation of the average asset allocation of pension plans across the major OECD countries according to OECD Global Pension Statistics.

Index	SAA	Risk-on	Risk-off
1. MSCI World (stocks)	25.0%	33.3%	12.5%
2. MSCI EM (stocks)	5.0%	6.7%	2.5%
3. FTSE/EPRA REIT (real estate)	10.0%	13.3%	5.0%
4. High-Yield Bonds (credit)	5.0%	6.7%	2.5%
5. EM High-Yield Bonds (credit)	5.0%	6.7%	2.5%
6. S&P GSCI Crude Oil WTI (commodity)	5.0%	6.7%	2.5%
7. S&P GSCI Gold (commodity)	5.0%	6.7%	2.5%
8. Corporate Bonds Inv Grade (fixed income)	10.0%	5.0%	17.5%
9. Inflation-Linked Bonds (fixed income)	10.0%	5.0%	17.5%
10. JPM Global GBI (fixed income)	20.0%	10.0%	35.0%

Table 5: The ten indices' weights in the risk-on and risk-off RBAA portfolios when $p = 0.5$, compared to their weights in the benchmark SAA portfolio.

positively correlated with DM stocks) is increased above 60% and the weight of fixed income is decreased below 40%. Risk-off is the opposite.¹⁰

The indices' weights are increased and decreased in proportion to their relative weights in the benchmark portfolio. The larger the percentage of the portfolio allocated to the RBAA strategy, the more the weights are increased and decreased. When $p = 0.5$, the weight of government bonds, for example, is 10% in the risk-on portfolio and 35% in the risk-off portfolio, compared to 20% in the SAA portfolio. Adjusting the weight of the risky assets relative to fixed income, rather than adjusting only the weights of stocks and government bonds, ensures a minimum level of diversification even when $p = 1$.

3 The hidden Markov model

Imagine a market that is either in a bullish or a bearish regime. When the market is in the bullish regime, the average return is positive and the volatility is low. When the market is in the bearish regime, the average return is negative and the volatility is high. Although the market regime can never be observed, it can reasonably be concluded based on the returns whether it is a bull or a bear market—that is, which state the market is in.

The use of HMMs to infer the state of financial markets has gained popularity over the last decade. The HMM is a black-box model, but the inferred states can often be linked to phases of the business cycle (see, e.g., Guidolin and Timmermann 2007). The possibility of interpreting the states, combined with the model's ability to reproduce stylized facts of financial returns, is part of the reason that HMMs have become increasingly popular.

¹⁰The weights in the RBAA portfolio depend on the percentage p of the portfolio that is allocated to the RBAA strategy and the regime X : $w^{\text{RBAA}}(p, X) = p \cdot w^{\text{risk-on/off}}(X) + (1 - p) \cdot w^{\text{SAA}}$. The regime-dependent portfolio weights are $w^{\text{risk-on/off}}(X) = (25, 5, 10, 5, 5, 5, 5, 0, 0, 0)^T / 60 \cdot \mathbf{1}_{\text{risk-on}}(X) + (0, 0, 0, 0, 0, 0, 10, 10, 20)^T / 40 \cdot \mathbf{1}_{\text{risk-off}}(X)$, where the indicator function $\mathbf{1}_{\text{risk-on}}(X) \equiv 1$ if $X = \text{risk-on}$ and $\mathbf{1}_{\text{risk-on}}(X) \equiv 0$ if $X = \text{risk-off}$.

In a hidden Markov model, the probability distribution that generates an observation depends on the state of an unobserved Markov chain. A sequence of discrete random variables $\{X_t : t \in \mathbb{N}\}$ is said to be a first-order Markov chain if, for all $t \in \mathbb{N}$, it satisfies the Markov property:

$$\Pr(X_{t+1} | X_t, \dots, X_1) = \Pr(X_{t+1} | X_t). \quad (1)$$

The conditional probabilities $\Pr(X_{t+1} = j | X_t = i) = \gamma_{ij}$ are called transition probabilities.

As an example, consider the two-state model with Gaussian conditional distributions:

$$Y_t | X_t \sim N(\mu_{X_t}, \sigma_{X_t}^2),$$

where

$$\mu_{X_t} = \begin{cases} \mu_1, & \text{if } X_t = 1, \\ \mu_2, & \text{if } X_t = 2, \end{cases} \quad \sigma_{X_t}^2 = \begin{cases} \sigma_1^2, & \text{if } X_t = 1, \\ \sigma_2^2, & \text{if } X_t = 2, \end{cases} \quad \text{and } \boldsymbol{\Gamma} = \begin{bmatrix} 1 - \gamma_{12} & \gamma_{12} \\ \gamma_{21} & 1 - \gamma_{21} \end{bmatrix}.$$

When the current state X_t is known, the distribution of Y_t is given—that is, the distribution of Y_t depends only on X_t .

The sojourn times are implicitly assumed to be geometrically distributed:

$$\Pr(\text{'staying } t \text{ time steps in state } i') = \gamma_{ii}^{t-1} (1 - \gamma_{ii}). \quad (2)$$

The geometric distribution is memoryless, implying that the time until the next transition out of the current state is independent of the time spent in the state.

HMMs can match the tendency of financial markets to change their behavior abruptly and the phenomenon that the new behavior often persists for several periods after a change (Ang and Timmermann 2012). They are well suited to capture the stylized behavior of many financial series including volatility clustering and leptokurtosis, as shown by Rydén et al. (1998).

Subsequent articles have extended the classical Gaussian HMM by considering other sojourn-time distributions than the memoryless geometric distribution (Bulla and Bulla 2006), other conditional distributions than the Gaussian distribution (Bulla 2011), and a continuous-time formulation as an alternative to the dominating discrete-time models (Nystrup et al. 2015b). In Nystrup et al. (2017b) it was found that the need to consider other sojourn-time distributions and other conditional distributions can be eliminated by adapting to the time-varying behavior of the underlying data process.

Parameter estimation

The parameters of an HMM are usually estimated using the maximum-likelihood method. Every observation is assumed to be of equal importance, no matter how

long the sample period is. This approach works well when the sample period is short and the underlying process does not change over time. The time-varying behavior of the parameters documented in previous studies (Rydén et al. 1998, Bulla 2011, Nystrup et al. 2017b) calls for an adaptive approach that assigns more weight to the most recent observations while keeping in mind past patterns at a reduced confidence.

In Nystrup et al. (2017b), an adaptive estimation approach based on weighting the observations with exponentially-decreasing weights—in other words, using exponential forgetting—was outlined. The same estimation approach was used in Nystrup et al. (2015a) and will be used in this article. The regime-switching model is still a two-state HMM with Gaussian conditional distributions, but one that adapts to the time-varying behavior of the underlying process in an effort to produce more robust state estimates.

4 State inference

Once the parameters of the hidden Markov model have been estimated, the hidden states can be inferred. The most likely sequence of states can be computed efficiently using the algorithm of Viterbi (1967). The entire output sequence $\{Y_t : t \in 1, 2, \dots, T\}$ must be observed before the state for any time step can be generated. A widely used approach is to break the input sequence into fixed-size windows and apply the Viterbi algorithm to each window. Larger windows lead to higher accuracy but result in higher latency.

Narasimhan et al. (2006) proposed an online step algorithm that makes it possible to dynamically trade off latency for expected accuracy, without having to choose a fixed window size up front. The essence of their algorithm is that the initial state becomes increasingly certain as more observations are included in the sequence and the latency increases. Once the certainty estimate reaches a dynamically-computed threshold, the identified initial state is outputted and the algorithm proceeds to estimate the next state in the sequence. The algorithm is shown in pseudo code in algorithm 1. Despite being very intuitive, the algorithm has never been applied in studies of RBAA.

Choice of threshold

Using the online step algorithm, the tradeoff between accuracy and latency can be made explicit by letting the threshold be a decreasing function of the latency. It can be argued, though, that this is not desirable in the present application; if the delay in classifying an observation is large, then part of the reallocation premium has been missed, and incurring unnecessary transaction costs would only make it worse.

Instead, a constant confidence threshold of $1 - 1/T \approx 0.9998$, where T is the number of observations, is chosen. This threshold is not comparable to the

Algorithm 1: Online step algorithm.

```

 $t = T = 1$ 
while  $T \leq$  the number of observations
    calculate the probabilities  $\Pr(X_t = i | Y_1, Y_2, \dots, Y_T)$  for all states  $i$  at time  $t \leq T$ 
    based on knowledge of the first  $T$  observations
    if  $\max_i \Pr(X_t = i | Y_1, Y_2, \dots, Y_T) >$  threshold
        classify state  $X_t = \arg \max_i \Pr(X_t = i | Y_1, Y_2, \dots, Y_T)$ 
         $t = t + 1$ 
         $T = \max(t, T)$ 
    else
         $T = T + 1$ 
    endif
endwhile

```

95% threshold applied in Nystrup et al. (2015a), where an observation was classified as belonging to the current regime unless it immediately and with 95% confidence could be classified as belonging to the other regime. In the algorithm proposed by Narasimhan et al. (2006), an observation is not classified until enough observations have been gathered that the confidence requirement is met.

With a constant threshold of 0.9998, the median delay in classifying an observation is 7 days (not trading days). The median delay in detecting regime changes is 25 days. By lowering the confidence threshold, the delay can be reduced, but this also leads to detection of more (spurious) regime changes and increased transaction costs.

For a given level of transaction costs, there is an optimal threshold that balances the cost of rebalancing with the cost of not reacting to regime changes or delaying the reaction. A confidence threshold that corresponds to an expectation of one misclassification for the entire sample may be too conservative. Attempting to find the optimal threshold, however, would introduce a backtesting bias.

5 Empirical results

The testing is done one day at a time in a live-sample setting to make it as realistic as possible. The model is fitted to the first t observations of the MSCI World index, assigning most weight to the most recent observations.¹¹ Based on the estimated parameters, the probability that on day t the market was in the high- and low-volatility states, respectively, is estimated.¹² The asset allocation remains unchanged if the certainty of the estimate does not exceed the threshold

¹¹An asymptotic memory length of 520 days is used when estimating the parameters (see Nystrup et al. 2017b).

¹²As the states are highly persistent ($\gamma_{ii} \gg 0.5$), the most likely state on day $t + 1$ will be the same state that was estimated to be most likely on day t .

of 0.9998. The closing price on day $t + 1$ is then included in the sample, the model is re-estimated, and the state probabilities for day t are estimated based on knowledge of the closing price on day $t + 1$. This procedure is repeated sequentially by including the observations, one at a time, until the certainty of the estimate exceeds the threshold and the state on day t can be classified.

Once the certainty exceeds the threshold and the state on day t has been classified based on knowledge of the first T observations, the asset allocation can be updated. If the estimated state on day t is different from the state that the current asset allocation is based on, then the allocation is changed based on the closing price at day $T + 1$ —that is, there is assumed to be a one-day delay in the implementation. Otherwise the asset allocation remains unchanged. If, based on knowledge of the first T observations, the states on day t and $t + 1$ can be classified simultaneously, then it is the state on day $t + 1$ that determines whether the asset allocation is changed.

When as many observations as possible have been classified based on knowledge of the first T observations, then the closing price on day $T + 1$ is included in the sample and the model is re-estimated. It is then the next day in the sequence that has to be classified—for instance, $t + 2$, if, based on knowledge of the first T observations, the states on day t and $t + 1$ were classified. This procedure is repeated sequentially by including the observations, one at a time, from January 1, 1998 all the way through the sample.¹³ The portfolio is rebalanced only when the allocation changes from risk-on to risk-off or vice versa.

¹³The log-returns from 1997 are used for initialization.

5.1 Dynamic allocation or diversification

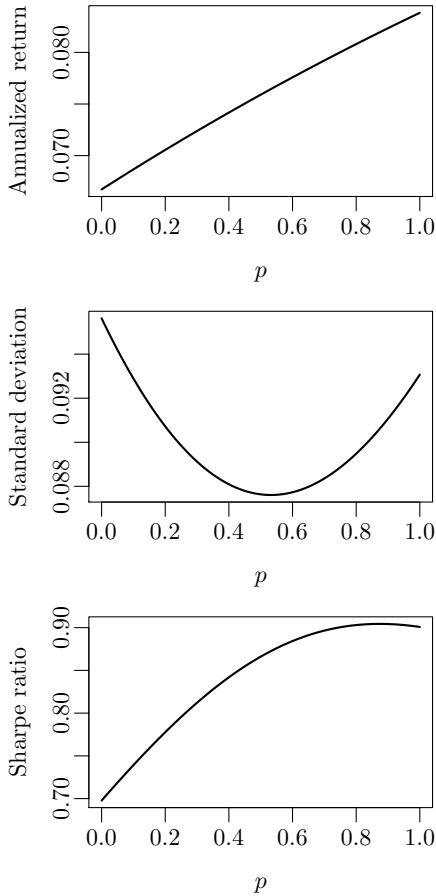


Figure 6: Annualized return, standard deviation, and Sharpe ratio as a function of the percentage of the portfolio that is allocated to the regime-based strategy.

Figure 6 shows the annualized return, standard deviation, and Sharpe ratio as a function of the percentage p of the portfolio that is allocated to the RBAA strategy; $p = 0$ corresponds to the benchmark 60/40 SAA portfolio rebalanced at the change points. In terms of the rebalancing frequency of the benchmark portfolio, it turns out that annual rebalancing would have been better than quarterly or monthly. This is a lower frequency than institutional investors typically use and indicates the presence of momentum in the asset returns. Rebalancing at the change points, however, performed almost as well as annual rebalancing. By rebalancing the benchmark portfolio at the same points in time as the allocation of the RBAA portfolios changes, the timing has no impact on the relative performance.

The annualized return of the RBAA portfolio increases linearly as a function of p . The annualized standard deviation (adjusted for autocorrelation) is minimized when p is around 0.5, and the Sharpe ratio is maximized when p is approximately 0.8. Although this is when there are no transaction costs, adding 10 basis point transaction costs does not change the shape of the graphs. The value of p that maximizes the Sharpe ratio would be much smaller if it was only the weight of DM stocks and govern-

ment bonds that was adjusted dynamically, because the decline in diversification would be steeper. In summary, RBAA increases portfolio return, decreases portfolio risk, and, thus, leads to increased risk-adjusted returns.

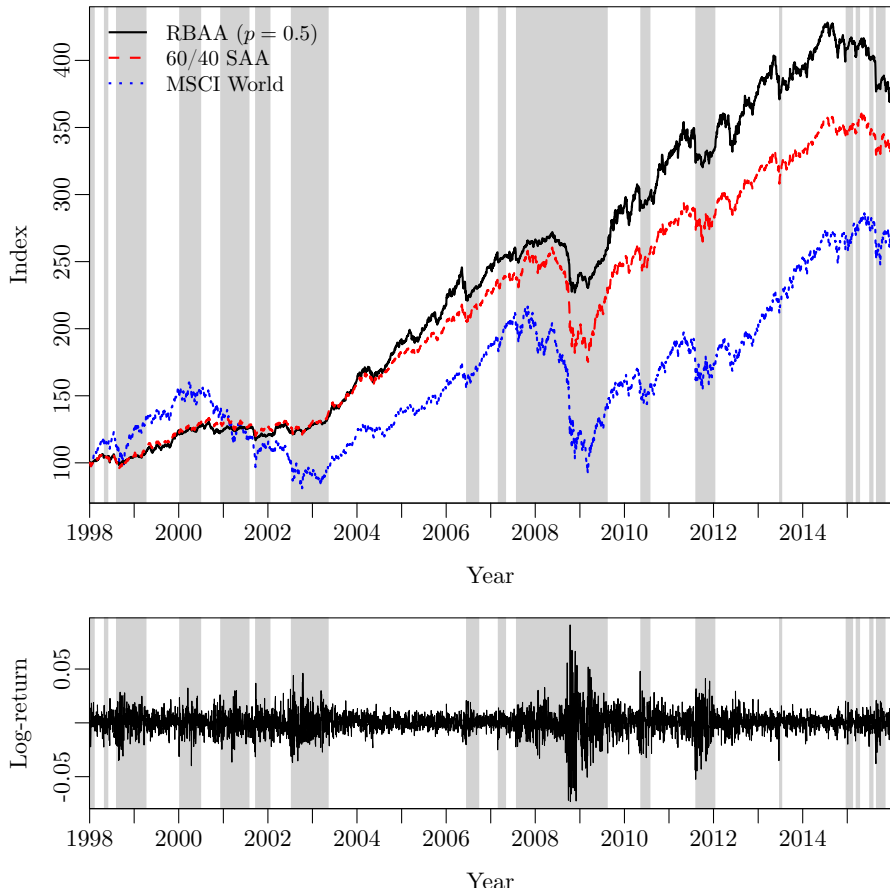


Figure 7: Development of RBAA strategy with $p = 0.5$ compared to 60/40 SAA portfolio and the MSCI World index across the inferred regimes. In the shaded, high-volatility periods, the allocation was risk-off.

5.2 Performance across the inferred regimes

In figure 7, the development of the RBAA strategy with $p = 0.5$ is compared to the 60/40 SAA portfolio and the MSCI World index over the period from 1998 to 2015. In the shaded periods, the allocation was risk-off. The 60/40 portfolio is in fact a suitable benchmark for this period, as it turns out that the RBAA strategy was risk-on 61% of the time—that is, the two portfolios had almost the same average allocation to fixed income.

The inferred regimes seem intuitive when looking at the log-returns of the MSCI World index in the lower panel of figure 7. A total of 34 regime changes are

	RBAA($p = 0.5$)	RBAA($p = 0.8$)	SAA
Annualized return	0.076	0.081	0.067
Standard deviation	0.088	0.089	0.096
Sharpe ratio	0.87	0.90	0.70
Maximum drawdown	0.17	0.18	0.30
Calmar ratio	0.46	0.46	0.22
Annual turnover	0.92	1.47	0.05

Table 8: Performance of RBAA portfolios compared to 60/40 SAA portfolio with rebalancing at the change points.

detected over the 18-year period. The length of the identified regimes varies considerably from a few weeks up to four years, which is different from what would be expected if the regimes were based on a business-cycle indicator.

The RBAA strategy with $p = 0.5$ outperforms both the 60/40 benchmark and the MSCI World index, when there are no transaction costs. The outperformance relative to the benchmark portfolio begins in 2003 and then slowly accumulates all the way through the crisis in 2008. Part of the outperformance is lost in the first half of 2009 when the market rebounds and the RBAA portfolio is still risk-off. Once the allocation is changed to risk-on in the second half of 2009, the RBAA strategy again starts to outperform the benchmark. In 2015, however, the RBAA strategy underperformed the SAA portfolio.

In table 8, the performance of the RBAA portfolio with $p = 0.5$ and $p = 0.8$, respectively, is compared to the 60/40 SAA portfolio rebalanced at the change points over the period 1998–2015. Recall from figure 6 that $p = 0.5$ was the percentage that minimized the standard deviation and the Sharpe ratio was maximized around $p = 0.8$. Although the annual turnover of the RBAA strategies is much higher than that of the benchmark portfolio, the Sharpe ratios exceed that of the SAA portfolio as long as transaction costs do not exceed 79 and 60 basis points per one-way transaction, respectively.

In addition, the maximum drawdown of the RBAA portfolios is much smaller than that of the SAA portfolio. This means that the Calmar ratio, which is the annualized return divided by the maximum drawdown, is more than twice as high for the RBAA portfolio than for the SAA portfolio.

5.3 Comparison with other approaches

In table 9, the performance of the RBAA portfolio with $p = 0.5$ and the SAA portfolio is compared with two other RBAA approaches. The first is based on the median filter that Bulla et al. (2011) applied to filter the state probabilities instead of the online step algorithm. The inferred state on day t is the median

	RBAA($p = 0.5$)	SAA	Median filter	EWMA
Annualized return	0.076	0.067	0.079	0.055
Standard deviation	0.088	0.096	0.103	0.094
Sharpe ratio	0.87	0.70	0.76	0.59
Maximum drawdown	0.17	0.30	0.21	0.23
Calmar ratio	0.46	0.22	0.38	0.25
Annual turnover	0.92	0.05	1.06	3.02

Table 9: Performance of RBAA portfolio and 60/40 SAA portfolio with rebalancing at the change points compared to a median filter and an EWMA approach. A percentage $p = 0.5$ of the portfolio was allocated to the RBAA strategy in all three cases.

of the most likely states over the last 21 days.¹⁴ The Sharpe ratio is almost the same regardless of whether the number of days is 5 or 21 (one week or one month), but the annual turnover is much higher when fewer days are considered.

The average allocation of the median-filter approach is 71% risk-on and 29% risk-off, meaning that the 60/40 SAA portfolio is not a suitable benchmark for this approach. Despite the lower average exposure to fixed income, the median-filter approach realizes a higher Sharpe ratio than that of the SAA portfolio. It relies on the same HMM as the RBAA portfolio to distinguish between market regimes, but realizes a lower Sharpe ratio with a higher turnover.

The second strategy is based on an exponentially-weighted moving average (EWMA) of the standard deviation of the MSCI World index. When the EWMA rises above its 60% quantile, the allocation is changed to risk-off, and when it falls below its 60% quantile, the allocation is changed to risk-on. By design, the average allocation of the RBAA strategy based on the EWMA is 60/40. The annual turnover is highly dependent on the memory length of the EWMA. Table 9 shows the result when using an effective memory length of 21 days. This value yields a reasonable tradeoff between Sharpe ratio (before transaction costs) and turnover.

The basic idea of the EWMA approach—to reduce risk exposure whenever higher volatility has been observed for a while—is the same as for the other RBAA approaches; however, it realizes a lower Sharpe ratio than does the SAA portfolio. The comparison emphasizes the value of the HMM for distinguishing between market regimes and the online step algorithm for filtering the regime probabilities.

¹⁴The inferred state on day t is $\widehat{X}_t^f = \left[\text{median} \left(\widehat{X}_{t-20}, \widehat{X}_{t-19}, \dots, \widehat{X}_t \right) \right]$, where $[\cdot]$ maps every number to its integer part and $\widehat{X}_t = \arg \max_i \Pr(X_t = i | Y_1, Y_2, \dots, Y_t)$.

6 Conclusion

The empirical results showed that regime-based asset allocation is profitable, even when compared to a diversified benchmark portfolio in a multi-asset universe. The proposed strategy was based on adjusting the weight of risky assets relative to safe assets (fixed income) to maintain a minimum level of diversification in all regimes.

The results are robust, because they are based on available market data with no assumptions about equilibrium returns, volatilities, correlations, or the ability to forecast their future values. As the parameters of the hidden Markov model used to identify the regimes were updated every day, the same approach should work in other time periods as well. It will remain a possibility for future research to try to improve the performance by including information from other asset classes, economic variables, interest rates, investor sentiment surveys, or other possible indicators.

The benchmark portfolio was chosen to mimic a 60/40 long-only SAA portfolio of an institutional investor to make the comparison as realistic as possible. The performance of RBAA was analyzed as a function of the percentage of the portfolio that was allocated dynamically. In order to minimize the portfolio standard deviation, 50% had to be allocated to the regime-based strategy. This corresponded to an 80/20 allocation in the low-volatility regimes and a 30/70 allocation in the high-volatility regimes. The lower standard deviation combined with a higher return led to an improved Sharpe ratio compared to the static, fixed-weight benchmark. Even more remarkable was the improvement in the ratio of average return to maximum drawdown, as this ratio more than doubled when allocating half of the portfolio dynamically.

The results have important implications for portfolio managers with a medium-to long-term investment horizon. The percentage of a multi-asset portfolio that, with advantage, can be allocated dynamically is strongly dependent on the effectiveness of the regime-detection process. Rebalancing to a static benchmark is not optimal, however, when market regimes are persistent. It is definitely worth considering a more dynamic approach to asset allocation, if only to reduce the tail risk.

References

- Ang, A. and G. Bekaert. "International asset allocation with regime shifts." *Review of Financial Studies*, vol. 15, no. 4 (2002), pp. 1137–1187.
- Ang, A. and G. Bekaert. "How regimes affect asset allocation." *Financial Analysts Journal*, vol. 60, no. 2 (2004), pp. 86–99.

- Ang, A. and A. Timmermann. "Regime changes and financial markets." *Annual Review of Financial Economics*, vol. 4, no. 1 (2012), pp. 313–337.
- Brunnermeier, M. K. and L. H. Pedersen. "Market liquidity and funding liquidity." *Review of Financial Studies*, vol. 22, no. 6 (2009), pp. 2201–2238.
- Bulla, J. "Hidden Markov models with t components. Increased persistence and other aspects." *Quantitative Finance*, vol. 11, no. 3 (2011), pp. 459–475.
- Bulla, J. and I. Bulla. "Stylized facts of financial time series and hidden semi-Markov models." *Computational Statistics & Data Analysis*, vol. 51, no. 4 (2006), pp. 2192–2209.
- Bulla, J., S. Mergner, I. Bulla, A. Sesboüé, and C. Chesneau. "Markov-switching asset allocation: Do profitable strategies exist?" *Journal of Asset Management*, vol. 12, no. 5 (2011), pp. 310–321.
- Cohn, A., J. Engelmann, E. Fehr, and M. A. Maréchal. "Evidence for counter-cyclical risk aversion: an experiment with financial professionals." *American Economic Review*, vol. 105, no. 2 (2015), pp. 860–885.
- DeMiguel, V., L. Garlappi, and R. Uppal. "Optimal versus naive diversification: How inefficient is the $1/N$ portfolio strategy?" *Review of Financial Studies*, vol. 22, no. 5 (2009b), pp. 1915–1953.
- Goyal, A., A. Ilmanen, and D. Kabiller. "Bad habits and good practices." *Journal of Portfolio Management*, vol. 41, no. 4 (2015), pp. 97–107.
- Guidolin, M. and A. Timmermann. "Asset allocation under multivariate regime switching." *Journal of Economic Dynamics and Control*, vol. 31, no. 11 (2007), pp. 3503–3544.
- Kinlaw, W., M. Kritzman, and D. Turkington. "The divergence of high- and low-frequency estimation: Implications for performance measurement." *Journal of Portfolio Management*, vol. 41, no. 3 (2015), pp. 14–21.
- Kritzman, M. and Y. Li. "Skulls, financial turbulence, and risk management." *Financial Analysts Journal*, vol. 66, no. 5 (2010), pp. 30–41.
- Kritzman, M., S. Page, and D. Turkington. "Regime shifts: Implications for dynamic strategies." *Financial Analysts Journal*, vol. 68, no. 3 (2012), pp. 22–39.
- Mandelbrot, B. "The variation of certain speculative prices." *Journal of Business*, vol. 36, no. 4 (1963), pp. 394–419.
- Narasimhan, M., P. Viola, and M. Shilman. "Online decoding of Markov models under latency constraints." In *Proceedings of the 23rd International Conference on Machine Learning* (2006), pp. 657–664.

- Nystrup, P., B. W. Hansen, H. Madsen, and E. Lindström. "Regime-based versus static asset allocation: Letting the data speak." *Journal of Portfolio Management*, vol. 42, no. 1 (2015a), pp. 103–109.
- Nystrup, P., H. Madsen, and E. Lindström. "Stylised facts of financial time series and hidden Markov models in continuous time." *Quantitative Finance*, vol. 15, no. 9 (2015b), pp. 1531–1541.
- Nystrup, P., H. Madsen, and E. Lindström. "Long memory of financial time series and hidden Markov models with time-varying parameters." *Journal of Forecasting*, vol. 36, no. 8 (2017b), pp. 989–1002.
- Rydén, T., T. Teräsvirta, and S. Åsbrink. "Stylized facts of daily return series and the hidden Markov model." *Journal of Applied Econometrics*, vol. 13, no. 3 (1998), pp. 217–244.
- Sheikh, A. Z. and J. Sun. "Regime change: Implications of macroeconomic shifts on asset class and portfolio performance." *Journal of Investing*, vol. 21, no. 3 (2012), pp. 36–54.
- Siegel, J. J. "Does it pay stock investors to forecast the business cycle?" *Journal of Portfolio Management*, vol. 18, no. 1 (1991), pp. 27–34.
- Viterbi, A. J. "Error bounds for convolutional codes and an asymptotically optimum decoding algorithm." *IEEE Transactions on Information Theory*, vol. 13, no. 2 (1967), pp. 260–269.

PAPER E

Originally published in the *Journal of Asset Management*

Detecting change points in VIX and S&P 500: A new approach to dynamic asset allocation

Peter Nystrup, Bo William Hansen, Henrik Madsen,
and Erik Lindström

Abstract

The purpose of dynamic asset allocation is to overcome the challenge that changing market conditions present to traditional strategic asset allocation by adjusting portfolio weights to take advantage of favorable conditions and reduce potential drawdowns. This article proposes a new approach to dynamic asset allocation that is based on detection of change points without fitting a model with a fixed number of regimes to the data, without estimating any parameters, and without assuming a specific distribution of the data. It is examined whether dynamic asset allocation is most profitable when based on changes in the CBOE Volatility Index (VIX) or change points detected in daily returns of the S&P 500 index. In an asset universe consisting of the S&P 500 index and cash, it is shown that a dynamic strategy based on detected change points significantly improves the Sharpe ratio and reduces the drawdown risk when compared to a static, fixed-weight benchmark.

Keywords: Regime changes; Change-point detection; Dynamic asset allocation; Volatility regimes; Daily returns; Nonparametric statistics.

1 Introduction

The financial crisis of 2007–2008 resulted in large losses for most static portfolios, leading to increased interest in dynamic approaches to asset allocation. The market ructions during the beginning of 2016 are a recent example of how abruptly the behavior of financial markets can change. Although some changes may be transitory, the new behavior often persists for several months after a change (Ang and Timmermann 2012). The mean, volatility, and correlation patterns in stock returns, for example, changed dramatically at the start of, and persisted through the crisis of 2007–2008.

Changes in market dynamics present a big challenge to traditional strategic asset allocation (SAA) that seeks to develop static “all-weather” portfolios that

optimize efficiency across a range of scenarios. The purpose of dynamic asset allocation (DAA) is to take advantage of favorable market conditions and reduce potential drawdowns by adjusting portfolio weights as new information arrives (Sheikh and Sun 2012). DAA is distinct from tactical asset allocation (TAA). While the latter relies on forecasting, DAA is based on reacting to changes in market conditions. The goal of DAA is not to predict change points or future market movements, but to identify when a regime shift has occurred and then benefit from persistence of equilibrium returns and volatilities.

Some approaches to DAA exploit the relationship between observed regimes in financial markets and the phases of the business cycle while other approaches are based solely on market data. Regime-switching models, such as the hidden Markov model (HMM), are a popular choice for modeling the hidden state of financial markets because they are able to reproduce stylized facts of financial returns, including volatility clustering and leptokurtosis (see, e.g., Rydén et al. 1998, Nystrup et al. 2017b). Furthermore, the inferred states can often be linked to phases of the business cycle (see Guidolin and Timmermann 2007). Several studies have shown the profitability of DAA strategies based on regime-switching models (see, e.g., Guidolin and Timmermann 2007, Bulla et al. 2011, Kritzman et al. 2012, Nystrup et al. 2015a).

A DAA strategy has two components: a method for detecting change points and a strategy for changing the portfolio when a change point has been detected. In case of a strategy based on a regime-switching model the two components fuse as the asset allocation is typically fully determined by the inferred regime. The pivotal question then becomes, how many regimes are needed and whether the regimes can be assumed to be stationary. Assuming a fixed number of regimes (typically between two and four) based on economic motivations, as it has often been done in the literature (see Guidolin 2011b), is unlikely to be optimal.

The approach taken in this article is very different. It is based on detection of change points without fitting a model with a fixed number of regimes to the data, without estimating any parameters, and without assuming a specific distribution of the data. The change points will not necessarily correspond to turning points in the business cycle. When a change point has been detected, the only knowledge of the new regime is the observations encountered between the change point and the time of detection. The portfolio adjustment is determined independently of the change-point detection.

This article presents a new approach to DAA. It examines whether DAA based on nonparametric change-point detection can provide better long-term results when compared to static, fixed-weight portfolios. The focus will be on stock returns as portfolio risk is typically dominated by stock market risk. It will be examined whether to test for location, scale, or more general distributional changes; and whether the CBOE Volatility Index (VIX) or past returns of the S&P 500 index yield the best proxy for the prevailing regime. Finally, it will be

examined whether DAA is most profitable when based on changes in the VIX or change points detected in daily returns of the S&P 500 index. The VIX is considered due to its forward-looking nature which will be discussed in the next section before introducing change-point detection and the empirical results in the following sections.

2 VIX and S&P 500

The CBOE Volatility Index (VIX), introduced by the Chicago Board Options Exchange (CBOE) in 1993, is an important benchmark for stock market volatility. The VIX estimates expected market volatility by averaging weighted prices of 30-calendar-day S&P 500 options over a range of strike prices. It considers a model-free estimator of implied volatility and, thus, does not depend on any particular option pricing framework.¹ The VIX essentially offers a market-determined, forward-looking estimate of one-month stock market volatility and is regarded as an indicator of market stress; the higher the VIX, the greater the fear (Whaley 2000).

There is a significantly negative relationship between changes in the VIX and contemporaneous returns of the S&P 500 index as depicted in figure 1. The negative correlation between stock returns and implied volatility captures the leverage effect first discussed by Black (1976). Racicot and Théoret (2016) found that the VIX imbeds many properties of other macroeconomic and financial uncertainty measures such as the growth of industrial production, the growth of consumer credit, long-term interest rates, term spreads, etc.

In figure 2, the VIX is compared to the realized volatility of the S&P 500 index one-month ahead.² It is evident that the VIX has had a persistent bias over realized volatility. The VIX is not a pure forecast, it is the price of volatility and, as such, includes a risk premium that varies over time. A negative risk premium for volatility partly explains the bias.

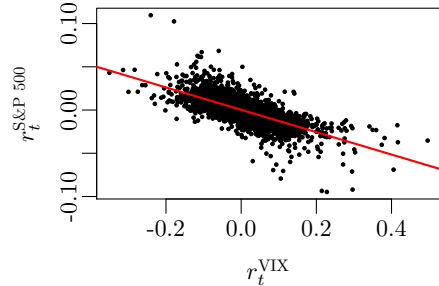


Figure 1: The leverage effect illustrated by contemporaneous log-returns of the VIX and the S&P 500 index.

¹The details of the computations are available at <http://www.cboe.com/micro/vix/vixwhite.pdf>.

²The realized volatility is calculated, in accordance with the methodology used by S&P Dow Jones Indices, as $RV_t = 100 \times \sqrt{12 \sum_{i=t-20}^t \log(P_i/P_{i-1})^2}$, where P_t is the closing price of the index on day t and \log is the natural logarithm.

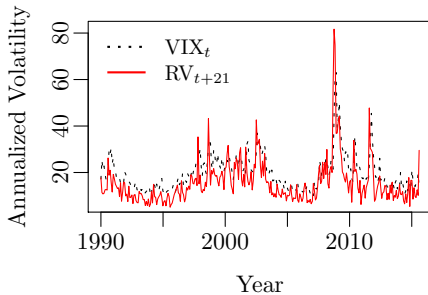


Figure 2: The VIX and the realized volatility of S&P 500 one-month ahead. Only one observation per month is shown.

From figure 2, it appears that spikes in realized volatility are followed by spikes in the VIX. Andersen et al. (2007) showed that monthly volatility forecasts based on past realized volatility are more efficient than the VIX model-free implied volatility. It may, however, still be the case that the VIX provides earlier signals about change points than past returns of the S&P 500 index.

The data analyzed is 6,485 daily log-returns of the VIX and the S&P 500 index covering the period from January 1990 through September 2015.

Figure 3 shows the two indices³ together with their log-returns.⁴ The volatility forms clusters as large movements tend to be followed by large movements and vice versa, as noted by Mandelbrot (1963).⁵ This is most pronounced in the log-returns of the S&P 500 index, although it can be seen in the VIX series as well.

The volatility of the VIX appears to be higher when the level of the VIX is high. Persistence in the volatility of the VIX corresponds to persistence in the kurtosis of the S&P 500 returns, as the second moment of the VIX corresponds to the fourth moment of the S&P 500 returns. DAA aims to exploit this persistence of the volatility, as risk-adjusted returns, on average, are substantially lower during turbulent periods, irrespective of the source of turbulence, as shown by Kritzman and Li (2010).

The log-return series are characterized by a large number of exceptional observations. Table 4 shows the first four moments of the log-returns of the two indices. The moments of the two return series are quite different, but the kurtosis is well above three for both series implying that the tails of the unconditional distributions are heavier than those of the Gaussian distribution. Assuming the data is Gaussian would cause occasional large values to be interpreted as change points, even though they should more correctly be classified as outliers, as discussed by Ross (2013).

³The S&P 500 index has been rescaled to start at 100 on January 2, 1990.

⁴The log-returns are calculated using $r_t = \log(P_t/P_{t-1})$.

⁵A quantitative manifestation of this fact is that while returns themselves are uncorrelated, absolute and squared returns display a positive, significant, and slowly decaying autocorrelation function.

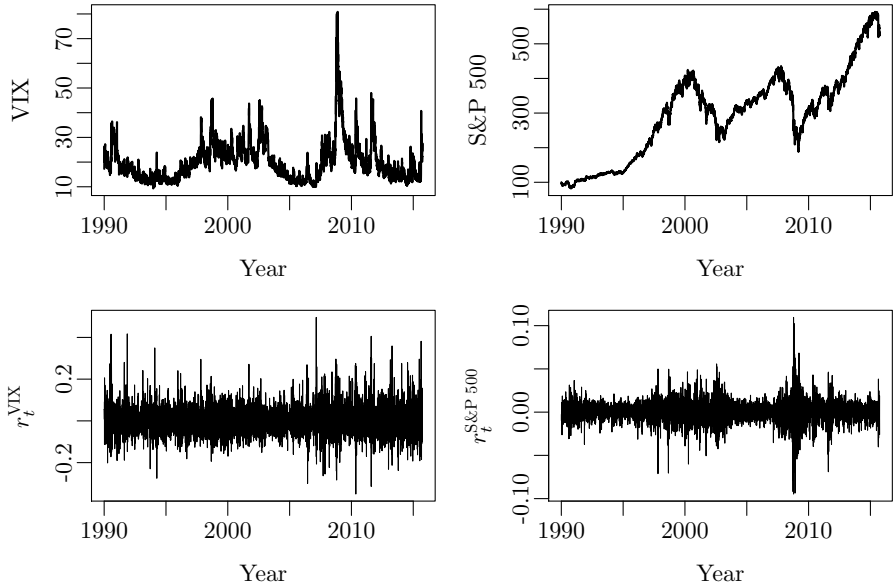


Figure 3: The VIX, the S&P 500 index, and their daily log-returns.

	VIX	S&P 500
Mean	0.000054	0.00026
Standard deviation	0.063	0.011
Skewness	0.69	-0.24
Kurtosis	7.2	11.7

Table 4: First four moments of the log-returns.

3 Change-point detection

A frequently used analogy for financial returns in the case of regime-switching models is that of a person's heart rate. While the person sleeps, a low average heart rate with low volatility is observed. When the person wakes up, there is a sudden rise in the heart rate's average level and its volatility. Without actually seeing the person, it can reasonably be concluded based on observations of the heart rate whether he or she is awake or sleeping. Rather than distinguishing between a fixed number of states, such as awake or sleeping, the aim of change-point detection is to detect when the distribution of the heart rate changes.

Change-detection problems, where the goal is to monitor for distributional shifts in a sequence of time-ordered observations, arise in many diverse areas. They have been studied extensively within the field of statistical process control where

the goal is to monitor the quality characteristics of an industrial process in order to detect and diagnose faults.

The task is to detect whether a data sequence contains a change point. If no change point exists, the observations are assumed to be identically distributed. If a change point exists at time τ , then the observations are distributed as:

$$X_i \sim \begin{cases} F^0 & \text{if } i < \tau, \\ F^1 & \text{if } i \geq \tau. \end{cases} \quad (1)$$

In other words, the variables are assumed iid with some distribution F^0 before the change point at $t = \tau$ and iid with a different distribution F^1 after. The location of the change point is unknown, and the problem is to detect it as soon as possible. The change-point methodology can also be applied to sequences that are not iid between change points, by first modeling the data sequence in a way that yields iid one-step-ahead forecast residuals and then performing change detection on these (Ross et al. 2011).

Most traditional approaches to change detection assume that the distributional form of the data is known before and after the change with only the parameters being unknown. Classical methods for this problem include the CUSUM method (Page 1954), exponentially-weighted moving-average charts (Roberts 1959), and generalized likelihood ratio tests (Siegmund and Venkatraman 1995). This assumption, however, rarely holds in sequential applications. Typically, there is no prior knowledge of the true distribution or assumptions made about the distribution may be incorrect.

A nonparametric approach

The nonparametric (distribution-free) change detection approach applied in this article is based on Ross et al. (2011) and the implementation by Ross (2015). It does not assume that anything is known about the distribution of the data before monitoring begins; it is thus an example of a self-starting technique. The main advantage of the approach being self-starting is that it can be deployed out-of-the-box without the need to estimate parameters of the data distribution from a reference sample prior to monitoring.

In a typical setting, a sequence of observations x_1, x_2, \dots are received from the random variables X_1, X_2, \dots . The distribution of X_i is given by (1), conditional on the change point τ which the task is to detect. Suppose t points from the sequence have been observed. For any fixed $k < t$ the hypothesis that a change point occurred at the k th observation can be written as

$$H_0 : \forall i \ X_i \sim F_0, \quad H_1 : X_i \sim \begin{cases} F_0 & \text{if } i < k, \\ F_1 & \text{if } i \geq k. \end{cases}$$

A two-sample hypothesis test can be used to test for a change point at k . Let $D_{k,t}$ be an appropriately chosen test statistic. For example, if the change is assumed to take the form of a shift in location and the data is assumed to be Gaussian, then $D_{k,t}$ will be the statistic associated with the usual t -test. If $D_{k,t} > h_{k,t}$ for some appropriately chosen threshold $h_{k,t}$, then a change is detected at location k . As no information is available concerning the location of the change point, $D_{k,t}$ has to be evaluated at all values of $1 < k < t$. If

$$D_{\max,t} = \max_k D_{k,t}, \quad (2)$$

then the hypothesis that no change has occurred before the t th observation is rejected if $D_{\max,t} > h_t$ for some threshold h_t . The estimate $\hat{\tau}$ of the change point is then the value of k which maximizes $D_{k,t}$. This formulation provides a general method for nonsequential change-point detection on a fixed size dataset. It can also be applied in the case where points are sequentially arriving over time, by repeatedly recomputing the test statistic as each new observation is received.

When the task is to detect a change in a data sequence where no information is available regarding the pre- or post-change distribution, the approach of Ross et al. (2011) is to replace $D_{k,t}$ with a nonparametric two-sample test statistic that can detect arbitrary changes in a distribution. The algorithm would proceed as above, with this statistic evaluated at every time point, and the maximum value being compared to a threshold h_t . In many situations a more powerful test can be found by restricting attention to the case when the pre-change distribution F_0 undergoes a change in either location or scale:

- Location Shift: $F_1(x) = F_0(x + \delta)$.
- Scale Shift: $F_1(x) = F_0(\delta x)$.

This corresponds to a change in either the mean or volatility of financial returns. Although it is slightly more restricted than testing for arbitrary changes, in practice any change in F_0 is likely to cause a shift in location or scale, and thus can be detected.

Nonparametric change detection is typically perceived to be less powerful than parametric change detection, but Ross et al. (2011) showed that, although parametric Gaussian change detection using the t - and F -test outperforms the nonparametric methods when detecting larger sized changes in the parameters of a Gaussian distribution, the difference in performance is not excessive, and the nonparametric tests actually outperform for smaller sized changes. For heavy-tailed data the nonparametric methods significantly outperform the parametric Gaussian methods.

Of the nonparametric test statistics that were considered for this article, the tests that—in agreement with Ross et al. (2011)—were found to be most powerful are the Mann–Whitney test for changes in location (Mann and Whitney 1947), the Mood test for changes in scale (Mood 1954), and the Lepage test for joint monitoring of changes in location and scale (Lepage 1971). The Cramér–von Mises and Kolmogorov–Smirnov tests (see Ross and Adams 2012) were also considered, but they were found to be slower at detecting distributional changes when compared to the Lepage test.

The mentioned tests use only the rank of the observations.⁶ The Mood test (Mood 1954), for example, is based on the observation that if $n = n_A + n_B$ points are spread over two samples A and B , then assuming no tied ranks, the expected rank of each point under the null hypothesis that both samples are identically distributed is $(n + 1)/2$. The Mood test uses a test statistic which measures the extent to which the rank of each observation deviates from the expected value:

$$M' = \sum_{x_i \in A} (r(x_i) - (n + 1)/2)^2, \quad (3)$$

where $r(x_i)$ denotes the rank of x_i in the pooled sample.

The distribution of the Mood statistic is independent of the distribution of the underlying random variables with mean and variance

$$\mu_{M'} = n_A(n^2 - 1)/12, \quad \sigma_{M'}^2 = n_A n_B (n + 1)(n^2 - 4)/180.$$

Taking the absolute value of the standardized test statistic

$$M = |(M' - \mu_{M'})/\sigma_{M'}| \quad (4)$$

ensures that both increases and decreases in scale can be detected.

4 Empirical results

The empirical testing shows that the best result is obtained by focusing on shifts in the scale parameter. It is not surprising that there is little information in the mean values (see, e.g., Merton 1980). Testing for more general distributional changes leads to approximately the same change points being identified with a larger detection delay compared to when focusing on shifts in scale. This finding applies to both the VIX and the S&P 500 return series.

⁶The rank of the i th observation at time t is defined as $r(x_i) = \sum_{i \neq j}^t I(x_i \geq x_j)$, where I is the indicator function.

In order to avoid a large number of false alarms the expected time between false positive detections, also referred to as the average run length, is set to 10,000. The choice of average run length is a tradeoff between false positive detections and the delay in detecting changes. A total of 27 change points are detected in each of the two series when using the Mood test for changes in scale (Mood 1954) as implemented by Ross (2015).

The detected change points are compared in figure 5. Every second regime is shaded to make it easier to identify the change points. There is no further information in the shading. The detected change points seem very intuitive when shown together with the S&P 500 returns due to the distinct volatility clusters, while the change points detected in the log-returns of the VIX seem more intuitive when shown together with the index. The distance between the change points varies considerably from a few days up to six years. This is different from what would be expected if the change points were based on a business cycle indicator.

Although it is interesting in itself to analyze the change points, it is the times of detection that really matter. It is not possible to conclude whether changes in the VIX or past returns on the S&P 500 index yield the earliest signal about change points as not all the detected change points coincide. The next step is, therefore, to implement and test a dynamic asset allocation strategy based on the detected change points in order to determine which of the indices provides the most profitable signals.

4.1 Test procedure

The testing is done one day at a time in a live-sample setting to make it as realistic as possible. The first 21 observations, corresponding to one month, are used to determine the initial allocation. From that point onwards it is tested each day whether a change point has occurred. If a change point is detected to have happened on day $\tau < t$ after the log-return of the index on day t has been added to the sample, then the observations from the time of the change

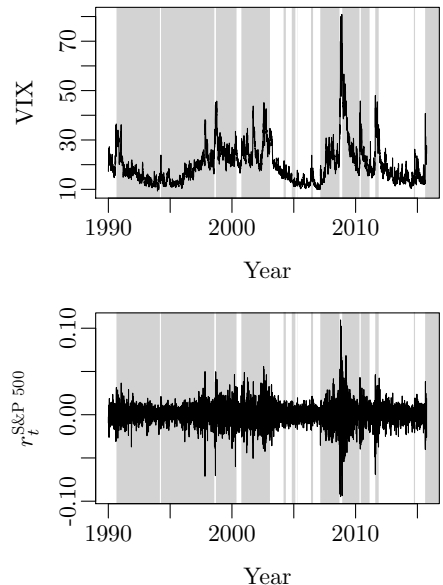


Figure 5: Comparison of the change points detected in the VIX and the S&P 500 log-returns.

point τ until the time of the detection t are used to estimate the volatility in the new regime. If, based on the new estimate of the volatility, the allocation to the stock index changes, then the new allocation is implemented at the closing of day $t + 1$, i.e., there is assumed to be a one-day delay in the implementation. The asset allocation remains unchanged otherwise. The closing level on day $t + 1$ is then included in the sample and it is tested whether a new change point has occurred. The portfolio is not rebalanced until the next change point is detected.

Upon the detection of a change point, the volatility is estimated as the square root of an exponentially-weighted moving average of the past variance

$$\text{EWMA}_t = \lambda \text{EWMA}_{t-1} + (1 - \lambda) r_t^2. \quad (5)$$

The forgetting parameter λ is set to 0.95, corresponding to an effective memory length of 20 trading days or roughly one month. This EWMA is found to be a better forecast of future, one-month volatility than the VIX.

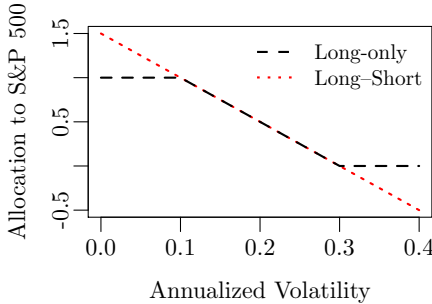


Figure 6: Two simple strategies where the allocation to S&P 500 is a function of the annualized volatility.

responds to the same allocation function with leverage and short-selling allowed. This strategy is referred to as Long–Short to distinguish it from the Long-only strategy. These strategies are likely not optimal, but attempting to optimize them may introduce a significant back-testing bias.

The tested strategies are fairly simple as the purpose is not to outline the optimal strategy but rather to discuss the profitability of a DAA approach based on change-point detection. Assuming the average long-term stock volatility is 20%, a simple strategy is to allocate 50% to stocks and 50% to cash when the volatility is 20%. If, instead, the volatility is 10%, then the entire portfolio is allocated to stocks. If the volatility is 30%, then the entire portfolio is allocated to cash. In figure 6, this simple (linear) long-only strategy with no leverage is shown as the dashed line. The dotted line corresponds to the same allocation function with leverage and short-selling allowed.

4.2 Performance of dynamic asset allocation strategies

S&P 500 change points. In table 7, the performance of the two dynamic strategies based on the S&P 500 change points is compared to the performance of the S&P 500 index and a static, fixed-weight portfolio. The static portfolio I is rebalanced daily to have a fixed allocation of 61% to the S&P 500 index which equals the average allocation of the Long-only strategy to the stock index

Index/Strategy	AR	SD	SR	MDD
S&P 500	0.071	0.18	0.39	0.57
Long-only strategy	0.056	0.09	0.62	0.31
Static portfolio I	0.047	0.11	0.43	0.39
Long–Short strategy	0.057	0.16	0.36	0.47

Table 7: Performance of two dynamic strategies based on the S&P 500 change points. The table summarizes the annualized return, standard deviation, Sharpe ratio, and maximum drawdown for the S&P 500 index, the two dynamic strategies based on the S&P 500 change points, and a static portfolio that has the same average exposure (61%) to the S&P 500 index as the Long-only strategy.

over the period from February 1990 through September 2015. The remaining 39% are allocated to cash which is assumed to yield zero interest.

The Long-only strategy has the highest Sharpe ratio (SR) with an annualized return (AR) of 5.6% and an annualized standard deviation (SD) of 9%.⁷ Although the realized return is lower than for the S&P 500 index, the SR is significantly higher. The Long–Short strategy has the same AR as the Long-only strategy but a higher SD and MDD, and, consequently, a lower SR.

The Long-only strategy has a lower SD and maximum drawdown⁸ (MDD) than the static portfolio I (that has the same average exposure to the S&P 500 index), but the realized return is higher as long as transaction costs do not exceed 188 basis points per one-way transaction. This is when ignoring the costs associated with rebalancing to static weights, so the break-even transaction cost is higher than 188 basis points.

Figure 8 shows the development of the Long-only strategy, the static portfolio I, and the S&P 500 index. The shaded areas show the Long-only strategy’s allocation to the stock index. The times of detection of the change points that result in allocation changes are visible from the plot. Based on the allocation changes the volatility forecasts can be inferred. There appears to be many different levels of volatility. The choice of not rebalancing the dynamic portfolio between change points tilts it towards a momentum strategy, but the effect appears to be moderate. In case of a short position, thought of as implemented using a futures contract, the effect of not rebalancing is the opposite, as the size of the short position increases when the index goes up and decreases when the index goes down.

Most of the Long-only strategy’s outperformance relative to the static, fixed-weight portfolio occurred during the financial crisis in 2008. It is clear why the

⁷Neither of the portfolio return series display enough autocorrelation that it is necessary to adjust the annualized standard deviations.

⁸The maximum drawdown is the largest relative decline from a historical peak in the index value.

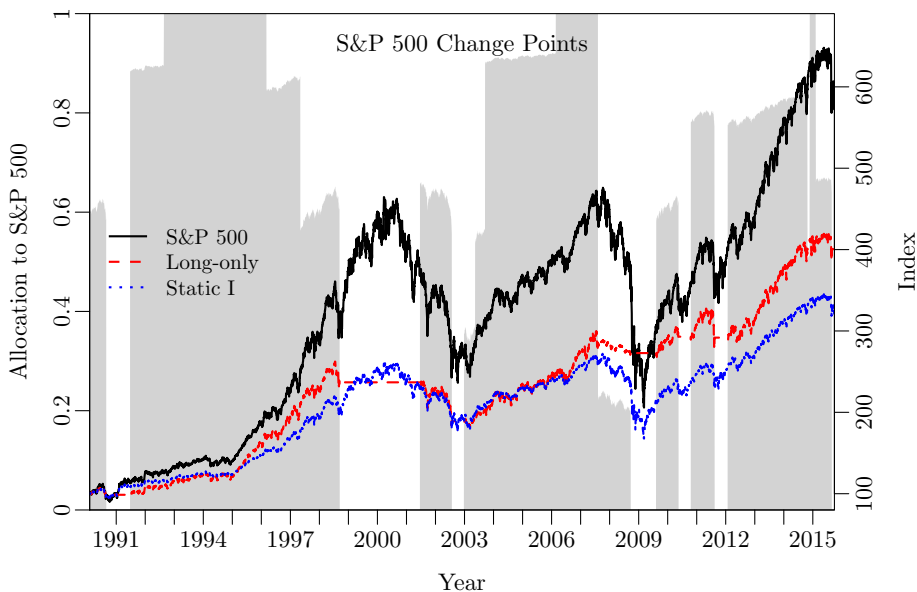


Figure 8: Development of the Long-only strategy based on the S&P 500 change points compared to a static, fixed-weight portfolio and the S&P 500 index (right axis). The shaded areas show the Long-only strategy's allocation to the S&P 500 index (left axis). The legends are sorted according to the final index value.

Long–Short strategy is not profitable as the Long-only strategy is primarily fully allocated to cash around the peak in 2000 and on the way out of the crisis in 2008, when the market rebounded.

VIX change points. Table 9 summarizes the performance of the same strategies when based on change points detected by analyzing the daily changes in the VIX. The static portfolio II has a fixed allocation of 64% to the S&P 500 index which equals the average allocation of the Long-only strategy to the stock index over the period.

The Long-only strategy has a higher AR and SR and a lower MDD than before. The AR is still lower than that of the index, but the difference is smaller. The AR of the Long-only strategy exceeds that of the static portfolio II as long as transaction costs do not exceed 372 basis points per one-way transaction.

The performance of the Long–Short strategy is similar to the index in terms of SR and it has a lower MDD. This is a significant improvement compared to when based on the S&P 500 change points, but it is still less profitable than the Long-only strategy.

Index/Strategy	AR	SD	SR	MDD
S&P 500	0.071	0.18	0.39	0.57
Long-only strategy	0.062	0.10	0.64	0.24
Static portfolio II	0.049	0.12	0.42	0.40
Long–Short strategy	0.059	0.15	0.40	0.37

Table 9: Performance of two dynamic strategies based on the VIX change points. The table summarizes the annualized return, standard deviation, Sharpe ratio, and maximum drawdown for the S&P 500 index, the two dynamic strategies based on the VIX change points, and a static portfolio that has the same average exposure (64%) to the S&P 500 index as the Long-only strategy.

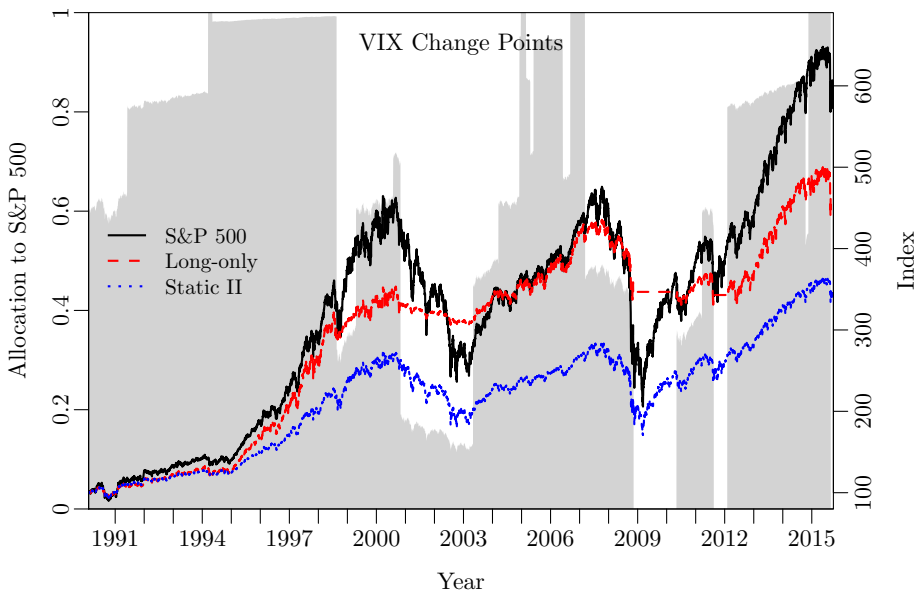


Figure 10: Development of the Long-only strategy based on the VIX change points compared to a static, fixed-weight portfolio and the S&P 500 index (right axis). The shaded areas show the Long-only strategy's allocation to the S&P 500 index (left axis). The legends are sorted according to the final index value.

Figure 10 shows the development of the Long-only strategy, the static portfolio II, and the S&P 500 index. It was evident from figure 5 that not all the change points are coinciding between the two series and by comparing figure 8 and figure 10 it appears that this is true for the detection times as well.

Compared to figure 8, the Long-only strategy based on the VIX change points performs better in the years leading up to the burst of the dot-com bubble in

year 2000. The allocation to S&P 500 is significantly reduced in 1998, around the same time as the allocation was reduced to zero when based on the S&P 500 change points, but the allocation is then increased to about 60% in 1999. This allocation is retained all the way to the peak in year 2000. Towards the peak in 2008, the Long-only strategy performs worse when based on the VIX change points. The allocation to S&P 500 is reduced for the first time already at the beginning of 2007, but it is not reduced all the way to zero until November 2008. In figure 8, the allocation was reduced to zero in September 2008, only a few days after Lehman Brothers filed for bankruptcy.

The superior performance of the Long-only strategy compared to the static portfolio II increases steadily towards the peak in year 2000, through the subsequent downturn, and towards the peak in year 2008. The difference in performance is then reduced over the following three years during the market rebound before it again increases. The outperformance is built up gradually through the 25-year period and does not come from the financial crisis in 2008, on the contrary, the gap in performance compared to the static portfolio shrunk a lot in the wake of the crisis.

4.3 Performance of switching strategies

Although the tested strategies are fairly simple, they can be made even simpler by only allowing one asset in the portfolio at a time. Rather than having the allocation to the S&P 500 index be a linear function of the forecasted volatility, the allocation is either 100% or 0% in the long-only case and 100% or -100% in the long-short case depending on whether the forecasted volatility is above or below 20%. This threshold is chosen based on the assumption that the average long-term stock volatility is 20%, which is an arbitrary choice. These simple switching strategies are similar to a regime-switching approach.

The testing of the switching strategies is carried out one day at a time in a live-sample setting exactly as before. The focus will be on the change points detected by analyzing the daily changes in the VIX, since the DAA strategies already tested were most profitable when based on these. Past returns of the S&P 500 index are still used to estimate the volatility upon the detection of a change point.

Table 11 summarizes the performance of the switching strategies based on the VIX change points. The static portfolio III is rebalanced daily to have a fixed allocation of 66% to the S&P 500 index, which equals the average allocation of the Long-only switching strategy to the stock index over the period.

The performance of the Long-only switching strategy is notable. Not only does it have a much higher SR and a significantly lower MDD than the S&P 500 index, it also has a higher realized return as long as transaction costs do not exceed 93 basis points per one-way transaction. This is under the assumption

Index/Strategy	AR	SD	SR	MDD
S&P 500	0.071	0.18	0.39	0.57
Long-only switching strategy	0.075	0.11	0.68	0.20
Static portfolio III	0.051	0.12	0.42	0.41
Long–Short switching strategy	0.074	0.15	0.50	0.44

Table 11: Performance of two switching strategies based on the VIX change points. The table summarizes the annualized return, standard deviation, Sharpe ratio, and maximum drawdown for the S&P 500 index, the two switching strategies based on the VIX change points, and a static portfolio that has the same average exposure (66%) to the S&P 500 index as the Long-only switching strategy.

that there is no interest on cash. The realized return of the Long-only switching strategy exceeds that of the static portfolio III as long as transaction costs do not exceed 627 basis points per one-way transaction and, at the same time, the MDD is less than half.

The Long–Short switching strategy is only rebalanced when the position changes from long to short or from short to long. This strategy also has a higher AR and a lower SD and MDD compared to the S&P 500 index. The SR of 0.50 is higher than that of the index, but it does not compare to that of the Long-only switching strategy.

Figure 12 shows the development of the Long-only switching strategy, the static portfolio III, and the S&P 500 index. The allocation is 100% whenever it was above 50% in figure 10 and 0% whenever it was below 50%.

Compared to the index, the switching strategy falls behind on the way towards the peak in year 2000, then it gets ahead during the subsequent downturn and retains its lead until the peak in year 2008 when the index catches up. The switching strategy gets far ahead during the crash in 2008 and the difference compared to the index is at its largest at the market trough in 2009. The lead almost diminishes during the turbulent second half of 2011, but the switching strategy retains a small lead all the way to the end of the sample. It is clear that if the big loss in 2008 was removed from the sample, the dynamic strategies would not outperform the index in terms of absolute return.

Compared to the static, fixed-weight portfolio, the Long-only switching strategy gradually extends its lead, with the exception of a few short periods, from the beginning of the sample to the market trough in 2009. The following three years the static portfolio regains some of the loss before the difference is again extended from 2012 to the end of the sample. The Long-only switching strategy is far in front of the static portfolio throughout the sample as evidenced by the break-even transaction cost of 627 basis points.

It is easy to get the impression from figure 12 that the applied change-point method is faster at detecting increases in the volatility than decreases, as the

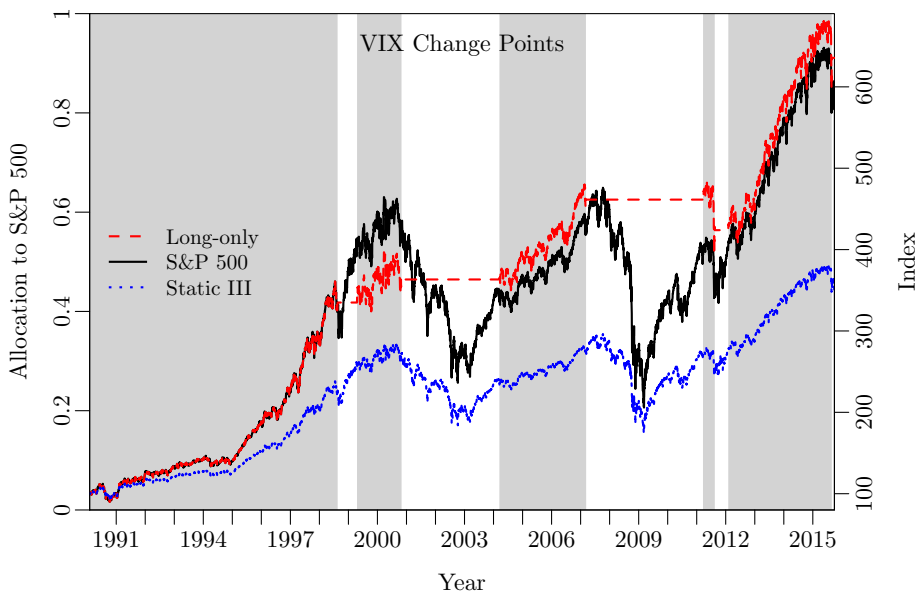


Figure 12: Development of the Long-only switching strategy based on the VIX change points compared to a static, fixed-weight portfolio and the S&P 500 index (right axis). The shaded areas show the Long-only strategy's allocation to the S&P 500 index (left axis). The legends are sorted according to the final index value.

switching strategy is much better at timing the downturns than the rebounds. The same conclusion was reached in Nystrup et al. (2015a) based on regimes inferred with an HMM with time-varying parameters. From a comparison with figure 10 it appears that the volatility remains high during the beginning of the rebound as the allocation is increased (to a level below 50%) sooner than it can be seen from figure 12. It is expected that gradual drift is harder to detect than abrupt changes.

4.4 Trading the VIX

Given the strong performance of the Long-only switching strategy based on the VIX change points, it is natural to wonder whether the performance can be replicated and possibly improved by trading the VIX itself. Instead of buying the S&P 500 when a change point is detected and the volatility is estimated to be below 20%, the replicating strategy would be to sell short-term VIX futures (see Ilmanen 2012, Whaley 2013, Simon and Campasano 2014).

As long as the volatility remains low, a short position will accrue a roll yield as the futures price converges to the spot price, reflecting the gap between realized

Index/Strategy	AR	SD	SR	MDD
S&P 500	0.044	0.21	0.21	0.57
Long-only switching strategy	0.045	0.09	0.47	0.18
VIX short-term futures inverse ER	0.117	0.64	0.18	0.92
Switching futures strategy	0.179	0.31	0.59	0.40

Table 13: Performance of two switching strategies based on the VIX change points. The table summarizes the annualized return, standard deviation, Sharpe ratio, and maximum drawdown for the S&P 500 index, the Long-only switching strategy, the S&P 500 VIX short-term futures inverse daily excess return index, and the switching futures strategy over the period from December 20, 2005 through September 30, 2015.

and implied volatility.⁹ When a new change point is detected and the volatility is estimated to be above 20%, the short position is terminated.

In table 13, the performance of the switching futures strategy is compared to the S&P 500 VIX short-term futures inverse daily excess return index, the Long-only switching strategy, and the S&P 500 index over the period from December 20, 2005 through September 30, 2015.¹⁰

The return from selling short-term VIX futures is more than three times as high as the return of the S&P 500 index and the Long-only strategy that switches in and out of S&P 500, but the strategy is also more volatile. The SR of the futures strategy is higher than that of the Long-only switching strategy when transaction costs are ignored. After accounting for transaction costs, the difference is most likely small, since the futures strategy involves more trading from rolling the short position (Whaley 2013).

5 Summary and discussion

The new approach to DAA presented in this article was based on sequential hypothesis testing to detect change points without fitting a model with a fixed number of regimes to the data, without estimating any parameters, and without making any assumptions about the distribution of the data. This approach is very robust given that it is not based on a model or any assumptions about the data that can change going forward. It is a useful tool for dividing financial time series into regimes without making any assumptions about the number of regimes or the distribution of the data within the regimes.

Daily returns of both the VIX and the S&P 500 index were considered as input to the change-point detection. The VIX was considered due to its forward-looking

⁹The VIX futures curve has historically been in contango most of the time, especially when the VIX was below 20, as documented by Simon and Campasano (2014).

¹⁰This is the longest history available for the S&P 500 VIX short-term futures inverse daily excess return index (SPVXSPI) provided by S&P Dow Jones Indices.

nature. It was not possible to conclude which of the two series that provided the earliest warning about change points as not all the detected change points coincided. However, the testing did show that DAA based on the VIX change points was most profitable.

Simple switching strategies performed better than strategies where the allocation to the stock index was a linear function of the estimated volatility despite the fact that the volatility assumed many different levels in the detected regimes.

The best performing strategy was a switching strategy that was fully invested in the S&P 500 index in the low-volatility state and cash in the high-volatility state. This strategy outperformed both the S&P 500 index and a static portfolio with the same average allocation to the stock index both in terms of Sharpe ratio and realized return and it had a significantly lower tail risk. Due to the assumption of zero interest on cash positions, there was no other source of performance than the index. A similar Sharpe ratio could be obtained by selling short-term VIX futures instead of buying the S&P 500 index in the low-volatility state.

The analysis focused on the S&P 500 price index because of its link to the VIX. If the price index was replaced by the total return version of the S&P 500 index and the return on cash was assumed to be the daily risk-free rate rather than zero, then the realized returns would be higher, but the relative performance of the strategies and the break-even transaction costs would be almost the same.

The tested strategies may be based on larger changes in allocation than most investors are willing to and/or allowed to implement. The excess return that can be obtained will simply be proportional to the fraction of the portfolio that is allocated to the dynamic strategy.

The presented results have important implications for portfolio managers with a medium to long-term investment horizon. Even without any level of forecasting skill it is not optimal to hold a static, fixed-weight portfolio. This new robust approach to DAA has the potential to improve (risk-adjusted) returns and reduce tail risk compared to traditional static SAA.

References

- Andersen, T. G., P. H. Frederiksen, and A. D. Staal. "The information content of realized volatility forecasts." Working paper, Northwestern University (2007).
- Ang, A. and A. Timmermann. "Regime changes and financial markets." *Annual Review of Financial Economics*, vol. 4, no. 1 (2012), pp. 313–337.
- Black, F. "Studies of stock price volatility changes." In *Proceedings of the 1976 Meetings of the American Statistical Association, Business and Economics Statistics Section* (1976), pp. 177–181.

- Bulla, J., S. Mergner, I. Bulla, A. Sesboüé, and C. Chesneau. “Markov-switching asset allocation: Do profitable strategies exist?” *Journal of Asset Management*, vol. 12, no. 5 (2011), pp. 310–321.
- Guidolin, M. “Markov switching models in empirical finance.” In *Missing Data Methods: Time-Series Methods and Applications*, edited by D. M. Drukker, vol. 27b of *Advances in Econometrics*. Emerald Group Publishing: Bingley (2011b), pp. 1–86.
- Guidolin, M. and A. Timmermann. “Asset allocation under multivariate regime switching.” *Journal of Economic Dynamics and Control*, vol. 31, no. 11 (2007), pp. 3503–3544.
- Ilmanen, A. “Do financial markets reward buying or selling insurance and lottery tickets?” *Financial Analysts Journal*, vol. 68, no. 5 (2012), pp. 26–36.
- Kritzman, M. and Y. Li. “Skulls, financial turbulence, and risk management.” *Financial Analysts Journal*, vol. 66, no. 5 (2010), pp. 30–41.
- Kritzman, M., S. Page, and D. Turkington. “Regime shifts: Implications for dynamic strategies.” *Financial Analysts Journal*, vol. 68, no. 3 (2012), pp. 22–39.
- Lepage, Y. “A combination of Wilcoxon’s and Ansari–Bradley’s statistics.” *Biometrika*, vol. 58, no. 1 (1971), pp. 213–217.
- Mandelbrot, B. “The variation of certain speculative prices.” *Journal of Business*, vol. 36, no. 4 (1963), pp. 394–419.
- Mann, H. B. and D. R. Whitney. “On a test of whether one of two random variables is stochastically larger than the other.” *Annals of Mathematical Statistics*, vol. 18, no. 1 (1947), pp. 50–60.
- Merton, R. C. “On estimating the expected return on the market: An exploratory investigation.” *Journal of Financial Economics*, vol. 8, no. 4 (1980), pp. 323–361.
- Mood, A. M. “On the asymptotic efficiency of certain nonparametric two-sample tests.” *Annals of Mathematical Statistics*, vol. 25, no. 3 (1954), pp. 514–522.
- Nystrup, P., B. W. Hansen, H. Madsen, and E. Lindström. “Regime-based versus static asset allocation: Letting the data speak.” *Journal of Portfolio Management*, vol. 42, no. 1 (2015a), pp. 103–109.
- Nystrup, P., H. Madsen, and E. Lindström. “Long memory of financial time series and hidden Markov models with time-varying parameters.” *Journal of Forecasting*, vol. 36, no. 8 (2017b), pp. 989–1002.

- Page, E. S. "Continuous inspection schemes." *Biometrika*, vol. 41, no. 1–2 (1954), pp. 100–115.
- Racicot, F. É. and R. Théoret. "Macroeconomic shocks, forward-looking dynamics, and the behavior of hedge funds." *Journal of Banking & Finance*, vol. 62 (2016), pp. 41–61.
- Roberts, S. W. "Control chart tests based on geometric moving averages." *Technometrics*, vol. 1, no. 3 (1959), pp. 239–250.
- Ross, G. J. "Modelling financial volatility in the presence of abrupt changes." *Physica A: Statistical Mechanics and its Applications*, vol. 392, no. 2 (2013), pp. 350–360.
- Ross, G. J. "Parametric and nonparametric sequential change detection in R: The cpm package." *Journal of Statistical Software*, vol. 66, no. 3 (2015), pp. 1–20.
- Ross, G. J. and N. M. Adams. "Two nonparametric control charts for detecting arbitrary distribution changes." *Journal of Quality Technology*, vol. 44, no. 2 (2012), p. 102.
- Ross, G. J., D. K. Tasoulis, and N. M. Adams. "Nonparametric monitoring of data streams for changes in location and scale." *Technometrics*, vol. 53, no. 4 (2011), pp. 379–389.
- Rydén, T., T. Teräsvirta, and S. Åsbrink. "Stylized facts of daily return series and the hidden Markov model." *Journal of Applied Econometrics*, vol. 13, no. 3 (1998), pp. 217–244.
- Sheikh, A. Z. and J. Sun. "Regime change: Implications of macroeconomic shifts on asset class and portfolio performance." *Journal of Investing*, vol. 21, no. 3 (2012), pp. 36–54.
- Siegmund, D. and E. S. Venkatraman. "Using the generalized likelihood ratio statistic for sequential detection of a change-point." *Annals of Statistics*, vol. 23, no. 1 (1995), pp. 255–271.
- Simon, D. P. and J. Campasano. "The VIX futures basis: Evidence and trading strategies." *Journal of Derivatives*, vol. 21, no. 3 (2014), pp. 54–69.
- Whaley, R. E. "The investor fear gauge." *Journal of Portfolio Management*, vol. 26, no. 3 (2000), pp. 12–17.
- Whaley, R. E. "Trading volatility: At what cost?" *Journal of Portfolio Management*, vol. 40, no. 1 (2013), pp. 95–108.

PAPER F

To appear in *Advances in Data Analysis and Classification*

Greedy Gaussian segmentation of multivariate time series

David Hallac, Peter Nystrup, and Stephen Boyd

Abstract

We consider the problem of breaking a multivariate (vector) time series into segments over which the data is well explained as independent samples from a Gaussian distribution. We formulate this as a covariance-regularized maximum likelihood problem, which can be reduced to a combinatorial optimization problem of searching over the possible breakpoints, or segment boundaries. This problem can be solved using dynamic programming, with complexity that grows with the square of the time series length. We propose a heuristic method that approximately solves the problem in linear time with respect to this length, and always yields a locally optimal choice, in the sense that no change of any one breakpoint improves the objective. Our method, which we call *greedy Gaussian segmentation* (GGS), easily scales to problems with vectors of dimension over 1,000 and time series of arbitrary length. We discuss methods that can be used to validate such a model using data, and also to automatically choose appropriate values of the two hyperparameters in the method. Finally, we illustrate our GGS approach on financial time series and Wikipedia text data.

Keywords: Time series analysis; Change-point detection; Financial regimes; Text segmentation; Covariance regularization; Greedy algorithms.

1 Introduction

Many applications, including weather measurements (Xu 2002), car sensors (Hallac et al. 2016), and financial returns (Nystrup et al. 2017a), contain long sequences of multivariate time series data. With datasets such as these, there are many benefits to partitioning the time series into segments, where each segment can be explained by as simple a model as possible. Partitioning can be used for denoising (Abonyi et al. 2005), anomaly detection (Rajagopalan and Ray 2006), regime-change identification (Nystrup et al. 2016), and more. Breaking a large dataset down into smaller, simpler components is also a key aspect of many unsupervised learning algorithms (Hastie et al. 2009, chapter 14).

In this paper, we analyze the time series partitioning problem by formulating it as a covariance-regularized likelihood maximization problem, where the data

in each segment can be explained as independent samples from a multivariate Gaussian distribution. We propose an efficient heuristic, which we call the *greedy Gaussian segmentation* (GGS) algorithm, that approximately finds the optimal breakpoints using a greedy homotopy approach based on the number of segments (Zangwill and Garcia 1981). The memory usage of the algorithm is a modest multiple of the memory used to represent the original data, and the time complexity is linear in the number of observations, with significant opportunities for exploiting parallelism. Our method is able to scale to arbitrarily long time series and multivariate vectors of dimension over 1,000. We also discuss several extensions of this approach, including a streaming algorithm for real-time partitioning, as well as a method of validating the model and selecting optimal values of the hyperparameters. Last, we implement the GGS algorithm in a Python software package `GGS`, available online at <https://github.com/cvxgrp/GGS>, and apply it to various financial time series and Wikipedia text data to illustrate our method’s accuracy, scalability, and interpretability.

1.1 Related work

This work relates to recent advancements in both optimization and time series segmentation. Many variants of our problem have been studied in several contexts, including Bayesian change-point detection (Booth and Smith 1982, Lee 1998, Son and Kim 2005, Cheon and Kim 2010, Bauwens and Rombouts 2012), change-point detection based on hypothesis testing (Crosier 1988, Venter and Steel 1996, De Gooijer 2006, Galeano and Wied 2014, Li 2015a), mixture models (Verbeek et al. 2003, Abonyi et al. 2005, Picard et al. 2011, Samé et al. 2011), hidden Markov models and the Viterbi algorithm (Rydén et al. 1998, Ge and Smyth 2001, Bulla 2011, Hu et al. 2015, Nystrup et al. 2017b), and convex segmentation (Katz and Crammer 2015), all trying to find breakpoints in time series data.

The different methods make different assumptions about the data (see Esling and Agon 2012, for a comprehensive survey). GGS assumes that, in each segment, the mean and covariance are constant and unrelated to the means and covariances in all other segments. This differs from ergodic hidden Markov models, which implicitly assume that the underlying segments will repeat themselves, with some structure to when the transitions are likely to occur. In a left-to-right hidden Markov model (Bakis 1976, Cappé et al. 2005), though, additional constraints are imposed to ensure non-repeatability of segments, similar to GGS. Alternatively, trend filtering problems (Kim et al. 2009) assume that neighboring segments have similar statistical parameters; when a transition occurs, the new parameters are not too far from the previous ones. Other models have tried to solve the problem of change-point detection when the number of breakpoints is unknown (Basseville and Nikiforov 1993, Chouakria-Douzal 2003), including in streaming settings (Guralnik and Srivastava 1999, Gustafsson 2000).

GGS uses a straightforward approach based on the maximum likelihood of the data (we address how to incorporate many of these alternative assumptions in section 5). In real world contexts, deciding on which approach to use depends entirely on the underlying structure of the data; a reasonable choice of method can be determined via cross-validation of the various models. Our work is novel in that it allows for an extremely scalable greedy algorithm to detect breakpoints in multivariate time series. That is, GGS is able to solve much larger problems than many of these other methods, both in terms of vector dimension and the length of the time series. Additionally, its robustness allows GGS to be used as a black-box method which can automatically determine an appropriate number of breakpoints, as well as the model parameters within each segment, using cross-validation.

Our greedy algorithm is based on a top-down approach to segmentation (Douglas and Peucker 1973), though there has also been related work using bottom-up methods (Keogh et al. 2004). While our algorithm does achieve a locally optimal solution, we note that it is possible to solve for the global optimum using dynamic programming (Bellman 1961, Fragkou et al. 2004, Kehagias et al. 2006). However, these globally optimal approaches have complexities that grow with the square of the time series length, whereas our heuristic method scales linearly with the time series length. Our model approximates ℓ_1/ℓ_2 trend filtering problems (Kim et al. 2009, Wahlberg et al. 2011, 2012), which typically use a penalty based on the fused group lasso (Tibshirani et al. 2005, Bleakley and Vert 2011) to couple together the model parameters at adjacent times. However, these models are unable to scale up to the sizes we are aiming for, so we develop a fast heuristic, similar to an ℓ_0 penalty (Candès et al. 2008), where each breakpoint splits the time series into two independent problems. To ensure robustness, we rely on covariance-regularized regression to avoid errors when there are more dimensions than samples in a segment (Witten and Tibshirani 2009).

1.2 Outline

The rest of this paper is structured as follows. In section 2, we formally define our optimization problem. In section 3, we explain the GGS algorithm for approximately solving the problem in a scalable way. In section 4, we describe a validation process for choosing the two hyperparameters in our model. We then examine in section 5 several extensions of this approach which allow us to apply our algorithm to new types of problems. Finally, we apply GGS to several real-world financial and Wikipedia datasets, as well as a synthetic example, in section 6.

2 Problem setup

2.1 Segmented Gaussian model

We consider a given time series $x_1, \dots, x_T \in \mathbb{R}^n$. (The times $t = 1, \dots, T$ need not be uniformly spaced in real time; all that matters in our model and method is that they are ordered.) We will assume that the x_t 's are independent samples with $x_t \sim \mathcal{N}(\mu_t, \Sigma_t)$, where the mean μ_t and covariance Σ_t only change at $K \ll T$ breakpoints b_1, \dots, b_K . These breakpoints divide the given T samples into $K + 1$ segments; in each segment, the x_t 's are generated from the same multivariate normal distribution. Our goal is to determine K , the breakpoints b_1, \dots, b_K , and the means and covariances

$$\mu^{(1)}, \dots, \mu^{(K+1)}, \quad \Sigma^{(1)}, \dots, \Sigma^{(K+1)}$$

in the $K + 1$ segments between the breakpoints.

Introducing breakpoints b_0 and b_{K+1} , the breakpoints must satisfy

$$1 = b_0 < b_1 < \dots < b_K < b_{K+1} = T + 1,$$

and the means and covariances are given by

$$(\mu_t, \Sigma_t) = (\mu^{(i)}, \Sigma^{(i)}), \quad b_{i-1} \leq t < b_i, \quad i = 1, \dots, K.$$

(The subscript t denotes time t ; the superscript (i) and subscript on b denotes segment i .)

We refer to this parametrized distribution of x_1, \dots, x_T as the *segmented Gaussian model* (SGM). The log-likelihood of the data x_1, \dots, x_T under this model is given by

$$\begin{aligned} \ell(b, \mu, \Sigma) &= \sum_{t=1}^T \left(-\frac{1}{2}(x_t - \mu_t)^T \Sigma_t^{-1} (x_t - \mu_t) - \frac{1}{2} \log \det \Sigma_t - \frac{n}{2} \log(2\pi) \right) \\ &= \sum_{i=1}^{K+1} \sum_{t=b_{i-1}}^{b_i-1} \left(-\frac{1}{2}(x_t - \mu^{(i)})^T (\Sigma^{(i)})^{-1} (x_t - \mu^{(i)}) \right. \\ &\quad \left. - \frac{1}{2} \log \det \Sigma^{(i)} - \frac{n}{2} \log(2\pi) \right) \\ &= \sum_{i=1}^{K+1} \ell^{(i)}(b_{i-1}, b_i, \mu^{(i)}, \Sigma^{(i)}), \end{aligned}$$

where

$$\begin{aligned}\ell^{(i)}(b_{i-1}, b_i, \mu^{(i)}, \Sigma^{(i)}) &= \sum_{t=b_{i-1}}^{b_i-1} \left(-\frac{1}{2}(x_t - \mu^{(i)})^T (\Sigma^{(i)})^{-1} (x_t - \mu^{(i)}) \right. \\ &\quad \left. - \frac{1}{2} \log \det \Sigma^{(i)} - \frac{n}{2} \log(2\pi) \right) \\ &= -\frac{1}{2} \sum_{t=b_{i-1}}^{b_i-1} (x_t - \mu^{(i)})^T (\Sigma^{(i)})^{-1} (x_t - \mu^{(i)}) \\ &\quad - \frac{b_i - b_{i-1}}{2} \left(\log \det \Sigma^{(i)} + n \log(2\pi) \right)\end{aligned}$$

is the contribution from the i 'th segment. Here we use the notation $b = (b_1, \dots, b_K)$, $\mu = (\mu^{(1)}, \dots, \mu^{(K+1)})$, and $\Sigma = (\Sigma^{(1)}, \dots, \Sigma^{(K+1)})$, for the parameters in the SGM. In all the expressions above we define $\log \det \Sigma$ as $-\infty$ if Σ is singular, i.e., not positive definite. Note that $b_i - b_{i-1}$ is the length of the i 'th segment.

2.2 Regularized maximum-likelihood estimation

We will choose the model parameters by maximizing the covariance-regularized log-likelihood for a given value of K , the number of breakpoints. We regularize the covariance to avoid errors when there are more dimensions than samples in a segment, a well-known problem in high-dimensional settings (Huang et al. 2006, Bickel and Levina 2008, Witten and Tibshirani 2009). Thus we choose b , μ , and Σ to maximize the regularized log-likelihood

$$\begin{aligned}\phi(b, \mu, \Sigma) &= \ell(b, \mu, \Sigma) - \lambda \sum_{i=1}^{K+1} \mathbf{Tr}(\Sigma^{(i)})^{-1} \\ &= \sum_{i=1}^{K+1} \left(\ell^{(i)}(b_{i-1}, b_i, \mu^{(i)}, \Sigma^{(i)}) - \lambda \mathbf{Tr}(\Sigma^{(i)})^{-1} \right),\end{aligned}\tag{1}$$

where $\lambda \geq 0$ is a regularization parameter, with K fixed. (We discuss the choice of the hyperparameters λ and K in section 4.) This is a mixed combinatorial and continuous optimization problem since it involves a search over the $\binom{T-1}{K}$ possible choices of the breakpoints b_1, \dots, b_K , as well as the parameters μ and Σ . For $\lambda = 0$, this reduces to maximum-likelihood estimation, but we will assume henceforth that $\lambda > 0$. This implies that we will only consider positive definite (invertible) estimated covariance matrices.

If the breakpoints b are fixed, the regularized maximum-likelihood problem has a simple analytical solution. The optimal value of the i 'th segment mean is the

empirical mean over the segment,

$$\mu^{(i)} = \frac{1}{b_i - b_{i-1}} \sum_{t=b_{i-1}}^{b_i-1} x_t, \quad (2)$$

and the optimal value of the i 'th segment covariance is

$$\Sigma^{(i)} = S^{(i)} + \frac{\lambda}{b_i - b_{i-1}} I, \quad (3)$$

where $S^{(i)}$ is the empirical covariance over the segment:

$$S^{(i)} = \frac{1}{b_i - b_{i-1}} \sum_{t=b_{i-1}}^{b_i-1} (x_t - \mu^{(i)})(x_t - \mu^{(i)})^T.$$

Note that the empirical covariance $S^{(i)}$ can be singular, for example when $b_i - b_{i-1} < n$, but for $\lambda > 0$ (which we assume), $\Sigma^{(i)}$ is always positive definite. Thus, for any fixed choice of breakpoints b , the mean and covariance parameters that maximize the regularized log-likelihood (1) are given by (2) and (3), respectively. The optimal value of the covariance (3) is similar to a Stein-type shrinkage estimator (Ledoit and Wolf 2004).

Using these optimal values of the mean and covariance parameters, the regularized log-likelihood (1) can be expressed in terms of b alone, as

$$\begin{aligned} \phi(b) &= C - \frac{1}{2} \sum_{i=1}^{K+1} \left((b_i - b_{i-1}) \log \det(S^{(i)} + \frac{\lambda}{b_i - b_{i-1}} I) \right. \\ &\quad \left. - \lambda \mathbf{Tr}(S^{(i)} + \frac{\lambda}{b_i - b_{i-1}} I)^{-1} \right) \\ &= C + \sum_{i=1}^{K+1} \psi(b_{i-1}, b_i), \end{aligned}$$

where $C = -(Tn/2)(\log(2\pi) + 1)$ is a constant that does not depend on b , and

$$\begin{aligned} \psi(b_{i-1}, b_i) &= -\frac{1}{2} \left((b_i - b_{i-1}) \log \det(S^{(i)} + \frac{\lambda}{b_i - b_{i-1}} I) \right. \\ &\quad \left. - \lambda \mathbf{Tr}(S^{(i)} + \frac{\lambda}{b_i - b_{i-1}} I)^{-1} \right). \end{aligned}$$

(Note that $S^{(i)}$ depends on b_{i-1} and b_i .) Without regularization, i.e., with $\lambda = 0$, we have

$$\psi(b_{i-1}, b_i) = -\frac{1}{2} (b_i - b_{i-1}) \log \det S^{(i)}.$$

More generally, we have reduced the regularized maximum-likelihood-estimation problem, for fixed values of K and λ , to the purely combinatorial problem

$$\begin{aligned} \text{maximize } & -\frac{1}{2} \sum_{i=1}^{K+1} \left((b_i - b_{i-1}) \log \det(S^{(i)}) + \frac{\lambda}{b_i - b_{i-1}} I \right. \\ & \quad \left. - \lambda \mathbf{Tr}(S^{(i)} + \frac{\lambda}{b_i - b_{i-1}} I)^{-1} \right), \end{aligned} \quad (4)$$

where the variable to be chosen is the collection of breakpoints $b = (b_1, \dots, b_K)$. These can take $\binom{T-1}{K}$ possible values. Note that the breakpoints b_i appear in the objective of (4) both explicitly and implicitly, through the empirical covariance matrices $S^{(i)}$, which depend on the breakpoints.

Efficiently computing the objective. For future reference, we mention how the objective in (4) can be computed given b . We first compute the empirical covariance matrices $S^{(i)}$, which costs order Tn^2 flops. This step can be carried out in parallel, on up to $K+1$ processors. The storage required to store these matrices is order Kn^2 doubles. For comparison, the storage required for the original problem data is Tn . Since we typically have $Kn \leq T$, i.e., the average segment length is at least n , the storage of $S^{(i)}$ is no more than the storage of the original data.

For each segment $i = 1, \dots, K+1$, we carry out the following steps (again, possibly in parallel) to evaluate $\psi(b_{i-1}, b_i)$. We first carry out the Cholesky factorization

$$LL^T = S^{(i)} + \frac{\lambda}{b_i - b_{i-1}} I,$$

where L is lower triangular with positive diagonal entries, which costs order n^3 flops. The log-determinant term can be computed in order n flops, as $2 \sum_{i=1}^n \log(L_{ii})$, and the trace term in order n^3 flops, as $\|L^{-1}\|_F^2$. The overall complexity of evaluating the objective is order $Tn^2 + Kn^3$ flops, and this can be easily parallelized into $K+1$ independent tasks. While we make no assumptions about T , n , and K (other than $K < T$), the two terms are equal in order when $T = Kn$, which means that the average segment length is on the order of n , the vector dimension. This is the threshold at which the empirical covariance matrices (can) become nonsingular, though in most applications, useful values of K are much smaller, which means the first term dominates (in order). With the assumption that the average segment length is at least n , the overall complexity of evaluating the objective is Tn^2 .

As an example, we might expect a serial implementation for a data set with $T = 1000$ and $n = 100$ to require on the order of 0.01 seconds to evaluate the objective, using the very conservative estimate of 1Gflop/sec for computer speed.

Globally optimal solution. The problem (4) can be solved globally by dynamic programming (Bellman 1961, Fragkou et al. 2004, Kehagias et al. 2006). We take as states the set of pairs (b_{i-1}, b_i) , with $b_{i-1} < b_i$, so the state space has cardinality $T(T - 1)/2$. We consider the selection of a sequence of K states, with the state transition constraint that (p, q) must be succeeded by a state of the form (q, r) . The complexity of this dynamic programming method is n^3KT^2 . Our interest, however, is in a method for large T , so we instead seek a heuristic method for solving (4) approximately, but with linear complexity in the time series length T .

Our method. In section 3, we describe a heuristic method for approximately solving problem (4). The method is not guaranteed to find the globally optimal choice of breakpoints, but it does find breakpoints with high (if not always highest) objective value, and the ones it finds are 1-OPT, meaning that no change of any one breakpoint can increase the objective. The storage requirements of the method are on the order of the storage required to evaluate the objective, and the computational cost is typically smaller than a few hundred evaluations of the objective function.

3 Greedy Gaussian segmentation

In this section we describe a greedy algorithm for fitting an SGM to data, which we call *greedy Gaussian segmentation*. GGS computes an approximate solution of (4) in a scalable way, in each iteration adding one breakpoint and then adjusting all the breakpoints to (approximately) maximize the objective. In the literature on time series segmentation, this is similar to the standard “top-down” approach (Keogh et al. 2004).

3.1 Split subroutine

The main building block of our algorithm is the Split subroutine. The function $\text{Split}(b_{i-1}, b_i)$ takes segment i and finds the t that maximizes $\psi(b_{i-1}, t) + \psi(t, b_i)$ over all values of t between b_{i-1} and b_i . (We assume that $b_i - b_{i-1} > 1$; otherwise we cannot split the i ’th segment into two segments.) The time $t = \text{Split}(b_{i-1}, b_i)$ is the optimal place to add a breakpoint between b_{i-1} and b_i . The value of $\psi(b_{i-1}, t) + \psi(t, b_i) - \psi(b_{i-1}, b_i)$ is the increase in the objective if we add a new breakpoint at t . This is highest when we choose $t = \text{Split}(b_{i-1}, b_i)$. Due to the regularization term, it is possible for this maximum increase to be negative, which means that adding any breakpoint between b_{i-1} and b_i actually decreases the objective. The Split subroutine is summarized in algorithm 1.

In Split, line 3, updating the empirical mean and covariance of the left and right segments resulting from adding a breakpoint at t is done in a recursive setting

Algorithm 1: Splitting a single interval into two separate segments.

Input: $x_{b_{i-1}}, \dots, x_{b_i}$, along with empirical mean μ and covariance Σ .

```

1: initialize  $\mu_{\text{left}} = 0$ ,  $\mu_{\text{right}} = \mu$ ,  $\Sigma_{\text{left}} = \lambda I$ ,  $\Sigma_{\text{right}} = \Sigma + \lambda I$ .
2: for  $t = b_{i-1} + 1, \dots, b_i - 1$  do
3:   Update  $\mu_{\text{left}}$ ,  $\mu_{\text{right}}$ ,  $\Sigma_{\text{left}}$ ,  $\Sigma_{\text{right}}$ .
4:   Calculate  $\psi_t = \psi(b_{i-1}, t) + \psi(t, b_i)$ .
5: end for
6: return The  $t$  which maximizes  $\psi_t$  and the value of  $\psi_t - \psi(b_{i-1}, b_i)$  for that  $t$ .
```

Algorithm 2: Greedy Gaussian segmentation.

Input: x_1, \dots, x_T , K^{\max} .

```

1: initialize  $b_0 = 1$ ,  $b_1 = T + 1$ .
2: for  $K = 0, \dots, K^{\max}-1$  do
   AddNewBreakpoint:
3:   for  $i = 1, \dots, K + 1$  do
4:      $(t_i, \psi_{\text{increase}}) = \text{Split}(b_{i-1}, b_i)$ .
5:   end for
6:   if All  $\psi_{\text{increase}}$ 's are negative and  $K > 0$  then
7:     return  $(b_1, \dots, b_K)$ .
8:   else if All  $\psi_{\text{increase}}$ 's are negative then
9:     return  $()$ .
10:  end if
11:  Add a new breakpoint at the  $t_i$  with the largest corresponding value of  $\psi_{\text{increase}}$ .
12:  Relabel the breakpoints so that  $1 = b_0 < b_1 < \dots < b_{K+1} < b_{K+2} = T + 1$ .
   AdjustBreakpoints:
13:  repeat
14:    for  $i = 1, \dots, K$  do
15:       $(t_i, \ell_{\text{increase}}) = \text{Split}(b_{i-1}, b_{i+1})$ .
16:      If  $t_i \neq b_i$ , set  $b_i = t_i$ .
17:    end for
18:  until Stationary.
19: end for
20: return  $(b_1, \dots, b_K)$ .
```

in order n^2 flops (Welford 1962). Line 4, evaluating ψ_t requires order n^3 flops, which dominates. The total cost of running Split is order $(b_i - b_{i-1})n^3$.

3.2 GGS algorithm

We can use the Split subroutine to develop a simple greedy method for finding good choices of K breakpoints, for $K = 1, \dots, K^{\max}$, by alternating between adding a new breakpoint to the current set of breakpoints, and then adjusting the positions of all breakpoints until the result is 1-OPT, i.e., no change of any one breakpoint improves the objective. This GGS approach is outlined in algorithm 2.

In line 2, we loop over the addition of new breakpoints, adding exactly one new breakpoint each iteration. Thus, the algorithm finds good sets of breakpoints, for $K = 1, \dots, K^{\max}$, unless it quits early in line 6. This occurs when the addition of any new breakpoint will decrease the objective. In `AdjustBreakpoints`, we loop over the current segmentation and adjust each breakpoint alone to maximize the objective. In this step the objective can either increase or stay the same, and we repeat until the current choice of breakpoints is 1-OPT. In `AdjustBreakpoints`, there is no need to call `Split(b_{i-1}, b_{i+1})` more than once if the arguments have not changed.

The outer loop over K must be run serially, since in each iteration we start with the breakpoints from the previous iteration. Lines 3 and 4 (in `AddNewBreakpoint`) can be run in parallel over the $K + 1$ segments. We can also parallelize `AdjustBreakpoints`, by alternately adjusting the even and odd breakpoints (each of which can be parallelized) until stationarity. GGS requires storage on the order of Kn^2 numbers. As already mentioned, this is typically the same order as, or less than, the storage required for the original data.

Ignoring opportunities for parallelization, running iteration K of GGS requires order KLn^3T flops, where L is the average number of iterations required in `AdjustBreakpoints`. When parallelized, the complexity drops to Ln^3T flops. While we do not know an upper bound on L , we have observed empirically that it is modest when K is not too large; that is, `AdjustBreakpoints` runs just a few outer loops over the breakpoints. Summing from $K = 1$ to $K = K^{\max}$, and assuming L is a constant, gives a complexity of order $(K^{\max})^2n^3T$ without parallelization, or $K^{\max}n^3T$ with parallelization. In contrast, the dynamic programming method (Bellman 1961, Fragkou et al. 2004, Kehagias et al. 2006) requires order $K^{\max}n^3T^2$ flops.

4 Validation and parameter selection

Our GGS method has just two hyperparameters: λ , which controls the amount of covariance regularization, and K^{\max} , the maximum number of breakpoints. In applications where the reason for segmentation is to identify interesting times where the statistics of the data change, K (and λ) might be chosen by hand, or by aesthetic or other considerations, such as whether the segmentation identifies known or suspected times when something changed. The hyperparameter values can also be chosen by a more principled method, such as Bayesian or Akaike information criterion (Hastie et al. 2009, chapter 7). In this section, we describe a simple method of selecting the hyperparameters through out-of-sample or cross validation. We first describe the basic idea with 10:1 out-of-sample validation.

We remove 10% of the data at random, leaving us with $0.9T$ remaining samples. The 10% of samples are our test set, and the remaining samples are the training set, which we use to fit our model. We choose some reasonable value for K^{\max} ,

such as $K^{\max} = (T/n)/3$ (which corresponds to the average segment length $3n$) or a much smaller number when T/n is large. For multiple values of λ , typically logarithmically spaced over a wide range, we run the GGS algorithm. This gives us one SGM for each value of λ and each value of K . For each of these SGMs, we note the log-likelihood on the training data, and also on the test data. (It is convenient to divide each of these by the number of data points, so they become the average log-likelihood per sample. In this way the numbers for the training and test sets can be compared.) To calculate the log-likelihood on the test set, we simply evaluate

$$\ell(x_t) = -\frac{1}{2}(x_t - \mu^{(i)})^T(\Sigma^{(i)})^{-1}(x_t - \mu^{(i)}) - \frac{1}{2}\log\det\Sigma^{(i)} - \frac{n}{2}\log(2\pi),$$

if t falls in the i 'th segment of the model. The overall test set log-likelihood is then defined, on a test set \mathcal{X} , as $\frac{1}{|\mathcal{X}|}\sum_{x_t \in \mathcal{X}}\ell(x_t)$. Note that when t is the time index of a sample in the test set, it cannot be a breakpoint of the model, since the model was developed using the data in the training set.

We then apply standard principles of validation. If for a particular SGM (found by GGS with a particular value of λ and K) the average log-likelihood on the training and test sets is similar, we conclude the model is not overfit, and therefore a reasonable candidate. Among candidate models, we then choose one that has a high value of average log-likelihood. If many models have reasonably high average log-likelihood, we choose one with a small value of K and a large value of λ . (In the former case to get the simplest model that explains the data, and in the latter case to get the least sensitive model that explains the data.)

Standard cross-validation is an extension of out-of-sample validation that can give us even more confidence in a proposed SGM. In cross-validation we divide the original data into ten equal size ‘folds’ of randomly chosen samples, and carry out out-of-sample validation ten times, with each fold as the test set. If the results are reasonably consistent across the folds, both in terms of training and test average log-likelihood and the breakpoints themselves, we can have confidence that the SGM fits the data.

5 Variations and extensions

The basic model and method can be extended in many ways, several of which we describe here.

Warm-start. GGS builds SGMs by increasing K , starting from $K = 0$. It can also be used in warm-start mode, meaning we start the algorithm from a given choice of initial breakpoints. As an extreme version, we can start with a random set of K breakpoints, and then run AdjustBreakpoints until we have a 1-OPT solution. The main benefit of a warm start is that it allows for a significant

computational speedup. Whereas a (parallelized) GGS algorithm has a runtime of $O(K^{\max} T n^3)$, this warm-start method takes only $O(T n^3)$, since it can skip the first $K^{\max} - 1$ steps of algorithm 2. However, as we will show in section 6.2, this speedup comes with a tradeoff, as the solution accuracy tends to drop when running GGS in warm-start mode as compared to the original algorithm.

Backtracking. In GGS, we add one breakpoint per iteration. While we adjust the previous breakpoints found, we never remove a breakpoint. One variation is to occasionally remove a breakpoint. This can be done using a subroutine called `Combine`. This function evaluates, for each breakpoint, the decrease in objective value if that breakpoint is removed. In a backtracking step, we remove the breakpoint that decreases the objective the least; we can then adjust the remaining breakpoints and continue with the GGS algorithm by adding a new breakpoint. (If we end up adding the breakpoint we removed back in, nothing has been achieved.) We also note that backtracking allows for GGS to be solved by a bottom-up method (Keogh et al. 2004, Borenstein and Ullman 2008). We do so by starting with $T - 1$ breakpoints and continually backtracking until only K breakpoints remain.

Streaming. We can deploy GGS when the data is streaming. We maintain a memory of the last M samples and run GGS on this data set. We could do this from scratch as each new data point or group of data points arrives, complete with selection of the hyperparameters and validation. Another option is to fix λ and K , and then run GGS in warm-start mode, which means that we keep the previous breakpoints (shifted appropriately), and then run `AdjustBreakpoints` from this starting point (as well as `AddBreakpoint` if a breakpoint has fallen off our memory).

In streaming mode, the GGS algorithm provides an estimate of the statistics of future time samples, namely, the mean and covariance in the SGM in the most recent segment.

Multiple samples at the same time. Our approach can easily incorporate the case where we have more than one data vector for any given time t . We simply change the sums over each segment for the empirical mean and covariance to include any data samples in the given time range.

Cyclic data. In cyclic data, the times t are interpreted modulo T , so x_T and x_1 are adjacent. A good example is a vector time series that represents daily measurements over multiple years; we simply map all measurements to $t = 1, \dots, 365$ (ignoring leap years), and modify the model and method to be cyclic. The only subtlety here arises in choosing the first breakpoint, since one breakpoint does not split a cyclic set of times into two segments. Evidently we need two breakpoints to split a cyclic set of times into two segments. We

modify GGS by arbitrarily choosing a first breakpoint, and then running as usual, including the ‘wrap-around’ segment as a segment. Thus, the first step chooses the second breakpoint, which splits the cyclic data into two segments. The `AdjustBreakpoints` method now adjusts both the chosen breakpoint and the arbitrarily chosen original one.

Regularization across time. In our current model, the estimates on either side of a breakpoint are independent of each other. We can, however, carry out a post-processing step to shrink models on either side of each breakpoint towards each other. We can do this by fixing the breakpoints and then adjusting the continuous model parameters to minimize our original objective minus a regularization term that penalizes deviations of $(\Sigma^{(i)}, \mu^{(i)})$ from $(\Sigma^{(i-1)}, \mu^{(i-1)})$.

Non-Gaussian data. Our segmented Gaussian model and associated regularized maximum-likelihood problem (4) can be generalized to other statistical models. The problem is tractable, at least in theory, when the associated regularized maximum-likelihood problem is convex. In this case we can compute the optimal parameters over a segment by solving a convex optimization problem, whereas in the SGM we have an analytical solution in terms of the empirical mean and covariance. Thus we can segment Poisson or Bernoulli data, or even heterogeneous exponential family distributions (Lee and Hastie 2015, Tansey et al. 2015).

6 Experiments

In this section, we describe our implementation of GGS, and the results of some numerical experiments to illustrate the model and the method.

6.1 Implementation

We have implemented GGS as a Python package `GGS` available at

<https://github.com/cvxgrp/GGS>.

`GGS` is capable of carrying out full ten-fold cross-validation to help users choose values of the hyperparameters. `GGS` uses `NumPy` for the numerical computations and the `multiprocessing` package to carry out the algorithm in parallel for different cross-validation folds for a single λ . (The current implementation does not support parallelism over the segments of a single fold, and the advantages of parallelism will only be seen when `GGS` is run on a computer with multiple cores.)

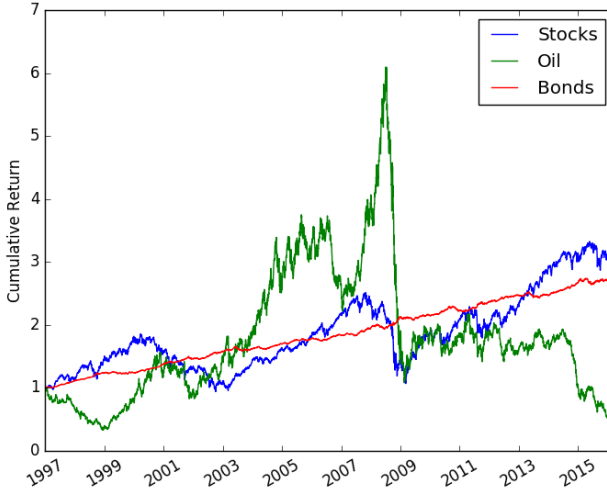


Figure 1: Cumulative returns over the 19-year period for a stock, oil, and bond index.

6.2 Financial indices

In financial markets, regime changes have been shown to have important implications for asset class and portfolio performance (Ang and Timmermann 2012, Sheikh and Sun 2012, Nystrup et al. 2015a, 2017a). We start with a small example with $n = 3$, where we can visualize and plot all entries of the segment parameters $\mu^{(i)}$ and $\Sigma^{(i)}$.

Dataset description. Our dataset consists of 19 years of daily returns, from January 1997 to December 2015, for $n = 3$ indices for stocks, oil, and government bonds: MSCI World, S&P GSCI Crude Oil, and J.P. Morgan Global Government Bonds. We use log-return data, i.e., the logarithm of the end-of-day price increase from the previous day. The time series length is $T = 4943$. Cumulative returns for the three indices are shown in figure 1. We can clearly see multiple ‘regimes’ in the return time series, although the individual behaviors of the three indices are quite different.

Running GGS We run GGS on the data with $K^{\max} = 30$ and $\lambda = 10^{-4}$. Figure 2 shows the value of the objective as a function of K , i.e., the objective value in each iteration of GGS. We see a sharp increase in the objective value up to around $K = 8$ or $K = 10$ —our first hint that a choice in this range would be reasonable. For this example n is very small, so the computation time is dominated by Python overhead. Still, our single-threaded GGS solver took less

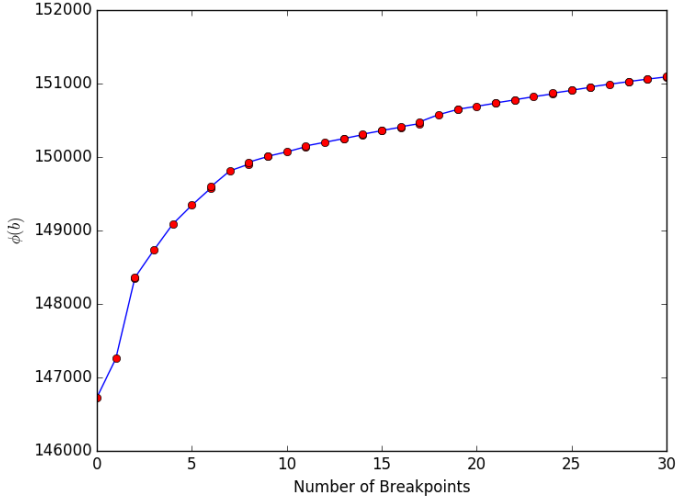


Figure 2: Objective value $\phi(b)$ as a function of the number of breakpoints for $\lambda = 10^{-4}$.

than 30 seconds to compute these 30 models on a standard laptop with a 1.7 GHz Intel i7 processor. The average number of passes through the data for the breakpoint adjustments was under two.

Cross-validation. We next use ten-fold cross-validation to determine reasonable values for K and λ . We plot the average log-likelihood over the ten folds as a function of K in figure 3 for various values of λ . When λ is large, the curves stop before $K = K^{\max}$, because GGS terminates early. These plots clearly show that increasing K above ten does not increase the average log-likelihood in the test set; and moreover past this point the log-likelihood on the test and training sets begin to diverge, meaning the model is overfit. Though figure 3 only goes up to $K = 30$, we find that for values of K above around 60, the log-likelihood begins to drop significantly. Furthermore, we see that values of λ up to $\lambda = 10^{-4}$ yield roughly the same high log-likelihood. This suggests that choices of $K = 10$ and $\lambda = 10^{-4}$ are reasonable, aligning with our general preference for models which are simple (small K) and not too sensitive to noise (large λ). Cross-validation also reveals that the choice of breakpoint locations is very stable for these values of K and λ , across the ten folds.

Results. Figure 4 shows the model obtained by GGS with $\lambda = 10^{-4}$ and $K = 10$. We plot the covariance matrix by showing the square root of the diagonal entries (i.e., the volatilities) and the three correlations as a function of t . During the financial crisis in 2008, the mean returns of stocks and oil

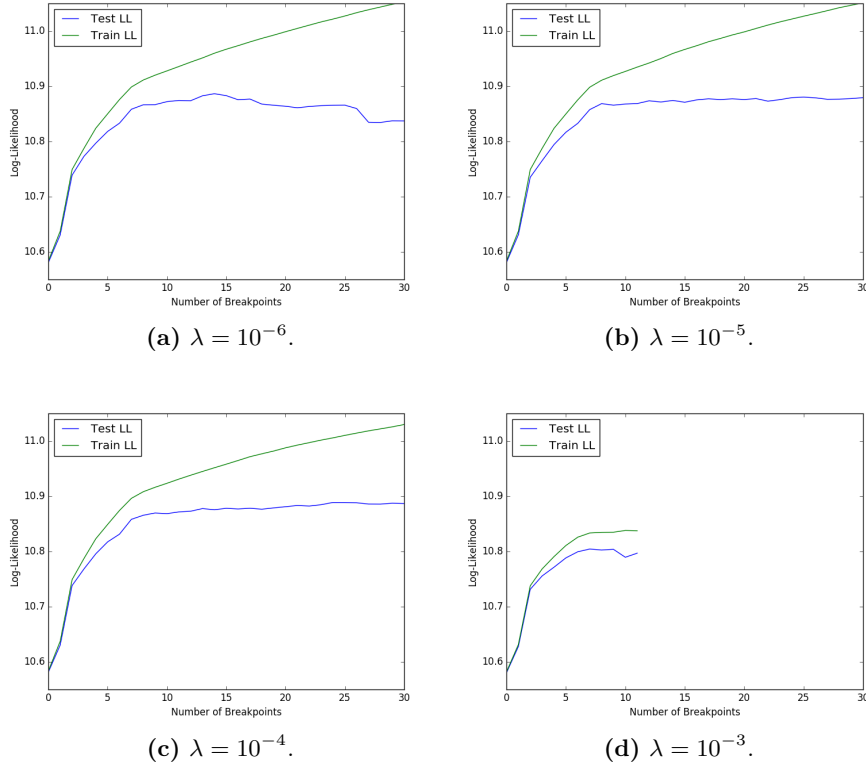


Figure 3: Average training- and test-set log-likelihood during ten-fold cross validation for various λ 's and across all values of $K \leq 30$.

were very negative and volatility was high. The stock market and the oil price were almost uncorrelated before 2008, but have been positively correlated since then. It is interesting to see how the correlation between stocks and bonds has varied over time: it was strongly positive in 1997 and very negative in 1998, in 2002, and in the five years from mid-2007 to mid-2012. The sudden shift in this correlation between 1997 and 1998 is why GGS yields two relatively short segments in the [1997, 1999] window, rather than breaking up a longer segment (such as [1999, 2002], where the correlation structure is more homogenous). The extent of these variations would be difficult to capture using a sliding window; the window would have to be very short, which would lead to noisy estimates. The segmentation approach yields a more interpretable partitioning with no dependence on a (prespecified, fixed) window length.

Approaches to risk modeling (Alexander 2000) and portfolio optimization (Par-

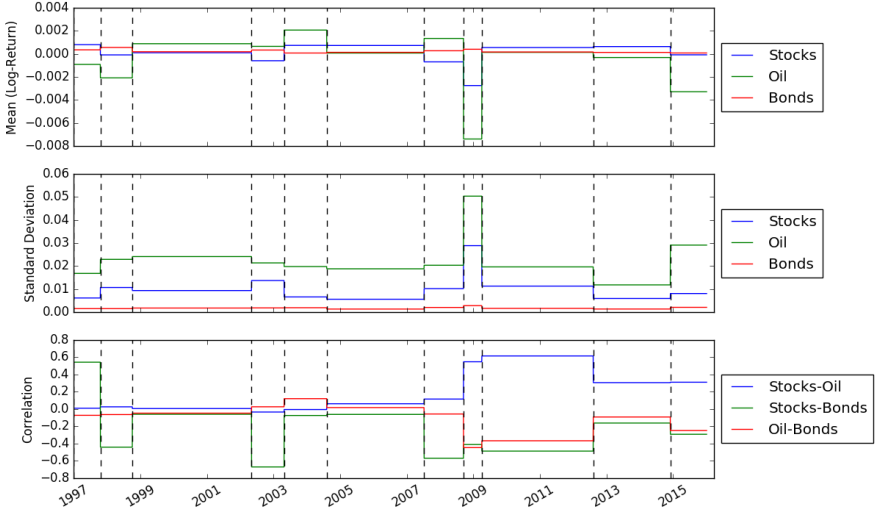


Figure 4: Segmented Gaussian model obtained with $\lambda = 10^{-4}$ and $K = 10$.

tovi and Caputo 2004, Meucci 2009) based on principal component analysis are questionable, when volatilities and correlations are changing as significantly as is the case in figure 4 (see also Fenn et al. 2011). We plot the cumulative index returns along with the chosen breakpoints in figure 5. We can clearly see natural segments and boundaries, for example the Russian default in 1998 and the 2008 financial crisis.

Comparison with random warm-start. We fix the hyperparameters $K = 10$ and $\lambda = 10^{-4}$, and attempt to find a better SGM using warm-start with random breakpoints. This step is not needed; we carry it out to demonstrate that while GGS does not find the model that globally maximizes the objective, it is effective. We run 10,000 warm-start random initial breakpoint computations, running AdjustBreakpoints until the model is 1-OPT and computing the objective found in each case. (In this case the number of passes over the data set far exceeds two, the typical number in GGS.) The complementary CDF of the objective for these 10,000 computations is shown in figure 6, as well as the objective values found by GGS for $K = 8$ through $K = 11$. We see that the random initializations can sometimes lead to very poor results: over 50% of the simulations, even though they are locally optimal, have smaller objectives than the $K = 9$ step of GGS. On the other hand, the random initializations do find some SGMs with objective slightly exceeding the one found by GGS, demonstrating that GGS did not find the globally optimal set of breakpoints. These

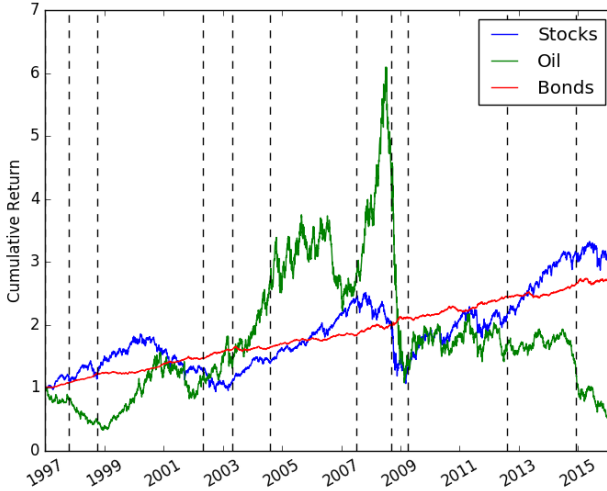


Figure 5: Cumulative returns with vertical bars at the model breakpoints.

SGMs have similar breakpoints, and similar cross-validated log-likelihood, as the one found by GGS. As a practical matter, these SGMs are no better than the one found by GGS. There are two advantages of GGS over the random search: first, it is much faster; and second, it finds models for a range of values of K , which is useful before we select the value of K to use.

6.3 Large-scale financial example

Dataset description. We next look at a larger example to emphasize the scalability of GGS. We look at all companies currently in the S&P 500 index that have been publicly listed for the entire 19-year period from before (from 1997 to 2015), which leaves 309 companies. Note that there are slightly fewer trading days for the S&P 500 each year than the global indices, since the S&P 500 does not trade during US holidays, while the global indices still move. The 19-year dataset yields a 309×4782 data matrix. We take daily log-returns for these stocks and run the GGS algorithm to detect relevant breakpoints.

GGS scalability. We run GGS on this much larger dataset up to $K^{\max} = 10$. Our serial implementation of the GGS algorithm, on the same 1.7 GHz Intel i7 processor, took 36 minutes, where `AdjustBreakpoint` took an average of 3.5 passes through the data at each K . Note that this aligns very closely with our predicted runtime from section 3.2, which was estimated as $(K^{\max})^2 L T n$.

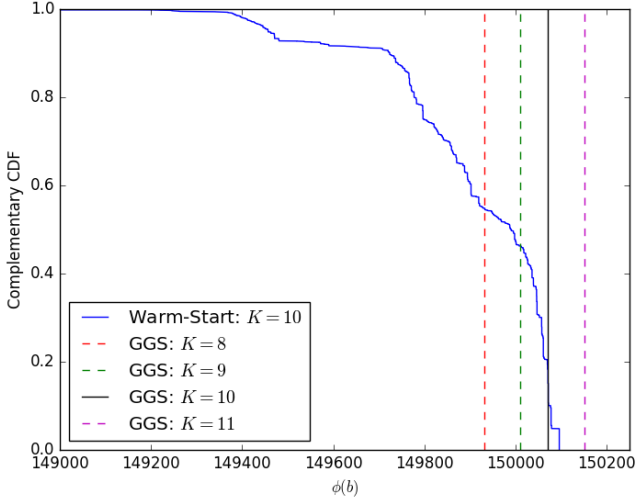


Figure 6: Empirical complementary CDF of $\phi(b)$ for 10,000 randomly initialized results for $K = 10$ and $\lambda = 10^{-4}$.

Cross-validation. We run ten-fold cross-validation to find good values of the hyperparameters K and λ . The average log-likelihood of the test and training sets are displayed in figure 7. From the results, we can see that the log-likelihood is maximized at a much smaller value of K , indicating fewer breakpoints. This is in part because, with $n = 309$, we need more samples in each segment to get an accurate estimate of the 309×309 covariance matrix, as opposed to the 3×3 covariance in the smaller example. Our cross-validation results suggest choosing $K = 3$ and $\lambda = 5 \times 10^{-2}$, and as in the small example, the results are very stable near these values.

Results. We plot the mean, standard deviation, and cumulative return of a uniform, buy-and-hold portfolio (i.e., investing \$1 into each of the 309 stocks in 1997). The results are shown in figure 8. Note that there is a selection bias in the dataset, since these companies all remained in the S&P 500 in 2016, and the total return is 8 \times over the 19-year period. Like before, the 2008 financial crisis stands out. It is the only segment with a negative mean value. The partitioning seems intuitively right. The first, highly volatile, segment includes both the build-up and burst of the dot-com bubble. The second segment is the bull market that led to the financial crisis in 2008. The third segment is the financial crisis and the fourth segment is the market rally that followed the crisis. These breakpoints were also found in the multi-asset example in figure 4 and figure 5.

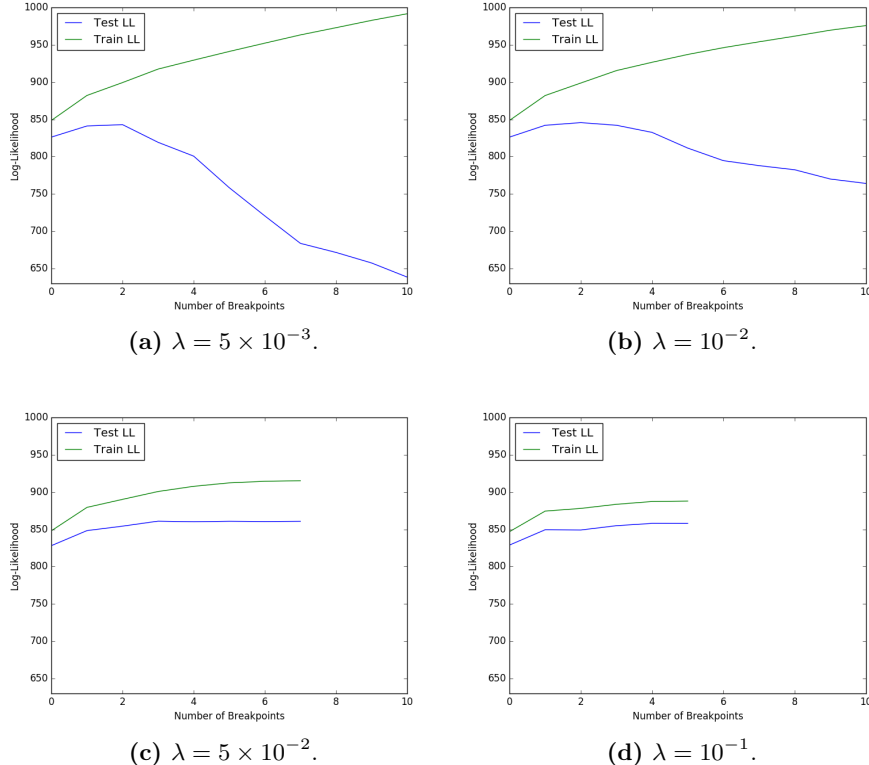


Figure 7: Average training- and test-set log-likelihood during ten-fold cross-validation for various λ 's for the 309-stock example. Note that not all λ 's go all the way up to $K = 10$ because our algorithm stops when it determines that it will no longer benefit from adding an additional split.

6.4 Wikipedia text data

We examine an example from the field of natural language processing (NLP) to illustrate how GGS can be applied to a very different type of dataset, beyond traditional time series examples.

Dataset description. We look at text data from English-language Wikipedia. We obtain our data by concatenating the introductions, i.e., the text that precedes the Table of Contents section on the Wikipedia webpage, of five separate articles, with titles George Clooney, Botany, Julius Caesar, Jazz, and Denmark. Here, the “time series” consists of the sequence of words from these five articles in order. After basic preprocessing (removing words that do not appear at least

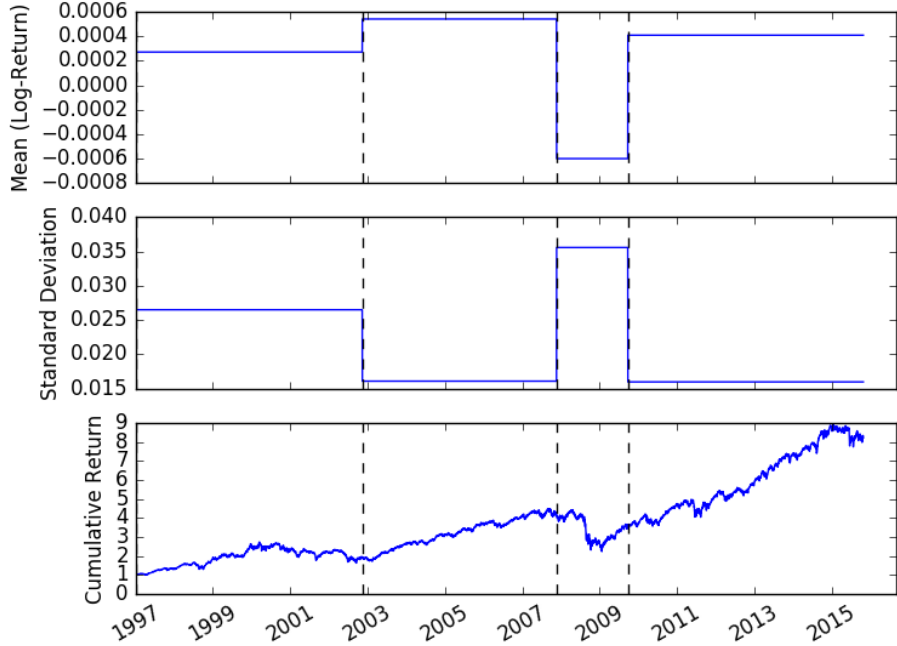


Figure 8: Mean, standard deviation, and cumulative return for a uniform portfolio with $K = 3$ and $\lambda = 5 \times 10^{-2}$.

five times and in multiple articles), our dataset consists of 1282 words, with each article contributing between 224 and 286 words. We then convert each word into a 300-dimensional vector using a pretrained Word2Vec embedding of three million unique words (or short phrases), trained on the Google News dataset of approximately 100 billion words, available at

<https://code.google.com/archive/p/word2vec/>.

This leaves us with a 300×1282 data matrix. Our hope is that GGS can detect the breakpoints between the five concatenated articles, based solely on the change in mean and covariance of the vectors associated with the words in our vector series.

GGS results. We run GGS to split the data into five segments—i.e., $K = 4$ —and use cross-validation to select $\lambda = 10^{-3}$. (We note, however, that this example is quite robust to the selection of λ , and any value from 10^{-6} to 10^{-3} yields the exact same breakpoint locations.) We plot the results in figure 9,

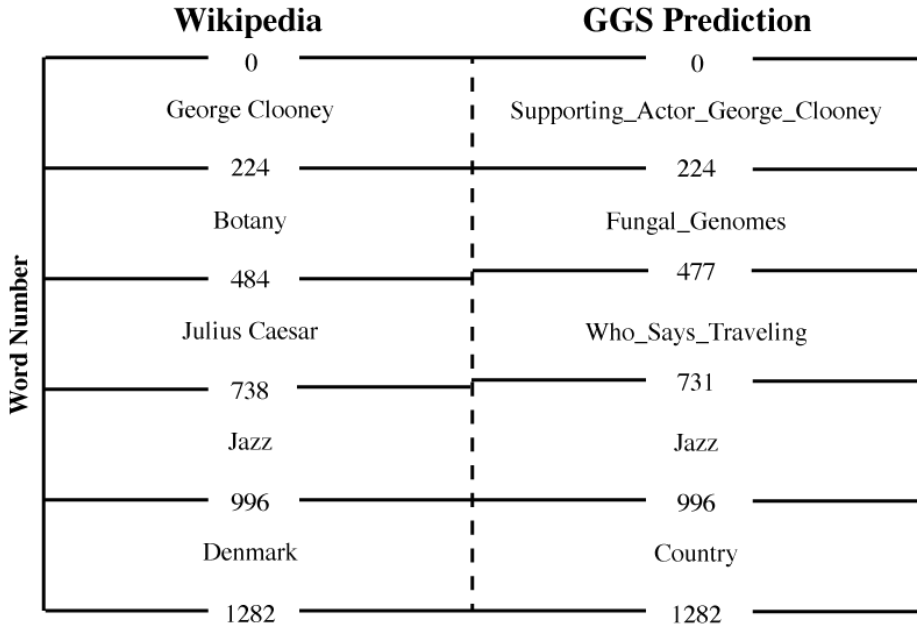
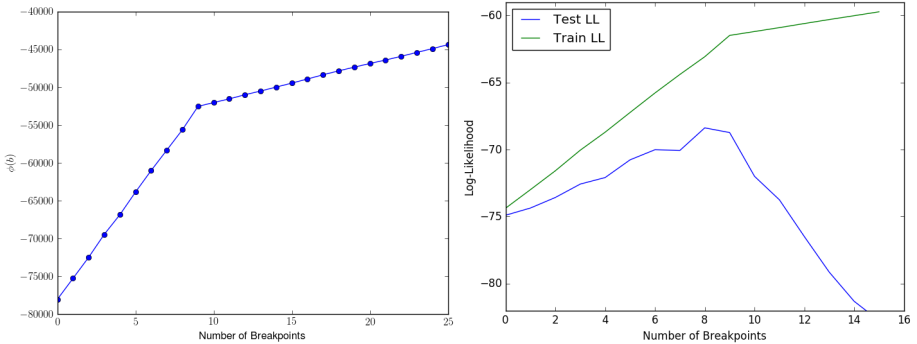


Figure 9: Actual and GGS-predicted breakpoints for the concatenation of the five Wikipedia articles, along with the predicted most similar word to the mean of each GGS segment.

which show GGS achieving a near-perfect split of the five articles. Figure 9 also shows a representative word (or short phrase) in the Google News dataset that is among the top five “most similar” words, out of the entire three million word corpus, to the average (mean) of each GGS segment, as measured by cosine similarity. We see that GGS correctly identifies both the breakpoint locations and the general topic of each segment.

6.5 Comparison with left-to-right HMM on synthetic data

We next analyze a synthetic example where observations are generated from a given sequence of segments. This provides a known ground truth, allowing us to compare GGS with a common baseline, a left-to-right hidden Markov model (HMM) (Bakis 1976, Cappé et al. 2005). Left-to-right HMMs, like GGS, split the data into non-repeatable segments, where each segment is defined by a Gaussian distribution. The HMMs in this experiment are implemented using the `rarhsmm` library (Xu and Liu 2017), which includes the same shrinkage estimator for the covariance matrices used in GGS (see section 2.2). The shrinkage estimator results in more reliable estimates not only of the covariance matrices but also of the transition matrix and the hidden states (Fiecas et al. 2017).



(a) Objective vs. breakpoints for $\lambda = 10$. (b) Average training and test log-likelihood.

Figure 10: GGS correctly identifies that there are ten underlying segments in the data (from the kink in the plots at $K = 9$).

Data set description. We start by generating ten random covariance matrices. We do so by setting $\Sigma_i = A^{(i)}A^{(i)T}$, $i = 1, \dots, 10$, where $A^{(i)} \in \mathbb{R}^{25 \times 25}$ is a random matrix where each element $A_{j,k}^{(i)}$ was generated independently from the standard normal distribution. Our synthetic data set then has ten ground truth segments (or $K = 9$ breakpoints), where segment i has zero mean and covariance Σ_i . Each segment is of length 100 (so the total time series has 1,000 observations). Each of the 100 readings per segment is sampled independently from the given distribution. Thus, our final data set consists of a 25×1000 data matrix, consisting of ten independent segments, each of length 100.

Results. We run both GGS and the left-to-right HMM on this data set. For GGS, we immediately notice a kink in the objective at $K = 9$, as shown in figure 10(a), indicating that the data should be split into $K + 1 = 10$ segments. We use cross-validation to choose an appropriate value of λ , which yields $\lambda = 10$. We plot the training- and test-set log-likelihoods for $\lambda = 10$ in figure 10(b). (Similar to the Wikipedia text example, though, the breakpoint locations are relatively robust to our selection of λ . GGS returns identical breakpoints for any λ between 10^{-3} and 10^3). For this value of λ (and thus for the whole range of λ between 10^{-3} and 10^3), we split the data perfectly, identifying the nine breakpoints at their *exact* locations.

Left-to-right HMMs have various methods for determining the number of segments, such as AIC or BIC. Here we instead simply use the correct number of segments, and initialize the transition matrix as its true value. Note that this is the best-case scenario for the left-to-right HMM. Even with this advantage, the left-to-right HMM struggles to properly split the time series. Whereas GGS

correctly identifies the breakpoints as [100, 200, 300, 400, 500, 600, 700, 800, 900], the left-to-right HMM gets at least one breakpoint completely wrong (and splits the data at, for example, [100, 200, 300, 400, 500, 600, 663, 700, 800]).

These results are consistent. In fact, when this experiment was repeated 100 times (with different randomly generated data), GGS identified the correct breakpoints every single time. We also note that GGS is robust to n (the dimension of the data), K (the number of breakpoints), and $T/(K+1)$ (the average segment length), perfectly splitting the data at the exact breakpoints for all tests across at least one order of magnitude in each of these three parameters. On the other hand, the 100 left-to-right HMM experiments correctly labeled on average just 7.46 of the nine true breakpoints (and never more than eight). In these HMM experiments, instead of ten segments of length 100, the shortest segment had an average length of 26, and the longest segment had an average length of 200. Additionally, the left-to-right HMM struggles as the parameters change, doing significantly worse when K increases and when T/K is small compared to n (though formal analysis of the robustness of left-to-right HMMs is outside the scope of this paper). This comes as no surprise, because finding the global maximum among all local maxima of the likelihood function for an HMM with many states is known to be difficult problem (Cappé et al. 2005, chapter 1.4). Therefore, as shown by these experiments, GGS appears to outperform left-to-right HMMs in this setting.

7 Summary

We have analyzed the problem of breaking a multivariate time series into segments, where the data in each segment could be modeled as independent samples from a multivariate Gaussian distribution. Our greedy Gaussian segmentation (GGS) algorithm is able to approximately maximize the covariance-regularized log-likelihood in an efficient manner, easily scaling to vectors with dimension over 1,000 and time series of any length. Examples on both small and large data sets yielded useful insights. Our implementation, available at <https://github.com/cvxgrp/GGS>, can be used to solve problems in a variety of applications. For example, the regularized parameter estimates obtained by GGS could be used as inputs to portfolio optimization, where correlations between different assets play an important role when determining optimal holdings.

References

- Abonyi, J., B. Feil, S. Nemeth, and P. Arva. “Modified Gath–Geva clustering for fuzzy segmentation of multivariate time-series.” *Fuzzy Sets and Systems*, vol. 149, no. 1 (2005), pp. 39–56.

- Alexander, C. “A primer on the orthogonal GARCH model.” (2000). Unpublished manuscript, ISMA Center, University of Reading, U.K.
- Ang, A. and A. Timmermann. “Regime changes and financial markets.” *Annual Review of Financial Economics*, vol. 4, no. 1 (2012), pp. 313–337.
- Bakis, R. “Continuous speech recognition via centisecond acoustic states.” *Journal of the Acoustical Society of America*, vol. 59, no. S1 (1976), p. S97.
- Basseville, M. and I. V. Nikiforov. *Detection of Abrupt Changes: Theory and Application*, vol. 104. Prentice Hall: Englewood Cliffs (1993).
- Bauwens, L. and J. Rombouts. “On marginal likelihood computation in change-point models.” *Computational Statistics & Data Analysis*, vol. 56, no. 11 (2012), pp. 3415–3429.
- Bellman, R. E. “On the approximation of curves by line segments using dynamic programming.” *Communications of the ACM*, vol. 4, no. 6 (1961), p. 284.
- Bickel, P. J. and E. Levina. “Regularized estimation of large covariance matrices.” *Annals of Statistics*, vol. 36, no. 1 (2008), pp. 199–227.
- Bleakley, K. and J. P. Vert. “The group fused lasso for multiple change-point detection.” *arXiv preprint arXiv:1106.4199* (2011).
- Booth, N. B. and A. F. M. Smith. “A Bayesian approach to retrospective identification of change-points.” *Journal of Econometrics*, vol. 19, no. 1 (1982), pp. 7–22.
- Borenstein, E. and S. Ullman. “Combined top-down/bottom-up segmentation.” *IEEE Transactions on Pattern Analysis and Machine Intelligence*, vol. 30, no. 12 (2008), pp. 2109–2125.
- Bulla, J. “Hidden Markov models with t components. Increased persistence and other aspects.” *Quantitative Finance*, vol. 11, no. 3 (2011), pp. 459–475.
- Candès, E. J., M. B. Wakin, and S. Boyd. “Enhancing sparsity by reweighted ℓ_1 minimization.” *Journal of Fourier Analysis and Applications*, vol. 14, no. 5–6 (2008), pp. 877–905.
- Cappé, O., E. Moulines, and T. Rydén. *Inference in Hidden Markov Models*. Springer: New York (2005).
- Cheon, S. and J. Kim. “Multiple change-point detection of multivariate mean vectors with the Bayesian approach.” *Computational Statistics & Data Analysis*, vol. 54, no. 2 (2010), pp. 406–415.

- Chouakria-Douzal, A. “Compression technique preserving correlations of a multivariate temporal sequence.” In *Advances in Intelligent Data Analysis V*, edited by M. R. Berthold, H.-J. Lenz, E. Bradley, R. Kruse, and C. Borgelt, vol. 2810 of *Lecture Notes in Computer Science*. Springer: Berlin (2003), pp. 566–577.
- Crosier, R. B. “Multivariate generalizations of cumulative sum quality-control schemes.” *Technometrics*, vol. 30, no. 3 (1988), pp. 291–303.
- De Gooijer, J. “Detecting change-points in multidimensional stochastic processes.” *Computational Statistics & Data Analysis*, vol. 51, no. 3 (2006), pp. 1892–1903.
- Douglas, D. H. and T. K. Peucker. “Algorithms for the reduction of the number of points required to represent a digitized line or its caricature.” *Cartographica: The International Journal for Geographic Information and Geovisualization*, vol. 10, no. 2 (1973), pp. 112–122.
- Esling, P. and C. Agon. “Time-series data mining.” *ACM Computing Surveys*, vol. 45, no. 1 (2012), p. 12.
- Fenn, D. J., M. A. Porter, S. Williams, M. McDonald, N. F. Johnson, and N. S. Jones. “Temporal evolution of financial-market correlations.” *Physical Review E*, vol. 84, no. 2 (2011), p. 026109.
- Fiecas, M., J. Franke, R. von Sachs, and J. T. Kamgaing. “Shrinkage estimation for multivariate hidden Markov models.” *Journal of the American Statistical Association*, vol. 112, no. 517 (2017), pp. 424–435.
- Fragkou, P., V. Petridis, and A. Kehagias. “A dynamic programming algorithm for linear text segmentation.” *Journal of Intelligent Information Systems*, vol. 23, no. 2 (2004), pp. 179–197.
- Galeano, P. and D. Wied. “Multiple break detection in the correlation structure of random variables.” *Computational Statistics & Data Analysis*, vol. 76 (2014), pp. 262–282.
- Ge, X. and P. Smyth. “Segmental semi-Markov models for endpoint detection in plasma etching.” *IEEE Transactions on Semiconductor Engineering*, vol. 259 (2001), pp. 201–209.
- Guralnik, V. and J. Srivastava. “Event detection from time series data.” In *Proceedings of the Fifth ACM SIGKDD International Conference on Knowledge Discovery and Data Mining* (1999), pp. 33–42.
- Gustafsson, F. *Adaptive Filtering and Change Detection*. Wiley: West Sussex (2000).

- Hallac, D., A. Sharang, R. Stahmann, A. Lamprecht, M. Huber, M. Roehder, R. Sosić, and J. Leskovec. “Driver identification using automobile sensor data from a single turn.” In *IEEE 19th International Conference on Intelligent Transport Systems* (2016), pp. 953–958.
- Hastie, T., R. Tibshirani, and J. Friedman. *The Elements of Statistical Learning*. Springer: New York, 2nd ed. (2009).
- Hu, B., T. Rakthanmanon, Y. Hao, S. Evans, S. Lonardi, and E. Keogh. “Using the minimum description length to discover the intrinsic cardinality and dimensionality of time series.” *Data Mining and Knowledge Discovery*, vol. 29, no. 2 (2015), pp. 358–399.
- Huang, J. Z., N. Liu, M. Pourahmadi, and L. Liu. “Covariance matrix selection and estimation via penalised normal likelihood.” *Biometrika*, vol. 93, no. 1 (2006), pp. 85–98.
- Katz, I. and K. Crammer. “Outlier-robust convex segmentation.” In *Proceedings of the 29th National Conference on Artificial Intelligence*, vol. 4 (2015), pp. 2701–2707.
- Kehagias, A., E. Nidokou, and V. Petridis. “A dynamic programming segmentation procedure for hydrological and environmental time series.” *Stochastic Environmental Research and Risk Assessment*, vol. 20, no. 1–2 (2006), pp. 77–94.
- Keogh, E., S. Chu, D. Hart, and M. Pazzani. “Segmenting time series: A survey and novel approach.” In *Data Mining in Time Series Databases*, edited by M. Last, A. Kandel, and H. Bunke, vol. 57 of *Series in Machine Perception and Artificial Intelligence*, chap. 1. World Scientific: Singapore (2004).
- Kim, S. J., K. Koh, S. Boyd, and D. Gorinevsky. “ ℓ_1 trend filtering.” *SIAM Review*, vol. 51, no. 2 (2009), pp. 339–360.
- Ledoit, O. and M. Wolf. “A well-conditioned estimator for large-dimensional covariance matrices.” *Journal of Multivariate Analysis*, vol. 88, no. 2 (2004), pp. 365–411.
- Lee, C. B. “Bayesian analysis of a change-point in exponential families with applications.” *Computational Statistics & Data Analysis*, vol. 27, no. 2 (1998), pp. 195–208.
- Lee, J. and T. Hastie. “Learning the structure of mixed graphical models.” *Journal of Computational and Graphical Statistics*, vol. 24, no. 1 (2015), pp. 230–253.

- Li, J. “Nonparametric multivariate statistical process control charts: a hypothesis testing-based approach.” *Journal of Nonparametric Statistics*, vol. 27, no. 3 (2015a), pp. 383–400.
- Meucci, A. “Managing diversification.” *Risk*, vol. 22, no. 5 (2009), pp. 74–79.
- Nystrup, P., B. W. Hansen, H. O. Larsen, H. Madsen, and E. Lindström. “Dynamic allocation or diversification: A regime-based approach to multiple assets.” *Journal of Portfolio Management*, vol. 44, no. 2 (2017a), pp. 62–73.
- Nystrup, P., B. W. Hansen, H. Madsen, and E. Lindström. “Regime-based versus static asset allocation: Letting the data speak.” *Journal of Portfolio Management*, vol. 42, no. 1 (2015a), pp. 103–109.
- Nystrup, P., B. W. Hansen, H. Madsen, and E. Lindström. “Detecting change points in VIX and S&P 500: A new approach to dynamic asset allocation.” *Journal of Asset Management*, vol. 17, no. 5 (2016), pp. 361–374.
- Nystrup, P., H. Madsen, and E. Lindström. “Long memory of financial time series and hidden Markov models with time-varying parameters.” *Journal of Forecasting*, vol. 36, no. 8 (2017b), pp. 989–1002.
- Partovi, M. H. and M. Caputo. “Principal portfolios: Recasting the efficient frontier.” *Economics Bulletin*, vol. 7, no. 3 (2004), pp. 1–10.
- Picard, F., É. Lebarbier, E. Budinská, and S. Robin. “Joint segmentation of multivariate Gaussian processes using mixed linear models.” *Computational Statistics & Data Analysis*, vol. 55, no. 2 (2011), pp. 1160–1170.
- Rajagopalan, V. and A. Ray. “Symbolic time series analysis via wavelet-based partitioning.” *Signal Processing*, vol. 86, no. 11 (2006), pp. 3309–3320.
- Rydén, T., T. Teräsvirta, and S. Åsbrink. “Stylized facts of daily return series and the hidden Markov model.” *Journal of Applied Econometrics*, vol. 13, no. 3 (1998), pp. 217–244.
- Samé, A., F. Chamroukhi, G. Govaert, and P. Aknin. “Model-based clustering and segmentation of time series with changes in regime.” *Advances in Data Analysis and Classification*, vol. 5, no. 4 (2011), pp. 301–321.
- Sheikh, A. Z. and J. Sun. “Regime change: Implications of macroeconomic shifts on asset class and portfolio performance.” *Journal of Investing*, vol. 21, no. 3 (2012), pp. 36–54.
- Son, Y. S. and S. Kim. “Bayesian single change point detection in a sequence of multivariate normal observations.” *Statistics*, vol. 39, no. 5 (2005), pp. 373–387.

- Tansey, W., O. H. M. Padilla, A. S. Suggala, and P. Ravikumar. “Vector-space Markov random fields via exponential families.” In *Proceedings of the 32nd International Conference on Machine Learning*, vol. 1 (2015), pp. 684–692.
- Tibshirani, R., M. Saunders, S. Rosset, J. Zhu, and K. Knight. “Sparsity and smoothness via the fused lasso.” *Journal of the Royal Statistical Society: Series B (Statistical Methodology)*, vol. 67, no. 1 (2005), pp. 91–108.
- Venter, J. H. and S. J. Steel. “Finding multiple abrupt change points.” *Computational Statistics & Data Analysis*, vol. 22, no. 5 (1996), pp. 481–504.
- Verbeek, J., N. Vlassis, and B. Kröse. “Efficient greedy learning of Gaussian mixture models.” *Neural Computation*, vol. 15, no. 2 (2003), pp. 469–485.
- Wahlberg, B., S. Boyd, M. Annegren, and Y. Wang. “An ADMM algorithm for a class of total variation regularized estimation problems.” *IFAC Proceedings Volumes*, vol. 45, no. 16 (2012), pp. 83–88.
- Wahlberg, B., C. Rojas, and M. Annegren. “On ℓ_1 mean and variance filtering.” In *Proceedings of the Forty Fifth Asilomar Conference on Signals, Systems and Computers* (2011), pp. 1913–1916.
- Welford, B. P. “Note on a method for calculating corrected sums of squares and products.” *Technometrics*, vol. 4, no. 3 (1962), pp. 419–420.
- Witten, D. and R. Tibshirani. “Covariance-regularized regression and classification for high dimensional problems.” *Journal of the Royal Statistical Society: Series B (Statistical Methodology)*, vol. 71, no. 3 (2009), pp. 615–636.
- Xu, N. “A survey of sensor network applications.” *IEEE Communications Magazine*, vol. 40, no. 8 (2002), pp. 102–114.
- Xu, Z. and Y. Liu. “Regularized autoregressive hidden semi Markov model.” <https://github.com/cran/rarhsmm> (2017).
- Zangwill, W. I. and C. B. Garcia. *Pathways to solutions, fixed points, and equilibria*. Prentice Hall: Englewood Cliffs (1981).

PAPER G

Originally published in *Quantitative Finance*

Dynamic portfolio optimization across hidden market regimes

Peter Nystrup, Henrik Madsen, and Erik Lindström

Abstract

Regime-based asset allocation has been shown to add value over rebalancing to static weights and, in particular, reduce potential drawdowns by reacting to changes in market conditions. The predominant approach in previous studies has been to specify in advance a static decision rule for changing the allocation based on the state of financial markets or the economy. In this article, model predictive control (MPC) is used to dynamically optimize a portfolio based on forecasts of the mean and variance of financial returns from a hidden Markov model with time-varying parameters. There are computational advantages to using MPC when estimates of future returns are updated every time a new observation becomes available, since the optimal control actions are reconsidered anyway. MPC outperforms a static decision rule for changing the allocation and realizes both a higher return and a significantly lower risk than a buy-and-hold investment in various major stock market indices. This is after accounting for transaction costs, with a one-day delay in the implementation of allocation changes, and with zero-interest cash as the only alternative to the stock indices. Imposing a trading penalty that reduces the number of trades is found to increase the robustness of the approach.

Keywords: Mean–variance optimization; Model predictive control; Hidden Markov model; Adaptive estimation; Forecasting.

1 Introduction

The objective of portfolio optimization is to find an optimal tradeoff between risk and return over a fixed planning horizon. Traditionally, investors decide on a strategic asset allocation (SAA) based on a single-period optimization, inspired by the mean–variance framework of Markowitz (1952). The purpose is to develop a static, “all-weather” portfolio that optimizes efficiency across a range of economic scenarios. Even if the SAA is reconsidered on an annual basis, it is unlikely to change significantly, as long as the purpose is “all-weather” efficiency.

In the presence of time-varying investment opportunities, portfolio weights should be adjusted as new information arrives to take advantage of favorable economic regimes and withstand adverse regimes (Sheikh and Sun 2012). The abrupt regime changes that financial markets tend to undergo present a big challenge to traditional SAA. Although some changes may be transitory, the new behavior often persists for several periods after a change (Ang and Timmermann 2012).

Regime-based asset allocation (RBAA) has indeed been shown to add value over rebalancing to static weights and, in particular, reduce potential drawdowns by reacting to changes in market conditions (see Ang and Bekaert 2004, Guidolin and Timmermann 2007, Bulla et al. 2011, Kritzman et al. 2012, Nystrup et al. 2015a, 2017a). The predominant approach is to specify in advance a static decision rule for changing the allocation based on the state of financial markets or the economy.

The parameters of the decision rule can be optimized in sample, but it does not guarantee that the decision rule is optimal for the problem at hand. A disadvantage is, therefore, that a large number of different specifications might have to be tried, in order to find a decision rule with good performance. Testing many different specifications increases the risk of inferior performance out of sample. Further, it can be argued that a static decision rule is hardly optimal when the underlying model used for regime inference is time varying, as in Bulla et al. (2011) and Nystrup et al. (2015a, 2017a).

An alternative approach is to dynamically optimize the portfolio based on the inferred regime probabilities and parameters taking into account transaction costs, risk aversion, and possibly other constraints. Herzog et al. (2007) and Boyd et al. (2014) proposed to use model predictive control (MPC) to solve this constrained, stochastic control problem. In MPC, a statistical model of the process is used to predict its future evolution and choose the best control action.

The great strength of MPC is the capability to solve control problems under constraints in a computationally feasible manner. Even so, it is commonly assumed that asset prices can be described by a linear factor model with constant variance and that there are no transaction costs in order to derive analytical expressions for when the allocation should be changed (see, e.g., Herzog et al. 2007, Costa and Araujo 2008, Calafiore 2008, 2009). This limits the practical impact of the results. Transaction costs are important when comparing the performance of static and dynamic strategies, because frequent rebalancing can offset the potential excess return of a dynamic strategy. Moreover, transaction costs stabilize the optimization problem (Brodie et al. 2009, Ho et al. 2015).

In this article, asset returns are modeled by a two-state hidden Markov model (HMM) with time-varying parameters, similar to the model considered in Nystrup et al. (2015a, 2017b,a). From a statistical perspective, the HMM is a more realistic description of asset price dynamics than a linear factor model

with constant variance. It is well suited to capture the stylized behavior of financial series, including volatility clustering, leptokurtosis, and time-varying correlations (see, e.g., Rydén et al. 1998, Ang and Timmermann 2012). From an economic perspective, the HMM can describe the abrupt changes in market conditions and investment opportunities that arise due to changes in risk aversion and structural changes in the state of the economy.

Instead of a static decision rule for changing the portfolio based on the inferred regime, MPC is used to dynamically optimize the portfolio based on forecasted means and variances. Using an HMM, the forecasts are mean-reverting and only change when the regime probabilities change. Thus, the allocation is still determined indirectly by the inferred regime. MPC, however, is applicable to forecasts from any type of model. The impact of transaction costs and risk aversion is analyzed in a live-sample setting using available market data. MPC is compared with previous approaches to RBAA under realistic assumptions about transaction costs and implementation.

The article is structured as follows: section 2 introduces the HMM, its estimation, and use for forecasting. Section 3 is concerned with dynamic portfolio optimization and MPC. The empirical results are presented in section 4. Finally, section 5 concludes.

2 The hidden Markov model

The HMM is a popular choice for inferring the hidden state of financial markets. It can match the tendency of financial markets to change their behavior abruptly and the phenomenon that the new behavior often persists for several periods after a change (Ang and Timmermann 2012). In addition, it is well suited to capture the stylized behavior of many financial series including volatility clustering and leptokurtosis, as shown by Rydén et al. (1998).

In an HMM, the probability distribution that generates an observation depends on the state of an unobserved Markov chain. A sequence of discrete random variables $\{S_t : t \in \mathbb{N}\}$ is said to be a first-order Markov chain if, for all $t \in \mathbb{N}$, it satisfies the Markov property:

$$\Pr(S_{t+1} | S_t, \dots, S_1) = \Pr(S_{t+1} | S_t). \quad (1)$$

The conditional probabilities $\Pr(S_{t+1} = j | S_t = i) = \gamma_{ij}$ are called transition probabilities. A Markov chain with transition probability matrix $\boldsymbol{\Gamma} = \{\gamma_{ij}\}$ has stationary distribution $\boldsymbol{\pi}$, if $\boldsymbol{\pi}^T \boldsymbol{\Gamma} = \boldsymbol{\pi}^T$ and $\mathbf{1}^T \boldsymbol{\pi} = 1$, where $\mathbf{1}$ is a column vector with all entries one. The Markov chain is said to be stationary if $\boldsymbol{\delta} = \boldsymbol{\pi}$, where $\boldsymbol{\delta}$ is the initial distribution, i.e., $\delta_i = \Pr(S_1 = i)$.

As an example, consider the two-state model with Gaussian conditional distributions:

$$Y_t | S_t \sim N(\mu_{S_t}, \sigma_{S_t}^2),$$

where

$$\mu_{S_t} = \begin{cases} \mu_1, & \text{if } S_t = 1, \\ \mu_2, & \text{if } S_t = 2, \end{cases} \quad \sigma_{S_t}^2 = \begin{cases} \sigma_1^2, & \text{if } S_t = 1, \\ \sigma_2^2, & \text{if } S_t = 2, \end{cases} \quad \text{and } \boldsymbol{\Gamma} = \begin{bmatrix} 1 - \gamma_{12} & \gamma_{12} \\ \gamma_{21} & 1 - \gamma_{21} \end{bmatrix}.$$

When the current state S_t is known, the distribution of Y_t depends only on S_t , and not on previous states or observations.

The sojourn times are implicitly assumed to be geometrically distributed:

$$\Pr(\text{'staying } t \text{ time steps in state } i) = \gamma_{ii}^{t-1} (1 - \gamma_{ii}). \quad (2)$$

The geometric distribution is memoryless, implying that the time until the next transition out of the current state is independent of the time spent in the state.

In order to improve its fit to the distributional and temporal properties of daily returns, the Gaussian HMM has been extended by considering other sojourn-time distributions than the memoryless geometric distribution (Bulla and Bulla 2006), other conditional distributions than the Gaussian distribution (Bulla 2011), and a continuous-time formulation as an alternative to the dominating discrete-time models (Nystrup et al. 2015b). As an alternative to increasing the model complexity, Nystrup et al. (2017b) obtained good results using an adaptive estimation approach that allowed for time variation in the parameters of a two-state Gaussian HMM. This approach was adopted in Nystrup et al. (2015a, 2017a) and will be adopted in this article as well.

2.1 Adaptive parameter estimation

The parameters of an HMM are usually estimated using the maximum-likelihood method. The two most popular approaches to maximizing the likelihood are direct numerical maximization and the Baum–Welch algorithm, a special case of the expectation–maximization (EM) algorithm (Baum et al. 1970, Dempster et al. 1977).

Every observation is assumed to be of equal importance, no matter how long the sample period is. This approach works well when the sample period is short and the underlying process does not change over time. The time-varying behavior of the parameters documented in previous studies (Rydén et al. 1998, Bulla 2011, Nystrup et al. 2017b), however, calls for an adaptive approach that assigns more weight to the most recent observations, while keeping in mind past patterns at a reduced confidence.

As pointed out by Cappé et al. (2005), it is possible to evaluate derivatives of the likelihood function with respect to the parameters for virtually any model that the EM algorithm can be applied to. As a consequence, instead of resorting to a specific algorithm such as the EM algorithm, the likelihood can be maximized using gradient-based methods. Lystig and Hughes (2002) described an algorithm

for exact computation of the score vector and the observed information matrix in HMMs that can be performed in a single pass through the data. Their algorithm was derived from the forward–backward algorithm.

The reason for exploring gradient-based methods is the flexibility to make the estimator recursive and adaptive.¹ The estimation of the parameters through a maximization of the conditional log-likelihood function can be done online using the estimator

$$\hat{\theta}_t = \arg \max_{\theta} \sum_{n=1}^t w_n \log \Pr(Y_n | Y_{n-1}, \dots, Y_1, \theta) = \arg \max_{\theta} \tilde{l}_t(\theta) \quad (3)$$

with $w_n = 1$.² The online estimator can be made adaptive by introducing a different weighting. A popular choice is to use exponential weights $w_n = f^{t-n}$, where $0 < f < 1$ is the forgetting factor (Parkum et al. 1992, Kulhavý and Zarrop 1993). The speed of adaption is then determined by the effective memory length

$$N_{\text{eff}} = \frac{1}{1-f}. \quad (4)$$

Maximizing the second-order Taylor expansion of $\tilde{l}_t(\theta)$ around $\hat{\theta}_{t-1}$ with respect to θ and defining the solution as the estimator $\hat{\theta}_t$ leads to

$$\hat{\theta}_t = \hat{\theta}_{t-1} - \left[\nabla_{\theta\theta} \tilde{l}_t(\hat{\theta}_{t-1}) \right]^{-1} \nabla_{\theta} \tilde{l}_t(\hat{\theta}_{t-1}). \quad (5)$$

This is equivalent to a specific case of the generalized autoregressive score (GAS) model of Creal et al. (2013). Using the estimator (5) it is possible to reach quadratic convergence, whereas the GAS model, in general, converges only linearly (see Cappé et al. 2005).

Scaling by the Hessian in (5) is equivalent to scaling by the variance of the score function, because the expectation of the score is zero. The variance of the score function is known as the Fisher information

$$I_t(\theta) = E[-\nabla_{\theta\theta} l_t] = E[\nabla_{\theta} l_t \nabla_{\theta} l_t^T]. \quad (6)$$

Approximating the Hessian by the Fisher information leads to the recursive, adaptive estimator

$$\hat{\theta}_t \approx \hat{\theta}_{t-1} + A \left[I_t(\hat{\theta}_{t-1}) \right]^{-1} \nabla_{\theta} \tilde{l}_t(\hat{\theta}_{t-1}). \quad (7)$$

¹See Khreich et al. (2012) for a survey of techniques for incremental learning of HMM parameters.

²An online estimator processes its input observation-by-observation in a sequential fashion, without having the entire input sequence available from the start.

The tuning constant A can be adjusted to increase or decrease the speed of convergence without changing the effective memory length, although it is common to choose $A \approx 1/N_{\text{eff}}$. The inverse of the Fisher information can be updated recursively using (6) and the matrix inversion lemma. It is necessary to apply a transformation to all constrained parameters for the estimator (7) to converge, and it is advisable to start the estimation at $t > 1$ to avoid large initial steps.

The time variation of the parameters is observation driven based on the score of the likelihood function. Although the parameters are stochastic, they are perfectly predictable given the past observations. This is contrary to parameter-driven models, in which the parameters are stochastic processes with their own source of error. No prior knowledge is assumed about the parameters, and no attempt is made to identify the drivers of the variations (see, e.g., Brennan et al. 1997).

The use of the score function for updating the parameters is intuitive, as it defines the steepest ascent direction for improving the model's local fit in terms of the likelihood at time t given the current parameter values (Creal et al. 2013). For HMMs, the score function must consider the previous observations and cannot reasonably be approximated by the score function of the most recent observation, as it is often done for other models (Khreich et al. 2012). This leads to a significant increase in computational complexity. In order to compute the weighted score function, the algorithm of Lystig and Hughes (2002) has to be run for each iteration and the contribution of each observation has to be weighted.

2.2 Forecasting

The first step toward calculating the forecast distributions is to estimate the current state probabilities given the past observations and parameters. The vector of state probabilities is

$$\boldsymbol{\alpha}_{T|T}^T = \frac{\boldsymbol{\delta}^T \mathbf{P}_1(y_1) \prod_{t=2}^T \boldsymbol{\Gamma}_t \mathbf{P}_t(y_t)}{\boldsymbol{\delta}^T \mathbf{P}_1(y_1) \left(\prod_{t=2}^T \boldsymbol{\Gamma}_t \mathbf{P}_t(y_t) \right) \mathbf{1}}, \quad (8)$$

where the i 'th entry is $(\boldsymbol{\alpha}_{T|T})_i = \Pr(S_T = i | Y_T, \dots, Y_1)$ and $\mathbf{P}_t(y_t)$ is a diagonal matrix with the conditional densities $p_i(y_t) = \Pr(Y_t = y_t | S_t = i, \theta_t)$ as entries.

Once the current state probabilities are estimated, the state probabilities k steps ahead can be calculated by multiplying $\boldsymbol{\alpha}_{T|T}$ with the transition probability matrix k times:

$$\boldsymbol{\alpha}_{T+k|T}^T = \boldsymbol{\alpha}_{T|T}^T \boldsymbol{\Gamma}_T^k. \quad (9)$$

The parameters are assumed to stay constant in the absence of a model describing their evolution.

The density forecast is the average of the state-dependent conditional densities weighted by the forecasted state probabilities. When the conditional distributions are distinct normal distributions, the forecast distribution will be a nonnormal mixture (Frühwirth-Schnatter 2006).³ Using Monte Carlo simulation, Boyd et al. (2014) showed that the results of dynamic portfolio optimization are not particularly sensitive to higher-order moments. Consequently, for the present application, only the first and second moment of the forecast distribution are considered.

The first two moments of a mixture distribution are

$$\mu = \sum_{i=1}^m \mu_i \alpha_i \quad (10)$$

$$\sigma^2 = \sum_{i=1}^m (\mu_i^2 + \sigma_i^2) \alpha_i - \mu^2 \quad (11)$$

with α_i denoting the weights—that is, the forecasted state probabilities.

Before calculating the moments of the mixture distribution, the conditional means and variances of the returns are calculated based on the moments of the log-returns. Within each state, the returns r_t are assumed to be iid with log-normal distribution

$$\log(1 + r_t) \sim N(\mu, \sigma^2),$$

where μ and σ^2 are the mean and variance of the log-returns. Thus, the mean and variance of the returns are given by

$$E[r_t] = \exp(\mu + \sigma^2/2) - 1 \quad (12)$$

$$\text{Var}[r_t] = (\exp(\sigma^2) - 1) \exp(2\mu + \sigma^2). \quad (13)$$

The forecasted mean and variance will be mean-reverting, as the forecast horizon extends and the state probabilities converge to the stationary distribution of the Markov chain. The rate of convergence is determined by the size of the second largest eigenvalue of the transition probability matrix, which for a two-state Markov chain is $|\lambda_2| = |\gamma_{11} + \gamma_{22} - 1|$. The more persistent the states are—or equivalently, the larger the size of λ_2 —the lower the rate of convergence.

³The nonnormality can easily be captured by generating scenarios using the current state probabilities as initial probabilities.

3 Dynamic portfolio optimization

The approach outlined in the previous section can be applied online to forecast the mean and variance of returns at discrete horizons. The forecasted means and variances are inputs to a multi-period portfolio optimization. Every day a decision has to be made whether or not to change the current portfolio allocation, knowing that the decision will be reconsidered the next day with new input. In the risk-neutral case, the possible gain or saving from changing allocation has to exceed the costs involved.

The planning horizon should at least be long enough to reach the stationary distribution of the underlying Markov chain, whereafter the forecast does not change. In principle, the forecast horizon should be infinitely long, but in reality no one has an infinite horizon.

There is a limit to how far ahead in time it is meaningful to make predictions. For sufficiently long horizons, it is not possible to make better predictions than the long-term mean and variance, which is also the reason that the forecasted mean and variance converge to their stationary values, when the forecast horizon extends. Thus, looking only a limited number of steps into the future is not just an approximation necessary to make the optimization problem computationally feasible, it also seems perfectly reasonable.

The formulation of the dynamic portfolio optimization problem as a stochastic control problem is inspired by Boyd et al. (2014). However, the objective function and the way transaction costs are handled are significantly different. Boyd et al. (2014) assumed that infinite amounts of cash could be entered into the portfolio on any given day. Although it would be possible to constrain the amount of cash that can be entered into the portfolio per day, it is for most purposes more realistic to assume that only a finite amount of cash is available initially. At any later point in time, the amount of cash available depends on the portfolio's development and transaction costs incurred.

3.1 Stochastic control formulation

Let $h_t \in \mathbb{R}^n$ denote the portfolio holdings at time t , where $(h_t)_i$ is the dollar value of asset i at the end of day t , with $(h_t)_i < 0$ meaning a short position in asset i . Assets can be bought and sold at the end of each day. Let $u_t \in \mathbb{R}^n$ denote the dollar values of the trades, with $(u_t)_i > 0$ meaning that asset i is bought at the end of day t .

The post-trade portfolio is defined as

$$h_t^+ = h_t + u_t, \quad t = 0, \dots, T-1, \quad (14)$$

which is also the portfolio at the beginning of day $t+1$. The total value of the portfolio before trading is $V_t = \mathbf{1}^T h_t$ and the total value of the post-trade

portfolio is $V_t^+ = \mathbf{1}^T h_t^+ \leq V_t$. Working with holdings h_t , rather than weights h_t/V_t , simplifies the notation.

The portfolio is assumed to be self-financing with transaction costs proportional to the total trade volume, that is,

$$\mathbf{1}^T u_t + \kappa^T |u_t| = 0, \quad t = 0, \dots, T-1, \quad (15)$$

where κ is a vector of commission rates and the absolute value is elementwise. The constraint states that $-\mathbf{1}^T u_t$, which is the total gross proceeds from sales minus the total gross proceeds from purchases, equals $\kappa^T |u_t|$, the total transaction cost for purchases and sales.

For optimization purposes, the constraint (15) is replaced by the convex relaxation

$$\mathbf{1}^T u_t + \kappa^T |u_t| \leq 0, \quad t = 0, \dots, T-1, \quad (16)$$

which allows the possibility of discarding money.

The post-trade portfolio is held until the end of the next day. The (pre-trade) portfolio at the end of the next day is given by

$$h_{t+1} = (\mathbf{1} + r_{t+1}) \circ h_t^+, \quad t = 0, \dots, T-1,$$

where $r_{t+1} \in \mathbb{R}^n$ is the vector of asset returns from day t to day $t+1$ and \circ denotes Hadamard (elementwise) multiplication of vectors. As illustrated in figure 1, the dynamics are linear, but unknown at time t .

The returns r_t are random variables with mean and covariance

$$\mathbb{E}[r_t] = \bar{r}_t, \quad \mathbb{E}\left[(r_t - \bar{r}_t)(r_t - \bar{r}_t)^T\right] = \Sigma_t, \quad t = 1, \dots, T.$$

The trades are determined in each period by a trading policy $\phi_t : \mathbb{R}^n \rightarrow \mathbb{R}^n$:

$$u_t = \phi_t(h_t), \quad t = 0, \dots, T-1.$$

Let $\mathcal{C}_t \subseteq \mathbb{R}^n$ denote the post-trade portfolio constraint set. Since \mathcal{C}_t is nonempty, it follows that for any value of h_t , there exists a u_t for which

$$h_t^+ = h_t + u_t \in \mathcal{C}_t.$$

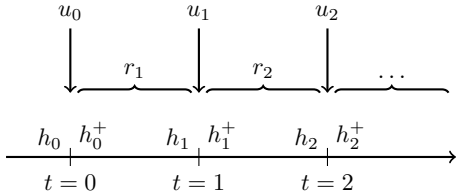


Figure 1: Timeline of portfolio dynamics.

Explicit constraints are imposed only on the post-trade portfolio h_t^+ , because this can be controlled by buying and selling (i.e., through u_t), whereas the pre-trade portfolio h_t is determined by the random return r_t in the previous period and, therefore, not directly controllable.

The portfolio may be subject to constraints on the post-trade holdings, such as minimum and maximum allowed holdings for each asset:

$$h_t^{\min} \leq h_t^+ \leq h_t^{\max}, \quad (17)$$

where the inequalities are elementwise and h_t^{\min} and h_t^{\max} are given vectors of minimum and maximum asset holdings in dollars. For a long-only portfolio with no short positions allowed $h^{\min} = 0$. Position limits can also be expressed relative to the total portfolio value, for example,

$$y_t^+ \leq V_t^+ H_t^{\max}, \quad (18)$$

with $H_t^{\max} \in \mathbb{R}^n$.

The overall objective is to maximize

$$J = \mathbb{E} \left[V_T - \sum_{t=0}^{T-1} \psi_t(h_t, u_t) \right], \quad (19)$$

where the expectation is over the sequence of returns r_1, \dots, r_T conditional on all past observations, $V_T = \mathbf{1}^T h_T$ is the terminal value of the portfolio, and $\psi_t : \mathbb{R}^n \times \mathbb{R}^n \rightarrow \mathbb{R}$ is a cost, with units of dollars, for period t . This is a stochastic control problem with linear dynamics and convex objective function, ensuring the existence of a unique solution (Boyd and Vandenberghe 2004). The data for the problem is the distribution of r_t , the stage costs ψ_t , and the initial portfolio h_0 .

Risk-averse control

The traditional risk-adjustment charge is proportional to the variance of the next period portfolio value given the current post-trade portfolio, which corresponds to

$$\psi_t(h_t, u_t) = \gamma \frac{\text{Var}[V_{t+1}|h_t^+]}{V_t^+} = \gamma \frac{(h_t^+)^T \Sigma_{t+1} h_t^+}{V_t^+}, \quad (20)$$

where $\gamma \geq 0$ is a unitless risk-aversion parameter. To ensure that the tradeoff between terminal value and variance does not depend on the portfolio value, the variance is scaled by the post-trade value V_t^+ .

If the returns are independent, then the sum of the variances is the variance of the terminal value. In that case, the objective function (19) with the risk-adjustment charge (20) is equivalent to the mean-variance criterion of Markowitz

(1952).⁴ It is a special case of expected utility maximization with a quadratic utility function. While the utility approach was theoretically justified by von Neumann and Morgenstern (1953), in practice few, if any, investors know their utility functions; nor do the functions which financial engineers and economists find analytically convenient necessarily represent a particular investor's attitude toward risk and return (Dai et al. 2010a). The mean–variance criterion remains the most commonly used in portfolio optimization (Meucci 2005).

As an alternative to including a risk penalty in the objective function, Boyd et al. (2014) proposed to constrain the portfolio standard deviation to a fraction of the portfolio value. In a single-period setting, the two formulations are equivalent. A risk limit might be preferable, because it is easier to quantify than a risk-aversion parameter. In a multi-period setting, however, a constraint on the portfolio standard deviation leads to excessive trading and inferior performance. The resulting constant-risk portfolio does not consider the attractiveness of the risk-return tradeoff. In order to maximize the return, the portfolio will be right at the risk limit most of the time, which leads to forced trading, whenever the volatility forecast increases unexpectedly.

Trading aversion

Boyd et al. (2014) gave examples of other convex constraints and cost terms that arise in practical investment problems and can easily be included. One option is to include a penalty for trading

$$\psi_t(u_t) = \rho^T |u_t|, \quad (21)$$

where ρ is a vector of trading-aversion parameters. This could reflect a conservatism toward trading, for example, due to the uncertainty related to the parameter estimates and forecasts. Inflating the transaction cost κ in (15)–(16) would have the same effect. In order to distinguish it from the actual transaction cost, the trading penalty (21) is instead included in the objective function (19), similarly to the variance penalty (20).

It is well known that estimation errors can cause mean–variance optimized portfolios to perform poorly (Michaud 1989, DeMiguel et al. 2009b). Brodie et al. (2009) reformulated the mean–variance optimization problem as a constrained, least-squares regression problem. Imposing a trading penalty (21) that is proportional to the trade volume is a convex relaxation of constraining the number of trades. Similar to the least absolute shrinkage and selection operator (lasso) in regression analysis (Tibshirani 1996), this ℓ_1 penalty regularizes the optimization problem and reduces the risk due to estimation errors (Ho et al. 2015).

⁴Everything is scaled by V_t .

3.2 Model predictive control

MPC, also referred to as receding horizon control or rolling horizon planning, is widely used in some industries; primarily for systems with slow dynamics such as energy systems, chemical plants, and supply chains (see, e.g., Bemporad 2006), but it is also used, for example, for steering autonomous vehicles (see, e.g., Falcone et al. 2007). MPC typically works very well in practice, even for short horizons.

MPC is based on the simple idea that in order to determine u_t , all future (unknown) returns are replaced by their forecasted mean values \hat{r}_τ , $\tau = t+1, \dots, T$. This turns the stochastic control problem into a deterministic optimization problem

$$\begin{aligned} &\text{maximize} && V_T - \sum_{\tau=t}^{T-1} \psi_\tau(h_\tau, u_\tau) \\ &\text{subject to} && h_{\tau+1} = (\mathbf{1} + \hat{r}_{\tau+1}) \circ (h_\tau + u_\tau), \quad \tau = t, \dots, T-1 \end{aligned} \quad (22)$$

with variables h_{t+1}, \dots, h_T and u_t, \dots, u_{T-1} . Note that h_t is not a variable, but the (known) current portfolio holdings.

Solving this convex optimization problem yields an optimal sequence of trades u_t^*, \dots, u_{T-1}^* . This sequence is a plan for future trades over the remaining trading horizon under the highly unrealistic assumption that future returns will be equal to their forecasted values. An alternative is to forecast the unconditional distribution and generate a number of scenarios, but this is computationally much more challenging.

The MPC policy takes $\phi^{\text{MPC}}(h_t) = u_t^*$, that is, only the first trade in the planned sequence of trades is executed. At the next step, the process is repeated, starting from the new portfolio h_{t+1} . In the case of a mean-variance objective function, Herzog et al. (2007) showed that future asset allocation decisions do not depend on the trajectory of the portfolio, but solely on the current tradeoff between satisfying the constraints and maximizing the objective. As emphasized by Boyd et al. (2014), there are computational advantages to using MPC in cases when estimates of future return statistics are updated online. In this case, the expected returns \bar{r}_t are simply replaced with the most recent return estimates.

MPC for stochastic systems is a suboptimal control strategy. However, it uses new information advantageously and is better than pure open-loop control (Herzog et al. 2007). The open-loop policy would be to execute the entire sequence of trades u_t^*, \dots, u_{T-1}^* based on the initial portfolio without recourse. Using Monte Carlo simulation, Boyd et al. (2014) showed that, in any practical sense, the MPC policy is optimal.

Truncated MPC

The MPC policy described in (22) plans a sequence of trades for the full time interval t, \dots, T . A common variation is to look a limited number of steps, K ,

Algorithm 1: MPC approach to dynamic portfolio optimization.

1. Update HMM parameters based on the most recent returns
 2. Forecast the mean and variance K steps into the future
 3. Compute an optimal sequence of trades $u_t^*, \dots, u_{t+K-1}^*$ based on the current portfolio
 4. Execute the first trade, u_t^* , in the sequence and return to step 1
-

into the future. At each time t the optimization problem is

$$\begin{aligned} & \text{maximize} && V_{t+K}^{\text{term}}(h_{t+K}) - \sum_{\tau=t}^{t+K-1} \psi_{\tau}(h_{\tau}, u_{\tau}) \\ & \text{subject to} && h_{\tau+1} = (\mathbf{1} + \hat{r}_{\tau+1}) \circ (h_{\tau} + u_{\tau}), \quad \tau = t, \dots, t+K-1 \end{aligned} \quad (23)$$

with variables h_{t+1}, \dots, h_{t+K} and u_t, \dots, u_{t+K-1} . Here K is the number of steps of look-ahead and V_{t+K}^{term} is the terminal value.

If the terminal value is appropriately chosen, then the truncated MPC policy is exactly the same as the full look-ahead policy. If K is large enough to reach the stationary distribution of the underlying Markov chain, then $V_{t+K}^{\text{term}}(h_{t+K})$ can be replaced by $V_{t+K} = \mathbf{1}^T h_{t+K}$, since the risk–return tradeoff does not change after this point. If transaction costs are very high, then the choice of K can affect the result, even when K is large enough to reach the stationary distribution of the underlying Markov chain. However, the choice should reflect how far ahead in time it is meaningful to make predictions.

Algorithm 1 summarizes the four steps in the MPC approach to solving the dynamic portfolio optimization problem. At time t , a new measurement is obtained, which is used to update the parameters of the HMM and forecast the mean and variance K steps into the future. The next step is to compute an optimal sequence of trades $u_t^*, \dots, u_{t+K-1}^*$ based on the current portfolio and the forecasts. Only the first trade in the sequence is executed before a new measurement is obtained and the procedure is repeated. Computing the optimal sequence of trades for $K = 100$ by solving the optimization problem (23) takes less than 18 milliseconds using CVXPY (Diamond and Boyd 2016) with the open-source solver ECOS (Domahidi et al. 2013).

4 Empirical results

4.1 Data

The asset universe considered consists of various major stock market indices and cash. Cash positions are assumed to be risk-free and yield zero interest;

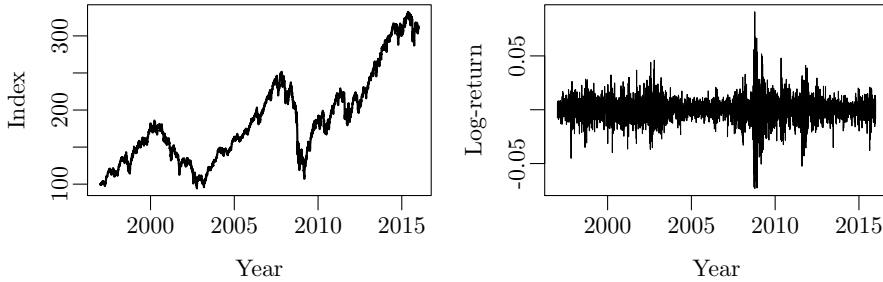


Figure 2: MSCI World Total Return Index and its daily log-returns.

hence, the only source of performance is the stock indices. The stock indices are considered one at a time. By only considering one risky asset and one risk-free asset, correlations can be disregarded. It is natural to focus on a stock index, since portfolio risk is typically dominated by stock market risk (see, e.g., Goyal et al. 2015). Previous studies on RBAA have also focused on stocks and cash, sometimes in combination with bonds (Ang and Bekaert 2004, Guidolin and Timmermann 2007, Bulla et al. 2011, Kritzman et al. 2012, Nystrup et al. 2015a).

In the first subsections, the data analyzed is 4,943 daily log-returns of the MSCI World Total Return Index covering the period from 1997 through 2015.⁵ Then in section 4.6, the analysis is repeated for S&P 500, TOPIX, DAX, FTSE, and MSCI EM. Figure 2 shows the MSCI World index and its daily log-returns over the 19-year data period. The volatility forms clusters, as large price movements tend to be followed by large price movements and vice versa, as noted by Mandelbrot (1963).⁶ RBAA aims to exploit this persistence of the volatility, since risk-adjusted returns, on average, are substantially lower during turbulent periods, irrespective of the source of turbulence, as shown by Kritzman and Li (2010).

Similar to previous studies, the regime detection will focus on the log-returns of the stock indices. Observed regimes in financial markets are related to the phases of the business cycle (Campbell 1999, Cochrane 2005). As argued in Nystrup et al. (2015a), the link is complex and difficult to exploit for investment purposes due to the large lag in the availability of data related to the business cycle. Besides, stock markets generally lead the economy (Siegel 1991). The

⁵The log-returns are calculated using $r_t = \log(P_t) - \log(P_{t-1})$, where P_t is the closing price of the index on day t and \log is the natural logarithm.

⁶A quantitative manifestation of this fact is that while returns themselves are uncorrelated, absolute and squared returns display a positive, significant, and slowly decaying autocorrelation function.

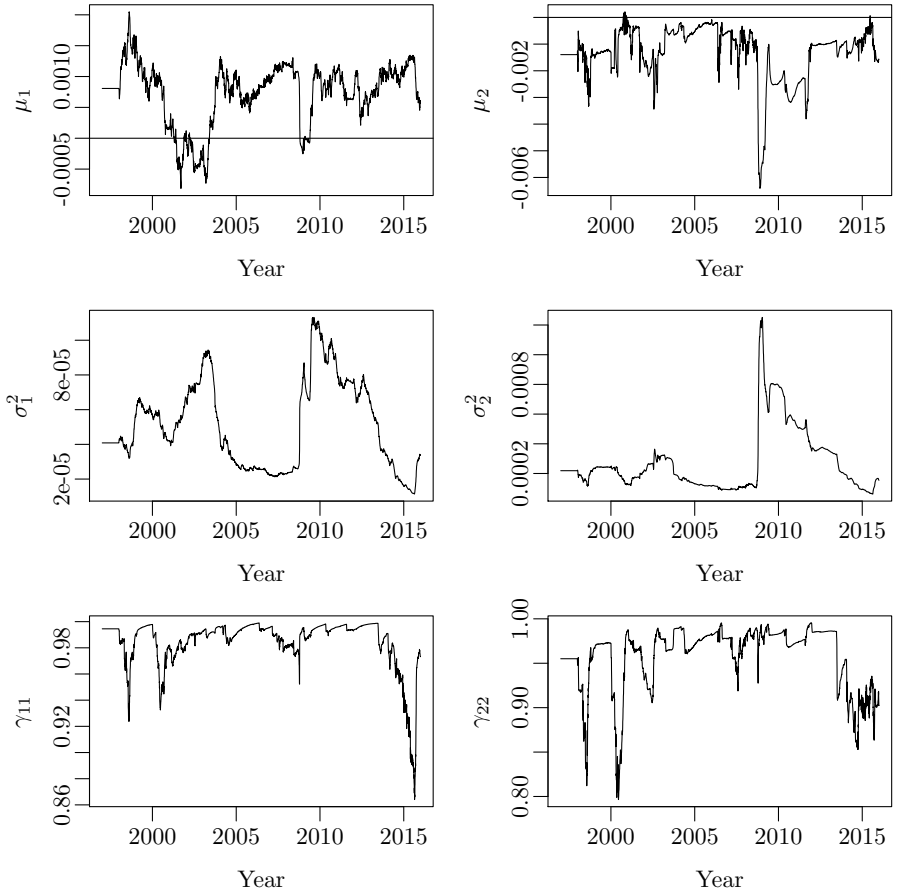


Figure 3: Parameters of a two-state Gaussian HMM estimated adaptively using an effective memory length of $N_{\text{eff}} = 260$ days.

focus is, therefore, on readily available market data instead of attempting to establish the link to the business cycle.

4.2 HMM parameters

Figure 3 shows the result of applying the adaptive estimator (10) on the daily log-returns of the MSCI World index to estimate the parameters of a two-state Gaussian HMM. An effective memory length of $N_{\text{eff}} = 260$ days was used with the tuning constant $A = 1/N_{\text{eff}}$. The first 260 observations were used for initialization.

The choice of memory length affects the parameter estimates and can be viewed

as a tradeoff between bias and variance. A shorter window yields a faster adaptation to changes, but larger variance of the estimates, as fewer observations are included in the estimation. In Nystrup et al. (2017b), an effective memory length of about one year was found to give the best forecasts. In agreement with this, forecasts based on a memory length of 260 days are found to give good results when used as inputs for MPC of an investment portfolio.

Similar to the finding in previous studies (Rydén et al. 1998, Bulla 2011, Nystrup et al. 2017b), the HMM parameters are seen to fluctuate a lot over the 19-year data period. State one is the most persistent, has the lowest variance, and—most of the time—has a positive mean. State two has a much higher variance and a negative mean value most of the time. The period in the early 2000s, when the mean return in both states was negative, exposes a weakness to having predefined rules for changing the portfolio based on the regime; regardless of the regime, an allocation to stocks would lose money in those years.

The probabilities of staying in the current state, γ_{11} and γ_{22} , appear to be less than 0.99 the majority of the time. A probability of 0.99 would imply an expected sojourn time of $1/(1 - 0.99) = 100$ days. The number of steps of look-ahead, K , is, therefore, chosen to be 100.⁷ This is found to be a sufficiently large number in that a further increase does not affect the results.

4.3 Optimal thresholds for changing allocation

The optimal thresholds for changing allocation depend on the specific parameter values. Using MPC, the current parameter values are taken into account when deciding whether to change the portfolio, instead of having a static decision rule for changing the allocation based on the inferred regime. As an example, figure 4 shows the optimal thresholds for changing allocation for different levels of risk aversion and transaction costs for a long-only portfolio based on the parameter values on January 2, 2012. The thresholds are not necessarily optimal ex post.

Based on the parameter values on January 2, 2012, a risk-neutral investor with $\gamma = 0$ that can trade at zero cost should be fully invested in stocks when the probability of currently being in state one (the state with low variance and positive mean) exceeds 0.55. Whenever the probability falls below 0.55, the risk-neutral investor should sell all stocks. The risk-neutral investor is always fully allocated to either stocks or cash.

A risk-averse investor with $\gamma = 2$ should be fully invested in stocks when the probability of currently being in state one exceeds 0.86 and—similar to a risk-neutral investor—fully allocated to cash when the probability is below 0.55. In between, the portfolio is a mix of stocks and cash.

⁷The number of steps of look-ahead, K , could also be chosen based on the maximum absolute value of the second largest eigenvalue of the transition probability matrix, $|\lambda_2| = |1 - \gamma_{11} - \gamma_{22}|$, which is just below 0.99.

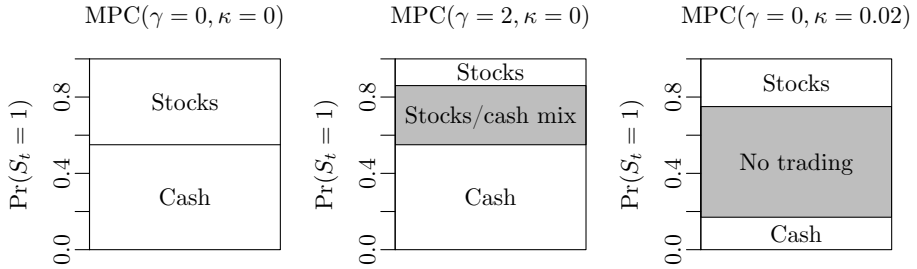


Figure 4: Optimal thresholds for changing allocation for different levels of risk aversion, γ , and transaction costs, κ , based on the parameter values on January 2, 2012.

A risk-neutral investor that can trade stocks at a cost of $\kappa = 0.02$ per transaction should buy stocks when the probability of currently being in state one exceeds 0.75 and sell all stocks when the probability falls below 0.17. In between, the risk-neutral investor should keep the initial portfolio. The thresholds are not symmetric, as $0.75 \neq 1 - 0.17$.

Institutional investors can trade stocks at a much lower cost than 2%, but this high value clearly illustrates that the presence of transaction costs leads to a no-trade zone. Based on the parameter values at the end of 2015, for example, a risk-neutral investor that can trade at a cost of 2% should never sell stocks, even if the probability of currently being in the good state is zero, because of the low persistence of the bad state and the not excessively negative mean value. The higher the transaction costs, the larger the no-trade zone. Dai et al. (2010b) derived similar results in a continuous-time framework.

4.4 Comparison of MPC results

Table 5 summarizes the performance of MPC with and without risk (20) and trading (21) aversion for $K = 100$ steps of look-ahead. Short positions were not allowed. Transaction costs of $\kappa = 0.001$ (10 basis points per transaction) have been deducted in all three cases. This is a realistic cost for an institutional investor.

The first approach, $\text{MPC}(\gamma = 0, \rho = 0)$, is pure return maximization with no risk or trading penalty (except for the 10 basis point transaction cost). This approach yields the highest annualized return (AR) despite having an annual turnover (AT) of 4.61. An AT of 4.61 means that the entire portfolio is shifted from stocks to cash or vice versa, on average, 4.61 times per year.

Introducing a risk penalty by setting $\gamma = 2$ increases the AT from 4.61 to 5.30 and leads to a lower standard deviation (SD), lower maximum drawdown

	MPC($\gamma = 0, \rho = 0$)	MPC($\gamma = 2, \rho = 0$)	MPC($\gamma = 0, \rho = 0.02$)
Annualized return	0.076	0.062	0.070
Standard deviation	0.12	0.10	0.11
Sharpe ratio	0.65	0.61	0.67
Maximum drawdown	0.26	0.21	0.23
Calmar ratio	0.29	0.29	0.31
Annual turnover	4.61	5.30	1.17

Table 5: Performance of MPC with and without risk and trading aversion.

(MDD)⁸, and lower AR. The Calmar ratio (CR)⁹ is unaffected. To ensure that the performance comparison is not distorted by autocorrelation in the daily returns, the reported SDs have been adjusted for autocorrelation using the procedure outlined by Kinlaw et al. (2015). As γ increases and more emphasis is put on the variance forecast, the Sharpe ratio (SR)¹⁰ deteriorates. This could indicate that the mean changes faster than the variance; however, the variance is crucial when distinguishing between market regimes (Nystrup et al. 2016). Basing the allocation decision on both the mean and variance forecasts adds another source of estimation error. This should be further explored in a future study encompassing more assets.

The third approach, MPC($\gamma = 0, \rho = 0.02$), is return maximization with a 2% trading penalty on top of the 10 basis point transaction cost. The trading penalty (21) with $\rho = 0.02$ is included in the objective function when determining the optimal sequence of trades in step 3 of algorithm 1, but the actual transaction cost applied is still $\kappa = 0.001$. This subjective trading penalty leads to a significantly lower AT and a slightly lower AR compared to the unpenalized case, while the SR and CR are roughly unchanged.

Figure 6 shows the transactions in the MSCI World index relative to the portfolio value at the time for the three approaches. Introducing a risk penalty by setting $\gamma = 2$ leads to more frequent trading and a higher AT compared to pure return maximization. A trading penalty, on the other hand, leads to significantly fewer trades. The trading penalty appears to be effective at reducing the number of trades that are reversed within a short timespan and may, therefore, be preferred in some applications.

⁸The maximum drawdown is the largest relative decline from a historical peak in the index value.

⁹The Calmar ratio is the annualized return divided by the maximum drawdown.

¹⁰The Sharpe ratio is the annualized return divided by the standard deviation adjusted for autocorrelation.

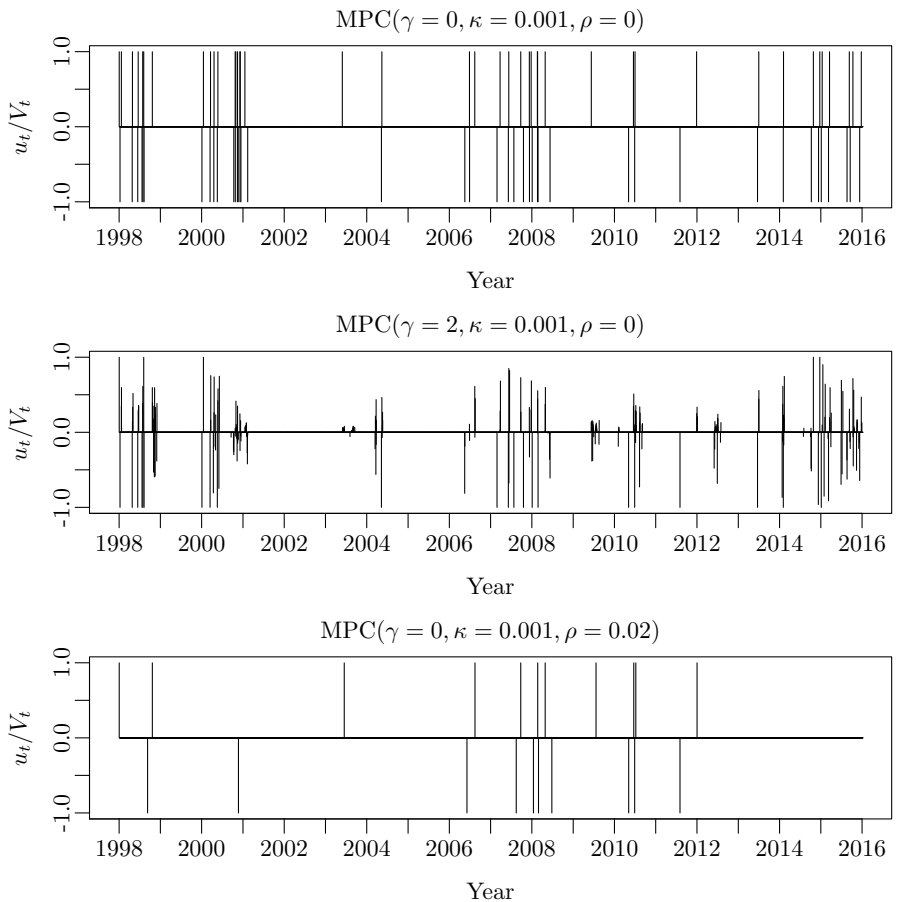


Figure 6: Trades in the MSCI World index relative to the portfolio value at the time based on MPC with and without risk and trading aversion.

	MPC($\gamma = 0, \rho = 0$)	MPC($\gamma = 0, \rho = 0.02$)	MSCI World	RBAA	SAA
Annualized return	0.065	0.069	0.056	0.046	0.041
Standard deviation	0.12	0.11	0.18	0.12	0.13
Sharpe ratio	0.56	0.63	0.30	0.38	0.32
Maximum drawdown	0.26	0.25	0.57	0.34	0.44
Calmar ratio	0.25	0.28	0.10	0.13	0.09
Annual turnover	4.16	1.17	0.00	1.94	0.09

Table 8: Performance of MPC with and without a trading penalty compared to the MSCI World index, rule-based RBAA, and SAA, when allocation changes are subject to a one-day delay.

4.5 Comparison with rule-based approach when allocation changes are delayed

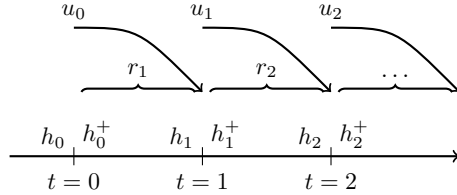


Figure 7: Timeline of portfolio dynamics when trades are delayed by one day.

The results presented in the previous subsection are based on the assumption that it is possible to trade at the closing price after it is known and the parameters and forecasts have been updated. It is often more realistic to assume that allocation changes cannot be implemented until the end of the next day, as illustrated in figure 7. To ensure that the long-only constraint is still satisfied at all times, trading decisions have to be implemented as fractions of the holding.¹¹

In table 8, the performance of the risk-neutral MPC approach with and without a trading penalty is reported when allocation changes are subject to a one-day delay. Transaction costs of 10 basis points have been deducted from the reported results. The AR of MPC with no risk or trading penalty is about one percentage point lower when allocation changes are delayed, in spite of the AT being lowered from 4.61 to 4.16.

Imposing a trading penalty actually increases the AR when allocation changes are subject to a one-day delay. The AR, SR, and CR of the risk-neutral MPC approach with trading aversion are almost unchanged compared to when there is no delay. This suggest that a trading penalty increases the robustness of the MPC approach, similarly to what it does in a single-period setting (Brodie et al. 2009, Ho et al. 2015). The delay has no impact on the AT of the penalized MPC approach that is still substantially lower than for the unpenalized approach.

¹¹If a decision is made on day t to sell \$80 worth of stocks out of a total holding of \$100, then 80% of the stocks are sold on day $t + 1$, regardless of their value.

In table 8, the performance of the risk-neutral MPC approaches is compared with the MSCI World index, a rule-based RBAA approach, and an SAA portfolio that is rebalanced monthly to a fixed allocation of 69% stocks and 31% cash, which equals the average allocation of the unpenalized MPC approach.

The rule-based RBAA approach is the same as in Nystrup et al. (2017a). Like the risk-neutral MPC approaches, it is either fully allocated to stocks or cash. The allocation is changed when the probability that a regime change has occurred exceeds a threshold of 0.9998. The underlying HMM is estimated using (7) with an effective memory length of two years, since this was found to give better results. A similar memory length was used in Nystrup et al. (2015a, 2017a).

The risk-neutral MPC approaches have realized the highest AR and have outperformed the MSCI World index that has a significantly higher SD and MDD. This is under the assumption that cash positions yield zero interest. Further, with approximately the same SD and a lower MDD than the RBAA and SAA portfolios, the MPC approaches have realized a substantially higher SR and CR.

RBAA outperforms both SAA and the index in terms of SR and CR. Its AT of 1.94 is higher than that of the penalized MPC approach, but less than half of that of the unpenalized MPC approach. The performance of RBAA relative to the index is not as convincing as when there are other alternatives to invest in than zero-interest cash (see Nystrup et al. 2015a, 2017a).

In figure 9, the performance of MPC with no trading or risk penalty is compared to the rule-based RBAA strategy and the MSCI World index when allocation changes are subject to a one-day delay. In the shaded periods, the MPC (top half) and the RBAA portfolios (bottom half) were fully allocated to cash. The allocations are different from what would be expected if the regimes were based on a business cycle indicator.

The MPC portfolio performs better than the RBAA portfolio during the build-up and burst of the dot-com bubble around the year 2000. It is fully allocated to stocks most of the time leading up to the peak and fully allocated to cash throughout the downturn. The MPC portfolio stays fully allocated to cash throughout the downturn, because the mean value in both states is negative in this period, cf. figure 3. The RBAA portfolio times the subsequent rebound better and does well by staying fully allocated to cash throughout the crash in 2008. The MPC portfolio times the rebound in 2009 better and gradually extends its lead over the following years.

The MPC portfolio is slightly behind the MSCI World index at the peak in year 2000, but then moves ahead of the index during the downturn. The lead is maintained in the following years leading up to the crash in 2008, during which the lead is significantly extended. Part of the lead is lost during the market rebound in the first half of 2009, before the MPC allocation is shifted

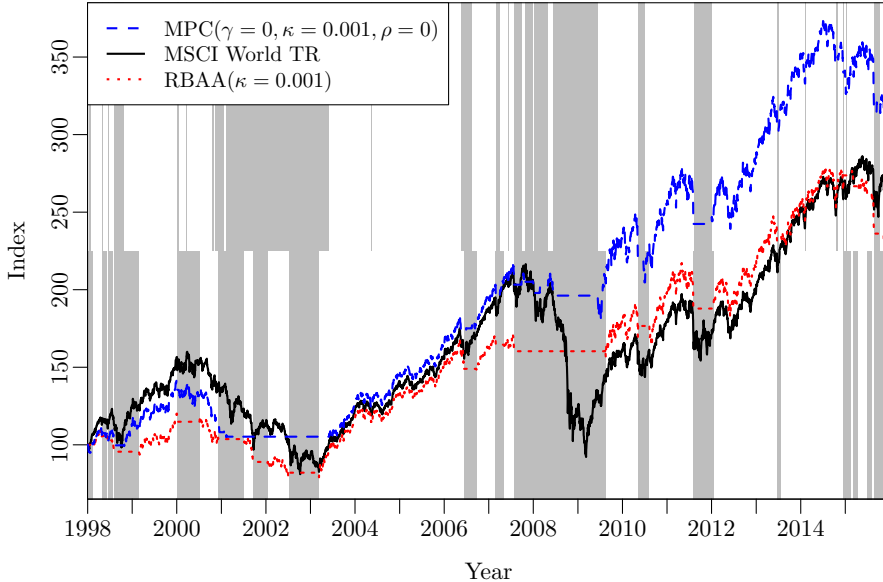


Figure 9: Performance of the return-maximizing MPC approach compared with rule-based RBAA and the MSCI World index. In the shaded periods, the MPC and the RBAA portfolios (top and bottom half, respectively) were fully allocated to cash.

to stocks. At the end of the sample, the performance gap is substantial. The outperformance relative to the index comes from the two major downturns, but this is hardly surprising, since there is no other source of return than the index itself. In risk-adjusted terms, the outperformance is conclusive.

4.6 Application to other indices

Table 10 summarizes the results from applying MPC with no risk or trading penalty (i.e., $MPC(\gamma = 0, \rho = 0)$) to various major stock market indices. For the MSCI World index, the numbers are the same that were reported in table 5. Recall that the testing period for the MSCI World index spans 1998 through 2015. For S&P 500, TOPIX, DAX, and FTSE, the data period includes 1984 through 2015. The first two years are used for initialization, leaving 30 years for testing. For the MSCI EM index, daily data is only available from 1988 and onwards, thus the testing period is four years shorter. All indices are net total return.

The MPC approach realizes a higher SR and CR than a buy-and-hold investment (as summarized in parentheses) in five out of six indices, with FTSE being the only exception. The best performance relative to the underlying index is

	MSCI World	S&P500	TOPIX	DAX	FTSE	MSCI EM
Annualized return	0.076 (0.056)	0.110 (0.108)	0.044 (0.025)	0.066 (0.073)	0.051 (0.078)	0.119 (0.072)
Standard deviation	0.12 (0.18)	0.14 (0.16)	0.17 (0.24)	0.16 (0.22)	0.14 (0.15)	0.18 (0.27)
Sharpe ratio	0.65 (0.30)	0.79 (0.68)	0.26 (0.10)	0.41 (0.33)	0.36 (0.54)	0.66 (0.27)
Maximum drawdown	0.26 (0.57)	0.36 (0.55)	0.48 (0.72)	0.39 (0.73)	0.36 (0.48)	0.38 (0.65)
Calmar ratio	0.29 (0.10)	0.30 (0.20)	0.09 (0.03)	0.17 (0.10)	0.14 (0.16)	0.31 (0.11)
Annual turnover	4.61 (0.00)	3.29 (0.00)	4.69 (0.00)	5.89 (0.00)	4.59 (0.00)	8.18 (0.00)

Table 10: Performance of MPC with no risk or trading penalty when applied to various major stock indices with no delay in allocation changes. The numbers in parentheses are the summary statistics for a buy-and-hold investment in the respective indices.

obtained for MSCI World, TOPIX, and MSCI EM. For all indices except DAX and FTSE, the AR of the MPC approach is higher than that of the underlying index despite high ATs—which could easily be reduced by introducing a trading penalty. In all six cases, the SD and MDD are lower than those of the underlying index. The results in table 10 show that the MPC approach in combination with the adaptively-estimated HMM has worked well for multiple major stock indices across different time periods. By introducing a trading penalty and calibrating its level to each index individually, it would be possible to further improve the results.

5 Conclusion

This article has shown the strength of using MPC for dynamic portfolio optimization in combination with an online method for forecasting the mean and variance of financial returns. There were computational advantages to using MPC in cases when estimates of future return statistics were updated every time a new observation becomes available, since the optimal control actions were reconsidered anyway.

Based on forecasts from an adaptively-estimated HMM, the MPC approach realized a higher return and a significantly lower risk than a buy-and-hold investment in various major stock indices. This was after accounting for transaction costs. Imposing an additional trading penalty increased the robustness, by reducing the number of trades, and improved the performance, when allocation changes were subject to a delay. MPC also outperformed RBAA based on a static decision rule for changing the portfolio. The performance of rule-based RBAA has been stronger in previous studies, where there were more investment opportunities than stocks and zero-interest cash. Thus, there is potential for using MPC for optimal control of multi-asset portfolios.

To keep things simple and illustrate the strength of the approach, the focus of this article was on stocks and cash, but it naturally extends to a multi-asset portfolio. Another possibility for future work would be to specify a model for the parameter changes, possibly including relevant explanatory variables, in an

attempt to improve the forecasts and take the stochasticity into account in the portfolio optimization.

References

- Ang, A. and G. Bekaert. "How regimes affect asset allocation." *Financial Analysts Journal*, vol. 60, no. 2 (2004), pp. 86–99.
- Ang, A. and A. Timmermann. "Regime changes and financial markets." *Annual Review of Financial Economics*, vol. 4, no. 1 (2012), pp. 313–337.
- Baum, L. E., T. Petrie, G. Soules, and N. Weiss. "A maximization technique occurring in the statistical analysis of probabilistic functions of Markov chains." *Annals of Mathematical Statistics*, vol. 41, no. 1 (1970), pp. 164–171.
- Bemporad, A. "Model predictive control design: New trends and tools." In *Proceedings of the 45th IEEE Conference on Decision and Control* (2006), pp. 6678–6683.
- Boyd, S., M. T. Mueller, B. O'Donoghue, and Y. Wang. "Performance bounds and suboptimal policies for multi-period investment." *Foundations and Trends in Optimization*, vol. 1, no. 1 (2014), pp. 1–72.
- Boyd, S. and L. Vandenberghe. *Convex Optimization*. Cambridge University Press: New York (2004).
- Brennan, M. J., E. S. Schwartz, and R. Lagnado. "Strategic asset allocation." *Journal of Economic Dynamics and Control*, vol. 21, no. 8–9 (1997), pp. 1377–1403.
- Brodie, J., I. Daubechies, C. D. Mol, D. Giannone, and I. Loris. "Sparse and stable Markowitz portfolios." *Proceedings of the National Academy of Sciences of the United States of America*, vol. 106, no. 30 (2009), pp. 12267–12272.
- Bulla, J. "Hidden Markov models with t components. Increased persistence and other aspects." *Quantitative Finance*, vol. 11, no. 3 (2011), pp. 459–475.
- Bulla, J. and I. Bulla. "Stylized facts of financial time series and hidden semi-Markov models." *Computational Statistics & Data Analysis*, vol. 51, no. 4 (2006), pp. 2192–2209.
- Bulla, J., S. Mergner, I. Bulla, A. Sesboüé, and C. Chesneau. "Markov-switching asset allocation: Do profitable strategies exist?" *Journal of Asset Management*, vol. 12, no. 5 (2011), pp. 310–321.
- Calafiori, G. C. "Multi-period portfolio optimization with linear control policies." *Automatica*, vol. 44, no. 10 (2008), pp. 2463–2473.

- Calafiori, G. C. “An affine control method for optimal dynamic asset allocation with transaction costs.” *SIAM Journal on Control and Optimization*, vol. 48, no. 4 (2009), pp. 2254–2274.
- Campbell, J. Y. “Asset prices, consumption, and the business cycle.” In *Handbook of Macroeconomics*, edited by J. B. Taylor and M. Woodford, vol. 1C, chap. 19. Elsevier: Amsterdam (1999), pp. 1231–1303.
- Cappé, O., E. Moulines, and T. Rydén. *Inference in Hidden Markov Models*. Springer: New York (2005).
- Cochrane, J. H. “Financial markets and the real economy.” *Foundations and Trends in Finance*, vol. 1, no. 1 (2005), pp. 1–101.
- Costa, O. L. and M. V. Araujo. “A generalized multi-period mean–variance portfolio optimization with Markov switching parameters.” *Automatica*, vol. 44, no. 10 (2008), pp. 2487–2497.
- Creal, D., S. J. Koopman, and A. Lucas. “Generalized autoregressive score models with applications.” *Journal of Applied Econometrics*, vol. 28, no. 5 (2013), pp. 777–795.
- Dai, M., Z. Q. Xu, and X. Y. Zhou. “Continuous-time Markowitz’s model with transaction costs.” *SIAM Journal on Financial Mathematics*, vol. 1, no. 1 (2010a), pp. 96–125.
- Dai, M., Q. Zhang, and Q. J. Zhu. “Trend following trading under a regime switching model.” *SIAM Journal on Financial Mathematics*, vol. 1, no. 1 (2010b), pp. 780–810.
- DeMiguel, V., L. Garlappi, and R. Uppal. “Optimal versus naive diversification: How inefficient is the $1/N$ portfolio strategy?” *Review of Financial Studies*, vol. 22, no. 5 (2009b), pp. 1915–1953.
- Dempster, A. P., N. M. Laird, and D. B. Rubin. “Maximum likelihood from incomplete data via the EM algorithm.” *Journal of the Royal Statistical Society. Series B (Methodological)*, vol. 39, no. 1 (1977), pp. 1–38.
- Diamond, S. and S. Boyd. “CVXPY: A Python-embedded modeling language for convex optimization.” *Journal of Machine Learning Research*, vol. 17, no. 83 (2016), pp. 1–5.
- Domahidi, A., E. Chu, and S. Boyd. “ECOS: An SOCP solver for embedded systems.” In *Proceedings of the 12th European Control Conference* (2013), pp. 3071–3076.
- Falcone, P., F. Borrelli, J. Asgari, H. E. Tseng, and D. Hrovat. “Predictive active steering control for autonomous vehicle systems.” *IEEE Transactions on control systems technology*, vol. 15, no. 3 (2007), pp. 566–580.

- Frühwirth-Schnatter, S. *Finite Mixture and Markov Switching Models*. Springer: New York (2006).
- Goyal, A., A. Ilmanen, and D. Kabiller. “Bad habits and good practices.” *Journal of Portfolio Management*, vol. 41, no. 4 (2015), pp. 97–107.
- Guidolin, M. and A. Timmermann. “Asset allocation under multivariate regime switching.” *Journal of Economic Dynamics and Control*, vol. 31, no. 11 (2007), pp. 3503–3544.
- Herzog, F., G. Dondi, and H. P. Geering. “Stochastic model predictive control and portfolio optimization.” *International Journal of Theoretical and Applied Finance*, vol. 10, no. 2 (2007), pp. 203–233.
- Ho, M., Z. Sun, and J. Xin. “Weighted elastic net penalized mean–variance portfolio design and computation.” *SIAM Journal on Financial Mathematics*, vol. 6, no. 1 (2015), pp. 1220–1244.
- Khreich, W., E. Granger, A. Miri, and R. Sabourin. “A survey of techniques for incremental learning of HMM parameters.” *Information Sciences*, vol. 197 (2012), pp. 105–130.
- Kinlaw, W., M. Kritzman, and D. Turkington. “The divergence of high- and low-frequency estimation: Implications for performance measurement.” *Journal of Portfolio Management*, vol. 41, no. 3 (2015), pp. 14–21.
- Kritzman, M. and Y. Li. “Skulls, financial turbulence, and risk management.” *Financial Analysts Journal*, vol. 66, no. 5 (2010), pp. 30–41.
- Kritzman, M., S. Page, and D. Turkington. “Regime shifts: Implications for dynamic strategies.” *Financial Analysts Journal*, vol. 68, no. 3 (2012), pp. 22–39.
- Kulhavý, R. and M. B. Zarrop. “On a general concept of forgetting.” *International Journal of Control*, vol. 58, no. 4 (1993), pp. 905–924.
- Lystig, T. C. and J. P. Hughes. “Exact computation of the observed information matrix for hidden Markov models.” *Journal of Computational and Graphical Statistics*, vol. 11, no. 3 (2002), pp. 678–689.
- Mandelbrot, B. “The variation of certain speculative prices.” *Journal of Business*, vol. 36, no. 4 (1963), pp. 394–419.
- Markowitz, H. “Portfolio selection.” *Journal of Finance*, vol. 7, no. 1 (1952), pp. 77–91.
- Meucci, A. *Risk and Asset Allocation*. Springer: Berlin (2005).

- Michaud, R. O. "The Markowitz optimization Enigma: Is 'optimized' optimal?" *Financial Analysts Journal*, vol. 45, no. 1 (1989), pp. 31–42.
- Nystrup, P., B. W. Hansen, H. O. Larsen, H. Madsen, and E. Lindström. "Dynamic allocation or diversification: A regime-based approach to multiple assets." *Journal of Portfolio Management*, vol. 44, no. 2 (2017a), pp. 62–73.
- Nystrup, P., B. W. Hansen, H. Madsen, and E. Lindström. "Regime-based versus static asset allocation: Letting the data speak." *Journal of Portfolio Management*, vol. 42, no. 1 (2015a), pp. 103–109.
- Nystrup, P., B. W. Hansen, H. Madsen, and E. Lindström. "Detecting change points in VIX and S&P 500: A new approach to dynamic asset allocation." *Journal of Asset Management*, vol. 17, no. 5 (2016), pp. 361–374.
- Nystrup, P., H. Madsen, and E. Lindström. "Stylised facts of financial time series and hidden Markov models in continuous time." *Quantitative Finance*, vol. 15, no. 9 (2015b), pp. 1531–1541.
- Nystrup, P., H. Madsen, and E. Lindström. "Long memory of financial time series and hidden Markov models with time-varying parameters." *Journal of Forecasting*, vol. 36, no. 8 (2017b), pp. 989–1002.
- Parkum, J. E., N. K. Poulsen, and J. Holst. "Recursive forgetting algorithms." *International Journal of Control*, vol. 55, no. 1 (1992), pp. 109–128.
- Rydén, T., T. Teräsvirta, and S. Åsbrink. "Stylized facts of daily return series and the hidden Markov model." *Journal of Applied Econometrics*, vol. 13, no. 3 (1998), pp. 217–244.
- Sheikh, A. Z. and J. Sun. "Regime change: Implications of macroeconomic shifts on asset class and portfolio performance." *Journal of Investing*, vol. 21, no. 3 (2012), pp. 36–54.
- Siegel, J. J. "Does it pay stock investors to forecast the business cycle?" *Journal of Portfolio Management*, vol. 18, no. 1 (1991), pp. 27–34.
- Tibshirani, R. "Regression shrinkage and selection via the lasso." *Journal of the Royal Statistical Society. Series B (Methodological)*, vol. 58, no. 1 (1996), pp. 267–288.
- von Neumann, J. and O. Morgenstern. *Theory of Games and Economic Behavior*. Princeton University Press: Princeton, 3rd ed. (1953).

PAPER H

Originally published in *Foundations and Trends in Optimization*

Multi-period trading via convex optimization

Stephen Boyd, Enzo Busseti, Steven Diamond, Ronald N. Kahn,
Kwangmoo Koh, Peter Nystrup, and Jan Speth

Abstract

We consider a basic model of multi-period trading, which can be used to evaluate the performance of a trading strategy. We describe a framework for single-period optimization, where the trades in each period are found by solving a convex optimization problem that trades off expected return, risk, transaction cost, and holding cost such as the borrowing cost for shorting assets. We then describe a multi-period version of the trading method, where optimization is used to plan a sequence of trades, with only the first one executed, using estimates of future quantities that are unknown when the trades are chosen. The single-period method traces back to Markowitz; the multi-period methods trace back to model predictive control. Our contribution is to describe the single- and multi-period methods in one simple framework, giving a clear description of the development and the approximations made. In this paper we do not address a critical component in a trading algorithm: the predictions or forecasts of future quantities. The methods we describe in this paper can be thought of as good ways to exploit predictions, no matter how they are made. We have also developed a companion open-source software library that implements many of the ideas and methods described in the paper.

Keywords: Optimization; Model predictive control.

1 Introduction

Single- and multi-period portfolio selection. Markowitz (1952) was the first to formulate the choice of an investment portfolio as an optimization problem trading off risk and return. Traditionally, this was done independently of the cost associated with trading, which can be significant when trades are made over multiple periods (Kolm et al. 2014). Goldsmith (1976) was among the first to consider the effect of transaction cost on portfolio selection in a single-period setting. It is possible to include many other costs and constraints in a single-period optimization formulation for portfolio selection (Lobo et al. 2007, Moallemi and Sağlam 2017).

In multi-period portfolio selection, the portfolio selection problem is to choose a sequence of trades to carry out over a set of periods. There has been much research on this topic since the work of Samuelson (1969) and Merton (1969, 1971). Constantinides (1979) extended Samuelson's discrete-time formulation to problems with proportional transaction costs. Davis and Norman (1990) and Dumas and Luciano (1991) derived similar results for the continuous-time formulation. Transaction costs, constraints, and time-varying forecasts are more naturally dealt with in a multi-period setting. Following Samuelson (1969) and Merton (1969, 1971), the literature on multi-period portfolio selection is predominantly based on dynamic programming (Bellman 1956, Bertsekas 1995), which properly takes into account the idea of recourse and updated information available as the sequence of trades are chosen (see Gârleanu and Pedersen 2013, and references therein). Unfortunately, actually carrying out dynamic programming for trade selection is impractical, except for some very special or small cases, due to the 'curse of dimensionality' (Powell 2007, Boyd et al. 2014). As a consequence, most studies include only a very limited number of assets and simple objectives and constraints. A large literature studies multi-period portfolio selection in the absence of transaction cost (see, e.g., Campbell and Viceira 2002, and references therein); in this special case, dynamic programming is tractable.

For practical implementation, various approximations of the dynamic programming approach are often used, such as approximate dynamic programming, or even simpler formulations that generalize the single-period formulations to multi-period optimization problems (Boyd et al. 2014). We will focus on these simple multi-period methods in this paper. While these simplified approaches can be criticized for only approximating the full dynamic programming trading policy, the performance loss is likely very small in practical problems, for several reasons. Boyd et al. (2014) developed a numerical bounding method that quantifies the loss of optimality when using a simplified approach, and found it to be very small in numerical examples. But in fact, the dynamic programming formulation is itself an approximation, based on assumptions (like independent or identically distributed returns) that need not hold well in practice, so the idea of an 'optimal strategy' itself should be regarded with some suspicion.

Why now? What is different now, compared to 10, 20, or 30 years ago, is vastly more powerful computers, better algorithms, specification languages for optimization, and access to much more data. These developments have changed how we can use optimization in multi-period investing. In particular, we can now quickly run full-blown optimization, run multi-period optimization, and search over hyperparameters in backtests. We can run end-to-end analyses, indeed many at a time in parallel. Earlier generations of investment researchers, relying on computers much less powerful than today, relied more on separate models and analyses to estimate parameter values, and tested signals using simplified (usually unconstrained) optimization.

Goal. In this tutorial paper we consider multi-period investment and trading. Our goal is to describe a simple model that takes into account the main practical issues that arise, and several simple and practical frameworks based on solving convex optimization problems (Boyd and Vandenberghe 2004) that determine the trades to make. We describe the approximations made, and briefly discuss how the methods can be used in practice. Our methods do not give a complete trading system, since we leave a critical part unspecified: forecasting future returns, volumes, volatilities, and other important quantities (see, e.g., Grinold and Kahn 2000). This paper describes good practical methods that can be used to trade, given forecasts.

The optimization-based trading methods we describe are practical and reliable when the problems to be solved are convex. Real-world single-period convex problems with thousands of assets can be solved using generic algorithms in well under a second, which is critical for evaluating a proposed algorithm with historical or simulated data, for many values of the parameters in the method.

Outline. We start in section 2 by describing a simple model of multi-period trading, taking into account returns, trading costs, holding costs, and (some) corporate actions. This model allows us to carry out simulation, used for what-if analyses, to see what would have happened under different conditions, or with a different trading strategy. The data in simulation can be realized past data (in a *backtest*) or simulated data that did not occur, but could have occurred (in a *what-if simulation*), or data chosen to be particularly challenging (in a *stress-test*). In section 3 we review several common metrics used to evaluate (realized or simulated) trading performance, such as active return and risk with respect to a benchmark.

We then turn to optimization-based trading strategies. In section 4 we describe *single-period optimization* (SPO), a simple but effective framework for trading based on optimizing the portfolio performance over a single period. In section 5 we consider *multi-period optimization* (MPO), where the trades are chosen by solving an optimization problem that covers multiple periods in the future.

Contribution. Most of the material that appears in this paper has appeared before, in other papers, books, or EE364A, the Stanford course on convex optimization. Our contribution is to collect in one place the basic definitions, a careful description of the model, and discussion of how convex optimization can be used in multi-period trading, all in a common notation and framework. Our goal is not to survey all the work done in this and related areas, but rather to give a unified, self-contained treatment. Our focus is not on theoretical issues, but on practical ones that arise in multi-period trading. To further this goal, we have developed an accompanying open-source software library implemented in Python, and available at

[https://github.com/cvxgrp/cvxportfolio.](https://github.com/cvxgrp/cvxportfolio)

Target audience. We assume that the reader has a background in the basic ideas of quantitative portfolio selection, trading, and finance, as described, for example, in the books by Grinold and Kahn (2000), Meucci (2005), or Narang (2013). We also assume that the reader has seen some basic mathematical optimization, specifically convex optimization (Boyd and Vandenberghe 2004). The reader certainly does not need to know more than the very basic ideas of convex optimization, for example the overview material covered in chapter 1 of Boyd and Vandenberghe (2004). In a nutshell, our target reader is a quantitative trader, or someone who works with or for, or employs, one.

2 The model

In this chapter, we set the notation and give some detail of our simplified model of multi-period trading. We develop our basic dynamic model of trading, which tells us how a portfolio and associated cash account change over time, due to trading, investment gains, and various costs associated with trading and holding portfolios. The model developed in this chapter is independent of any method for choosing or evaluating the trades or portfolio strategy, and independent of any method used to evaluate the performance of the trading.

2.1 Portfolio asset and cash holdings

Portfolio. We consider a portfolio of holdings in n assets, plus a cash account, over a finite time horizon, which is divided into discrete time periods labeled $t = 1, \dots, T$. These time periods need not be uniformly spaced in real time or be of equal length; for example, when they represent trading days, the periods are one (calendar) day during the week and three (calendar) days over a weekend. We use the label t to refer to both a point in time, the beginning of time period t , as well as the time interval from time t to $t + 1$. The time period in our model is arbitrary, and could be daily, weekly, or one hour intervals, for example. We will occasionally give examples where the time indexes trading days, but the same notation and model apply to any other time period.

Our investments will be in a *universe* of n assets, along with an associated cash account. We let $h_t \in \mathbb{R}^{n+1}$ denote the portfolio (or vector of positions or holdings) at the beginning of time period t , where $(h_t)_i$ is the *dollar value* of asset i at the beginning of time period t , with $(h_t)_i < 0$ meaning a short position in asset i , for $i = 1, \dots, n$. The portfolio is *long-only* when the asset holdings are all nonnegative, i.e., $(h_t)_i \geq 0$ for $i = 1, \dots, n$.

The value of $(h_t)_{n+1}$ is the *cash balance*, with $(h_t)_{n+1} < 0$ meaning that money is owed (or borrowed). The dollar value for the assets is determined using the reference prices $p_t \in \mathbb{R}_+^n$, defined as the average of the bid and ask prices at the

beginning of time period t . When $(h_t)_{n+1} = 0$, the portfolio is *fully invested*, meaning that we hold (or owe) zero cash, and all our holdings (long and short) are in assets.

Total value, exposure, and leverage. The total value (or *net asset value*, NAV) v_t of the portfolio, in dollars, at time t is $v_t = \mathbf{1}^T h_t$, where $\mathbf{1}$ is the vector with all entries one. (This is not quite the amount of cash the portfolio would yield on liquidation, due to transaction costs, discussed below.) Throughout this paper we will assume that $v_t > 0$, i.e., the total portfolio value is positive.

The vector

$$(h_t)_{1:n} = ((h_t)_1, \dots, (h_t)_n)$$

gives the asset holdings. The *gross exposure* can be expressed as

$$\|(h_t)_{1:n}\|_1 = |(h_t)_1| + \dots + |(h_t)_n|,$$

the sum of the absolute values of the asset positions. The *leverage* of the portfolio is the gross exposure divided by the value, $\|(h_t)_{1:n}\|_1/v_t$. (Several other definitions of leverage are also used, such as half the quantity above.) The leverage of a fully invested long-only portfolio is one.

Weights. We will also describe the portfolio using weights or fractions of total value. The *weights* (or weight vector) $w_t \in \mathbb{R}^{n+1}$ associated with the portfolio h_t are defined as $w_t = h_t/v_t$. (Recall our assumption that $v_t > 0$.) By definition the weights sum to one, $\mathbf{1}^T w_t = 1$, and are unitless. The weight $(w_t)_{n+1}$ is the fraction of the total portfolio value held in cash. The weights are all nonnegative when the asset positions are long and the cash balance is nonnegative. The dollar value holdings vector can be expressed in terms of the weights as $h_t = v_t w_t$. The leverage of the portfolio can be expressed in terms of the weights as $\|w_{1:n}\|_1$, the ℓ_1 norm of the asset weights.

2.2 Trades

Trade vector. In our simplified model we assume that all trading—i.e., buying and selling of assets—occurs at the beginning of each time period. (In reality the trades would likely be spread over at least some part of the period.) We let $u_t \in \mathbb{R}^n$ denote the dollar values of the trades, at the current price: $(u_t)_i > 0$ means we buy asset i and $(u_t)_i < 0$ means we sell asset i , at the beginning of time period t , for $i = 1, \dots, n$. The number $(u_t)_{n+1}$ is the amount we put into the cash account (or take out, if it is negative). The vector $z_t = u_t/v_t$ gives the trades normalized by the total value. Like the weight vector w_t , it is unitless.

Post-trade portfolio. The post-trade portfolio is denoted

$$h_t^+ = h_t + u_t, \quad t = 1, \dots, T.$$

This is the portfolio in time period t immediately after trading. The post-trade portfolio value is $v_t^+ = \mathbf{1}^T h_t^+$. The change in total portfolio value from the trades is given by

$$v_t^+ - v_t = \mathbf{1}^T h_t^+ - \mathbf{1}^T h_t = \mathbf{1}^T u_t.$$

The vector $(u_t)_{1:n} \in \mathbb{R}^n$ is the set of (non-cash) asset trades. Half its ℓ_1 norm $\|(u_t)_{1:n}\|_1/2$ is the *turnover* (in dollars) in period t . This is often expressed as a percentage of total value, as $\|(u_t)_{1:n}\|_1/(2v_t) = \|z_{1:n}\|_1/2$.

We can express the post-trade portfolio, normalized by the portfolio value, in terms of the weights $w_t = h_t/v_t$ and normalized trades as

$$h_t^+/v_t = w_t + z_t.$$

Note that this normalized quantity does not necessarily add up to one.

2.3 Transaction cost

The trading incurs a trading or transaction cost (in dollars), which we denote as $\phi_t^{\text{trade}}(u_t)$, where $\phi_t^{\text{trade}} : \mathbb{R}^{n+1} \rightarrow \mathbb{R}$ is the (dollar) transaction-cost function. We will assume that ϕ_t^{trade} does not depend on $(u_t)_{n+1}$, i.e., there is no transaction cost associated with the cash account. To emphasize this we will sometimes write the transaction cost as $\phi_t^{\text{trade}}((u_t)_{1:n})$. We assume that $\phi_t^{\text{trade}}(0) = 0$, i.e., there is no transaction cost when we do not trade. While $\phi_t^{\text{trade}}(u_t)$ is typically nonnegative, it can be negative in some cases, discussed below. We assume that the transaction-cost function ϕ_t^{trade} is *separable*, which means it has the form

$$\phi_t^{\text{trade}}(x) = \sum_{i=1}^n (\phi_t^{\text{trade}})_i(x_i),$$

i.e., the transaction cost breaks into a sum of transaction costs associated with the individual assets. We refer to $(\phi_t^{\text{trade}})_i$, which is a function from \mathbb{R} into \mathbb{R} , as the transaction-cost function for asset i , period t . We note that some authors have used models of transaction cost which are not separable, for example the quadratic dynamic model of Grinold (2006).

A generic transaction-cost model. A reasonable, generic model for the scalar transaction-cost functions $(\phi_t^{\text{trade}})_i$ is

$$x \mapsto a|x| + b\sigma \frac{|x|^{3/2}}{V^{1/2}} + cx, \quad (1)$$

where a , b , σ , V , and c are real numbers described below, and x is a dollar trade amount (Grinold and Kahn 2000). The number a is one half the bid-ask spread for the asset at the beginning of the time period, expressed as a fraction of the asset price (and so is unitless). We can also include in this term broker

commissions or fees which are a linear function of the number of shares (or dollar value) bought or sold. The number b is a positive constant with unit inverse dollars. The number V is the total market volume traded for the asset in the time period, expressed in dollar value, so $|x|^{3/2}/V^{1/2}$ has units of dollars. The number σ the corresponding price volatility (standard deviation) over recent time periods, in dollars. According to a standard rule of thumb, trading one day's volume moves the price by about one day's volatility, which suggests that the value of the number b is around one. (In practice, however, the value of b is determined by fitting the model above to data on realized transaction costs.) The number c is used to create asymmetry in the transaction-cost function. When $c = 0$, the transaction cost is the same for buying and selling; it is a function of $|x|$. When $c > 0$, it is cheaper to sell than to buy the asset, which generally occurs in a market where the buyers are providing more liquidity than the sellers (e.g., if the book is not balanced in a limit order exchange). The asymmetry in transaction cost can also be used to model price movement during trade execution. Negative transaction cost can occur when $|c| > |a|$. The constants in the transaction-cost model (1) vary with asset, and with trading period, i.e., they are indexed by i and t . This 3/2-power transaction-cost model is widely known and employed by practitioners.

We are not aware of empirical tests of the specific transaction-cost model (1), but several references describe and validate similar models (Lillo et al. 2003, Moro et al. 2009, Bershova and Rakhlin 2013, Gomes and Waelbroeck 2015). In particular, these empirical works suggest that transaction cost grows (approximately) with the 3/2 power of transaction size.

Normalized transaction cost. The transaction-cost model(1) is in dollars. We can normalize it by v_t , the total portfolio value, and express it in terms of z_i , the normalized trade of asset i , resulting in the function (with t suppressed for simplicity)

$$a_i|z_i| + b_i\sigma_i \frac{|z_i|^{3/2}}{(V_i/v)^{1/2}} + c_iz_i. \quad (2)$$

The only difference with (1) is that we use the normalized asset volume V_i/v instead of the dollar volume V_i . This shows that the same transaction-cost formula can be used to express the dollar transaction cost as a function of the dollar trade, with the volume denoted in dollars, or the normalized transaction cost as a function of the normalized trade, with the volume normalized by the portfolio value.

With some abuse of notation, we will write the normalized transaction cost in period t as $\phi_t^{\text{trade}}(z_t)$. When the argument to the transaction-cost function is normalized, we use the version where asset volume is also normalized. The normalized transaction cost $\phi_t^{\text{trade}}(z_t)$ depends on the portfolio value v_t , as well

as the current values of the other parameters, but we suppress this dependence to lighten the notation.

Other transaction-cost models. Other transaction-cost models can be used. Common variants include a piecewise linear model, or adding a term that is quadratic in the trade value z_i (Almgren and Chriss 2001, Grinold 2006, Gărleanu and Pedersen 2013). Almost all of these are convex functions. An example of a transaction-cost term that is not convex is a fixed fee for any nonzero trading in an asset. For simulation, however, the transaction-cost function can be arbitrary.

2.4 Holding cost

We will hold the post-trade portfolio h_t^+ over the t 'th period. This will incur a holding-based cost (in dollars) $\phi_t^{\text{hold}}(h_t^+)$, where $\phi_t^{\text{hold}} : \mathbb{R}^{n+1} \rightarrow \mathbb{R}$ is the holding-cost function. Like transaction cost, it is typically nonnegative, but it can also be negative in certain cases, discussed below. The holding cost can include a factor related to the length of the period; for example, if our periods are trading days, but holding costs are assessed on all days (including weekend and holidays), the Friday holding cost might be multiplied by three. For simplicity, we will assume that the holding-cost function does not depend on the post-trade cash balance $(h_t^+)_{n+1}$.

A basic holding-cost model includes a charge for borrowing assets when going short, which has the form

$$\phi_t^{\text{hold}}(h_t^+) = s_t^T (h_t^+)_-, \quad (3)$$

where $(s_t)_i \geq 0$ is the borrowing fee, in period t , for shorting asset i , and $(z)_- = \max\{-z, 0\}$ denotes the negative part of a number z . This is the fee for shorting the post-trade assets, over the investment period, and here we are paying this fee in advance, at the beginning of the period. Our assumption that the holding cost does not depend on the cash account requires $(s_t)_{n+1} = 0$. But we can include a cash borrow cost if needed, in which case $(s_t)_{n+1} > 0$. This is the premium for borrowing, and not the interest rate, which is included in another part of our model, discussed below.

The holding cost (3), normalized by portfolio value, can be expressed in terms of weights and normalized trades as

$$\phi_t^{\text{hold}}(h_t^+)/v_t = s_t^T (w_t + z_t)_-. \quad (4)$$

As with the transaction cost, with some abuse of notation we use the same function symbol to denote the normalized holding cost, writing the quantity above as $\phi_t^{\text{hold}}(w_t + z_t)$. (For the particular form of holding cost described

above, there is no abuse of notation since ϕ_t^{hold} is the same when expressed in dollars or normalized form.)

More complex holding-cost functions arise, for example when the assets include ETFs (exchange-traded funds). A long position incurs a fee proportional to h_i ; when we hold a short position, we *earn* the same fee. This is readily modeled as a linear term in the holding cost. (We can in addition have a standard fee for shorting.) This leads to a holding cost of the form

$$\phi_t^{\text{hold}}(w_t + z_t) = s_t^T(w_t + z_t)_- + f_t^T(w_t + z_t),$$

where f_t is a vector with $(f_t)_i$ representing the per-period management fee for asset i , when asset i is an ETF.

Even more complex holding-cost models can be used. One example is a piecewise linear model for the borrowing cost, which increases the marginal borrow charge rate when the short position exceeds some threshold. These more general holding-cost functions are almost always convex. For simulation, however, the holding-cost function can be arbitrary.

2.5 Self-financing condition

We assume that no external cash is put into or taken out of the portfolio, and that the trading and holding costs are paid from the cash account at the beginning of the period. This *self-financing condition* can be expressed as

$$\mathbf{1}^T u_t + \phi_t^{\text{trade}}(u_t) + \phi_t^{\text{hold}}(h_t^+) = 0. \quad (5)$$

Here $-\mathbf{1}^T u_t$ is the total cash out of the portfolio from the trades; (5) says that this cash out must balance the cash cost incurred, i.e., the transaction cost plus the holding cost. The self-financing condition implies $v_t^+ = v_t - \phi_t^{\text{trade}}(u_t) - \phi_t^{\text{hold}}(h_t^+)$, i.e., the post-trade value is the pre-trade value minus the transaction and holding costs.

The self-financing condition (5) connects the cash trade amount $(u_t)_{n+1}$ to the asset trades, $(u_t)_{1:n}$, by

$$(u_t)_{n+1} = -(\mathbf{1}^T(u_t)_{1:n} + \phi_t^{\text{trade}}((h_t + u_t)_{1:n}) + \phi_t^{\text{hold}}((u_t)_{1:n})). \quad (6)$$

Here we use the assumption that the transaction and holding costs do not depend on the $n+1$ (cash) component by explicitly writing the argument as the first n components, i.e., those associated with the (non-cash) assets. The formula (6) shows that if we are given the trade values for the non-cash assets, i.e., $(u_t)_{1:n}$, we can find the cash trade value $(u_t)_{n+1}$ that satisfies the self-financing condition (5).

We mention here a subtlety that will come up later. A trading algorithm chooses the asset trades $(u_t)_{1:n}$ before the transaction-cost function ϕ_t^{trade} and (possibly)

the holding-cost function ϕ_t^{hold} are known. The trading algorithm must use *estimates* of these functions to make its choice of trades. The formula (6) gives the cash trade amount that is *realized*.

Normalized self-financing. By dividing the dollar self-financing condition (5) by the portfolio value v_t , we can express the self-financing condition in terms of weights and normalized trades as

$$\mathbf{1}^T z_t + \phi_t^{\text{trade}}(v_t z_t)/v_t + \phi_t^{\text{hold}}(v_t(w_t + z_t))/v_t = 0,$$

where we use $u_t = v_t z_t$ and $h_t^+ = v_t(w_t + z_t)$, and the cost functions above are the dollar value versions. Expressing the costs in terms of normalized values we get

$$\mathbf{1}^T z_t + \phi_t^{\text{trade}}(z_t) + \phi_t^{\text{hold}}(w_t + z_t) = 0, \quad (7)$$

where here the costs are the normalized versions.

As in the dollar version, and assuming that the costs do not depend on the cash values, we can express the cash trade value $(z_t)_{n+1}$ in terms of the non-cash asset trade values $(z_t)_{1:n}$ as

$$(z_t)_{n+1} = -(\mathbf{1}^T(z_t)_{1:n} + \phi_t^{\text{trade}}((w_t + z_t)_{1:n}) + \phi_t^{\text{hold}}((z_t)_{1:n})). \quad (8)$$

2.6 Investment

The post-trade portfolio and cash are invested for one period, until the beginning of the next time period. The portfolio at the next time period is given by

$$h_{t+1} = h_t^+ + r_t \circ h_t^+ = (\mathbf{1} + r_t) \circ h_t^+, \quad t = 1, \dots, T-1,$$

where $r_t \in \mathbb{R}^{n+1}$ is the vector of asset and cash returns from period t to period $t+1$ and \circ denotes Hadamard (elementwise) multiplication of vectors. The return of asset i over period t is defined as

$$(r_t)_i = \frac{(p_{t+1})_i - (p_t)_i}{(p_t)_i}, \quad i = 1, \dots, n,$$

the fractional increase in the asset price over the investment period. We assume here that the prices and returns are adjusted to include the effects of stock splits and dividends. We will assume that the prices are nonnegative, so $\mathbf{1} + r_t \geq 0$ (where the inequality means elementwise). We mention an alternative to our definition above, the *log-return*,

$$\log \frac{(p_{t+1})_i}{(p_t)_i} = \log(1 + (r_t)_i), \quad i = 1, \dots, n.$$

For returns that are small compared to one, the log-return is very close to the return defined above.

The number $(r_t)_{n+1}$ is the return to cash, i.e., the risk-free interest rate. In the simple model, the cash interest rate is the same for cash deposits and loans. We can also include a premium for borrowing cash (say) in the holding-cost function, by taking $(s_t)_{n+1} > 0$ in (3). When the asset trades $(u_t)_{1:n}$ are chosen, the asset returns $(r_t)_{1:n}$ are not known. It is reasonable to assume that the cash interest rate $(r_t)_{n+1}$ is known.

Next period portfolio value. For future reference we work out some useful formulas for the next period portfolio value. We have

$$\begin{aligned} v_{t+1} &= \mathbf{1}^T h_{t+1} \\ &= (\mathbf{1} + r_t)^T h_t^+ \\ &= v_t + r_t^T h_t + (\mathbf{1} + r_t)^T u_t \\ &= v_t + r_t^T h_t + r_t^T u_t - \phi_t^{\text{trade}}(u_t) - \phi_t^{\text{hold}}(h_t^+). \end{aligned}$$

Portfolio return. The *portfolio realized return* in period t is defined as

$$R_t^p = \frac{v_{t+1} - v_t}{v_t},$$

the fractional increase in portfolio value over the period. It can be expressed as

$$R_t^p = r_t^T w_t + r_t^T z_t - \phi_t^{\text{trade}}(z_t) - \phi_t^{\text{hold}}(w_t + z_t). \quad (9)$$

This is easily interpreted. The portfolio return over period t consists of four parts:

- $r_t^T w_t$ is the portfolio return without trades or holding cost,
- $r_t^T z_t$ is the return on the trades,
- $-\phi_t^{\text{trade}}(z_t)$ is the transaction cost, and
- $-\phi_t^{\text{hold}}(w_t + z_t)$ is the holding cost.

Next period weights. We can derive a formula for the next period weights w_{t+1} in terms of the current weights w_t and the normalized trades z_t , and the return r_t , using the equations above. Simple algebra gives

$$w_{t+1} = \frac{1}{1 + R_t^p} (\mathbf{1} + r_t) \circ (w_t + z_t). \quad (10)$$

By definition, we have $\mathbf{1}^T w_{t+1} = 1$. This complicated formula reduces to $w_{t+1} = w_t + z_t$ when $r_t = 0$. We note for future use that when the per-period returns are small compared to one, we have $w_{t+1} \approx w_t + z_t$.

2.7 Aspects not modeled

We list here some aspects of real trading that our model ignores, and discuss some approaches to handle them if needed.

External cash. Our self-financing condition (5) assumes that no external cash enters or leaves the portfolio. We can easily include external deposits and withdrawals of cash by replacing the right-hand side of (5) with the external cash put into the account (which is positive for cash deposited into the account and negative for cash withdrawn).

Dividends. Dividends are usually included in the asset return, which implicitly means they are re-invested. Alternatively we can include cash dividends from assets in the holding cost, by adding the term $-d_t^T h_t$, where d_t is the vector of dividend rates (in dollars per dollar of the asset held) in period t . In other words, we can treat cash dividends as negative holding costs.

Non-instant trading. Our model assumes all trades are carried out instantly at the beginning of each investment period, but the trades are really executed over some fraction of the period. This can be modeled using the linear term in the transaction cost, which can account for the movement of the price during the execution. We can also change the dynamics equation

$$h_{t+1} = (\mathbf{1} + r_t) \circ (h_t + u_t)$$

to

$$h_{t+1} = (\mathbf{1} + r_t) \circ h_t + (1 - \theta_t/2)(\mathbf{1} + r_t) \circ u_t,$$

where θ_t is the fraction of the period over which the trades occur. In this modification, we do not get the full period return on the trades when $\theta_t > 0$, since we are moving into the position as the price moves.

The simplest method to handle non-instant trading is to use a shorter period. For example, if we are interested in daily trading, but the trades are carried out over the whole trading day and we wish to model this effect, we can move to an hourly model.

Imperfect execution. Here we distinguish between u_t^{req} , the requested trade, and u_t , the actual realized trade (Perold 1988). In a backtest simulation we might assume that some (very small) fraction of the requested trades are only partially completed.

Multi-period price impact. This is the effect of a large order in one period affecting the asset price in future periods (Almgren and Chriss 2001, Obizhaeva and Wang 2013). In our model the transaction cost is only a function of the current period trade vector, not previous ones.

Trade settlement. In trade settlement we keep track of cash from trades one day and two days ago (in daily simulation), as well as the usual (unencumbered) cash account which includes all cash from trades that occurred three or more days ago, which have already settled. Shorting expenses come from the unencumbered cash, and trade-related cash moves immediately into the one day ago category (for daily trading).

Merger/acquisition. In a certain period one company buys another, converting the shares of the acquired company into shares of the acquiring company at some rate. This modifies the asset holdings update. In a cash buyout, positions in the acquired company are converted to cash.

Bankruptcy or dissolution. The holdings in an asset are reduced to zero, possibly with a cash payout.

Trading freeze. A similar action is a trading freeze, where in some time periods an asset cannot be bought, or sold, or both.

2.8 Simulation

Our model can be used to simulate the evolution of a portfolio over the periods $t = 1, \dots, T$. This requires the following data, when the standard model described above is used. (If more general transaction- or holding-cost functions are used, any data required for them is also needed.)

- Starting portfolio and cash account values, $h_1 \in \mathbb{R}^{n+1}$.
- Asset trade vectors $(u_t)_{1:n}$. The cash trade value $(u_t)_{n+1}$ is determined from the self-financing condition by (6).
- Transaction-cost model parameters $a_t \in \mathbb{R}^n$, $b_t \in \mathbb{R}^n$, $c_t \in \mathbb{R}^n$, $\sigma_t \in \mathbb{R}^n$, and $V_t \in \mathbb{R}^n$.
- Shorting rates $s_t \in \mathbb{R}^n$.
- Returns $r_t \in \mathbb{R}^{n+1}$.
- Cash dividend rates $d_t \in \mathbb{R}^n$, if they are not included in the returns.

Backtest. In a backtest the values would be past realized values, with $(u_t)_{1:n}$ the trades proposed by the trading algorithm being tested. Such a test estimates what the evolution of the portfolio would have been with different trades or a different trading algorithm. The simulation determines the portfolio and cash account values over the simulation period, from which other metrics, described

in section 3 below, can be computed. As a simple example, we can compare the performance of rebalancing to a given target portfolio daily, weekly, or quarterly.

A simple but informative backtest is to simulate the portfolio evolution using the actual trades that were executed in a portfolio. We can then compare the actual and simulated or predicted portfolio holdings and total value over some time period. The true and simulated portfolio values will not be identical, since our model relies on estimates of transaction and holding costs, assumes instantaneous trade execution, and so on.

What-if simulations. In a what-if simulation, we change the data used to carry out the simulation, i.e., returns, volumes, and so on. The values used are ones that (presumably) could have occurred. This can be used to stress-test a trading algorithm, by using data that did not occur, but would have been very challenging.

Adding uncertainty in simulations. Any simulation of portfolio evolution relies on models of transaction and holding costs, which in turn depend on parameters. These parameters are not known exactly, and in any case, the models are not exactly correct. So the question arises, to what extent should we trust our simulations? One simple way to check this is to carry out multiple simulations, where we randomly perturb the model parameters by reasonable amounts. For example, we might vary the daily volumes from their true (realized) values by 10% each day. If simulation with parameters that are perturbed by reasonable amounts yields divergent results, we know that (unfortunately) we cannot trust the simulations.

3 Metrics

Several generic performance metrics can be used to evaluate the portfolio performance.

3.1 Absolute metrics

We first consider metrics that measure the growth of portfolio value in absolute terms, not in comparison to a benchmark portfolio or the risk-free rate.

Return and growth rate. The average realized return over periods $t = 1, \dots, T$ is

$$\overline{R^p} = \frac{1}{T} \sum_{t=1}^T R_t^p.$$

An alternative measure of return is the *growth rate* (or log-return) of the portfolio in period t , defined as

$$G_t^p = \log(v_{t+1}/v_t) = \log(1 + R_t^p).$$

The average growth rate of the portfolio is the average value of G_t^p over the periods $t = 1, \dots, T$. For per-period returns that are small compared to one (which is almost always the case in practice) G_t^p is very close to R_t^p .

The return and growth rates given above are per-period. For interpretability they are typically *annualized* (Bacon 2008): return and growth rates are multiplied by P , where P is the number of periods in one year. (For periods that are trading days, we have $P \approx 250$.)

Volatility and risk. The realized *volatility* (Black 1976) is the standard deviation of the portfolio return time series,

$$\sigma^p = \left(\frac{1}{T} \sum_{t=1}^T (R_t^p - \bar{R}^p)^2 \right)^{1/2}.$$

(This is the maximum-likelihood estimate; for an unbiased estimate we replace $1/T$ with $1/(T - 1)$). The square of the volatility is the *quadratic risk*. When R_t^p are small (in comparison to 1), a good approximation of the quadratic risk is the second moment of the return,

$$(\sigma^p)^2 \approx \frac{1}{T} \sum_{t=1}^T (R_t^p)^2.$$

The volatility and quadratic risk given above are per-period. For interpretability they are typically annualized. To get the annualized values we multiply volatility by \sqrt{P} , and quadratic risk by P . (This scaling is based on the idea that the returns in different periods are independent random variables.)

3.2 Metrics relative to a benchmark

Benchmark weights. It is common to measure the portfolio performance against a *benchmark*, given as a set of weights $w_t^b \in \mathbb{R}^{n+1}$, which are fractions of the assets (including cash), and satisfy $\mathbf{1}^T w_t^b = 1$. We will assume the benchmark weights are nonnegative, i.e., the entries in w_t^b are nonnegative. The benchmark weight $w_t^b = e_{n+1}$ (the unit vector with value 0 for all entries except the last, which has value 1) represents the cash, or risk-free, benchmark. More commonly the benchmark consists of a particular set of assets with weights proportional to their capitalization. The benchmark return in period t is $R_t^b = r_t^T w_t^b$. (When the benchmark is cash, this is the risk-free interest rate $(r_t)_{n+1}$.)

Active and excess return. The *active* return (Sharpe 1991, Grinold and Kahn 2000) (of the portfolio, with respect to a benchmark) is given by

$$R_t^a = R_t^p - R_t^b.$$

In the special case when the benchmark consists of cash (so that the benchmark return is the risk-free rate) this is known as *excess return*, denoted

$$R_t^e = R_t^p - (r_t)_{n+1}.$$

We define the average *active return* \bar{R}^a , relative to the benchmark, as the average of R_t^a . We have

$$\begin{aligned} R_t^a &= R_t^p - R_t^b \\ &= r_t^T (w_t - w_t^b) + r_t^T z_t - \phi_t^{\text{trade}}(z_t) - \phi_t^{\text{hold}}(w_t + z_t). \end{aligned}$$

Note that if $z_t = 0$ and $w_t = w_t^b$, i.e., we hold the benchmark weights and do not trade, the active return is zero. (This relies on the assumption that the benchmark weights are nonnegative, so $\phi_t^{\text{hold}}(w_t^b) = 0$.)

Active risk. The standard deviation of R_t^a , denoted σ^a , is the risk relative to the benchmark, or *active risk*. When the benchmark is cash, this is the excess risk σ^e . When the risk-free interest rate is constant, this is the same as the risk σ^p .

Information and Sharpe ratio. The (realized) *information ratio* (IR) of the portfolio relative to a benchmark is the average of the active returns \bar{R}^a over the standard deviation of the active returns σ^a (Grinold and Kahn 2000),

$$\text{IR} = \bar{R}^a / \sigma^a.$$

In the special case of a cash benchmark this is known as *Sharpe ratio* (SR) (Sharpe 1966, 1994)

$$\text{SR} = \bar{R}^e / \sigma^e.$$

Both IR and SR are typically given using the annualized values of the return and risk (Bacon 2008).

4 Single-period optimization

In this section we consider optimization-based trading strategies where at the beginning of period t , using all the data available, we determine the asset portion of the current trade vector $(u_t)_{1:n}$ (or the normalized asset trades $(z_t)_{1:n}$). The cash component of the trade vector $(z_t)_{n+1}$ is then determined by the self-financing equation (8), once we know the realized costs. We formulate this as

a convex optimization problem, which takes into account the portfolio performance over one period, the constraints on the portfolio, and investment risk (described below). The idea goes back to Markowitz (1952), who was the first to formulate the choice of a portfolio as an optimization problem. (We will consider multi-period optimization in the next section.)

When we choose $(z_t)_{1:n}$, we do not know r_t and the other market parameters (and therefore the transaction-cost function ϕ_t^{trade}), so instead we must rely on estimates of these quantities and functions. We will denote an estimate of the quantity or function Z , made at the beginning of period t (i.e., when we choose $(z_t)_{1:n}$), as \hat{Z} . For example, $\hat{\phi}_t^{\text{trade}}$ is our estimate of the current period transaction-cost function (which depends on the market volume and other parameters, which are predicted or estimated). The most important quantity that we estimate is the return over the current period r_t , which we denote as \hat{r}_t . (Return forecasts are sometimes called *signals*.) If we adopt a stochastic model of returns and other quantities, \hat{Z} could be the conditional expectation of Z , given all data that is available at the beginning of period t , when the asset trades are chosen.

Before proceeding we note that most of the effort in developing a good trading algorithm goes into forming the estimates or forecasts, especially of the return r_t (Campbell et al. 1997, Grinold and Kahn 2000). In this paper, however, we consider the estimates as given. Thus we focus on the question, given a set of estimates, what is a good way to trade based on them? Even though we do not focus on how the estimates should be constructed, the ideas in this paper are useful in the development of estimates, since the value of a set of estimates can depend considerably on how they are exploited, i.e., how the estimates are turned into trades. To properly assess the value of a proposed set of estimates or forecasts, we must evaluate them using a realistic simulation with a good trading algorithm.

We write our *estimated* portfolio return as

$$\hat{R}_t^p = \hat{r}_t^T w_t + \hat{r}_t^T z_t - \hat{\phi}_t^{\text{trade}}(z_t) - \hat{\phi}_t^{\text{hold}}(w_t + z_t),$$

which is (9), with the unknown return r_t replaced with the estimate \hat{r}_t . The estimated active return is

$$\hat{R}_t^a = \hat{r}_t^T (w_t - w_t^b) + \hat{r}_t^T z_t - \hat{\phi}_t^{\text{trade}}(z_t) - \hat{\phi}_t^{\text{hold}}(w_t + z_t).$$

Each of these consists of a term that does not depend on the trades, plus

$$\hat{r}_t^T z_t - \hat{\phi}_t^{\text{trade}}(z_t) - \hat{\phi}_t^{\text{hold}}(w_t + z_t), \quad (11)$$

the return on the trades minus the transaction and holding costs.

4.1 Risk–return optimization

In a basic optimization-based trading strategy, we determine the normalized asset trades z_t by solving the optimization problem

$$\begin{aligned} & \text{maximize} && \hat{R}_t^p - \gamma_t \psi_t(w_t + z_t) \\ & \text{subject to} && z_t \in \mathcal{Z}_t, \quad w_t + z_t \in \mathcal{W}_t \\ & && \mathbf{1}^T z_t + \hat{\phi}_t^{\text{trade}}(z_t) + \hat{\phi}_t^{\text{hold}}(w_t + z_t) = 0, \end{aligned} \tag{12}$$

with variable z_t . Here $\psi_t : \mathbb{R}^{n+1} \rightarrow \mathbb{R}$ is a risk function, described below, and $\gamma_t > 0$ is the *risk-aversion parameter*. The objective in (12) is called the *risk-adjusted estimated return*. The sets \mathcal{Z}_t and \mathcal{W}_t are the trading and holdings constraint sets, respectively, also described in more detail below. The current portfolio weight w_t is known, i.e., a parameter, in the problem (12). The risk function, constraint sets, and estimated transaction and holding costs can all depend on the portfolio value v_t , but we suppress this dependence to keep the notation light.

To optimize performance against the risk-free interest rate or a benchmark portfolio, we replace \hat{R}_t^p in (12) with \hat{R}_t^e or \hat{R}_t^a . By (11), these all have the form of a constant that does not depend on z_t , plus

$$\hat{r}_t^T z_t - \hat{\phi}_t^{\text{trade}}(z_t) - \hat{\phi}_t^{\text{hold}}(w_t + z_t).$$

So in all three cases we get the same trades by solving the problem

$$\begin{aligned} & \text{maximize} && \hat{r}_t^T z_t - \hat{\phi}_t^{\text{trade}}(z_t) - \hat{\phi}_t^{\text{hold}}(w_t + z_t) - \gamma_t \psi_t(w_t + z_t) \\ & \text{subject to} && z_t \in \mathcal{Z}_t, \quad w_t + z_t \in \mathcal{W}_t \\ & && \mathbf{1}^T z_t + \hat{\phi}_t^{\text{trade}}(z_t) + \hat{\phi}_t^{\text{hold}}(w_t + z_t) = 0, \end{aligned} \tag{13}$$

with variable z_t . (We will see later that the risk functions are not the same for absolute, excess, and active return.) The objective has four terms: the first is the estimated return for the trades, the second is the estimated transaction cost, the third term is the holding cost of the post-trade portfolio, and the last is the risk of the post-trade portfolio. Note that the first two depend on the trades z_t and the last two depend on the post-trade portfolio $w_t + z_t$. (Similarly, the first constraint depends on the trades, and the second on the post-trade portfolio.)

Estimated versus realized transaction and holding costs. The asset trades we choose are given by $(z_t)_{1:n} = (z_t^*)_{1:n}$, where z_t^* is optimal for (13). In dollar terms, the asset trades are $(u_t)_{1:n} = v_t(z_t^*)_{1:n}$. The true normalized cash trade value $(z_t)_{n+1}$ is found by the self-financing condition (8) from the non-cash asset trades $(z_t^*)_{1:n}$ and the realized costs. This is not (in general) the same as $(z_t^*)_{n+1}$, the normalized cash trade value found by solving the optimization problem (13). The quantity $(z_t)_{n+1}$ is the normalized cash trade

value with the *realized* costs, while $(z_t^*)_n$ is the normalized cash trade value with the *estimated* costs.

The (small) discrepancy between the realized cash trade value $(z_t)_n$ and the planned or estimated cash trade value $(z_t^*)_n$ has an implication for the post-trade holding constraint $w_t + z_t^* \in \mathcal{W}_t$. When we solve (13) we require that the post-trade portfolio with the *estimated* cash balance satisfies the constraints, which is not quite the same as requiring that the post-trade portfolio with the *realized* cash balance satisfies the constraints. The discrepancy is typically very small, since our estimation errors for the transaction cost are typically small compared to the true transaction costs, which in turn are small compared to the total portfolio value. But it should be remembered that the realized post-trade portfolio $w_t + z_t$ can (slightly) violate the constraints since we only constrain the estimated post-trade portfolio $w_t + z_t^*$ to satisfy the constraints. (Assuming perfect trade execution, constraints relating to the asset portion of the post-trade portfolio $(w_t + z_t^*)_{1:n}$ will hold exactly.)

Simplifying the self-financing constraint. We can simplify problem (13) by replacing the self-financing constraint

$$\mathbf{1}^T z_t + \hat{\phi}_t^{\text{trade}}(z_t) + \hat{\phi}_t^{\text{hold}}(w_t + z_t) = 0$$

with the constraint $\mathbf{1}^T z_t = 0$. In all practical cases, the cost terms are small compared to the total portfolio value, so the approximation is good. At first glance it appears that by using the simplified constraint $\mathbf{1}^T z = 0$ in the optimization problem, we are essentially ignoring the transaction and holding costs, which would not produce good results. But we still take the transaction and holding costs into account in the objective.

With this approximation we obtain the simplified problem

$$\begin{aligned} & \text{maximize} && \hat{r}_t^T z_t - \hat{\phi}_t^{\text{trade}}(z_t) - \hat{\phi}_t^{\text{hold}}(w_t + z_t) - \gamma_t \psi_t(w_t + z_t) \\ & \text{subject to} && \mathbf{1}^T z_t = 0, \quad z_t \in \mathcal{Z}_t, \quad w_t + z_t \in \mathcal{W}_t. \end{aligned} \quad (14)$$

The solution z_t^* to the simplified problem slightly over-estimates the realized cash trade $(z_t)_n$, and therefore the post-trade cash balance $(w_t + z_t)_n$. The cost functions used in optimization are only estimates of what the realized values will be; in most practical cases this estimation error is much larger than the approximation introduced with the simplification $\mathbf{1}^T z_t = 0$. One small advantage (that will be useful in the multi-period trading case) is that in the optimization problem (14), $w_t + z_t$ is a bona fide set of weights, i.e., $\mathbf{1}^T (w_t + z_t) = 1$; whereas in (13), $\mathbf{1}^T (w_t + z_t)$ is (typically) slightly less than one.

We can re-write the problem (14) in terms of the variable $w_{t+1} = w_t + z_t$, which we interpret as the post-trade portfolio weights:

$$\begin{aligned} & \text{maximize} && \hat{r}_t^T w_{t+1} - \hat{\phi}_t^{\text{trade}}(w_{t+1} - w_t) - \hat{\phi}_t^{\text{hold}}(w_{t+1}) - \gamma_t \psi_t(w_{t+1}) \\ & \text{subject to} && \mathbf{1}^T w_{t+1} = 1, \quad w_{t+1} - w_t \in \mathcal{Z}_t, \quad w_{t+1} \in \mathcal{W}_t, \end{aligned} \quad (15)$$

with variable w_{t+1} .

4.2 Risk measures

The risk measure ψ_t in (13) or (14) is traditionally an estimate of the variance of the return, using a stochastic model of the returns (Markowitz 1952, Kolm et al. 2014), but it can be any function that measures our perceived risk of holding a portfolio (Frittelli and Gianin 2002). We first describe the traditional risk measures.

Absolute risk. Under the assumption that the returns r_t are stochastic, with covariance matrix $\Sigma_t \in \mathbb{R}^{(n+1) \times (n+1)}$, the variance of R_t^P is given by

$$\text{var}[R_t^P] = (w_t + z_t)^T \Sigma_t (w_t + z_t).$$

This gives the traditional quadratic risk measure for period t ,

$$\psi_t(x) = x^T \Sigma_t x.$$

It must be emphasized that Σ_t is an *estimate* of the return covariance under the assumption that the returns are stochastic. It is usually assumed that the cash return (risk-free interest rate) $(r_t)_{n+1}$ is known, in which case the last row and column of Σ_t are zero.

Active risk. With the assumption that r_t is stochastic with covariance Σ_t , the variance of the active return R_t^A is

$$\text{var}[R_t^A] = (w_t + z_t - w_t^B)^T \Sigma_t (w_t + z_t - w_t^B).$$

This gives the traditional quadratic active risk measure

$$\psi_t(x) = (x - w_t^B)^T \Sigma_t (x - w_t^B).$$

When the benchmark is cash, this reduces to $x^T \Sigma_t x$, the absolute risk, since the last row and column of Σ_t are zero. In the sequel we will work with the active risk, which reduces to the absolute or excess risk when the benchmark is cash.

Risk-aversion parameter. The risk-aversion parameter γ_t in (13) or (14) is used to scale the relative importance of the estimated return and the estimated risk. Here we describe how the particular value $\gamma_t = 1/2$ arises in an approximation of maximizing expected growth rate, neglecting costs. Assuming that the returns r_t are independent samples from a distribution, and w is fixed, the portfolio return $R_t^P = w^T r_t$ is a (scalar) random variable. The weight vector that maximizes the expected portfolio growth rate $\mathbf{E}[\log(1 + R_t^P)]$ (subject to $\mathbf{1}^T w = 1$, $w \geq 0$) is called the *Kelly optimal portfolio* or *log-optimal portfolio*

(Kelly 1956, Busseti et al. 2016). Using the quadratic approximation of the logarithm $\log(1 + a) \approx a - (1/2)a^2$ we obtain

$$\begin{aligned}\mathbf{E}[\log(1 + R_t^p)] &\approx \mathbf{E}[R_t^p - (1/2)(R_t^p)^2] \\ &= \mu^T w - (1/2)w^T(\Sigma + \mu\mu^T)w,\end{aligned}$$

where $\mu = \mathbf{E}[r_t]$ and $\Sigma = \mathbf{E}[(r_t - \mu)(r_t - \mu)^T]$ are the mean and covariance of the return r_t . Assuming that the term $\mu\mu^T$ is small compared to Σ (which is the case for realistic daily returns and covariance), the expected growth rate can be well approximated as $\mu^T w - (1/2)w^T\Sigma w$. So the choice of risk-aversion parameter $\gamma_t = 1/2$ in the single-period optimization problems (13) or (14) corresponds to approximately maximizing growth rate, i.e., Kelly optimal trading. In practice it is found that Kelly optimal portfolios tend to have too much risk (Busseti et al. 2016), so we expect that useful values of the risk-aversion parameter γ_t are bigger than 1/2.

Factor model. When the number of assets n is large, the covariance estimate Σ_t is typically specified as a low rank ('factor') component, plus a diagonal matrix,

$$\Sigma_t = F_t \Sigma_t^f F_t^T + D_t,$$

which is called a *factor model* (for quadratic risk). Here $F_t \in \mathbb{R}^{(n+1) \times k}$ is the *factor-loading matrix*, $\Sigma_t^f \in \mathbb{R}^{k \times k}$ is an estimate of the covariance of $F^T r_t$ (the vector of *factor returns*), and $D_t \in \mathbb{R}^{(n+1) \times (n+1)}$ is a nonnegative diagonal matrix.

The number of factors k is much less than n (Chan et al. 1999) (typically, tens versus thousands). Each entry $(F_t)_{ij}$ is the loading (or *exposure*) of asset i to factor j . Factors can represent economic concepts such as industrial sectors, exposure to specific countries, accounting measures, and so on. For example, a technology factor would have loadings of 1 for technology assets and 0 for assets in other industries. But the factor-loading matrices can be found using many other methods, for example by a purely data-driven analysis. The matrix D_t accounts for the additional variance in individual asset returns beyond that predicted by the factor model, known as the *idiosyncratic risk*.

When a factor model is used in the problems (13) or (14), it can offer a very substantial increase in the speed of solution (Perold 1984, Boyd and Vandenberghe 2004). Provided the problem is formulated in such a way that the solver can exploit the factor model, the computational complexity drops from $O(n^3)$ to $O(nk^2)$ flops, for a savings of $O((n/k)^2)$. The speedup can be substantial when (as is typical) n is on the order of thousands and k on the order of tens. (Computational issues are discussed in more detail in section 4.7.)

We now mention some less traditional risk functions that can be very useful in practice.

Transformed risk. We can apply a nonlinear transformation to the usual quadratic risk,

$$\psi_t(x) = \varphi((x - w_t^b)^T \Sigma_t (x - w_t^b)),$$

where $\varphi : \mathbb{R} \rightarrow \mathbb{R}$ is a nondecreasing function. (It should also be convex, to keep the optimization problem tractable, as we will discuss below.) This allows us to shape our aversion to different levels of quadratic risk. For example, we can take $\varphi(x) = (x - a)_+$. In this case the transformed risk assesses no cost for quadratic risk levels up to a . This can be useful to hit a target risk level, or to be maximally aggressive in seeking returns, up to the risk threshold a . Another option is $\varphi(x) = \exp(x/\eta)$, where $\eta > 0$ is a parameter. This assesses a strong cost to risks substantially larger than η , and is closely related to risk aversion used in stochastic optimization.

The solution of the optimization problem (13) with transformed risk is the same as the solution with the traditional risk function, but with a different value of the risk-aversion parameter. So we can think of transformed risk aversion as a method to automatically tune the risk-aversion parameter, increasing it as the risk increases.

Worst-case quadratic risk. We now move beyond the traditional quadratic risk to create a risk function that is more robust to unpredicted changes in market conditions. We define the *worst-case* risk for portfolio x as

$$\psi_t(x) = \max_{i=1,\dots,M} (x - w_t^b)^T \Sigma_t^{(i)} (x - w_t^b).$$

Here $\Sigma^{(i)}$, $i = 1, \dots, M$, are M given covariance matrices; we refer to i as the *scenario*. We can motivate the worst-case risk by imagining that the returns are generated from one of M distributions, with covariances $\Sigma^{(i)}$ depending on which scenario occurs. In each period, we do not know, and do not attempt to predict, which scenario will occur. The worst-case risk is the largest risk under the M scenarios.

If we estimate the probabilities of occurrence of the scenarios, and weight the scenario covariance matrices by these probabilities, we end up back with a single quadratic risk measure, the weighted sum of the scenario covariances. It is critical that we combine them using the maximum, and not a weighted sum. (Although other nonlinear combining functions would also work.) We should think of the scenarios as describing situations that could arise, but that we cannot or do not attempt to predict.

The scenario covariances $\Sigma^{(i)}$ can be found by many reasonable methods. They can be empirical covariances estimated from realized (past) returns conditioned on the scenario, for example, high or low market volatility, high or low interest rates, high or low oil prices, and so on (Meucci 2010). They could be an analyst's best guess for what the asset covariance would be in a situation that could occur.

4.3 Forecast-error risk

The risk measures considered above attempt to model the period to period variation in asset returns, and the associated period to period variation in the portfolio return they induce. In this section we consider terms that take into account errors in our prediction of return and covariance. (The same ideas can be applied to other parameters that we estimate, like volume.) Estimation errors can significantly impact the resulting portfolio weights, resulting in poor out-of-sample performance (Jorion 1985, Michaud 1989, Chopra and Ziemba 1993, Kan and Zhou 2007, DeMiguel et al. 2009b, Fabozzi et al. 2010, Kolm et al. 2014, Bailey et al. 2017).

Return-forecast-error risk. We assume our forecasts of the return vector \hat{r} are uncertain: any forecast $\hat{r} + \delta$ with $|\delta| \leq \rho$ and $\rho \in \mathbb{R}^n$ is possible and consistent with what we know. In other words, ρ is a vector of uncertainties on our return prediction \hat{r} . If we are confident in our (nominal) forecast of the return of asset i , we take ρ_i small; conversely large ρ_i means that we are not very confident in our forecast. The uncertainty in return forecast is readily interpreted when annualized; for example, our uncertain return forecast for an asset might be described as $6\% \pm 2\%$, meaning any forecast return between 4% and 8% is possible.

The post-trade estimated return is then $(\hat{r}_t + \delta_t)^T(w_t + z_t)$; we define the minimum of this over $|\delta| \leq \rho$ as the *worst-case return forecast*. It is easy to see what the worst-case value of δ is: if we hold a long position, the return (for that asset) should take its minimum value $\hat{r}_i + \rho_i$; if we hold a short position, it should take its maximum allowed value $\hat{r}_i - \rho_i$. The worst-case return forecast has the value

$$\hat{R}_t^{\text{wc}} = \hat{r}_t^T(w_t + z_t - w_t^{\text{b}}) - \rho^T|w_t + z_t - w_t^{\text{b}}|.$$

The first term here is our original estimate (including the constant terms we neglect in (13) and (14)); the second term (which is always nonpositive) is the worst possible value of our estimated active return over the allowed values of δ . It is a risk associated with forecast uncertainty. This gives

$$\psi_t(x) = \rho^T|x - w_t^{\text{b}}|. \quad (16)$$

(This would typically be added to a traditional quadratic risk measure.) This term is a weighted ℓ_1 norm of the deviation from the weights, and encourages weights that deviate sparsely from the benchmark, i.e., weights with some or many entries equal to those of the benchmark (Tibshirani 1996, Fastrich et al. 2015, Ho et al. 2015, Li 2015b).

Covariance-forecast-error risk. In a similar way we can add a term that corresponds to risk of errors in forecasting the covariance matrix in a traditional

quadratic risk model. As an example, suppose that we are given a nominal covariance matrix Σ , and consider the *perturbed covariance matrix*

$$\Sigma^{\text{pert}} = \Sigma + \Delta,$$

where Δ is a symmetric perturbation matrix with

$$|\Delta_{ij}| \leq \kappa (\Sigma_{ii} \Sigma_{jj})^{1/2}, \quad (17)$$

where $\kappa \in [0, 1]$ is a parameter. This perturbation model means that the diagonal entries of covariance can change by the fraction κ ; ignoring the change in the diagonal entries, the asset correlations can change by up to (roughly) κ . The value of κ depends on our confidence in the covariance matrix; reasonable values are $\kappa = 0.02, 0.05$, or more.

With $v = x - w_t^b$, the maximum (worst-case) value of the quadratic risk over this set of perturbations is given by

$$\begin{aligned} \max_{|\Delta_{ij}| \leq \kappa (\Sigma_{ii} \Sigma_{jj})^{1/2}} v^T (\Sigma^{\text{pert}}) v &= \max_{|\Delta_{ij}| \leq \kappa (\Sigma_{ii} \Sigma_{jj})^{1/2}} v^T (\Sigma + \Delta) v \\ &= v^T \Sigma v + \max_{|\Delta_{ij}| \leq \kappa (\Sigma_{ii} \Sigma_{jj})^{1/2}} \sum_{ij} v_i v_j \Delta_{ij} \\ &= v^T \Sigma v + \kappa \sum_{ij} |v_i v_j| (\Sigma_{ii} \Sigma_{jj})^{1/2} \\ &= v^T \Sigma v + \kappa \left(\sum_i \Sigma_{ii}^{1/2} |v_i| \right)^2. \end{aligned}$$

This shows that the worst-case covariance, over all perturbed covariance matrices consistent with our risk forecast error assumption (17), is given by

$$\psi_t(x) = (x - w_t^b)^T \Sigma (x - w_t^b) + \kappa (\sigma^T |x - w_t^b|)^2, \quad (18)$$

where $\sigma = (\Sigma_{11}^{1/2}, \dots, \Sigma_{nn}^{1/2})$ is the vector of asset volatilities. The first term is the usual quadratic risk with the nominal covariance matrix; the second term can be interpreted as risk associated with covariance forecasting error (Ho et al. 2015, Li 2015b). It is the square of a weighted ℓ_1 norm of the deviation of the weights from the benchmark. (With cash benchmark, this directly penalizes large leverage.)

4.4 Holding constraints

Holding constraints restrict our choice of normalized post-trade portfolio $w_t + z_t$. They may be surrogates for constraints on w_{t+1} , which we cannot constrain directly since it depends on the unknown returns. Usually returns are small

and w_{t+1} is close to $w_t + z_t$, so constraints on $w_t + z_t$ are good approximations for constraints on w_{t+1} . Some types of constraints always hold exactly for w_{t+1} when they hold for $w_t + z_t$.

Holding constraints may be mandatory, imposed by law or the investor, or discretionary, included to avoid certain undesirable portfolios. We discuss common holding constraints below. Depending on the specific situation, each of these constraints could be imposed on the *active* holdings $w_t + z_t - w_t^b$ instead of the absolute holdings $w_t + z_t$, which we use here for notational simplicity.

Long only. This constraint requires that only long asset positions are held,

$$w_t + z_t \geq 0.$$

If only the assets must be long, this becomes $(w_t + z_t)_{1:n} \geq 0$. When a long-only constraint is imposed on the post-trade weight $w_t + z_t$, it automatically holds on the next period value $(\mathbf{1} + r_t) \circ (h_t + z_t)$, since $\mathbf{1} + r_t \geq 0$.

Leverage constraint. The leverage can be limited with the constraint

$$\|(w_t + z_t)_{1:n}\|_1 \leq L^{\max},$$

which requires the post-trade portfolio leverage to not exceed L^{\max} . (Note that the leverage of the next period portfolio can be slightly larger than L^{\max} , due to the returns over the period.)

Limits relative to asset capitalization. Holdings are commonly limited so that the investor does not own too large a portion of the company total value. Let C_t denote the vector of asset capitalization, in dollars. The constraint

$$(w_t + z_t)_i \leq \delta \circ C_t / v_t,$$

where $\delta \geq 0$ is a vector of fraction limits, and $/$ is interpreted elementwise, limits the long post-trade position in asset i to be no more than the fraction δ_i of the capitalization. We can impose a similar limit on short positions, relative to asset capitalization, total outstanding short value, or some combination.

Limits relative to portfolio. We can limit our holdings in each asset to lie between a minimum and a maximum fraction of the portfolio value,

$$-w^{\min} \leq w_t + z_t \leq w^{\max},$$

where w^{\min} and w^{\max} are nonnegative vectors of the maximum short and long allowed fractions, respectively. For example, with $w^{\max} = w^{\min} = (0.05)\mathbf{1}$, we are not allowed to hold more than 5% of the portfolio value in any one asset, long or short.

Minimum cash balance. Often the cash balance must stay above a minimum dollar threshold c_{\min} (which can be negative). We express a minimum cash balance as the constraint

$$(w_t + z_t)_{n+1} \geq c_{\min}/v_t.$$

This constraint can be slightly violated by the realized values, due to our error in estimation of the costs.

No-hold constraints. A no-hold constraint on asset i forbids holding a position in asset i , i.e.,

$$(w_t + z_t)_i = 0.$$

β -neutrality. A β -neutral portfolio is one whose return R^p is uncorrelated with the benchmark return R^b , according to our estimate Σ_t of $\text{cov}[r_t]$. The constraint that $w_t + z_t$ be β neutral takes the form

$$(w_t^b)^T \Sigma_t (w_t + z_t) = 0.$$

Factor neutrality. In the factor covariance model, the estimated portfolio risk σ_i^F due to factor i is given by

$$(\sigma_i^F)^2 = (w_t + z_t)^T (F_t)_i (\Sigma_t^F)_{ii} (F_t)_i^T (w_t + z_t).$$

The constraint that the portfolio be neutral to factor i means that $\sigma_i^F = 0$, which occurs when

$$(F_t)_i^T (w_t + z_t) = 0.$$

Stress constraints. Stress constraints protect the portfolio against unexpected changes in market conditions. Consider scenarios $1, \dots, K$, each representing a market shock event such as a sudden change in oil prices, a general reversal in momentum, or a collapse in real estate prices. Each scenario i has an associated (estimated) return c_i . The c_i could be based on past occurrences of scenario i or predicted by analysts if scenario i has never occurred before.

Stress constraints take the form

$$c_i^T (w_t + z_t) \geq R^{\min},$$

i.e., the portfolio return in scenario i is above R^{\min} . (Typically R^{\min} is negative; here we are limiting the decrease in portfolio value should scenario i actually occur.) Stress constraints are related to chance constraints such as value at risk in the sense that they restrict the probability of large losses due to shocks.

Liquidation-loss constraint. We can bound the loss of value incurred by liquidating the portfolio over T^{liq} periods. A constraint on liquidation loss will deter the optimizer from investing in illiquid assets. We model liquidation as the transaction cost to trade h^+ over T^{liq} periods. If we use the transaction-cost estimate $\hat{\phi}$ for all periods, the optimal schedule is to trade $(w_t + z_t)/T^{\text{liq}}$ each period. The constraint that the liquidation loss is no more than the fraction δ of the portfolio value is given by

$$T^{\text{liq}} \hat{\phi}_t^{\text{trade}}((w_t + z_t)/T^{\text{liq}}) \leq \delta.$$

(For optimization against a benchmark, we replace this with the cost to trade the portfolio to the benchmark over T^{liq} periods.)

Concentration limit. As an example of a non-traditional constraint, we consider a *concentration limit*, which requires that no more than a given fraction ω of the portfolio value can be held in some given fraction (or just a specific number K) of assets. This can be written as

$$\sum_{i=1}^K (w_t + z_t)_{[i]} \leq \omega,$$

where the notation $a_{[i]}$ refers to the i 'th largest element of the vector a . The left-hand side is the sum of the K largest post-trade positions. For example, with $K = 20$ and $\omega = 0.4$, this constraint prohibits holding more than 40% of the total value in any 20 assets. (It is not well known that this constraint is convex, and indeed, easily handled; see Boyd and Vandenberghe (2004, section 3.2.3). It is easily extended to the case where K is not an integer.)

4.5 Trading constraints

Trading constraints restrict the choice of normalized trades z_t . Constraints on the non-cash trades $(z_t)_{1:n}$ are exact (since we assume that our trades are executed in full), while constraints on the cash trade $(z_t)_{n+1}$ are approximate, due to our estimation of the costs. As with holding constraints, trading constraints may be mandatory or discretionary.

Turnover limit. The turnover of a portfolio in period t is given by $\|(z_t)_{1:n}\|_1/2$. It is common to limit the turnover to a fraction δ (of portfolio value), i.e.,

$$\|(z_t)_{1:n}\|_1/2 \leq \delta.$$

Limits relative to trading volume. Trades in non-cash assets may be restricted to a certain fraction δ of the current period market volume V_t (estimate),

$$|(z_t)_{1:n}| \leq \delta(V_t/v_t),$$

where the division on the right-hand side means elementwise.

No-buy, sell, or trade restriction. A no-buy restriction on asset i imposes the constraint

$$(z_t)_i \leq 0,$$

while a no-sell restriction imposes the constraint

$$(z_t)_i \geq 0.$$

A no-trade restriction imposes both a no-buy and no-sell restriction.

4.6 Soft constraints

Any of the constraints on holdings or transactions can be made *soft*, which means that are not strictly enforced. We explain this in a general setting. For a vector equality constraint $h(x) = 0$ on the variable or expression x , we replace it with a term subtracted the objective of the form $\gamma\|h(x)\|_1$, where $\gamma > 0$ is the *priority* of the constraint. (We can generalize this to $\gamma^T|h(x)|$, with γ a vector, to give different priorities to the different components of $h(x)$.)

In a similar way we can replace an inequality constraint $h(x) \leq 0$ with a term, subtracted from the objective, of the form $\gamma^T(h(x))_+$, where $\gamma > 0$ is a vector of priorities. Replacing the hard constraints with these *penalty* terms results in *soft constraints*. For large enough values of the priorities, the constraints hold exactly; for smaller values, the constraints are (roughly speaking) violated only when they need to be.

As an example, we can convert a set of factor-neutrality constraints $F_t^T(w_t + z_t) = 0$ to soft constraints, by subtracting a term $\gamma\|F_t^T(w_t + z_t)\|_1$ from the objective, where $\gamma > 0$ is the priority. For larger values of γ factor neutrality $F_t^T(w_t + z_t) = 0$ will hold (exactly, when possible); for smaller values some factor exposures can become nonzero, depending on other objective terms and constraints.

4.7 Convexity

The portfolio optimization problem (13) can be solved quickly and reliably using readily available software so long as the problem is convex. This requires that the risk and estimated transaction- and holding-cost functions are convex, and the trade and holding constraint sets are convex. All the functions and constraints discussed above are convex, except for the self-financing constraint

$$\mathbf{1}^T z_t + \hat{\phi}_t^{\text{trade}}(z_t) + \hat{\phi}_t^{\text{hold}}(w_t + z_t) = 0,$$

which must be relaxed to the inequality

$$\mathbf{1}^T z_t + \hat{\phi}_t^{\text{trade}}(z_t) + \hat{\phi}_t^{\text{hold}}(w_t + z_t) \leq 0.$$

The inequality will be tight at the optimum of (13). Alternatively, the self-financing constraint can be replaced with the simplified version $\mathbf{1}^T z_t = 0$ as in problem (14).

Solution times. The SPO problems described above, except for the multi-covariance risk model, can be solved using standard interior-point methods (Nesterov and Nemirovskii 1994) with a complexity $O(nk^2)$ flops, where n is the number of assets and k is the number of factors. (Without the factor model, we replace k with n .) The coefficient in front is on the order of 100, which includes the interior-point iteration count and other computation. This should be the case even for complex leverage constraints, the 3/2-power transaction cost, limits on trading and holding, and so on.

This means that a typical current single core (or thread) of a processor can solve an SPO problem with 1,500 assets and 50 factors in under one half second (based conservatively on a computation speed of 1G flop/sec). This is more than fast enough to use the methods to carry out trading with periods on the order of a second. But the speed is still very important even when the trading is daily, in order to carry out backtesting. For daily trading, one year of backtesting, around 250 trading days, can be carried out in a few minutes or less. A generic 32 core computer, running 64 threads, can carry out a backtest on five years of data, with 64 different choices of parameters (see below), in under 10 minutes. This involves solving 80,000 convex optimization problems. All of these times scale linearly with the number of assets, and quadratically with the number of factors. For a problem with, say, 4,500 assets and 100 factors, the computation times would be around 12 \times longer. Our estimates are conservatively based on a computation speed of 1G flop/sec; for these or larger problems multi-threaded optimized linear algebra routines can achieve 100G flop/sec, making the backtesting 100 \times faster.

We mention one special case that can be solved much faster. If the objective is quadratic, which means that the risk and costs are quadratic functions, and the only constraints are linear equality constraints (e.g., factor neutrality), the problem can be solved with the same $O(nk^2)$ complexity, but the coefficient in front is closer to 2, around 50 times faster than using an interior-point method.

Custom solvers, or solvers targeted to specific platforms like GPUs, can solve SPO problems much faster (O'Donoghue et al. 2016). For example, the first order operator-splitting method implemented in POGS (Fougner and Boyd 2018) running on a GPU can solve extremely large SPO problems. POGS can solve a problem with 100,000 assets and 1,000 factors (which is much larger than any practical problem) in a few seconds or less. At the other extreme, code generation systems like CVXGEN (Mattingley and Boyd 2012) can solve smaller SPO problems with stunning speed; for example, a problem with 30 assets in well under one millisecond.

Problem specification. New frameworks for convex optimization such as CVX (Fougner and Boyd 2018), CVXPY (Diamond and Boyd 2016), and Convex.jl (Udell et al. 2014), based on the idea of disciplined convex programming

(Grant et al. 2006), make it very easy to specify and modify the SPO problem in just a handful of lines of easy to understand code. These frameworks make it easy to experiment with non-standard trading and holding constraints, or risk and cost functions.

Nonconvexity. The presence of nonconvex constraints or terms in the optimization problem greatly complicates its solution, making its solution time much longer, and sometimes very much longer. This may not be a problem in the production trading engine that determines one trade per day, or per hour. But nonconvexity makes backtesting much slower at the least, and in many cases simply impractical. This greatly reduces the effectiveness of the whole optimization-based approach. For this reason, nonconvex constraints or terms should be strenuously avoided.

Nonconvex constraints generally arise only when someone who does not understand this adds a reasonable sounding constraint, unaware of the trouble he or she is making. As an example, consider imposing a minimum trade condition, which states that if $(z_t)_i$ is nonzero, it must satisfy $|(z_t)_i| \geq \epsilon$, where $\epsilon > 0$. This constraint seems reasonable enough, but makes the problem nonconvex. If the intention was to achieve sparse trading, or to avoid many very small trades, this can be accomplished (in a far better way) using convex constraints or cost terms.

Other examples of nonconvex constraints (that should be avoided) include limits on the number of assets held, minimum values of nonzero holdings, or restricting trades to be integer numbers of share lots, or restricting the total number of assets we can trade. The requirement that we must trade integer numbers of shares is also nonconvex, but irrelevant for any practical portfolio. The error induced by rounding our trade lists (which contain real numbers) to an integer number of shares is negligible for reasonably sized portfolios.

While nonconvex constraints and objective terms should be avoided, and are generally not needed, it is possible to handle many of them using simple powerful heuristics, such as solving a relaxation, fixing the nonconvex terms, and then solving the convex problem again (Diamond et al. 2018). As a simple example of this approach, consider the minimum nonzero trade requirement $|(z_t)_i| \geq \epsilon$ for $(z_t)_i \neq 0$. We first solve the SPO problem without this constraint, finding a solution \tilde{z} . We use this tentative trade vector to determine which entries of z will be zero, negative, or positive (i.e., which assets we hold, sell, or buy). We now impose these sign constraints on the trade vector: we require $(z_t)_i = 0$ if $(\tilde{z}_t)_i = 0$, $(z_t)_i \geq 0$ if $(\tilde{z}_t)_i > 0$, and $(z_t)_i \leq 0$ if $(\tilde{z}_t)_i < 0$. We solve the SPO again, with these sign constraints, and the minimum-trade constraints as well, which are now linear, and therefore convex. This simple method will work very well in practice.

As another example, suppose that we are limited to make at most K nonzero trades in any given period. A very simple scheme, based on convex optimization, will work extremely well. First we solve the problem ignoring the limit, and possibly with an additional ℓ_1 transaction cost added in, to discourage trading. We take this trade list and find the K largest trades (buy or sell). We then add the constraint to our problem that we will only trade these assets, and we solve the portfolio optimization problem again, using only these trades. As in the example described above, this approach will yield extremely good, if not optimal, trades. This approximation will have no effect on the real metrics of interest, i.e., the portfolio performance.

There is generally no need to solve the nonconvex problem globally, since this greatly increases the solve time and delivers no practical benefit in terms of trading performance. The best method for handling nonconvex problems in portfolio optimization is to avoid them.

4.8 Using single-period optimization

The idea. In this section we briefly explain, at a high level, how the SPO trading algorithm is used in practice. We do not discuss what is perhaps the most critical part, the return (and other parameter) estimates and forecasts. Instead, we assume the forecasts are given, and focus on how to use SPO to exploit them.

In SPO, the parameters that appear in the transaction and holding costs can be inspired or motivated by our estimates of what their true values will be, but it is better to think of them as ‘knobs’ that we turn to achieve trading behavior that we like (see, e.g., Jagannathan and Ma 2003, Cornuejols and Tütüncü 2006, DeMiguel et al. 2009a, Li 2015b), as verified by backtesting, what-if simulation, and stress-testing.

As a crude but important example, we can scale the entire transaction-cost function ϕ_t^{trade} by a *trading-aversion factor* γ^{trade} . (The name emphasizes the analogy with the risk-aversion parameter, which scales the risk term in the objective.) Increasing the trading-aversion parameter will deter trading or reduce turnover; decreasing it will increase trading and turnover. We can even think of $1/\gamma^{\text{trade}}$ as the number of periods over which we will amortize the transaction cost we incur (Grinold 2006). As a more sophisticated example, the transaction-cost parameters a_t , meant to model bid-ask spread, can be scaled up or down. If we increase them, the trades become more sparse, i.e., there are many periods in which we do not trade each asset. If we scale the 3/2-power term, we encourage or discourage large trades. Indeed, we could add a quadratic transaction term to the SPO problem, not because we think it is a good model of transaction costs, but to discourage large trades even more than the 3/2-power term does. Any SPO variation, such as scaling certain terms, or adding new ones, is assessed by backtesting and stress-testing.

The same ideas apply to the holding cost. We can scale the holding-cost rates by a positive *holdings-aversion parameter* γ_t^{hold} to encourage, or discourage, holding positions that incur holding costs, such as short positions. If the holding cost reflects the cost of holding short positions, the parameter γ_t^{hold} scales our aversion to holding short positions. We can modify the holding cost by adding a quadratic term of the short positions $\kappa^T(w_t + z_t)_-^2$, (with the square interpreted elementwise and $\kappa \geq 0$), not because our actual borrow-cost rates increase with large short positions, but to send the message to the SPO algorithm that we wish to avoid holding large short positions.

As another example, we can add a liquidation loss term to the holding cost, with a scale factor to control its effect. We add this term not because we intend to liquidate the portfolio, but to avoid building up large positions in illiquid assets. By increasing the scale factor for the liquidation loss term, we discourage the SPO algorithm from holding illiquid positions.

Trade-, hold-, and risk-aversion parameters. The discussion above suggests that we modify the objective in (14) with scaling parameters for transaction and holding costs, in addition to the traditional risk-aversion parameter, which yields the SPO problem

$$\begin{aligned} & \text{maximize} \quad \left(\hat{r}_t^T z_t - \gamma_t^{\text{trade}} \hat{\phi}_t^{\text{trade}}(z_t) \right. \\ & \quad \left. - \gamma_t^{\text{hold}} \hat{\phi}_t^{\text{hold}}(w_t + z_t) - \gamma_t^{\text{risk}} \psi_t(w_t + z_t) \right) \\ & \text{subject to} \quad \mathbf{1}^T z_t = 0, \quad z_t \in \mathcal{Z}_t, \quad w_t + z_t \in \mathcal{W}_t. \end{aligned} \quad (19)$$

where γ_t^{trade} , γ_t^{hold} , and γ_t^{risk} are positive parameters used to scale the respective costs. These parameters are sometimes called *hyperparameters*, which emphasizes the analogy to the hyperparameters used when fitting statistical models to data. The hyperparameters are ‘knobs’ that we ‘turn’ (i.e., choose or change) to obtain good performance, which we evaluate by backtesting. We can have even more than three hyperparameters, which scale individual terms in the holding and transaction costs. The choice of hyperparameters can greatly affect the performance of the SPO method. They should be chosen using backtesting, what-if testing, and stress-testing.

This style for using SPO is similar to how optimization is used in many other applied areas, for example control systems or machine learning. In machine learning, for example, the goal is to find a model that makes good predictions on new data. Most methods for constructing a model use optimization to minimize a so-called loss function, which penalizes not fitting the observed data, plus a regularizer, which penalizes model sensitivity or complexity. Each of these functions is inspired by a (simplistic) theoretical model of how the data were generated. But the final choice of these functions, and the (hyperparameter) scale factor between them, is done by out-of-sample validation or cross

validation, i.e., testing the model on data it has not seen (Hastie et al. 2009). For general discussion of how convex optimization is used in this spirit, in applications such as control or estimation, see Boyd and Vandenberghe (2004).

Judging value of forecasts. In this paper we do not consider forecasts, which of course are critically important in trading. The most basic test of a new proposed return estimate or forecast is that it does well predicting returns. This is typically judged using a simple model that evaluates Sharpe ratio or information ratio, implicitly ignoring all portfolio constraints and costs. If a forecast fails these simple SR or IR tests, it is unlikely to be useful in a trading algorithm.

But the true value of a proposed estimate or forecast in the context of multi-period trading can be very different from what is suggested by the simple SR or IR prediction tests, due to costs, portfolio constraints, and other issues. A new proposed forecast should be judged in the context of the portfolio constraints, other forecasts (say, of volume), transaction costs, holding costs, trading constraints, and choice of parameters such as risk aversion. This can be done using simulation, carrying out backtests, what-if simulations, and stress-tests, in each case varying the parameters to achieve the best performance. The result of this testing is that the forecast might be less valuable (the usual case) or more valuable (the less usual case) than it appeared from the simple SR and IR tests. One consequence of this is that the true value of a forecast can depend considerably on the type and size of the portfolio being traded; for example, a forecast could be very valuable for a small long-short portfolio with modest leverage, and much less valuable for a large long-only portfolio.

5 Multi-period optimization

5.1 Motivation

In this chapter we discuss optimization-based strategies that consider information about multiple periods when choosing trades for the current period. Before delving into the details, we should consider what we hope to gain over the single-period approach. Predicting the returns for the current period is difficult enough. Why attempt to forecast returns in future periods?

One reason is to better account for transaction costs. In the absence of transaction cost (and other limitations on trading), a greedy strategy that only considers one period at a time is optimal, since performance for the current period does not depend on previous holdings. However, in any realistic model current holdings strongly affect whether a return prediction can be profitably acted on. We should therefore consider whether the trades we make in the current period put us in a good or bad position to trade in future periods. While this idea can

be incorporated into single-period optimization, it is more naturally handled in multi-period optimization.

For example, suppose our single-period optimization-based strategy tells us to go very long in a rarely traded asset. We may not want to make the trade because we know that unwinding the position will incur large transaction costs. The single-period problem models the cost of moving into the position, but not the cost of moving out of it. To model the fact that we will over time revert positions towards the benchmark, and thus must eventually sell the positions we buy, we need to model time beyond the current period. (One standard trick in single-period optimization is to double the transaction cost, which is then called the *round-trip cost*.)

Another advantage of multi-period optimization is that it naturally handles multiple, possibly conflicting return estimates on different time scales (see, e.g., Gărleanu and Pedersen 2013, Nystrup et al. 2018b). As an example, suppose we predict that a return will be positive over a short period, but over a longer period it will be negative. The first prediction might be relevant for only a day, while the second for a month or longer. In a single-period optimization framework, it is not clear how to account for the different time scales when blending the return predictions. Combining the two predictions would likely cancel them, or have us move according to whichever prediction is larger. But the resulting behavior could be quite non-optimal. If the trading cost is high, taking no action is likely the right choice, since we will have to reverse any trade based on the fast prediction as we follow the slow prediction in future periods. If the trading cost is low, however, the right choice is to follow the fast prediction, since unwinding the position is cheap. This behavior falls naturally out of a multi-period optimization, but is difficult to capture in a single-period problem.

There are many other situations where predictions over multiple periods, as opposed to just the current period, can be taken advantage of in multi-period optimization. We describe a few of them here.

- *Signal decay and time-varying return predictions.* Generalizing the discussion above on fast versus slow signals, we may assign an exponential *decay-rate* to every return prediction signal. (This can be estimated historically, for example, by fitting an auto-regressive model to the signal values.) Then it is easy to compute return estimates at any time scale. The decay in prediction accuracy is also called mean-reversion or alpha decay (see, e.g., Campbell et al. 1997, Grinold 2006, Gărleanu and Pedersen 2013).
- *Known future changes in volatility or risk.* If we know that a future event will increase the risk, we may want to exit some of the risky positions in advance. In MPO, trading towards a lower risk position starts well before the increase in risk, trading it off with the transaction costs. In SPO,

(larger) trading to a lower risk position occurs only once the risk has increased, leading to larger transaction costs. Conversely, known periods of low risk can be exploited as well.

- *Changing constraints over multiple periods.* As an example, assume we want to de-leverage the portfolio over multiple periods, i.e., reduce the leverage constraint L^{\max} over some number of periods to a lower value. If we use a multi-period optimization framework we will likely incur lower trading cost than by some ad-hoc approach, while still exploiting our returns predictions.
- *Known future changes in liquidity or volume.* Future volume or volatility predictions can be exploited for transaction-cost optimization, for example by delaying some trades until they will be cheaper. Market volumes V_t have much better predictability than market returns.
- *Setting up, shutting down, or transferring a portfolio.* These transitions can all be handled naturally by MPO, with a combination of constraints and objective terms changing over time.

5.2 Multi-period optimization

In multi-period optimization, we choose the current trade vector z_t by solving an optimization problem over a *planning horizon* that extends H periods into the future,

$$t, t+1, \dots, t+H-1.$$

(Single-period optimization corresponds to the case $H = 1$.)

Many quantities at times $t, t+1, \dots, t+H-1$ are unknown at time t , when the optimization problem is solved and the asset trades are chosen, so as in the single-period case, we will estimate them. For any quantity or function Z , we let $\hat{Z}_{\tau|t}$ denote our estimate of Z_τ given all information available to us at the beginning of period t . (Presumably $\tau \geq t$; otherwise we can take $\hat{Z}_{\tau|t} = Z_\tau$, the realized value of Z at time τ .) For example, $\hat{r}_{\tau|t}$ is the estimate made at time t of the return at time τ (which we denoted \hat{r}_t in the section on single-period optimization); $\hat{r}_{t+2|t}$ is the estimate made at time t of the return at time $t+2$.

We can develop a multi-period optimization problem starting from (13). Let

$$z_t, z_{t+1}, \dots, z_{t+H-1}$$

denote our sequence of planned trades over the horizon. A natural objective is the total risk-adjusted return over the horizon,

$$\sum_{\tau=t}^{t+H-1} \left(\hat{r}_{\tau|t}^T (w_\tau + z_\tau) - \gamma_\tau \psi_\tau (w_\tau + z_\tau) - \hat{\phi}_\tau^{\text{hold}} (w_\tau + z_\tau) - \hat{\phi}_\tau^{\text{trade}} (z_\tau) \right).$$

(This expression drops a constant that does not depend on the trades, and handles absolute or active return.) In this expression, w_t is known, but w_{t+1}, \dots, w_{t+H} are not, since they depend on the trades z_t, \dots, z_{t+H-1} (which we will choose) and the unknown returns, via the dynamics equation (10),

$$w_{t+1} = \frac{1}{1 + R_t^p} (\mathbf{1} + r_t) \circ (w_t + z_t),$$

which propagates the current weight vector to the next one, given the trading and return vectors. (This true dynamics equation ensures that if $\mathbf{1}^T w_t = 1$, we have $\mathbf{1}^T w_{t+1} = 1$.)

In adding the risk terms $\gamma_\tau \psi_\tau(w_\tau + z_\tau)$ in this objective, we are implicitly relying on the idea that the returns are independent random variables, so the variance of the sum is the sum of the variances. We can also interpret $\gamma_\tau \psi_\tau(w_\tau + z_\tau)$ as cost terms that discourage us from holding certain portfolios.

Simplifying the dynamics. We now make a simplifying approximation: for the purpose of propagating w_t and z_t to w_{t+1} in our planning exercise, we will assume $R_t^p = 0$ and $r_t = 0$ (i.e., that the one period returns are small compared to one). This results in the much simpler dynamics equation $w_{t+1} = w_t + z_t$. With this approximation, we must add the constraints $\mathbf{1}^T z_t = 0$ to ensure that the weights in our planning exercise add to one, i.e., $\mathbf{1}^T w_\tau = 1$, $\tau = t+1, \dots, t+H$. So we will impose the constraints

$$\mathbf{1}^T z_\tau = 0, \quad \tau = t+1, \dots, t+H-1.$$

The current portfolio weights w_t are given, and satisfy $\mathbf{1}^T w_t = 1$; we get that $\mathbf{1}^T w_\tau = 1$ for $\tau = t+1, \dots, t+H$ due to the constraints. (Implications of the dynamics simplification are discussed below.)

Multi-period optimization problem. With the dynamics simplification we arrive at the MPO problem

$$\begin{aligned} & \text{maximize}_{\tau=t}^{t+H-1} \left(\hat{r}_{\tau|t}^T (w_\tau + z_\tau) - \gamma_\tau \psi_\tau(w_\tau + z_\tau) \right. \\ & \quad \left. - \hat{\phi}_\tau^{\text{hold}}(w_\tau + z_\tau) - \hat{\phi}_\tau^{\text{trade}}(z_\tau) \right) \\ & \text{subject to } \mathbf{1}^T z_\tau = 0, \quad z_\tau \in \mathcal{Z}_\tau, \quad w_\tau + z_\tau \in \mathcal{W}_\tau, \\ & \quad w_{\tau+1} = w_\tau + z_\tau, \quad \tau = t, \dots, t+H-1, \end{aligned} \tag{20}$$

with variables $z_t, z_{t+1}, \dots, z_{t+H-1}$ and w_{t+1}, \dots, w_{t+H} . Note that w_t is not a variable, but the (known) current portfolio weights. When $H = 1$, the multi-period problem reduces to the simplified single-period problem (14). (We can ignore the constant $\hat{r}_{t|t}^T w_t$, which does not depend on the variables, that appears in (20) but not (14).)

Using $w_{\tau+1} = w_\tau + z_\tau$ we can eliminate the trading variables z_τ to obtain the equivalent problem

$$\begin{aligned} \text{maximize} \quad & \sum_{\tau=t+1}^{t+H} \left(\hat{r}_{\tau|t}^T w_\tau - \gamma_\tau \psi_\tau(w_\tau) \right. \\ & \quad \left. - \hat{\phi}_\tau^{\text{hold}}(w_\tau) - \hat{\phi}_\tau^{\text{trade}}(w_\tau - w_{\tau-1}) \right) \\ \text{subject to} \quad & \mathbf{1}^T w_\tau = 1, \quad w_\tau - w_{\tau-1} \in \mathcal{Z}_\tau, \quad w_\tau \in \mathcal{W}_\tau, \\ & \tau = t+1, \dots, t+H, \end{aligned} \quad (21)$$

with variables w_{t+1}, \dots, w_{t+H} , the planned weights over the next H periods. This is the multi-period analog of (15).

Both MPO formulations (20) and (21) are convex optimization problems, provided the transaction cost, holding cost, risk functions, and trading and holding constraints are all convex.

Interpretation of MPO. The MPO problems (20) or (21) can be interpreted as follows. The variables constitute a *trading plan*, i.e., a set of trades to be executed over the next H periods. Solving (20) or (21) is forming a trading plan, based on forecasts of critical quantities over the planning horizon, and some simplifying assumptions. We do not intend to execute this sequence of trades, except for the first one z_t . It is reasonable to ask then why we optimize over the future trades $z_{t+1}, \dots, z_{t+H-1}$, since we do not intend to execute them. The answer is simple: we optimize over them as part of a *planning exercise*, just to be sure we don't carry out any trades now (i.e., z_t) that will put us in a bad position in the future. The idea of carrying out a planning exercise, but only executing the current action, occurs and is used in many fields, such as automatic control (where it is called model predictive control, MPC, or receding horizon control) (Kwon and Han 2005, Bemporad 2006, Mattingley et al. 2011), supply chain optimization (Cho et al. 2003), and others. Applications of MPC in finance include Herzog et al. (2007), Boyd et al. (2014), Bemporad et al. (2014), Busseti and Boyd (2015), Nystrup et al. (2018b).

About the dynamics simplification. Before proceeding let us discuss the simplification of the dynamics equation, where we replace the exact weight update

$$w_{t+1} = \frac{1}{1 + R_t^p} (\mathbf{1} + r_t) \circ (w_t + z_t)$$

with the simplified version $w_{t+1} = w_t + z_t$, by assuming that $r_t = 0$. At first glance it appears to be a gross simplification, but this assumption is only made for the purpose of propagating the portfolio forward in our planning process; we do take the returns into account in the first term of our objective. We are thus neglecting *second-order* terms, and we cannot be too far off if the per period returns are small compared to one.

In a similar way, adding the constraints $\mathbf{1}^T z_\tau = 0$ for $\tau = t + 1, \dots, t + H - 1$ suggests that we are ignoring the transaction and holding costs, since if z_τ were a realized trade we would have $\mathbf{1}^T z_\tau = -\phi_\tau^{\text{trade}}(z_\tau) - \phi_\tau^{\text{hold}}(w_\tau + z_\tau)$. As above, this assumption is only made for the purpose of propagating our portfolio forward in our planning exercise; we do take the costs into account in the objective.

Terminal constraints. In MPO, with a reasonably long horizon, we can add a terminal (equality) constraint, which requires the final planned weight to take some specific value, $w_{t+H} = w^{\text{term}}$. A reasonable choice for the terminal portfolio weight is (our estimate of) the benchmark weight w^b at period $t + H$.

For optimization of absolute or excess return, the terminal weight would be cash, i.e., $w^{\text{term}} = e_{n+1}$. This means that our planning exercise should finish with the portfolio all cash. This does not mean we intend to liquidate the portfolio in H periods; rather, it means we should carry out our planning as if this were the case. This will keep us from making the mistake of moving into what appears, in terms of our returns predictions, to be an attractive position that it is, however, expensive to unwind. For optimization relative to a benchmark, the natural terminal constraint is to be in the (predicted) benchmark.

Note that adding a terminal constraint reduces the number of variables. We solve the problem (20), but with w_{t+H} a given constant, not a variable. The initial weight w_t is also a given constant; the intermediate weights $w_{t+1}, \dots, w_{t+H-1}$ are variables.

5.3 Computation

The MPO problem (21) has Hn variables. In general the complexity of a convex optimization increases as the cube of the number of variables, but in this case the special structure of the problem can be exploited so that the computational effort grows linearly in H , the horizon. Thus, solving the MPO problem (21) should be a factor H slower than solving the SPO problem (15). For modest H (say, a few tens), this is not a problem. But for $H = 100$ (say) solving the MPO problem can be very challenging. Distributed methods based on ADMM (Boyd et al. 2011, 2014) can be used to solve the MPO problem using multiple processors.

In most cases we can solve the MPO problem in production. The issue is backtesting, since we must solve the problem many times, and with many variations of the parameters.

5.4 How MPO is used

All of the general ideas about how SPO is used apply to MPO as well; for example, we consider the parameters in the MPO problem as knobs that we adjust to achieve good performance under backtest and stress-test. In MPO, we

must provide forecasts of each quantity for each period over the next H periods. This can be done using sophisticated forecasts, with possibly different forecasts for each period, or in a very simple way, with predictions that are constant.

5.5 Multi-scale optimization

MPO trading requires estimates of all relevant quantities, like returns, transaction costs, and risks, over H trading periods into the future. In this section we describe a simplification of MPO that requires fewer predictions, as well as less computation to carry out the optimization required in each period. We still create a plan for trades and weights over the next H periods, but we assume that trades take place only a few times over the horizon; in other time periods the planned portfolio is maintained with no trading. This preserves the idea that we have recourse; but it greatly simplifies the problem (20). We describe the idea for three trades, taken in the short term, medium term, and long term, and an additional trade at the end to satisfy a terminal constraint $w_{t+H} = w^b$.

Specifically we add the constraint that in (20), trading (i.e., $z_\tau \neq 0$) only occurs at specific periods in the future, for

$$\tau = t, \quad \tau = t + T^{\text{med}}, \quad \tau = t + T^{\text{long}}, \quad \tau = t + H - 1,$$

where

$$1 < T^{\text{med}} < T^{\text{long}} < H - 1.$$

We interpret $z^{\text{short}} = z_t$ as our short term trade, $z^{\text{med}} = z_{t+T^{\text{med}}}$ as our medium term trade, and $z^{\text{long}} = z_{t+T^{\text{long}}}$ as our long term trade, in our trading plan. The final nonzero trade z_{t+H-1} is determined by the terminal constraint.

For example, we might take $T^{\text{med}} = 5$ and $T^{\text{long}} = 21$, with $H = 100$. If the periods represent days, we plan to trade now (short term), in a week (medium term) and in month (longer term); in 99 days, we trade to the benchmark. The only variables we have are the short, medium, and long term trades, and the associated weights, given by

$$w^{\text{short}} = w_t + z^{\text{short}}, \quad w^{\text{med}} = w^{\text{short}} + z^{\text{med}}, \quad w^{\text{long}} = w^{\text{med}} + z^{\text{long}}.$$

To determine the trades to make, we solve (20) with all other z_τ set to zero, and using the weights given above. This results in an optimization problem with the same form as (20), but with only three variables each for trading and weights, and three terms in the objective, plus an additional term that represents the transaction cost associated with the final trade to the benchmark at time $t + H - 1$.

6 Implementation

We have developed an open-source Python package **CVXPortfolio** (Busseti et al. 2017) that implements the portfolio simulation and optimization concepts dis-

cussed in the paper. The package relies on Pandas (McKinney 2012) for managing data. Pandas implements structured data types as in-memory databases (similar to R dataframes) and provides a rich API for accessing and manipulating them. Through Pandas, it is easy to couple our package with database backends. The package uses the convex optimization modeling framework CVXPY (Diamond and Boyd 2016) to construct and solve portfolio optimization problems.

The package provides an object-oriented framework with classes representing return, risk measures, transaction costs, holding constraints, trading constraints, etc. Single-period and multi-period optimization models are constructed from instances of these classes. Each instance generates CVXPY expressions and constraints for any given period t , making it easy to combine the instances into a single convex model. In section 7 we give some simple numerical examples that use `CVXPortfolio`.

6.1 Components

We briefly review the major classes in the software package. Implementing additional classes, such as novel policies or risk measures, is straightforward.

Return estimates. Instances of the `ReturnsForecast` class generate a return estimate \hat{r}_t for period t using only information available at that period. The simplest `ReturnsForecast` instance wraps a Pandas dataframe with return estimates for each period:

```
r_hat = ReturnsForecast(return_estimates_dataframe)
```

Multiple `ReturnsForecast` instances can be blended into a linear combination.

Risk measures. Instances of a risk measure class, contained in the `risks` submodule, generate a convex cost representing a risk measure at a given period t . For example, the `FullSigma` class generates the cost $(w_t + z_t)^T \Sigma_t (w_t + z_t)$ where $\Sigma_t \in \mathbb{R}^{(n+1) \times (n+1)}$ is an explicit matrix, whereas the `FactorModel` class generates the cost with a factor model of Σ_t . Any risk measure can be switched to absolute or active risk and weighted with a risk-aversion parameter. The package provides all the risk measures discussed in section 4.2.

Costs. Instances of the `TcostModel` and `HcostModel` classes generate transaction- and holding-cost estimates, respectively. The same classes work both for modeling costs in a portfolio optimization problem and calculating realized costs in a trading simulation. Cost objects can also be used to express other objective terms like soft constraints.

Constraints. The package provides classes representing each of the constraints discussed in section 4.4 and section 4.5. For example, instances of the class `LeverageLimit` generate a leverage limit constraint that can vary by period. Constraint objects can be converted into soft constraints, which are cost objects.

Policies. Instances of a policy class take holdings w_t and value v_t and output trades z_t using information available in period t . Single-period optimization policies are constructed using the `SinglePeriodOpt` class. The constructor takes a `ReturnsForecast`, a list of costs, including risk models (multiplied by their coefficients), and constraints. For example, the following code snippet constructs a SPO policy:

```
spo_policy = SinglePeriodOpt(r_hat,
                             [gamma_risk*factor_risk,
                              gamma_trade*tcost_model,
                              gamma_hold*hcost_model],
                             [leverage_limit])
```

Multi-period optimization policies are constructed similarly. The package also provides classes for simple policies such as periodic rebalancing.

Simulator. The `MarketSimulator` class is used to run trading simulations, or backtests. Instances are constructed with historical returns and other market data, as well as transaction- and holding-cost models. Given a `MarketSimulator` instance `market_sim`, a backtest is run by calling the `run_backtest` method with an initial portfolio, policy, and start and end periods:

```
backtest_results = market_sim.run_backtest(init_portfolio,
                                           policy,
                                           start_t, end_t)
```

Multiple backtests can be run in parallel with different conditions. The backtest results include all the metrics discussed in section 3.

7 Examples

In this section we present simple numerical examples illustrating the ideas developed above, all carried out using `CVXPortfolio` and open-source market data (and some approximations where no open source data is available). The code for these is available at <http://github.com/cvxgrp/cvxportfolio/tree/master/examples>. Given our approximations, and other short-comings of our simulations that we will mention below, the particular numerical results

we show should not be taken too seriously. But the simulations are good enough for us to illustrate real phenomena, such as the critical role transaction costs can play, or how important hyperparameter search can be.

7.1 Data for simulation

We work with a period of five years, from January 2012 through December 2016, on the components of the S&P 500 index as of December 2016. We select the ones continuously traded in the period. (By doing this we introduce survivorship bias (Elton et al. 1996).) We collect open-source market data from Quandl (2016). The data consists of realized daily market returns r_t (computed using closing prices) and volumes V_t . We use the federal reserve overnight rate for the cash return. Following Almgren (2009) we approximate the daily volatility with a simple estimator, $(\sigma_t)_i = |\log(p_t^{\text{open}})_i - \log(p_t^{\text{close}})_i|$, where $(p_t^{\text{open}})_i$ and $(p_t^{\text{close}})_i$ are the open and close prices for asset i in period t . We could not find open-source data for the bid-ask spread, so we used the value $a_t = 0.05\%$ (five basis points) for all assets and periods. As holding costs we use $s_t = 0.01\%$ (one basis point) for all assets and periods. We chose standard values for the other parameters of the transaction- and holding-cost models: $b_t = 1$, $c_t = 0$, $d_t = 0$ for all assets and periods.

7.2 Portfolio simulation

To illustrate backtest portfolio simulation, we consider a portfolio that is meant to track the *uniform portfolio* benchmark, which has weight $w^b = (1/n, 0)$, i.e., equal fraction of value in all non-cash assets. This is not a particularly interesting or good benchmark portfolio; we use it only as a simple example to illustrate the effects of transaction costs. The portfolio starts with $w_1 = w^b$, and due to asset returns drifts from this weight vector. We periodically rebalance, which means using trade vector $z_t = w^b - w_t$. For other values of t (i.e., the periods in which we do not rebalance) we have $z_t = 0$.

We carry out six backtest simulations for each of two initial portfolio values, \$100M and \$10B. The six simulations vary in rebalancing frequency: daily, weekly, monthly, quarterly, annually, or never (also called ‘hold’ or ‘buy-and-hold’). For each simulation we give the portfolio active return \bar{R}^a and active risk σ^a (defined in section 3.2), the annualized average transaction cost $\frac{250}{T} \sum_{t=1}^T \phi_t^{\text{trade}}(z_t)$, and the annualized average turnover $\frac{250}{T} \sum_{t=1}^T \|(z_t)_{1:n}\|_1/2$.

Table 1 shows the results. (The active return is also included for completeness.) We observe that transaction cost depends on the total value of the portfolio, as expected, and that the choice of rebalancing frequency trades off transaction cost and active risk. (The active risk is not exactly zero when rebalancing daily because of the variability of the transaction cost, which is included in the

Initial value	Rebalancing frequency	Active return	Active risk	Trans. cost	Turnover
\$100M	Daily	-0.07%	0.00%	0.07%	220.53%
	Weekly	-0.07%	0.09%	0.04%	105.67%
	Monthly	-0.12%	0.21%	0.02%	52.71%
	Quarterly	-0.11%	0.35%	0.01%	29.98%
	Annually	-0.10%	0.63%	0.01%	12.54%
	Hold	-0.36%	1.53%	0.00%	0.00%
\$10B	Daily	-0.25%	0.01%	0.25%	220.53%
	Weekly	-0.19%	0.09%	0.16%	105.67%
	Monthly	-0.20%	0.21%	0.10%	52.71%
	Quarterly	-0.17%	0.35%	0.07%	29.99%
	Annually	-0.13%	0.63%	0.04%	12.54%
	Hold	-0.36%	1.53%	0.00%	0.00%

Table 1: Portfolio simulation results with different initial value and different rebalancing frequencies. All values are annualized.

portfolio return.) Figure 2 shows, separately for the two portfolio sizes, the active risk versus the transaction cost.

7.3 Single-period optimization

In this section we show a simple example of the single-period optimization model developed in section 4. The portfolio starts with total value $v_1 = \$100M$ and allocation equal to the uniform portfolio $w_1 = (1/n, 0)$. We impose a leverage constraint of $L^{\max} = 3$. This simulation uses the market data defined in section 7.1. The forecasts and risk model used in the SPO are described below.

Risk model. Proprietary risk models, e.g., from MSCI (formerly Barra), are widely used. Here we use a simple factor risk model estimated from past realized returns, using a similar procedure to Almgren (2009). We estimate it on the first day of each month, and use it for the rest of the month. Let t be an estimation time period, and $t - M^{\text{risk}}$ the time period two years before. Consider the second moment of the window of realized returns $\Sigma^{\text{exp}} = \frac{1}{M^{\text{risk}}} \sum_{\tau=t-M^{\text{risk}}}^{t-1} r_\tau r_\tau^T$, and its eigenvalue decomposition $\Sigma^{\text{exp}} = \sum_{i=1}^n \lambda_i q_i q_i^T$, where the eigenvalues λ_i are in descending order. Our factor risk model is

$$F = [q_1 \cdots q_k], \quad \Sigma^f = \text{diag}(\lambda_1, \dots, \lambda_k), \quad D = \sum_{i=k+1}^n \lambda_i \text{diag}(q_i) \text{diag}(q_i),$$

with $k = 15$. (The diagonal matrix D is chosen so the factor model $F\Sigma^f F^T + D$ and the empirical second moment Σ^{exp} have the same diagonal elements.)

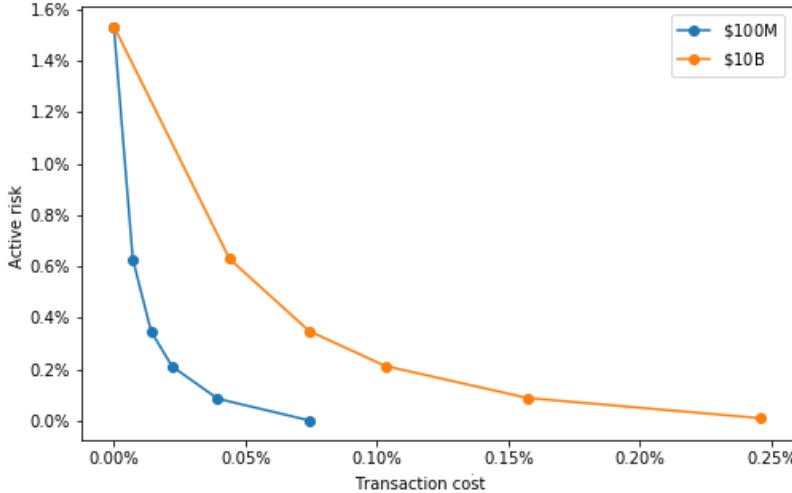


Figure 2: Active risk versus transaction cost, for the two initial portfolio sizes. The points on the lines correspond to rebalancing frequencies.

Return forecasts. The risk-free interest rates are known exactly, $(\hat{r}_t)_{n+1} = (r_t)_{n+1}$ for all t . Return forecasts for the non-cash assets are always proprietary. They are generated using many methods, ranging from analyst predictions to sophisticated machine learning techniques, based on a variety of data feeds and sources. For these examples we generate simulated return forecasts by adding zero-mean noise to the realized returns and then rescaling, to obtain return estimates that would (approximately) minimize mean squared error. Of course this is not a real return forecast, since it uses the actual realized return; but our purpose here is only to illustrate the ideas and methods.

For all t the return estimates for non-cash assets are

$$(\hat{r}_t)_{1:n} = \alpha((r_t)_{1:n} + \epsilon_t), \quad (22)$$

where $\epsilon_t \sim \mathcal{N}(0, \sigma_\epsilon^2 I)$ are independent. We use noise variance $\sigma_\epsilon^2 = 0.02$, so the noise components have standard deviation around 14%, around a factor of ten larger than the standard deviation of the realized returns. The scale factor α is chosen to minimize the mean squared error $\mathbf{E}[((\hat{r}_t)_{1:n} - (r_t)_{1:n})^2]$, if we think of r_t as a random variable with variance σ_r , i.e., $\alpha = \sigma_r^2 / (\sigma_r^2 + \sigma_\epsilon^2)$. We use the typical value $\sigma_r^2 = 0.0005$, i.e., a realized return standard deviation of around 2%, so $\alpha = 0.024$. Our typical return forecast is on the order of $\pm 0.3\%$. This corresponds to an information ratio $\sqrt{\alpha} \approx 0.15$, which is on the high end of what might be expected in practice (Grinold and Kahn 2000).

With this level of noise and scaling, our return forecasts have an accuracy on the order of what we might expect from a proprietary forecast. For example, across all the assets and all days, the sign of predicted return agrees with the sign of the real return around 54% of the times.

Volume and volatility forecasts. We use simple estimates of total market volumes and daily volatilities (used in the transaction-cost model), as moving averages of the realized values with a window of length ten. For example, the volume forecast at time period t and asset i is $(\hat{V}_t)_i = \frac{1}{10} \sum_{\tau=1}^{10} (V_{t-\tau})_i$.

SPO backtests. We carry out multiple backtest simulations over the whole period, varying the risk-aversion parameter γ^{risk} , the trading-aversion parameter γ^{trade} , and the holding-cost multiplier γ^{hold} (all defined and discussed in section 4.8). We first perform a coarse grid search in the hyperparameter space, testing all combinations of

$$\begin{aligned}\gamma^{\text{risk}} &= 0.1, 0.3, 1, 3, 10, 30, 100, 300, 1000, \\ \gamma^{\text{trade}} &= 1, 2, 5, 10, 20, \\ \gamma^{\text{hold}} &= 1,\end{aligned}$$

a total of 45 backtest simulations. (Logarithmic spacing is common in hyperparameter searches.)

Figure 3 shows mean excess portfolio return \bar{R}^e versus excess volatility σ^e (defined in section 3.2), for these combinations of parameters. For each value of γ^{trade} , we connect with a line the points corresponding to the different values of γ^{risk} , obtaining a risk–return tradeoff curve for that choice of γ^{trade} and γ^{hold} . These show the expected tradeoff between mean return and risk. We see that the choice of trading-aversion parameter is critical: for some values of γ^{trade} the results are so poor that the resulting curve does not even fit in the plotting area. Values of γ^{trade} around five seem to give the best results.

We then perform a fine hyperparameter search, focusing on trade-aversion parameters values around five,

$$\gamma^{\text{trade}} = 4, 5, 6, 7, 8,$$

and the same values of γ^{risk} and γ^{hold} . Figure 4 shows the resulting curves of excess return versus excess risk. A value around $\gamma^{\text{trade}} = 6$ seems to be best.

For our last set of simulations we use a finer range of risk-aversion parameters, focus on an even narrower range of the trading-aversion parameter, and also

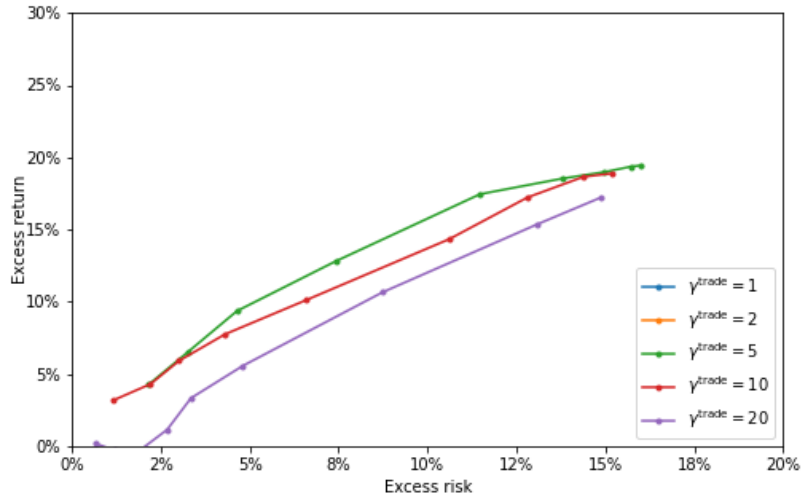


Figure 3: SPO example, coarse hyperparameter grid search. (Some curves do not fit in the plot.)

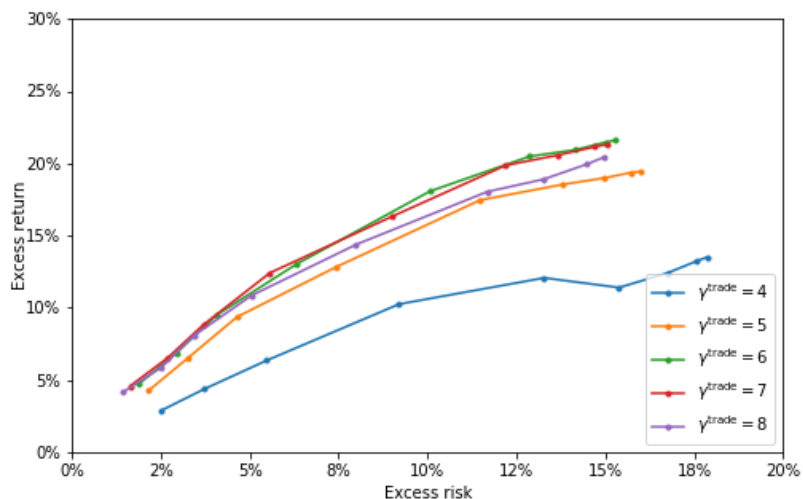


Figure 4: SPO example, fine hyperparameter grid search.

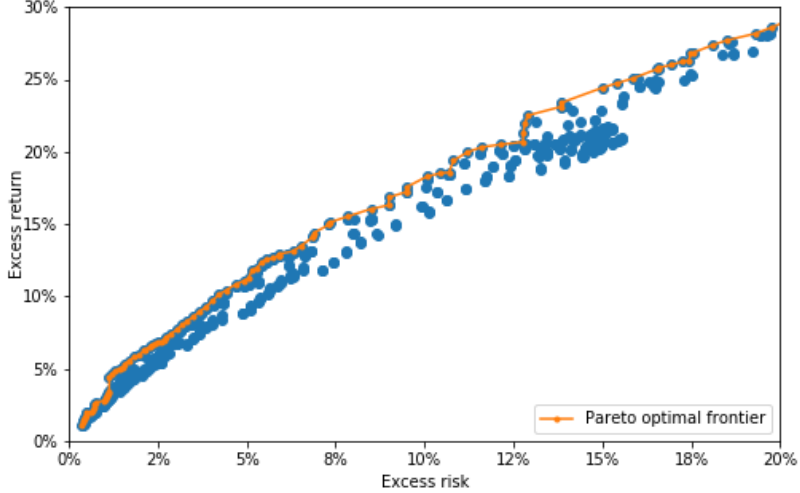


Figure 5: SPO example, grid search over 510 hyperparameter combinations. The line connects the Pareto optimal points.

vary the hold-aversion parameter. We test all combinations of

$$\begin{aligned}\gamma^{\text{risk}} &= 0.1, 0.178, 0.316, 0.562, 1, 2, 3, 6, 10, 18, 32, 56, \\ &\quad 100, 178, 316, 562, 1000, \\ \gamma^{\text{trade}} &= 5.5, 6, 6.5, 7, 7.5, 8, \\ \gamma^{\text{hold}} &= 0.1, 1, 10, 100, 1000,\end{aligned}$$

a total of 510 backtest simulations. The results are plotted in figure 5 as points in the risk–return plane. The Pareto optimal points, i.e., those with the lowest risk for a given level of return, are connected by a line. Table 6 lists a selection of the Pareto optimal points, giving the associated hyperparameter values.

From this curve and table we can make some interesting observations. The first is that we do substantially better with large values of the holding-cost multiplier parameter compared to $\gamma^{\text{hold}} = 1$, even though the actual holding cost (used by the simulator to update the portfolio each day) is very small, one basis point. This is a good example of regularization in SPO; our large holding-cost multiplier parameter tells the SPO algorithm to avoid short positions, and the result is that the overall portfolio performance is better.

It is hardly surprising that the risk-aversion parameter varies over this selection of Pareto optimal points; after all, this is the parameter most directly related

γ^{risk}	γ^{trade}	γ^{hold}	Excess return	Excess risk
1000.00	8.0	100	1.33%	0.39%
562.00	6.0	100	2.49%	0.74%
316.00	7.0	100	2.98%	1.02%
1000.00	7.5	10	4.64%	1.22%
562.00	8.0	10	5.31%	1.56%
316.00	7.5	10	6.53%	2.27%
316.00	6.5	10	6.88%	2.61%
178.00	6.5	10	8.04%	3.20%
100.00	8.0	10	8.26%	3.32%
32.00	7.0	10	12.35%	5.43%
18.00	6.5	0.1	14.96%	7.32%
6.00	7.5	10	18.51%	10.44%
2.00	6.5	10	23.40%	13.87%
0.32	6.5	10	26.79%	17.50%
0.18	7.0	10	28.16%	19.30%

Table 6: SPO example, selection of Pareto optimal points (ordered by increasing risk and return).

to the risk–return tradeoff. One surprise is that the value of the hold-aversion hyperparameter varies considerably as well.

In practice, we would backtest many more combinations of these three hyperparameters. Indeed we would also carry out backtests varying combinations of other parameters in the SPO algorithm, for example the leverage, or the individual terms in transaction-cost functions. In addition, we would carry out stress-tests and other what-if simulations, to get an idea of how our SPO algorithm might perform in other, or more stressful, market conditions. (This would be especially appropriate given our choice of backtest date range, which was entirely a bull market.) Since these backtests can be carried out in parallel, there is no reason to not carry out a large number of them.

7.4 Multi-period optimization

In this section we show the simplest possible example of the multi-period optimization model developed in section 5, using planning horizon $H = 2$. This means that in each time period the MPO algorithm plans both current day and next day trades, and then executes only the current day trades. As a practical matter, we would not expect a great performance improvement over SPO using a planning horizon of $H = 2$ days compared to SPO, which uses $H = 1$ day. Our point here is to demonstrate that it is different.

The simulations are carried out using the market data described in section 7.1.

The portfolio starts with total value $v_1 = \$100M$ and uniform allocation $w_1 = (\mathbf{1}/n, 0)$. We impose a leverage constraint of $L^{\max} = 3$. The risk model is the same one used in the SPO example. The volume and volatility estimates (for both the current and next period) are also the same as those used in the SPO example.

Return forecasts. We use the same return forecast we generated for the previous example, but at every time period we provide both the forecast for the current time period and the one for the next:

$$\hat{r}_{t|t} = \hat{r}_t, \quad \hat{r}_{t+1|t} = \hat{r}_{t+1},$$

where \hat{r}_t and \hat{r}_{t+1} are the same ones used in the SPO example, given in (22). The MPO trading algorithm thus sees each return forecast twice, $\hat{r}_{t+1} = \hat{r}_{t+1|t} = \hat{r}_{t+1|t+1}$, i.e., today's forecast of tomorrow's return is the same as tomorrow's forecast of tomorrow's return.

As in the SPO case, this is clearly not a practical forecast, since it uses the realized return. In addition, in a real setting the return forecast would be updated at every time period, so that $\hat{r}_{t+1|t} \neq \hat{r}_{t+1|t+1}$. Our goal in choosing these simulated return forecasts is to have ones that are similar to the ones used in the SPO example, in order to compare the results of the two optimization procedures.

Backtests. We carry out multiple backtest simulations varying the parameters γ^{risk} , γ^{trade} , and γ^{hold} . We first perform a coarse grid search in the hyperparameter space, with the same parameters as in the SPO example. We test all combinations of

$$\begin{aligned}\gamma^{\text{risk}} &= 0.1, 0.3, 1, 3, 10, 30, 100, 300, 1000, \\ \gamma^{\text{trade}} &= 1, 2, 5, 10, 20, \\ \gamma^{\text{hold}} &= 1,\end{aligned}$$

a total of 45 backtest simulations.

The results are shown in figure 7, where we plot mean excess portfolio return \bar{R}^e versus excess risk σ^e . For some trading-aversion parameter values the results were so bad that they did not fit in the plotting area.

We then perform a more accurate hyperparameter search using a finer range for γ^{risk} , focusing on the values around $\gamma^{\text{trade}} = 10$, and also varying the hold-aversion parameter. We test all combinations of

$$\begin{aligned}\gamma^{\text{risk}} &= 1, 2, 3, 6, 10, 18, 32, 56, 100, 178, 316, 562, 1000, \\ \gamma^{\text{trade}} &= 7, 8, 9, 10, 11, 12, \\ \gamma^{\text{hold}} &= 0.1, 1, 10, 100, 1000,\end{aligned}$$

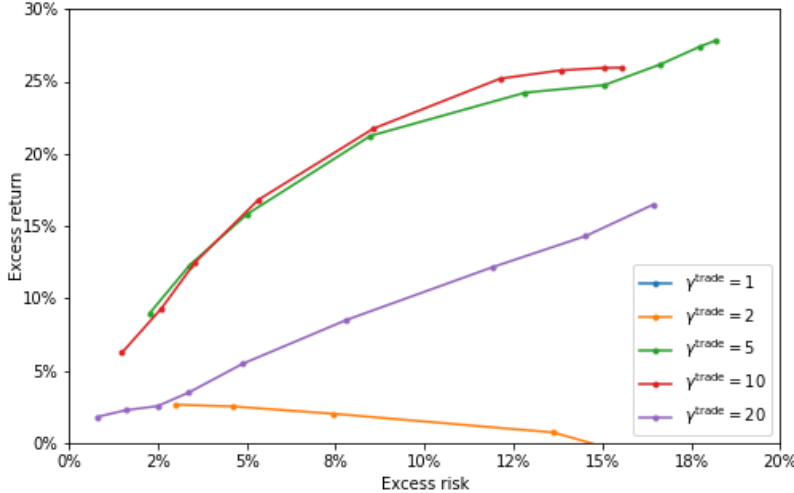


Figure 7: MPO example, coarse hyperparameter grid search.

for a total of 390 backtest simulations. The results are plotted in figure 8 as points in the risk–return plane. The Pareto optimal points are connected by a line.

Finally we compare the results obtained with the SPO and MPO examples. Figure 9 shows the Pareto optimal frontiers for both cases. We see that the MPO method has a substantial advantage over the SPO method, mostly explained by the advantage of a forecast for tomorrow’s, as well as today’s, return.

7.5 Simulation time

Here we give some rough idea of the computation time required to carry out the simulation examples shown above, focusing on the SPO case. The backtest simulation is single-threaded, so multiple backtests can be carried out on separate threads.

Figure 10 gives the breakdown of execution time for a backtest, showing the time taken for each step of simulation, broken down into the simulator, the numerical solver, and the rest of the policy (data management and CVXPY manipulations). We can see that simulating one day takes around 0.25 seconds, so a back test over five years takes around five minutes. The bulk of this (around 0.15 seconds) is the optimization carried out each day. The simulator time is, as expected, negligible.

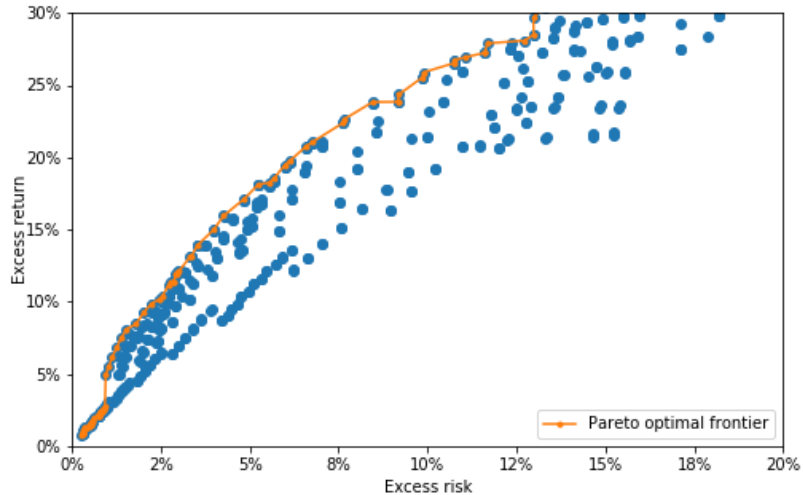


Figure 8: MPO example, grid search over 390 hyperparameter combinations. The line connects the Pareto optimal points.

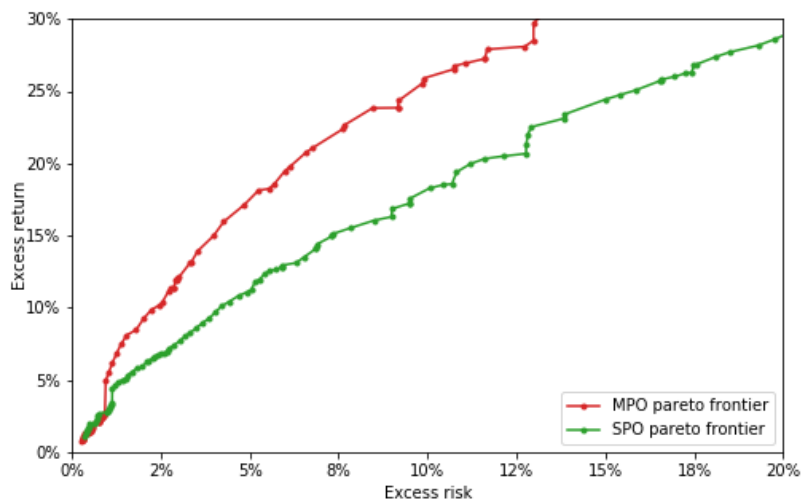


Figure 9: Pareto optimal frontiers for SPO and MPO.

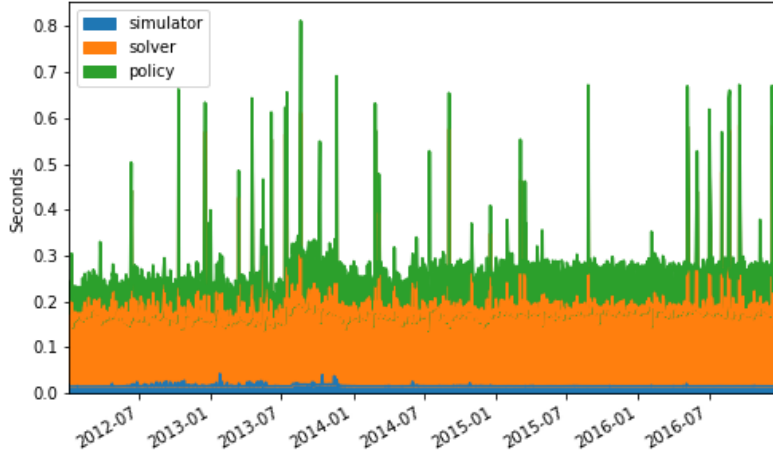


Figure 10: Execution time for each day for one SPO backtest.

We carried out the multiple backtests using a 32 core machine that can execute 64 threads simultaneously. Carrying out 510 backtests, which entails solving around a half million convex optimization problems, thus takes around thirty minutes. (In fact, it takes a bit longer, due to system overhead.)

We close by making a few comments about these optimization times. First, they can be considerably reduced by avoiding the $3/2$ -power transaction-cost terms, which slow the optimizer. By replacing these terms with square transaction-cost terms, we can obtain a speedup of more than a factor of two. Replacing the default generic solver ECOS (Domahidi et al. 2013) used in CVXPY with a custom solver, such as one based on operator-splitting methods (Boyd et al. 2011), would result in an even more substantial speedup.

References

- Almgren, R. “High frequency volatility.” Available at <http://cims.nyu.edu/~almgren/timeseries/notes7.pdf> (2009).
- Almgren, R. and N. Chriss. “Optimal execution of portfolio transactions.” *Journal of Risk*, vol. 3, no. 2 (2001), pp. 5–39.
- Bacon, C. R. *Practical Portfolio Performance Measurement and Attribution*. Wiley: West Sussex, 2nd ed. (2008).

- Bailey, D. H., J. M. Borwein, M. L. de Prado, and Q. J. Zhu. “The probability of backtest overfitting.” *Journal of Computational Finance*, vol. 20, no. 4 (2017), pp. 39–69.
- Bellman, R. E. “Dynamic programming and Lagrange multipliers.” *Proceedings of the National Academy of Sciences*, vol. 42, no. 10 (1956), pp. 767–769.
- Bemporad, A. “Model predictive control design: New trends and tools.” In *Proceedings of the 45th IEEE Conference on Decision and Control* (2006), pp. 6678–6683.
- Bemporad, A., L. Bellucci, and T. Gabbriellini. “Dynamic option hedging via stochastic model predictive control based on scenario simulation.” *Quantitative Finance*, vol. 14, no. 10 (2014), pp. 1739–1751.
- Bershova, N. and D. Raklin. “The non-linear market impact of large trades: evidence from buy-side order flow.” *Quantitative Finance*, vol. 13, no. 11 (2013), pp. 1759–1778.
- Bertsekas, D. P. *Dynamic Programming and Optimal Control*. Athena Scientific: Belmont (1995).
- Black, F. “Studies of stock price volatility changes.” In *Proceedings of the 1976 Meetings of the American Statistical Association, Business and Economics Statistics Section* (1976), pp. 177–181.
- Boyd, S., M. T. Mueller, B. O’Donoghue, and Y. Wang. “Performance bounds and suboptimal policies for multi-period investment.” *Foundations and Trends in Optimization*, vol. 1, no. 1 (2014), pp. 1–72.
- Boyd, S., N. Parikh, E. Chu, B. Peleato, and J. Eckstein. “Distributed optimization and statistical learning via the alternating direction method of multipliers.” *Foundations and Trends in Machine Learning*, vol. 3, no. 1 (2011), pp. 1–122.
- Boyd, S. and L. Vandenberghe. *Convex Optimization*. Cambridge University Press: New York (2004).
- Busseti, E. and S. Boyd. “Volume weighted average price optimal execution.” (2015).
- Busseti, E., S. Diamond, S. Boyd, and BlackRock. “CVXPortfolio.” (2017). Available at <https://github.com/cvxgrp/cvxportfolio>.
- Busseti, E., E. K. Ryu, and S. Boyd. “Risk-constrained Kelly gambling.” *Journal of Investing*, vol. 25, no. 3 (2016), pp. 118–134.
- Campbell, J. Y., A. W. Lo, and A. C. MacKinlay. *The Econometrics of Financial Markets*. Princeton University Press: Princeton (1997).

- Campbell, J. Y. and L. M. Viceira. *Strategic Asset Allocation: Portfolio Choice for Long-Term Investors*. Oxford University Press: New York (2002).
- Chan, L. K. C., J. Karceski, and J. Lakonishok. “On portfolio optimization: Forecasting covariances and choosing the risk model.” *Review of Financial Studies*, vol. 12, no. 5 (1999), pp. 937–974.
- Cho, E. G., K. A. Thoney, T. J. Hodgson, and R. E. King. “Rolling horizon scheduling of multi-factory supply chains.” In *Proceedings of the 2003 Winter Simulation Conference* (2003), pp. 1409–1416.
- Chopra, V. K. and W. T. Ziemba. “The effect of errors in means, variances, and covariances on optimal portfolio choice.” *Journal of Portfolio Management*, vol. 19, no. 2 (1993), pp. 6–11.
- Constantinides, G. M. “Multiperiod consumption and investment behavior with convex transactions costs.” *Management Science*, vol. 25, no. 11 (1979), pp. 1127–1137.
- Cornuejols, G. and R. Tütüncü. *Optimization Methods in Finance*. Cambridge University Press: New York (2006).
- Davis, M. H. A. and A. R. Norman. “Portfolio selection with transaction costs.” *Mathematics of Operations Research*, vol. 15, no. 4 (1990), pp. 676–713.
- DeMiguel, V., L. Garlappi, F. Nogales, and R. Uppal. “A generalized approach to portfolio optimization: Improving performance by constraining portfolio norms.” *Management Science*, vol. 55, no. 5 (2009a), pp. 798–812.
- DeMiguel, V., L. Garlappi, and R. Uppal. “Optimal versus naive diversification: How inefficient is the $1/N$ portfolio strategy?” *Review of Financial Studies*, vol. 22, no. 5 (2009b), pp. 1915–1953.
- Diamond, S. and S. Boyd. “CVXPY: A Python-embedded modeling language for convex optimization.” *Journal of Machine Learning Research*, vol. 17, no. 83 (2016), pp. 1–5.
- Diamond, S., R. Takapoui, and S. Boyd. “A general system for heuristic minimization of convex functions over non-convex sets.” *Optimization Methods and Software*, vol. 33, no. 1 (2018), pp. 165–193.
- Domahidi, A., E. Chu, and S. Boyd. “ECOS: An SOCP solver for embedded systems.” In *Proceedings of the 12th European Control Conference* (2013), pp. 3071–3076.
- Dumas, B. and E. Luciano. “An exact solution to a dynamic portfolio choice problem under transactions costs.” *Journal of Finance*, vol. 46, no. 2 (1991), pp. 577–595.

- Elton, E. J., M. J. Gruber, and C. R. Blake. "Survivor bias and mutual fund performance." *Review of Financial Studies*, vol. 9, no. 4 (1996), pp. 1097–1120.
- Fabozzi, F. J., D. Huang, and G. Zhou. "Robust portfolios: contributions from operations research and finance." *Annals of Operations Research*, vol. 176, no. 1 (2010), pp. 191–220.
- Fastrich, B., S. Paterlini, and P. Winker. "Constructing optimal sparse portfolios using regularization methods." *Computational Management Science*, vol. 12, no. 3 (2015), pp. 417–434.
- Fougner, C. and S. Boyd. "Parameter selection and pre-conditioning for a graph form solver." In *Emerging Applications of Control and System Theory*, edited by R. Tempo, S. Yurkovich, and P. Misra, chap. 4. Springer: Cham (2018), pp. 41–61.
- Frittelli, M. and E. R. Gianin. "Putting order in risk measures." *Journal of Banking & Finance*, vol. 26, no. 7 (2002), pp. 1473–1486.
- Gărleanu, N. and L. H. Pedersen. "Dynamic trading with predictable returns and transaction costs." *Journal of Finance*, vol. 68, no. 6 (2013), pp. 2309–2340.
- Goldsmith, D. "Transactions costs and the theory of portfolio selection." *Journal of Finance*, vol. 31, no. 4 (1976), pp. 1127–1139.
- Gomes, C. and H. Waelbroeck. "Is market impact a measure of the information value of trades? Market response to liquidity vs. informed metaorders." *Quantitative Finance*, vol. 15, no. 5 (2015), pp. 773–793.
- Grant, M., S. Boyd, and Y. Ye. "Disciplined convex programming." In *Global Optimization: From Theory to Implementation*, edited by L. Liberti and N. Maculan, vol. 84 of *Nonconvex Optimization and Its Applications*. Springer: New York (2006), pp. 155–210.
- Grinold, R. C. "A dynamic model of portfolio management." *Journal of Investment Management*, vol. 4, no. 2 (2006), pp. 5–22.
- Grinold, R. C. and R. N. Kahn. *Active Portfolio Management: A Quantitative Approach for Providing Superior Returns and Controlling Risk*. McGraw–Hill: New York, 2nd ed. (2000).
- Hastie, T., R. Tibshirani, and J. Friedman. *The Elements of Statistical Learning*. Springer: New York, 2nd ed. (2009).
- Herzog, F., G. Dondi, and H. P. Geering. "Stochastic model predictive control and portfolio optimization." *International Journal of Theoretical and Applied Finance*, vol. 10, no. 2 (2007), pp. 203–233.

- Ho, M., Z. Sun, and J. Xin. “Weighted elastic net penalized mean–variance portfolio design and computation.” *SIAM Journal on Financial Mathematics*, vol. 6, no. 1 (2015), pp. 1220–1244.
- Jagannathan, R. and T. Ma. “Risk reduction in large portfolios: Why imposing the wrong constraints helps.” *Journal of Finance*, vol. 58, no. 4 (2003), pp. 1651–1683.
- Jorion, P. “International portfolio diversification with estimation risk.” *Journal of Business*, vol. 58, no. 3 (1985), pp. 259–278.
- Kan, R. and G. Zhou. “Optimal portfolio choice with parameter uncertainty.” *Journal of Financial and Quantitative Analysis*, vol. 42, no. 3 (2007), pp. 621–656.
- Kelly, J. L., Jr. “A new interpretation of information rate.” *IRE Transactions on Information Theory*, vol. 2, no. 3 (1956), pp. 185–189.
- Kolm, P., R. Tütüncü, and F. Fabozzi. “60 years of portfolio optimization: Practical challenges and current trends.” *European Journal of Operational Research*, vol. 234, no. 2 (2014), pp. 356–371.
- Kwon, W. H. and S. H. Han. *Receding Horizon Control: Model Predictive Control for State Models*. Springer: London (2005).
- Li, J. “Sparse and stable portfolio selection with parameter uncertainty.” *Journal of Business & Economic Statistics*, vol. 33, no. 3 (2015b), pp. 381–392.
- Lillo, F., J. D. Farmer, and R. N. Mantegna. “Master curve for price-impact function.” *Nature*, vol. 421, no. 6919 (2003), p. 129.
- Lobo, M. S., M. Fazel, and S. Boyd. “Portfolio optimization with linear and fixed transaction costs.” *Annals of Operations Research*, vol. 152, no. 1 (2007), pp. 341–365.
- Markowitz, H. “Portfolio selection.” *Journal of Finance*, vol. 7, no. 1 (1952), pp. 77–91.
- Mattingley, J. and S. Boyd. “CVXGEN: A code generator for embedded convex optimization.” *Optimization and Engineering*, vol. 13, no. 1 (2012), pp. 1–27.
- Mattingley, J., Y. Wang, and S. Boyd. “Receding horizon control: Automatic generation of high-speed solvers.” *IEEE Control Systems Magazine*, vol. 31, no. 3 (2011), pp. 52–65.
- McKinney, W. *Python for Data Analysis: Data Wrangling with Pandas, NumPy, and IPython*. O’Reilly Media: Sebastopol (2012).

- Merton, R. C. "Lifetime portfolio selection under uncertainty: The continuous-time case." *Review of Economics and Statistics*, vol. 51, no. 3 (1969), pp. 247–257.
- Merton, R. C. "Optimum consumption and portfolio rules in a continuous-time model." *Journal of Economic Theory*, vol. 3, no. 4 (1971), pp. 373–413.
- Meucci, A. *Risk and Asset Allocation*. Springer: Berlin (2005).
- Meucci, A. "Historical scenarios with fully flexible probabilities." *GARP Risk Professional* (2010), pp. 47–51.
- Michaud, R. O. "The Markowitz optimization Enigma: Is 'optimized' optimal?" *Financial Analysts Journal*, vol. 45, no. 1 (1989), pp. 31–42.
- Moallemi, C. C. and M. Sağlam. "Dynamic portfolio choice with linear rebalancing rules." *Journal of Financial and Quantitative Analysis*, vol. 52, no. 3 (2017), pp. 1247–1278.
- Moro, E., J. Vicente, L. G. Moyano, A. Gerig, J. D. Farmer, G. Vaglica, F. Lillo, and R. N. Mantegna. "Market impact and trading profile of hidden orders in stock markets." *Physical Review E*, vol. 80, no. 6 (2009), p. 066102.
- Narang, R. K. *Inside the Black Box: A Simple Guide to Quantitative and High Frequency Trading*. Wiley: Hoboken, 2nd ed. (2013).
- Nesterov, Y. and A. Nemirovskii. *Interior-point Polynomial Algorithms in Convex Programming*. SIAM: Philadelphia (1994).
- Nystrup, P., H. Madsen, and E. Lindström. "Dynamic portfolio optimization across hidden market regimes." *Quantitative Finance*, vol. 18, no. 1 (2018b), pp. 83–95.
- Obizhaeva, A. A. and J. Wang. "Optimal trading strategy and supply/demand dynamics." *Journal of Financial Markets*, vol. 16, no. 1 (2013), pp. 1–32.
- O'Donoghue, B., E. Chu, N. Parikh, and S. Boyd. "Conic optimization via operator splitting and homogeneous self-dual embedding." *Journal of Optimization Theory and Applications*, vol. 169, no. 3 (2016), pp. 1042–1068.
- Perold, A. F. "Large-scale portfolio optimization." *Management Science*, vol. 30, no. 10 (1984), pp. 1143–1160.
- Perold, A. F. "The implementation shortfall: Paper versus reality." *Journal of Portfolio Management*, vol. 14, no. 3 (1988), pp. 4–9.
- Powell, W. B. *Approximate Dynamic Programming: Solving the Curses of Dimensionality*. Wiley: Hoboken (2007).

- Quandl. “WIKI end-of-day data.” (2016). Available at <https://www.quandl.com/data/WIKI>.
- Samuelson, P. A. “Lifetime portfolio selection by dynamic stochastic programming.” *Review of Economics and Statistics*, vol. 51, no. 3 (1969), pp. 239–246.
- Sharpe, W. F. “Mutual fund performance.” *Journal of Business*, vol. 39, no. 1 (1966), pp. 119–138.
- Sharpe, W. F. “The arithmetic of active management.” *Financial Analysts Journal*, vol. 47, no. 1 (1991), pp. 7–9.
- Sharpe, W. F. “The Sharpe ratio.” *Journal of Portfolio Management*, vol. 21, no. 1 (1994), pp. 49–58.
- Tibshirani, R. “Regression shrinkage and selection via the lasso.” *Journal of the Royal Statistical Society. Series B (Methodological)*, vol. 58, no. 1 (1996), pp. 267–288.
- Udell, M., K. Mohan, D. Zeng, J. Hong, S. Diamond, and S. Boyd. “Convex optimization in Julia.” In *First Workshop for High Performance Technical Computing in Dynamic Languages* (2014), pp. 18–28.

PAPER

To appear in *Annals of Operations Research*

Multi-period portfolio selection with drawdown control

Peter Nystrup, Stephen Boyd, Erik Lindström, and Henrik Madsen

Abstract

In this article, model predictive control is used to dynamically optimize an investment portfolio and control drawdowns. The control is based on multi-period forecasts of the mean and covariance of financial returns from a multivariate hidden Markov model with time-varying parameters. There are computational advantages to using model predictive control when estimates of future returns are updated every time new observations become available, because the optimal control actions are reconsidered anyway. Transaction and holding costs are discussed as a means to address estimation error and regularize the optimization problem. The proposed approach to multi-period portfolio selection is tested out of sample over two decades based on available market indices chosen to mimic the major liquid asset classes typically considered by institutional investors. By adjusting the risk aversion based on realized drawdown, it successfully controls drawdowns with little or no sacrifice of mean–variance efficiency. Using leverage it is possible to further increase the return without increasing the maximum drawdown.

Keywords: Risk management; Maximum drawdown; Dynamic asset allocation; Model predictive control; Regime switching; Forecasting.

1 Introduction

Financial risk management is about spending a risk budget in the most efficient way. Generally speaking, two different approaches exist. The first approach consists of diversification, that is, reducing risk through optimal asset allocation on the basis of imperfectly correlated assets. The second approach consists of hedging, that is, reducing risk by giving up the potential for gain or by paying a premium to retain some potential for gain. The latter is also referred to as insurance, which is hedging only when needed.

The 2008 financial crisis clearly showed that diversification is not sufficient to avoid large drawdowns (Nystrup et al. 2017a). Diversification fails, when needed the most, because correlations between risky assets tend to strengthen during times of crisis (see, e.g., Pedersen 2009, Ibragimov et al. 2011). Large drawdowns challenge investors' financial and psychological tolerance and lead to fund

redemption and firing of portfolio managers. Thus, a reasonably low maximum drawdown (MDD) is critical to the success of any portfolio. As pointed out by Zhou and Zhu (2010), drawdowns of similar magnitude to the 2008 financial crisis are more likely than a “once-in-a-century” event. Yet, if focusing on tail events when constructing a portfolio, the portfolio will tend to underperform over time (Lim et al. 2011, Ilmanen 2012, Downing et al. 2015).

As argued by Goltz et al. (2008), portfolio insurance can be regarded as the most general form of dynamic—as opposed to static—asset allocation. It is known from Merton’s (1973) replicating-argument interpretation of the Black and Scholes (1973) formula that nonlinear payoffs based on an underlying asset can be replicated by dynamic trading in the underlying asset and a risk-free asset. As a result, investors willing and able to engage in dynamic asset allocation (DAA) can generate the most basic form of risk management possible, which encompasses both static diversification and dynamic hedging (Goltz et al. 2008).

Although DAA is a multi-period problem, it is often approximated by a sequence of myopic, single-period optimizations, thus making it impossible to properly account for the consequences of trading, constraints, time-varying forecasts, etc. Following Mossin (1968), Samuelson (1969), and Merton (1969), the literature on multi-period portfolio selection is predominantly based on dynamic programming, which properly takes into account the idea of recourse and updated information available as a sequence of trades is chosen (see Gărleanu and Pedersen 2013, Cui et al. 2014, and references therein). Unfortunately, actually carrying out dynamic programming for trade selection is impractical, except for some very special or small cases, due to the “curse of dimensionality” (Bellman 1956, Boyd et al. 2014). As a consequence, most studies include only a limited number of assets and simple objectives and constraints (Mei et al. 2016).

The opportunity to select portfolio constituents from a large universe of assets corresponds with a large potential to diversify risk. Exploiting such potential can be difficult, however, as the presence of error increases when the number of assets increases relative to the number of observations, often resulting in worse out-of-sample performance (see, e.g., Brodie et al. 2009, Fastrich et al. 2015). Transaction and holding costs not only have great practical importance but are also a means to address estimation error and regularize the optimization problem.

Multi-period investment problems taking into account the stochastic nature of financial markets are usually solved in practice by scenario approximations of stochastic programming models, which is computationally challenging (see, e.g., Dantzig and Infanger 1993, Mulvey and Shetty 2004, Gülpinar and Rustem 2007, Pinar 2007, Zenios 2007). Herzog et al. (2007) proposed the benefit of model predictive control (MPC) for multi-period portfolio selection (see also Meindl and Primbs 2008, Bemporad et al. 2014, Boyd et al. 2014). The idea is to control a portfolio based on forecasts of asset returns and relevant parameters.

It is an intuitive approach with potential in practical applications, because it is computationally fast. This makes it feasible to consider large numbers of assets and impose important constraints and costs (see Boyd et al. 2017).

This article implements a specific case of the methods of Boyd et al. (2017), with an additional mode that controls for drawdown by adjusting the risk aversion based on realized drawdown. The proposed approach to drawdown control is a practical solution to an important investment problem and demonstrates the theoretical link to DAA. A second contribution is the empirical implementation based on available market indices chosen to mimic the major liquid asset classes typically considered by institutional investors. The testing shows that the MPC approach works well in practice and indeed makes it computationally feasible to solve realistic multi-period portfolio optimization problems and search over hyperparameters in backtests. When combined with drawdown control and use of leverage, it is possible to increase returns substantially without increasing the MDD.

The implementation is based on forecasts from a multivariate hidden Markov model (HMM) with time-varying parameters, which is a third contribution. The combination of an adaptive forecasting method and MPC is a flexible framework for incorporating new information into a portfolio, as it becomes available. Compared to Nystrup et al. (2018b), it is an extension from a single- to a multi-asset universe, which requires a different estimation approach. The HMM could be replaced by another return-prediction model, as model estimation and forecasting are treated separately from portfolio selection. Obviously, the better the forecasts, the more value can be added. The choice of an HMM is motivated by numerous studies showing that DAA based on regime-switching models can add value over rebalancing to static weights and, in particular, reduce potential drawdowns (Ang and Bekaert 2004, Guidolin and Timmermann 2007, Bulla et al. 2011, Kritzman et al. 2012, Bae et al. 2014, Nystrup et al. 2015a, 2017a, 2018b).

The article is structured as follows: section 2 outlines the MPC approach to multi-period portfolio selection with drawdown control. Section 3 describes the HMM, its estimation, and use for forecasting. The empirical results are presented in section 4. Finally, section 5 concludes.

2 Multi-period portfolio selection

Multi-period portfolio selection is a well-established research field since the work of Mossin (1968), Samuelson (1969), and Merton (1969). Since then, it is well understood that short-term portfolio optimization can be very different from long-term portfolio optimization. For sufficiently long horizons, however, it is not possible to make better predictions than the long-term average. Hence, it is really about choosing a sequence of trades to carry out over the next days

and weeks (Gârleanu and Pedersen 2013, Boyd et al. 2017). Looking only a limited number of steps into the future is not just an approximation necessary to make the optimization problem computationally feasible; it also seems perfectly reasonable.

Recent work has shown the importance of the frequency of the input estimates to the portfolio optimization being consistent with the time-horizon that performance is evaluated over (Kinlaw et al. 2014, 2015, Chaudhuri and Lo 2016). Even for long-term investors, though, performance is evaluated continually. The problem is that risk premiums and covariances do not remain invariant over long periods. In a single-period setting, the only way of taking this time variation into account is by blending short- and long-term estimates or the resulting allocations together, which is not optimal. In a multi-period framework, differences in short- and long-term forecasts as well as trading and holding costs can be properly modeled. Multi-period optimization, naturally, leads to a dynamic strategy.

2.1 Stochastic control formulation

The formulation of the multi-period portfolio selection problem as a stochastic control problem is based on Boyd et al. (2017). Every day a decision has to be made whether or not to change the current portfolio, knowing that the decision will be reconsidered the next day with new input. Possible benefits from changing allocation should be traded off against risks and costs.

Let $w_t \in \mathbb{R}^{n+1}$ denote the portfolio weights at time t , where $(w_t)_i$ is the fraction of the total portfolio value V_t invested in asset i , with $(w_t)_i < 0$ meaning a short position in asset i . It is assumed that the portfolio value is positive. The weight $(w_t)_{n+1}$ is the fraction of the total portfolio value held in cash, i.e., the risk-free asset. By definition, the weights sum to one, $\mathbf{1}^T w_t = 1$, where $\mathbf{1}$ is a column vector with all entries one, and are unitless.

A natural objective is to maximize the present value of future, risk-adjusted expected returns less transaction and holding costs over the investment horizon T ,

$$\begin{aligned} \mathbb{E} \left[\sum_{t=0}^{T-1} \eta^{t+1} & \left(r_{t+1}^T w_{t+1} - \gamma_{t+1} \psi_{t+1}(w_{t+1}) \right) \right. \\ & \left. - \eta^t (\phi_t^{\text{trade}}(w_{t+1} - w_t) + \phi_t^{\text{hold}}(w_{t+1})) \right], \end{aligned} \tag{1}$$

where the expectation is over the sequence of returns $r_1, \dots, r_T \in \mathbb{R}^{n+1}$ conditional on all past observations, $\psi_t : \mathbb{R}^{n+1} \rightarrow \mathbb{R}$ is a risk function (described in section 2.3), γ_t is a risk-aversion parameter used to scale the relative importance of risk and return, $\phi_t^{\text{trade}} : \mathbb{R}^{n+1} \rightarrow \mathbb{R}$ is a transaction-cost function (described

in section 2.5), $\phi_t^{\text{hold}} : \mathbb{R}^{n+1} \rightarrow \mathbb{R}$ is a holding-cost function (described in section 2.5), and $\eta \in (0, 1)$ is a discount factor (typically equal to the inverse of one plus the risk-free rate).

2.2 Model predictive control

MPC is based on the simple idea that in order to determine the trades to make, all future (unknown) quantities are replaced by their forecasted values over a planning horizon H . For example, the future returns are replaced by their forecasted mean values $\hat{\mu}_{\tau|t}$, $\tau = t+1, \dots, t+H$, where $\hat{\mu}_{\tau|t}$ is the forecast made at time t of the return at time τ . This turns the stochastic control problem into a deterministic optimization problem:

$$\begin{aligned} \text{maximize} \quad & \sum_{\tau=t+1}^{t+H} \left(\hat{\mu}_{\tau|t}^T w_{\tau} - \hat{\phi}_{\tau|t}^{\text{trade}} (w_{\tau} - w_{\tau-1}) \right. \\ & \quad \left. - \hat{\phi}_{\tau|t}^{\text{hold}} (w_{\tau}) - \gamma_{\tau} \hat{\psi}_{\tau|t} (w_{\tau}) \right) \\ \text{subject to} \quad & \mathbf{1}^T w_{\tau} = 1, \quad \tau = t+1, \dots, t+H, \end{aligned} \quad (2)$$

with variables w_{t+1}, \dots, w_{t+H} (see Boyd et al. 2017, for a detailed derivation). Note that w_t is not a variable, but the known, current portfolio weights. In formulation (2), $\hat{\phi}^{\text{trade}}$ and $\hat{\phi}^{\text{hold}}$ can be estimates of actual transaction- and holding-cost functions or arbitrary functions found to give good performance in backtest (see section 2.5).

Suboptimal control

Solving the optimization problem (2) yields an optimal sequence of weights $w_{t+1}^*, \dots, w_{t+H}^*$. The difference of this sequence is a plan for future trades over the planning horizon H under the highly unrealistic assumption that all future (unknown) quantities will be equal to their forecasted values. Only the first trade $w_{t+1}^* - w_t$ in the planned sequence of trades is executed. At the next step, the process is repeated, starting from the new portfolio w_{t+1} . The planning horizon H can typically be much shorter than the investment horizon T , without it affecting the solution. This is why discounting is ignored in formulation (2) compared to (1).

In the case of a mean–variance objective function, Herzog et al. (2007) showed that future asset allocation decisions do not depend on the trajectory of the portfolio, but solely on the current tradeoff between satisfying the constraints and maximizing the objective. MPC for stochastic systems is a suboptimal control strategy; however, it uses new information advantageously and is better than pure open-loop control. The open-loop policy would be to execute the entire sequence of trades based on the initial portfolio without recourse.

While the MPC approach can be criticized for only approximating the full dynamic programming trading policy, the performance loss is likely very small in

Algorithm 1: MPC approach to multi-period portfolio selection.

1. Update model parameters based on the most recent observation
 2. Forecast future values of all unknown quantities H steps into the future
 3. Compute the optimal sequence of weights $w_{t+1}^*, \dots, w_{t+H}^*$ based on the current portfolio w_t
 4. Execute the first trade $w_{t+1}^* - w_t$ and return to step 1
-

practical problems. Boyd et al. (2014) developed a numerical bounding method that quantifies the loss of optimality when using simplified approaches, such as MPC, and found it to be very small in numerical examples. In fact, the dynamic programming formulation is itself an approximation, based on assumptions—like independent and identically distributed returns—that need not hold well in practice, so the idea of an “optimal strategy” itself should be regarded with some suspicion (Boyd et al. 2017).

Computation

Algorithm 1 summarizes the four steps in the MPC approach to multi-period portfolio selection. There are computational advantages to using MPC in cases when estimates of future return statistics are updated every time a new observation becomes available, since the optimal control actions are reconsidered anyway.

Formulation (2) is a convex optimization problem, provided the risk function and the transaction and holding costs and constraints are convex (Boyd and Vandenberghe 2004). Computing the optimal sequence of trades for $H = 15$ with $n = 10$ assets by solving the optimization problem (2) with the risk-function and transaction and holding costs and constraints described in section 2.3 and section 2.5, respectively, takes less than 0.02 seconds using CVXPY (Diamond and Boyd 2016) with the open-source solver ECOS (Domahidi et al. 2013) on a standard Windows laptop.

Using a custom solver, or a code generator such as CVXGEN (Mattingley and Boyd 2012), would result in an even faster solution time. These solvers are more than fast enough to run in real-time. The practical advantage of the high speed is the ability to carry out a large number of backtests quickly. For example at 0.02 seconds per solve, each year of a backtest with daily trading can be carried out in around five seconds. In one hour, a 32-core machine can carry out five-year backtests with 4,000 different combinations of hyperparameters.

2.3 Risk-averse control

The traditional risk-adjustment charge is proportional to the variance of the portfolio return given the portfolio weights, which corresponds to

$$\psi_t(w_t) = w_t^T \Sigma_t w_t. \quad (3)$$

Note that Σ_t is an estimate of the return covariance under the assumption that the returns are stochastic. It can be interpreted as a cost term that discourages holding portfolios with high variance.

Objective function (1) with risk function (3) corresponds to mean–variance preferences over the changes in portfolio value in each time period (net of the risk-free return). If the returns are independent random variables, then the objective is equivalent to the mean–variance criterion of Markowitz (1952).¹ It is a special case of expected utility maximization with a quadratic utility function. While the utility approach was theoretically justified by von Neumann and Morgenstern (1953), in practice few, if any, investors know their utility functions; nor do the functions which financial engineers and economists find analytically convenient necessarily represent a particular investor’s attitude toward risk and return (Dai et al. 2010a, Markowitz 2014). The mean–variance criterion remains the most commonly used in portfolio selection (Kolm et al. 2014).

There is keen interest in other risk measures beyond the quadratic risk (3), for many good reasons (see, e.g., Zenios 2007, Scutellà and Recchia 2013). Many of these are convex and thus would work in this framework. A popular alternative is expected shortfall, also known as conditional value-at-risk, defined as the expected loss in the worst $q\%$ of cases. It is a coherent measure of risk and a convex function of the portfolio weights (Artzner et al. 1999, Rockafellar and Uryasev 2000, Bertsimas et al. 2004). Unlike the quadratic measure (3), it only penalizes down-side risk.² In practice, portfolios constructed to minimize expected shortfall often realize a higher shortfall out of sample than minimum-variance portfolios because of forecast uncertainty (Lim et al. 2011, Stoyanov et al. 2012, Downing et al. 2015). The lower the quantile level q , the larger the uncertainty. For investors concerned with tail risk, drawdown control is an appealing alternative since it, unlike expected-shortfall optimization, prevents a portfolio from losing more than a given limit.

2.4 Drawdown control

A portfolio is often subject to a maximum drawdown constraint, meaning that, at each point in time, it cannot lose more than a fixed percentage of the maxi-

¹When $H = 1$, the multi-period problem (2) with the risk function (3) reduces to the single-period mean–variance problem studied by Markowitz (1952).

²If the underlying return distribution is Gaussian with known parameters, then the portfolio that minimizes expected shortfall for a given expected return is equivalent to the portfolio that minimizes variance with the same expected return (Rockafellar and Uryasev 2000).

mum value it has achieved up to that time. Recall that V_t denotes the portfolio value at time t . If the maximum value achieved in the past—sometimes referred to as a high-water mark—is

$$M_t = \max_{\tau \leq t} V_\tau, \quad (4)$$

then the drawdown at time t is defined as

$$D_t = 1 - \frac{V_t}{M_t}. \quad (5)$$

Controlling drawdown through DAA may appear similar to the constant-proportion portfolio insurance (CPPI) policy introduced by Black and Jones (1987), Black and Perold (1992). However, they considered the problem of portfolio selection under the constraint that the portfolio value never falls below a fixed floor, rather than a fixed fraction of its maximum-to-date. The CPPI procedure dynamically allocates total assets to a risky asset in proportion to a multiple of the difference between the portfolio value and the desired protective floor. This produces an effect similar to owning a put option (under the assumption that it is possible to trade continuously when asset prices fall), which is the idea behind option-based portfolio insurance (OBPI), proposed by Leland (1980), Rubinstein and Leland (1981).

Grossman and Zhou (1993) were first to study portfolio selection under the constraint that the portfolio value never falls below a fixed fraction of its maximum-to-date. They extended the CPPI policy of Black and Jones (1987), Black and Perold (1992) to a stochastic floor in a frictionless financial market comprised of a risky asset with random-walk return dynamics and a risk-free asset with constant return. They showed that, for constant relative risk aversion utility functions, the optimal allocation to risky assets at time t is in proportion to the cushion $D^{\max} - D_t$, where $D^{\max} \in (0, 1)$ is the maximum acceptable drawdown. This is implemented by adjusting the risk-aversion parameter in response to changes to the cushion.

Let γ_0 be the risk aversion when the drawdown $D_t = 0$, i.e., when $V_t = M_t$. This is the initial risk aversion, since $V_0 = M_0$, and it is the minimum risk aversion at any later point in time, because the drawdown can never be negative. When $D_t = D^{\max}$, then the allocation to risky assets should be zero, meaning that the risk aversion should be infinite. This leads to

$$\gamma_t = \gamma_0 \frac{D^{\max}}{D^{\max} - D_t}. \quad (6)$$

In practice, the cushion in the denominator is replaced by $\max(D^{\max} - D_t, \epsilon)$, where ϵ is some small number, to avoid division by zero or negative numbers in case the drawdown limit is breached. Moreover, γ_τ is only adjusted based on the realized drawdown, which means keeping $\gamma_\tau = \gamma_t$ for $\tau = t + 1, \dots, t + H$ when

solving(2). Note that it is straight forward to implement another relationship between γ_t and γ_0 than (6).

Drawdown control is a reactive mechanism that seeks to limit losses as they evolve (Pedersen 2015). It will, by construction, increase risk aversion in the domain of losses, implying a path-dependent utility function (see, e.g., Dohi and Osaki 1993). If the drawdown gets too close to the limit, it can be impossible to escape it (depending on the risk-free rate). The lower the drawdown limit D^{\max} and initial risk-aversion parameter γ_0 , the larger the risk of getting trapped at the limit. In practice, a portfolio manager that gets trapped at a drawdown limit will need to contact the client or the board to get a new limit—or a dismissal.

2.5 Forecast-error risk

Data-driven portfolio optimization involves estimated statistics that are subject to estimation errors (Merton 1980). Practitioners tend to trust history for input estimation, because it is objective, interpretable, and available, but the nonstationary nature of financial returns limits the number of relevant observations obtainable. As a result, the benefits of diversification often are more than offset by estimation errors (Jorion 1985, Michaud 1989, Black and Litterman 1992, Broadie 1993, Chopra and Ziemba 1993, Garlappi et al. 2006, Kan and Zhou 2007, Ardia et al. 2017). Including transaction and holding costs and constraining portfolio weights are ways to regularize the optimization problem and reduce the risk due to estimation errors.

Transaction costs

Transaction costs are important when comparing the performance of dynamic and static strategies, as frequent trading can offset a dynamic strategy's potential excess return. In order to regularize the optimization problem and reduce the risk of trading too much, a penalty for trading,

$$\phi_t^{\text{trade}} (w_t - w_{t-1}) = \kappa_1^T |w_t - w_{t-1}| + \kappa_2^T (w_t - w_{t-1})^2, \quad (7)$$

should be included in the objective function, where κ_1 and κ_2 are vectors of penalty factors and the absolute and squared value are elementwise. This could reflect actual transaction costs or a conservatism toward trading, for example, due to the uncertainty related to the parameter estimates and forecasts.

The weighted elastic-net penalty (7) is a convex combination of ℓ_1 - and squared ℓ_2 -norm penalties. It reduces the number of trades like the ℓ_1 penalty and the size of trades like the squared ℓ_2 penalty. The ℓ_1 penalty is similar to the standard proportional transaction cost and is a convex relaxation of constraining the number of trades. The squared ℓ_2 penalty is used to model price impact (Alm-

gren and Chriss 2001, Boyd et al. 2017); it shrinks together trades in correlated assets and splits trades over multiple days.³

Many alternative formulations are possible. Popular models of transaction costs include $|w_t - w_{t-1}|^{3/2}$, which is another convex function, possibly scaled by the asset standard deviations and volumes (Grinold and Kahn 2000, Boyd et al. 2017). Grinold (2006) and Gârleanu and Pedersen (2013) argued for a cost of the type $(w_t - w_{t-1})^T \Sigma_t (w_t - w_{t-1})$ —closely related to the risk-adjustment charge (3)—which captures the increased cost of trading when volatility rises.

Holding costs

Holding the portfolio w_t over the t 'th period can incur a holding-based cost. A basic holding-cost model includes a charge for borrowing assets when going short, which has the form

$$\phi_t^{\text{hold}}(w_t) = s_t^T (w_t)_-, \quad (8)$$

where $(s_t)_i \geq 0$ is the borrowing fee for shorting asset i in period t , and $(w)_- = \max\{-w, 0\}$ denotes the negative part of (the elements of) w . This is a fee for shorting the assets over one investment period. A cash borrow cost can easily be included if needed, in which case $(s_t)_{n+1} > 0$. This is the premium for borrowing, and not the interest rate. When short positions are implemented using futures, the holding cost is (at least) equal to the risk-free rate.

Another option is to include a holding cost similar to

$$\phi_t^{\text{hold}}(w_t) = \rho_1^T |w_t| + \rho_2^T w_t^2, \quad (9)$$

where ρ_1 and ρ_2 are vectors of penalty factors and the absolute and squared value are elementwise. For sufficiently large holding costs (8) and (9), the portfolio will be long only, because the weights always sum to one (see (2)). Hence, including holding costs is a means of controlling portfolio leverage.

The weighted elastic-net penalty (9) can be justified by reformulating the mean-variance criterion as a robust optimization problem (Ho et al. 2015, Boyd et al. 2017). It reduces the number of holdings like the ℓ_1 penalty and the size of holdings like the squared ℓ_2 penalty. The ℓ_1 penalty is a convex relaxation of constraining the number of holdings. It can be regarded as a shrinkage estimator of the expected return (Stein 1956, Fabozzi et al. 2010). The squared ℓ_2 penalty shrinks together holdings in correlated assets; it corresponds to adding a diagonal matrix to the forecasted covariance matrix in (3), similar to a Stein-type shrinkage estimator (Ledoit and Wolf 2004).

³Price impact is the price movement against the trader that tends to occur when a large order is executed.

Constraints

Another way to improve the out-of-sample performance is to impose constraints on the portfolio weights, which is equivalent to shrinking the covariance matrix (Jagannathan and Ma 2003, Ledoit and Wolf 2003, 2004, DeMiguel et al. 2009a, Li 2015b). Different constraints correspond to different prior beliefs about the asset weights. The portfolio may be subject to constraints on the asset weights, such as minimum and maximum allowed positions for each asset:

$$-w^{\min} \leq w_t \leq w^{\max}, \quad (10)$$

where the inequalities are elementwise and w^{\min} and w^{\max} are nonnegative vectors of the maximum short and long allowed fractions, respectively. A long-only portfolio corresponds to $w^{\min} = 0$.

Portfolio leverage can be limited with a constraint

$$\|(w_t)_{1:n}\|_1 \leq L^{\max}, \quad (11)$$

which requires the leverage to not exceed L^{\max} . Refer to Boyd et al. (2017) for examples of many other convex holding and trading costs and constraints that arise in practical investment problems and can easily be included.

3 Data model

The volatility of asset prices forms clusters, as large price movements tend to be followed by large price movements and vice versa, as noted by Mandelbrot (1963).⁴ The choice of a regime-switching model aims to exploit this persistence of the volatility, since risk-adjusted returns, on average, are substantially lower during turbulent periods, irrespective of the source of turbulence (Fleming et al. 2001, Kritzman and Li 2010, Moreira and Muir 2017).

Clustering asset returns into time periods with similar behavior is different from other types of clustering, such as k -means, due to the time dependence (Dias et al. 2015). In machine learning, the task of inferring a function to describe a hidden structure from unlabeled data is called unsupervised learning. The data is unlabeled, because the regimes are unobservable. When the transition between different regimes is controlled by a Markov chain, the regime-switching model is called a hidden Markov model.

The HMM is a popular choice for inferring the hidden state of financial markets, because it is well suited to capture the stylized behavior of many financial time series including volatility clustering and leptokurtosis, as shown by Rydén et al. (1998). In addition, it can match the tendency of financial markets

⁴A quantitative manifestation of this fact is that while returns themselves are uncorrelated, absolute and squared returns display a positive, significant, and slowly decaying autocorrelation function.

to change their behavior abruptly and the phenomenon that the new behavior often persists for several periods after a change (Ang and Timmermann 2012).

3.1 The hidden Markov model

In an HMM, the probability distribution that generates an observation depends on the state of an unobserved Markov chain. A sequence of discrete random variables $\{s_t : t \in \mathbb{N}\}$ is said to be a first-order Markov chain if, for all $t \in \mathbb{N}$, it satisfies the Markov property:

$$\Pr(s_{t+1} | s_1, \dots, s_t) = \Pr(s_{t+1} | s_t).$$

The conditional probabilities $\Pr(s_{t+1} = j | s_t = i) = \gamma_{ij}$ are called transition probabilities. A Markov chain with transition probability matrix $\Gamma = \{\gamma_{ij}\}$ has stationary distribution π , if $\pi^T \Gamma = \pi^T$ and $\mathbf{1}^T \pi = 1$.

Future (excess) returns and covariances are forecasted using a model with multivariate Gaussian conditional distributions:

$$o_t | s_t \sim N(\mu_{s_t}, \Sigma_{s_t}).$$

When the current state s_t is known, the distribution of the observation o_t depends only on s_t and not on previous states or observations. The sojourn times are implicitly assumed to be geometrically distributed, implying that the time until the next transition out of the current state is independent of the time spent in the state.

3.2 Estimation

Using the online version of the expectation–maximization algorithm proposed by Stenger et al. (2001), estimates of the model parameters are updated after each sample value.⁵ The idea is that forward variables α_t are updated in every step. These variables give the probability of observing o_1, \dots, o_t and being in state $i \in \mathcal{S}$ at time t :

$$(\alpha_t)_i = \Pr(s_t = i, o_1, \dots, o_t), \quad i \in \mathcal{S}.$$

In the first step, the forward variables are set to

$$(\alpha_1)_i = (\delta)_i \Pr(o_1 | s_1 = i), \quad i \in \mathcal{S},$$

where δ is the initial state distribution, i.e., $(\delta)_i = \Pr(s_1 = i)$.

With every observation, the α values are updated by summing the probabilities over all possible paths which end in the new state $j \in \mathcal{S}$:

$$(\alpha_t)_j = \left[\sum_{i \in \mathcal{S}} (\alpha_{t-1})_i \gamma_{ij} \right] \Pr(o_t | s_t = j), \quad j \in \mathcal{S}.$$

⁵See also the survey by Khreich et al. (2012).

The filtering probability of being in a particular state $i \in \mathcal{S}$ at time t , given the observations, is

$$(\xi_t)_i = \Pr(s_t = i | o_1, \dots, o_t) = \frac{\Pr(s_t = i, o_1, \dots, o_t)}{\Pr(o_1, \dots, o_t)} = \frac{(\alpha_t)_i}{\mathbf{1}^T \alpha_t}.$$

The probability of a certain state transition i to j , given the observations, is

$$\begin{aligned} (\zeta_t)_{ij} &= \Pr(s_{t-1} = i, s_t = j | o_1, \dots, o_t) \\ &= \frac{\Pr(s_{t-1} = i, o_1, \dots, o_{t-1}) \Pr(s_t = j | s_{t-1} = i) \Pr(o_t | s_t = j)}{\Pr(o_1, \dots, o_t)} \\ &= \frac{(\alpha_{t-1})_i \gamma_{ij} \Pr(o_t | s_t = j)}{\mathbf{1}^T \alpha_t}. \end{aligned}$$

These formulas provide the re-estimation scheme. At every time step t , the probabilities ξ_t and ζ_t are computed and used to update the model parameters ($\forall i, j \in \mathcal{S}$):

$$\begin{aligned} \hat{\gamma}_{ij}^t &= \frac{\sum_{\tau=2}^t \Pr(s_{\tau-1} = i, s_\tau = j | o_1, \dots, o_\tau)}{\sum_{\tau=2}^t (\xi_\tau)_i} \\ &= \frac{\sum_{\tau=2}^{t-1} (\xi_\tau)_i \hat{\gamma}_{ij}^{t-1}}{\sum_{\tau=2}^t (\xi_\tau)_i} + \frac{(\zeta_t)_{ij}}{\sum_{\tau=2}^t (\xi_\tau)_i} \end{aligned} \quad (12)$$

$$\hat{\mu}_i^t = \frac{\sum_{\tau=1}^t (\xi_\tau)_i o_\tau}{\sum_{\tau=1}^t (\xi_\tau)_i} = \frac{\sum_{\tau=1}^{t-1} (\xi_\tau)_i \hat{\mu}_i^{t-1}}{\sum_{\tau=1}^t (\xi_\tau)_i} + \frac{(\xi_t)_i o_t}{\sum_{\tau=1}^t (\xi_\tau)_i} \quad (13)$$

$$\begin{aligned} \hat{\Sigma}_i^t &= \frac{\sum_{\tau=1}^t (\xi_\tau)_i (o_\tau - \hat{\mu}_i^t) (o_\tau - \hat{\mu}_i^t)^T}{\sum_{\tau=1}^t (\xi_\tau)_i} \\ &= \frac{\sum_{\tau=1}^{t-1} (\xi_\tau)_i \hat{\Sigma}_i^{t-1}}{\sum_{\tau=1}^t (\xi_\tau)_i} + \frac{(\xi_t)_i (o_t - \hat{\mu}_i^t) (o_t - \hat{\mu}_i^t)^T}{\sum_{\tau=1}^t (\xi_\tau)_i}. \end{aligned} \quad (14)$$

The sums in these equations are computed by storing the values and adding the new terms at each time step. This can be seen as continually updating the sufficient statistics, which are used to compute the new parameters.

Exponential forgetting

A problem with this method is that all values from $t = 1$ to the current time instant are used to compute the sufficient statistics. If the initial parameter values are far away from the true values, this will slow down the convergence process. Moreover, nonstationary data are not well handled. As a solution to these problems, Stenger et al. (2001) proposed to compute the sufficient statistics using exponential forgetting, by which estimates prior in time receive less weight.

The idea is to replace the sums in the re-estimation formulas (12)–(14) by variables which are updated recursively. For example, the term $\sum_{\tau=1}^t \xi_\tau$ is replaced by variables S_t^ξ which are updated as

$$S_t^\xi = \lambda S_{t-1}^\xi + (1 - \lambda) \xi_t,$$

where $\lambda \in (0, 1)$ is the forgetting factor. This approach discounts old observations exponentially, such that an observation that is τ samples old carries a weight that is equal to λ^τ times the weight of the most recent observation. Hence, the effective memory length is $T^{\text{eff}} = 1 / (1 - \lambda)$.

Exponential forgetting is a natural choice when parameters are believed to follow a random walk (Smidl and Gustafsson 2012). The choice of memory length is a tradeoff between adaptivity to parameter changes and sensitivity to noise. In order to reduce estimation noise, exponential forgetting is typically unable to capture abrupt changes. In an HMM, however, the mean and covariance are free to jump from one state to another at every time step—or instantaneously, if a continuous-time model is employed (Nystrup et al. 2015b)—even when the time variation of the underlying parameters is assumed to be smooth. In this way, the adaptively-estimated HMM combines abrupt changes and smooth variations (Nystrup et al. 2017b).

Shrinkage estimation

The usual issues when estimating a high-dimensional covariance matrix also arise in the context of HMMs, causing unstable estimates of the transition matrix and of the hidden states, as shown by Fiecas et al. (2017). In fact, the problem is even more pronounced, as some regimes could be seldom visited, in which case the effective sample size for estimating the covariance matrix will be very small. Furthermore, when applying exponential forgetting, the sample size is bounded by the effective memory length.

One possible solution, as proposed by Fiecas et al. (2017), is to apply a Stein-type shrinkage estimator

$$\hat{\Sigma}_i^{\text{shrink}} = (1 - \nu_i) \hat{\Sigma}_i + \nu_i \text{tr}(\hat{\Sigma}_i) n^{-1} I_n, \quad (15)$$

where $\nu_i \in [0, 1]$ is the shrinkage factor and I_n is the $n \times n$ identity matrix. In order to further stabilize the state classification, it can be necessary to consider only a subset of the indices when estimating the state probabilities (see section 4.2).

3.3 Forecasting

The first step toward calculating the forecast distribution is to estimate the current state probabilities given the past observations and parameters. This

is the ξ_t that is estimated as part of the online algorithm. Once the current state probabilities are estimated, the state probabilities h steps ahead can be forecasted by multiplying the state estimate $\hat{\xi}_{t|t}$ with the transition probability matrix h times:

$$\hat{\xi}_{t+h|t}^T = \hat{\xi}_{t|t}^T \Gamma^h. \quad (16)$$

The parameters are assumed to stay constant in the absence of a model describing their evolution.

The density forecast is the average of the state-dependent conditional densities weighted by the forecasted state probabilities. When the conditional distributions are distinct Gaussian distributions, the forecast distribution will be a mixture with non-Gaussian distribution (Frühwirth-Schnatter 2006). Using Monte Carlo simulation, Boyd et al. (2014) found that the results of dynamic portfolio optimization are not particularly sensitive to higher-order moments. For the present application, only the first and second moment of the forecast distribution are considered.

The first two unconditional moments of a multivariate mixture distribution are

$$\mu = \sum_{i \in \mathcal{S}} (\xi)_i \mu_i, \quad (17)$$

$$\Sigma = \sum_{i \in \mathcal{S}} (\xi)_i \Sigma_i + \sum_{i \in \mathcal{S}} (\xi)_i (\mu_i - \mu) (\mu_i - \mu)^T, \quad (18)$$

with $(\xi)_i$ denoting the weights, that is, the forecasted state probabilities.

Before calculating the unconditional moments of the mixture distribution, the conditional means and covariances of the returns r_t are calculated based on the estimated moments of the log-returns. Within each state, the log-returns are assumed to be independent and identically distributed with Gaussian distribution:

$$\log(1 + r_t) \sim N(\mu_{s_t}^{\log}, \Sigma_{s_t}^{\log}),$$

where $\mu_{s_t}^{\log}$ and $\Sigma_{s_t}^{\log}$ are the conditional mean and covariance of the log-returns. Thus, the conditional mean and covariance of the returns r_t are given by

$$(\mu_s)_i = \exp \left\{ (\mu_s^{\log})_i + \frac{1}{2} (\Sigma_s^{\log})_{ii} \right\} - 1, \quad (19)$$

$$(\Sigma_s)_{ij} = \exp \left\{ (\mu_s^{\log})_i + (\mu_s^{\log})_j + \frac{1}{2} \left\{ (\Sigma_s^{\log})_{ii} + (\Sigma_s^{\log})_{jj} \right\} \right\} \cdot \left\{ \exp \left\{ (\Sigma_s^{\log})_{ij} \right\} - 1 \right\}. \quad (20)$$

Note that i and j in (19) and (20) refer to elements of the conditional mean and covariance, i.e., specific assets, whereas s refers to a state.

The forecasted mean and covariance will be mean-reverting as the forecast horizon extends and the state probabilities converge to the stationary distribution of the Markov chain. The more persistent the states are, the slower the rate of convergence.

4 Empirical results

The empirical testing is divided into two parts. The purpose of the in-sample training is to determine the optimal number of regimes, memory length in the estimation, shrinkage factors, and values of the hyper-parameters in the MPC problem (2). In the out-of-sample test, the performance of the MPC approach to multi-period portfolio selection with drawdown control is evaluated for the particular choice of hyper-parameters and compared to various benchmarks.

4.1 Data

In sample

The choice of time period is a tradeoff between historical data availability and asset universe coverage. The in-sample asset universe consists of developed market (DM) and emerging market (EM) stocks, listed DM real estate, DM high-yield bonds, gold, oil, corporate bonds, and U.S. government bonds.⁶ All indices measure the total net return in USD with a total of 2,316 daily closing prices per index covering the period from 1990 through 1998.⁷ The first two years are used for initialization and the last seven years are used for training.

This is only a subset of the indices considered in the out-of-sample test, as historical data is not available for EM high-yield bonds and inflation-linked bonds. Furthermore, U.S. government bonds are a substitute for the Citi G7 government-bond index in sample.

Out of sample

The asset universe considered in the out-of-sample test consists of DM and EM stocks, listed DM real estate, DM and EM high-yield bonds, gold, oil, corporate bonds, inflation-linked bonds, and government bonds.⁸ All indices measure the

⁶The eight indices are MSCI World, MSCI Emerging Markets, FTSE EPRA/NAREIT Developed Real Estate, BofA Merrill Lynch U.S. High Yield, S&P GSCI Crude Oil (funded futures roll), LBMA Gold Price, Barclays U.S. Aggregate Corporate Bonds, and Bloomberg Barclays U.S. Government Bonds.

⁷Days on which more than half of the indices had zero price change (27 days in total) have been removed. In the few months where only monthly prices are available for DM high-yield bonds, linear interpolation with Gaussian noise has been used to fill the gaps.

⁸The ten indices are MSCI World, MSCI Emerging Markets, FTSE EPRA/NAREIT Developed Real Estate, BofA Merrill Lynch U.S. High Yield, Barclays Emerging Markets High Yield, S&P GSCI Crude Oil (funded futures roll), LBMA Gold Price, Barclays U.S. Aggregate Corporate Bonds,

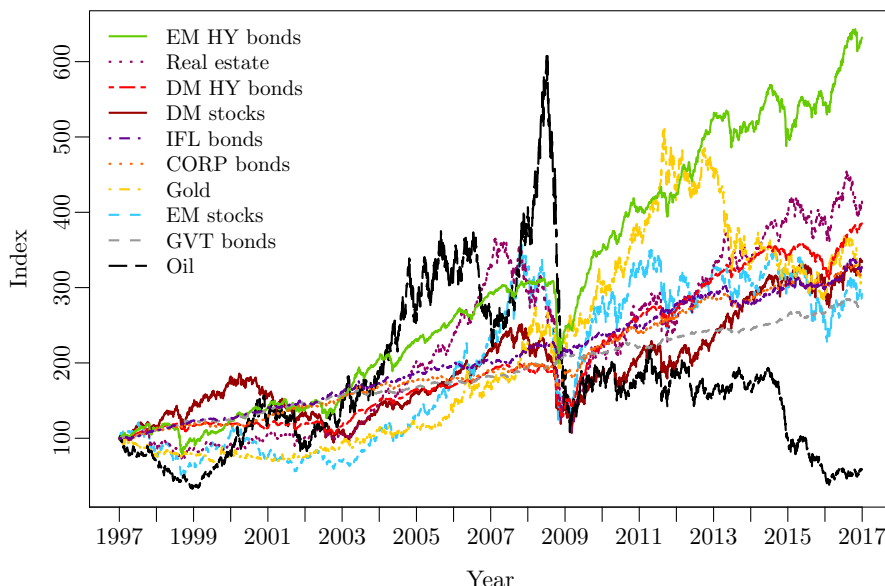


Figure 1: Development of the ten indices over the 20-year out-of-sample period.

total net return in USD with a total of 5,185 daily closing prices per index covering the period from 1997 through 2016.⁹ The first two years are used for initialization and the last 18 years are used for out-of-sample testing.

Figure 1 shows the ten indices' development over the 20-year out-of-sample period. There are large differences in the asset classes' behavior. The financial crisis in 2008 stands out, in that respect, as the majority of the indices suffered large losses in this period.

Table 2 summarizes the indices' annualized excess return, excess risk, Sharpe ratio (SR)¹⁰, maximum drawdown¹¹, and Calmar ratio (CR)¹². The risk-free rate is assumed to be the daily equivalent of the yield on a one-month U.S. treasury bill. The reported excess risks have been adjusted for autocorrelation using the procedure outlined by Kinlaw et al. (2014, 2015).¹³

Barclays World Inflation-Linked Bonds (hedged to USD), and Citi G7 Government Bonds (hedged to USD).

⁹Days on which more than half of the indices had zero price change (19 days in total) have been removed.

¹⁰The Sharpe ratio is the excess return divided by the excess risk (Sharpe 1966, 1994).

¹¹The maximum drawdown is the largest relative decline from a historical peak in the index value, as defined in section 2.4.

¹²The Calmar ratio is the annualized excess return divided by the maximum drawdown.

¹³The adjustment leads to the reported excess risks being higher than had they been annualized

Index	Excess return	Excess risk	Sharpe ratio	Maximum drawdown	Calmar ratio
1. DM stocks	0.042	0.18	0.24	0.57	0.07
2. EM stocks	0.035	0.28	0.12	0.65	0.05
3. Real estate	0.054	0.22	0.24	0.72	0.07
4. DM high-yield bonds	0.050	0.12	0.42	0.35	0.14
5. EM high-yield bonds	0.077	0.13	0.61	0.36	0.21
6. Oil	-0.046	0.42	-0.11	0.94	-0.05
7. Gold	0.038	0.16	0.23	0.45	0.09
8. Corporate bonds	0.040	0.06	0.68	0.16	0.25
9. Inflation-linked bonds	0.041	0.04	0.99	0.10	0.40
10. Government bonds	0.032	0.03	1.17	0.05	0.65

Table 2: Annualized performance of the ten indices over the 20-year out-of-sample period in excess of the risk-free rate.

The differences in performance are substantial. The oil price index is the only index that has had a negative excess return. The EM high-yield bond index realized the highest excess return while inflation-linked and government bonds realized the highest Sharpe and Calmar ratios. Fixed income benefited from falling interest rates over the considered period.

4.2 In-sample training

In the in-sample training, the risk-aversion parameter is fixed at $\gamma = 5$ and portfolio performance is evaluated in terms of SR, excess return, and annual turnover. The choice of $\gamma = 5$ results in portfolios with an excess risk similar to that of the equally-weighted $1/n$ portfolio (in section 4.4 results are shown for a range of values of the risk-aversion parameter). Training is carried out solely for a long-only (LO) portfolio with no leverage. Realized transaction costs, including bid–ask spread, are assumed to be 10 basis points, and there is no transaction cost associated with the risk-free asset. The assets are assumed to be liquid enough compared to the total portfolio value that price impact can be ignored. Further, it is assumed that there are no holding costs.

Many of the hyper-parameters are mutually dependent, which makes the in-sample training more challenging. For example, if the MPC planning horizon is doubled, transaction costs also have to be doubled in order to maintain an approximately similar turnover.¹⁴ In addition, the optimal values of the MPC

under the assumption of independence, as most of the indices display positive autocorrelation. The largest impact was on the excess risk of EM stocks that went from 0.20 to 0.28 and the excess risk of DM high-yield bonds that went from 0.05 to 0.12.

¹⁴See Grinold (2006), Boyd et al. (2017) for more on amortization of transaction and holding costs.

hyper-parameters depend on the choice of forecasting model.

To simplify the training task, it is divided into two steps. First, reasonable values of the MPC parameters are chosen and then used when testing different forecasting models. Second, the optimal MPC hyper-parameters are found for the selected forecasting model. A final check is done to ensure that the model is still optimal for that choice of MPC hyper-parameters.

Forecasting model

Number of regimes and indices. At first, a multivariate HMM is fitted to all indices at once. This results in a state sequence with low persistence and frequent switches, leading to excessive portfolio turnover and poor results. This is surprising given the large number of studies showing the value of DAA based on regime-switching models, in particular Nystrup et al. (2017a) who used a univariate HMM of daily stock returns to switch between predefined risk-on and risk-off multi-asset portfolios. Inspired by this approach, the states are instead estimated based on the two stock indices (DM and EM). The mean vector and covariance matrix in each state is still estimated based on all indices, but the underlying state is estimated solely based on the two stock indices. This leads to a more persistent state sequence with fewer switches and better portfolio performance. There is no benefit to including additional indices in the state estimation, as it increases the uncertainty. The stock indices appear to be sufficient in order to capture important changes in risk and return. Models with two, three, and four regimes are tested. There is no benefit in going from two to three regimes and it is very hard to distinguish between four regimes out of sample.

Effective memory length. Effective memory lengths of $T^{\text{eff}} = 65, 130, 260, 520$ days are tested. The shorter the memory length used in the estimation, the higher the risk of having states with no visits and, consequently, probabilities converging to zero and never recovering. This happens with memory lengths shorter than 100 days. The more regimes, the longer the optimal memory length. With only two regimes, 130 days appear to be optimal.

Shrinkage factors. The shorter the memory length, the higher the optimal shrinkage factor. Shrinkage factors of $\nu_i = 0.1, 0.2, \dots, 0.5$ are tried in each of the two regimes. A shrinkage factor of 0.2 in the most frequent regime and 0.4 in the least visited regime performs best. The use of shrinkage significantly improves the results, although they are not overly sensitive to the specific choice of shrinkage factor within the tested range.

MPC parameters

Planning horizon. Planning horizons of $H = 10, 15, \dots, 30$ days are tested. 10 days are found to be too few, while it appears that there is no benefit in going beyond 15 days.

Maximum holding constraint. Maximum holding constraints $w^{\max} = 0.2, 0.3, \dots, 0.5$ are tried. A maximum holding constraint ensures a minimum level of diversification, but with $w^{\max} = 0.2$ there is limited possibility for deviating from the equally-weighted portfolio. As a compromise, a value of $w^{\max} = 0.4$ is selected.

Transaction costs. Transaction costs $(\kappa_1)_{1:n} = 0.0005, 0.001, \dots, 0.0055$ are tested, while there is no transaction cost associated with the risk-free asset, i.e., $(\kappa_1)_{n+1} = 0$. The term $\kappa_1^T |w_t - w_{t-1}|$ is very effective at reducing portfolio turnover. When this penalty is included, there is no additional benefit from including a second term $\kappa_2^T (w_t - w_{t-1})^2$. This squared term reduces the size of trades, but it appears that it simply means that trades are split over multiple days and therefore delayed. This is not beneficial given the assumption that there is no realized price-impact cost. The value $(\kappa_1)_{1:n} = 0.004$ is selected.

Holding costs. Holding costs $\rho_2 = 0, 0.0005, \dots, 0.002$ are tested. The holding cost $\rho_2^T w_t^2$ has a similar effect as the weight constraint (10): it encourages diversification and reduces the risk due to uncertainty in the covariance forecasts. Increasing ρ_2 leads to a more diversified and stable portfolio. If $(\rho_2)_{n+1} = 0$, this will at the same time increase the allocation to cash, which is undesirable. The value $\rho_2 = 0.0005$ is selected. There is no benefit to including an ℓ_1 term $\rho_1^T |w_t|$, which leads to a more sparse portfolio.

4.3 Out-of-sample test results for $\gamma_0 = 5$

Below, the performance of the MPC approach is evaluated for the above choice of hyper-parameters and compared to various benchmarks. First, results when $\gamma_0 = 5$ are reported, and then in section 4.4 results are analyzed for a range of values of γ_0 . In all cases it is assumed that assets can be bought and sold at the end of each trading day, subject to a 10 basis point transaction cost, and the fee for shorting assets is assumed to be equal to the risk-free rate. It is assumed that there are no price-impact or holding costs.

Allocations

Figure 3 and figure 4 show the asset weights over time for a long-only and a long–short (LS) portfolio and for a leveraged long-only (LLO) portfolio with and without drawdown control, respectively. The cost and weight parameters not

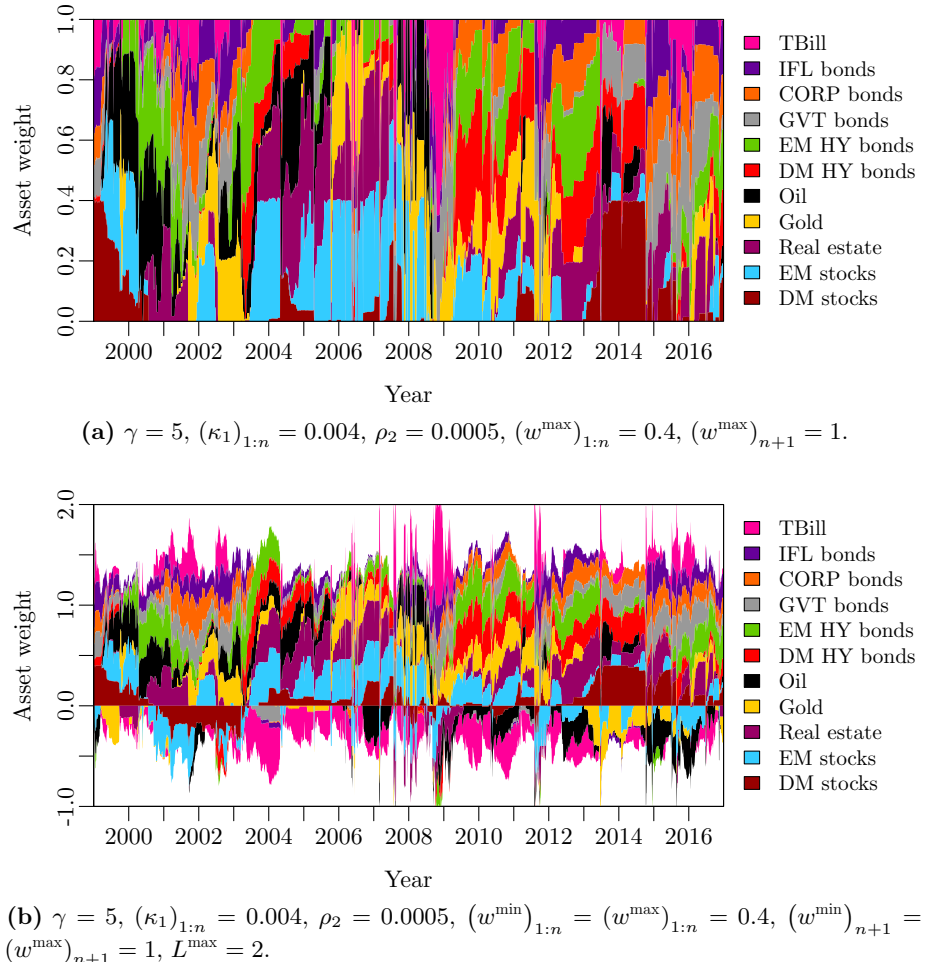


Figure 3: Asset weights over time for a long-only and a long–short portfolio.

mentioned in the figure captions are equal to zero. The portfolios always include multiple assets at a time due to the imposed maximum holding $(w^{\max})_{1:n} = 0.4$. The allocations change quite a bit over the test period, especially in the LS portfolio.

Leverage is primarily used between 2003 and mid-2006 and again from 2010 until mid-2013. With the exception of these two periods, the four portfolios include holdings in the risk-free asset most of the time in addition to some short positions in the LS portfolio. The impact of drawdown control on the allocation is most

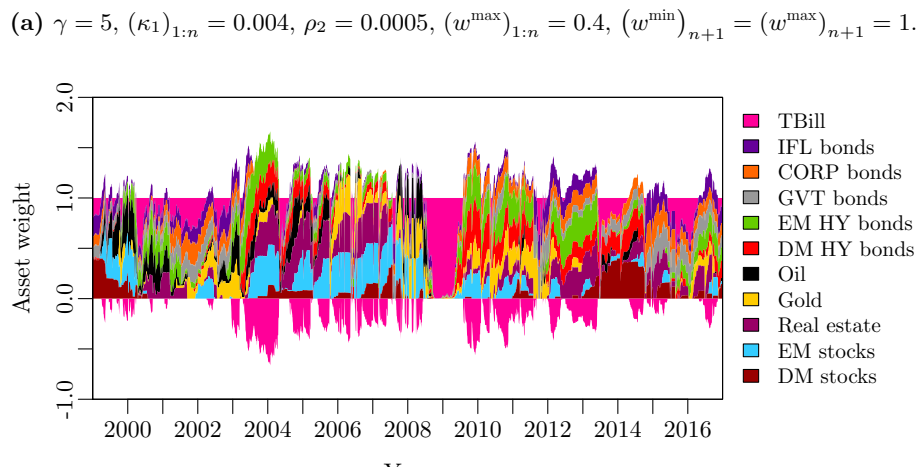
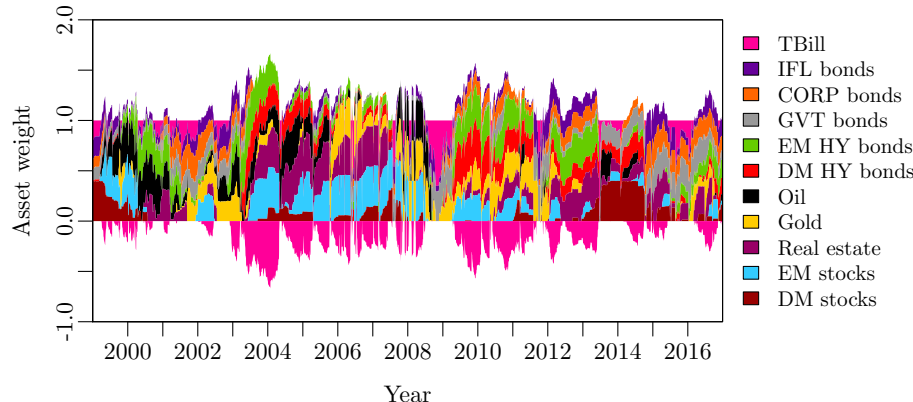


Figure 4: Asset weights over time for a leveraged long-only portfolio with and without drawdown control.

	LO	LLO	$\text{LLO}_{D^{\max}=0.1}$	LS	FM	$1/n$
Excess return	0.10	0.13	0.11	0.12	0.06	0.06
Excess risk	0.11	0.12	0.11	0.12	0.12	0.11
Sharpe ratio	0.97	1.01	1.00	1.01	0.51	0.52
Maximum drawdown	0.19	0.19	0.10	0.23	0.38	0.37
Calmar ratio	0.56	0.65	1.07	0.54	0.16	0.16
Annual turnover	2.93	3.22	3.24	6.75	0.16	0.16

Table 5: Annualized performance of MPC portfolios with $\gamma_0 = 5$ compared to fixed mix and $1/n$.

evident during the 2008 crisis, where the LLO portfolio subject to drawdown control is fully allocated to cash.

Performance compared to fixed mix and $1/n$

In table 5, the MPC portfolios' annualized performance in excess of the risk-free rate when $\gamma_0 = 5$ is compared to a fixed-mix (FM) portfolio and an equally-weighted ($1/n$) portfolio. The FM portfolio is rebalanced monthly to the average allocation of the LO portfolio over the entire 18-year test period. This means that the LO and the FM portfolios have the same average allocation. Thus, differences in performance can only be attributed to timing and transaction costs. The $1/n$ portfolio is rebalanced monthly to an equal allocation across all risky assets. The performance of FM and $1/n$ is fairly similar.

The LO portfolio's excess return is 445 basis points higher than that of the FM portfolio. This, combined with a slightly lower excess risk, leads to a SR of 0.97 compared to 0.51. DAA, even without drawdown control, leads to a MDD of 0.19 compared to the FM portfolio's 0.38. This leads to a CR that is more than three times as high (0.56 compared to 0.16). The LO portfolio's annual turnover of 2.93 is a lot higher than that of the FM portfolio, but the reported results are net of transaction costs of 10 basis points per one-way transaction.

Allowing a maximum leverage of $L^{\max} = 2$ leads to a higher turnover and a slightly higher excess return, excess risk, and SR when $\gamma_0 = 5$. The LLO portfolio's MDD is the same as that of the LO portfolio. This leads to a CR of 0.65 compared to the LO portfolio's 0.56.

By allowing leverage and imposing a maximum acceptable drawdown of $D^{\max} = 0.1$, the CR can be further improved. The reduction in MDD more than offsets the loss of excess return, leading to a CR of 1.07. Note that the imposition of a drawdown limit only leads to a slightly higher turnover.

The LS portfolio's SR and CR are similar to those of the LO portfolio. Its annual turnover of 6.75 is by far the highest of any of the portfolios. This could easily be reduced, though, by imposing a higher trading penalty in the optimization.

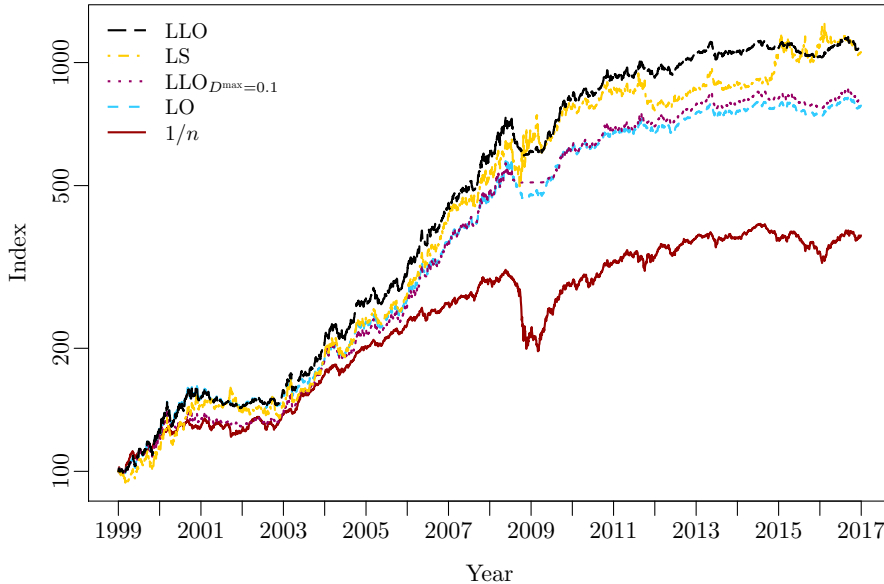


Figure 6: Performance over time of MPC portfolios with $\gamma_0 = 5$ compared to an equally-weighted portfolio.

Another way to reduce turnover is to reconsider the allocation less frequently. Weekly rather than daily adjustments reduce the turnover by more than one, but lead to a slightly lower return and higher risk.¹⁵ The savings in terms of transaction costs are not enough to compensate for the lost opportunities. The Calmar ratio deteriorates more so than the Sharpe ratio, because drawdown control does not work as well when allowing less frequent allocation changes. In addition, portfolio constraints can be violated. Yet, the Sharpe ratio is relatively stable, which indicates that the regime-switching approach is robust.

Figure 6 shows the value of the portfolios from table 5 over time on a log scale. The MPC portfolios outperform the equally-weighted portfolio throughout the 18-year period. The leveraged portfolios, in particular, have benefited from the bull market from 2003 until 2008 and again after the financial crisis. The MPC portfolios lost value in 2008, but they lost much less than the $1/n$ portfolio. None of the portfolios have gained much value in 2014 and 2015.

¹⁵Note that all hyperparameters were selected in sample based on a daily update frequency (section 4.2). When these parameters are used with a lower update frequency, as expected, the results are worse.

4.4 Drawdown control results

Long only

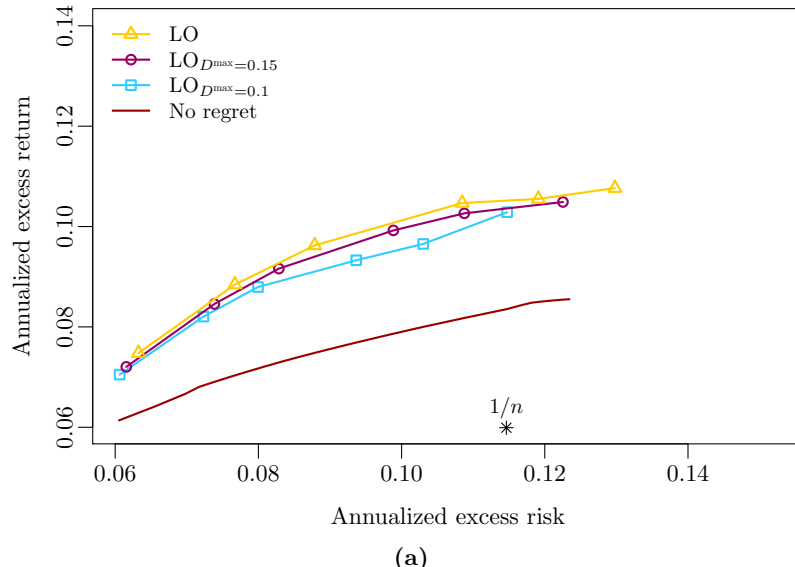
Figure 7 shows the annualized excess return net of transaction costs as a function of (a) annualized excess risk and (b) maximum drawdown for different values of γ_0 and D^{\max} for a long-only portfolio. For comparison, the ex-post mean-variance efficient frontier and the $1/n$ portfolio are shown. Note that the risk of the $1/n$ portfolio could be changed by allocating part of the portfolio to the risk-free asset. The ex-post efficient frontier shows the maximum excess return obtainable for a given excess risk for a fixed-mix, long-only portfolio subject to the maximum holding constraint $(w^{\max})_{1:n} = 0.4$, conditional on knowing the returns beforehand. It is referred to as a no-regret frontier (Bell 1982). It more or less overlaps with the ex-post mean-MDD efficient frontier in both risk spaces; therefore, only the former is shown.

The dynamic frontiers are clearly superior to the static, no-regret frontier. This is impressive considering that the no-regret frontier is constructed in hindsight and, thus, not obtainable in practice. In other words, even if they knew future returns when choosing their benchmark, investors who insist on rebalancing to a static, diversified benchmark could not have outperformed the dynamic strategies net of transaction costs over the 18-year test period in terms of SR nor CR. The opportunity for DAA significantly expands the investment opportunity set; even so, this is a noteworthy result.

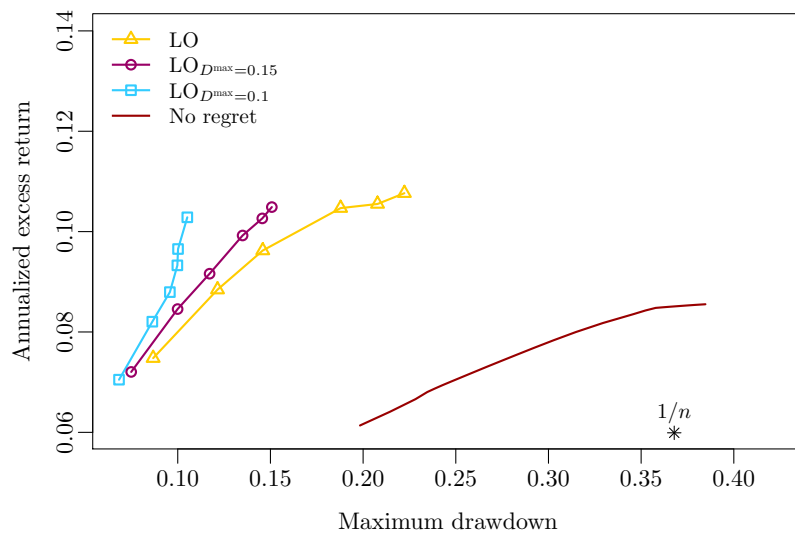
The $1/n$ portfolio is inefficient regardless of whether risk is measured by standard deviation or MDD. This is no surprise given that it is based on a naive prior assumption of equal returns, risks, and correlations across all assets. Yet, equally-weighted portfolios are often found to outperform mean-variance optimized portfolios out of sample (DeMiguel et al. 2009b, López de Prado 2016). This suggests that the no-regret frontier would likely be closer to the $1/n$ portfolio than to the dynamic frontiers, had it not benefited from hindsight.

Looking at the frontiers with and without drawdown control in figure 7(a), it appears that drawdown control can be implemented with little loss of mean-variance efficiency. By increasing the risk-aversion parameter as the drawdown approaches the maximum acceptable drawdown D^{\max} , a larger fraction of the portfolio is allocated to the risk-free asset, cf. figure 4(b). Except for the transaction costs involved, this does not lead to a worse SR per se, but reduced risk-taking in periods with above-average SRs would. This is clearly not the case. Drawdown control simply leads to a higher average risk aversion.

From figure 7(b) it can be seen that the drawdown limit is breached—although not by much—when $\gamma_0 = 1$. The success of the proposed approach to drawdown control is not very sensitive to the choice of initial risk-aversion parameter γ_0 . Essentially, any value $\gamma_0 \geq 3$ will work with a drawdown limit as tight as $D^{\max} = 0.1$. Drawdown control is more sensitive to the allocation-update fre-



(a)



(b)

Figure 7: Efficient frontiers for different values of D^{\max} compared to a no-regret frontier and an equally-weighted portfolio, when no leverage is allowed. The points, from right to left, correspond to $\gamma_0 = 1, 3, 5, 10, 15, 25$.

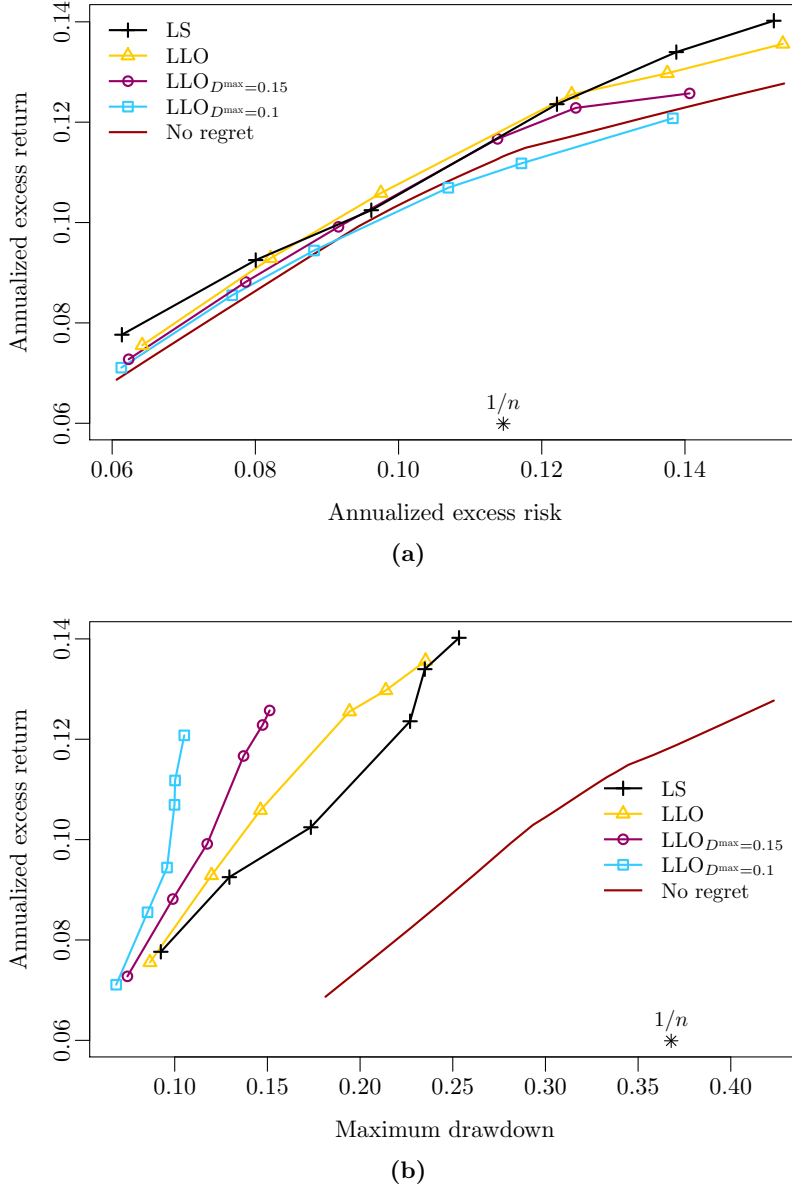


Figure 8: Efficient frontiers for different values of D^{\max} compared to a no-regret frontier and an equally-weighted portfolio, when leverage and short-positions are allowed. The points, from right to left, correspond to $\gamma_0 = 1, 3, 5, 10, 15, 25$.

quency, since optimal drawdown control requires continuous trading. Yet, daily allocation updates are sufficient for it to work for reasonable values of γ_0 and D^{\max} .

Long–short

Figure 8 shows the annualized excess return net of transaction costs as a function of (a) annualized excess risk and (b) maximum drawdown for different values of γ_0 and D^{\max} for LS and LLO portfolios. For comparison, the ex-post mean–variance efficient frontier and the $1/n$ portfolio are shown. The ex-post efficient frontier gives the maximum excess return obtainable for a given excess risk for a fixed-mix, long–short portfolio subject to the same holding and leverage constraints, $(w^{\min})_{1:n} = (w^{\max})_{1:n} = 0.4$ and $L^{\max} = 2$, conditional on knowing the returns beforehand.

In figure 8(a), the possibility of using leverage or taking short positions extends the efficient frontier. Leverage can be applied to increase risk while maintaining diversification, rather than concentrating the portfolio in a few assets. This reduces the gap between the dynamic frontiers and the no-regret frontier.

In figure 8(b), the difference between the dynamic frontiers and the no-regret frontier is still substantial. Again, the ex-post mean–variance efficient frontier more or less overlaps with the ex-post mean–MDD efficient frontier; therefore, only the former is shown. By taking a dynamic approach, the maximum drawdown can be reduced by 0.25, while maintaining the same excess return.

The combination of leverage and drawdown control is powerful. Compared to figure 7(b), it is possible to increase the excess return by several hundred basis points without suffering a larger MDD by combining the use of leverage with drawdown control. The possible excess return is bounded by the drawdown limit. Seeking excess return beyond this boundary by removing the drawdown limit and lowering γ_0 comes at the cost of a significantly increased MDD. This is true regardless of whether leverage can be applied.

5 Conclusion

By adjusting the risk aversion based on realized drawdown, the proposed approach to multi-period portfolio selection based on MPC successfully controlled drawdowns with little or no sacrifice of mean–variance efficiency. The empirical testing showed that performance could be significantly improved by reducing realized risk and MDD using this dynamic approach. In fact, even if they knew future returns when choosing their benchmark, investors who insisted on rebalancing to a static benchmark allocation could not have outperformed the dynamic approach net of transaction costs over the 18-year out-of-sample test period. The combination of leverage and drawdown control was particularly

successful, as it was possible to increase the excess return by several hundred basis points without suffering a larger MDD.

The MPC approach to multi-period portfolio selection has potential in practical applications, because it is computationally fast. This makes it feasible to consider a large universe of assets and implement important constraints and costs. When combined with an adaptive forecasting method it provides a flexible framework for incorporating new information into a portfolio as it becomes available. This should definitely be useful in future research, when evaluating the performance of return-prediction models.

References

- Almgren, R. and N. Chriss. "Optimal execution of portfolio transactions." *Journal of Risk*, vol. 3, no. 2 (2001), pp. 5–39.
- Ang, A. and G. Bekaert. "How regimes affect asset allocation." *Financial Analysts Journal*, vol. 60, no. 2 (2004), pp. 86–99.
- Ang, A. and A. Timmermann. "Regime changes and financial markets." *Annual Review of Financial Economics*, vol. 4, no. 1 (2012), pp. 313–337.
- Ardia, D., G. Bolliger, K. Boudt, and J. P. Gagnon-Fleury. "The impact of covariance misspecification in risk-based portfolios." *Annals of Operations Research*, vol. 254, no. 1-2 (2017), pp. 1–16.
- Artzner, P., F. Delbaen, J. M. Eber, and D. Heath. "Coherent measures of risk." *Mathematical Finance*, vol. 9, no. 3 (1999), pp. 203–228.
- Bae, G. I., W. C. Kim, and J. M. Mulvey. "Dynamic asset allocation for varied financial markets under regime switching framework." *European Journal of Operational Research*, vol. 234, no. 2 (2014), pp. 450–458.
- Bell, D. E. "Regret in decision making under uncertainty." *Operations Research*, vol. 30, no. 5 (1982), pp. 961–981.
- Bellman, R. E. "Dynamic programming and Lagrange multipliers." *Proceedings of the National Academy of Sciences*, vol. 42, no. 10 (1956), pp. 767–769.
- Bemporad, A., L. Bellucci, and T. Gabbriellini. "Dynamic option hedging via stochastic model predictive control based on scenario simulation." *Quantitative Finance*, vol. 14, no. 10 (2014), pp. 1739–1751.
- Bertsimas, D., G. J. Lauprete, and A. Samarov. "Shortfall as a risk measure: properties, optimization and applications." *Journal of Economic Dynamics & Control*, vol. 28, no. 7 (2004), pp. 1353–1381.

- Black, F. and R. W. Jones. "Simplifying portfolio insurance." *Journal of Portfolio Management*, vol. 14, no. 1 (1987), pp. 48–51.
- Black, F. and R. Litterman. "Global portfolio optimization." *Financial Analysts Journal*, vol. 48, no. 5 (1992), pp. 28–43.
- Black, F. and A. F. Perold. "Theory of constant proportion portfolio insurance." *Journal of Economic Dynamics & Control*, vol. 16, no. 3–4 (1992), pp. 403–426.
- Black, F. and M. Scholes. "The pricing of options and corporate liabilities." *Journal of Political Economy*, vol. 81, no. 3 (1973), pp. 637–654.
- Boyd, S., E. Busseti, S. Diamond, R. N. Kahn, K. Koh, P. Nystrup, and J. Speth. "Multi-period trading via convex optimization." *Foundations and Trends in Optimization*, vol. 3, no. 1 (2017), pp. 1–76.
- Boyd, S., M. T. Mueller, B. O'Donoghue, and Y. Wang. "Performance bounds and suboptimal policies for multi-period investment." *Foundations and Trends in Optimization*, vol. 1, no. 1 (2014), pp. 1–72.
- Boyd, S. and L. Vandenberghe. *Convex Optimization*. Cambridge University Press: New York (2004).
- Broadie, M. "Computing efficient frontiers using estimated parameters." *Annals of Operations Research*, vol. 45, no. 1 (1993), pp. 21–58.
- Brodie, J., I. Daubechies, C. D. Mol, D. Giannone, and I. Loris. "Sparse and stable Markowitz portfolios." *Proceedings of the National Academy of Sciences of the United States of America*, vol. 106, no. 30 (2009), pp. 12267–12272.
- Bulla, J., S. Mergner, I. Bulla, A. Sesboüé, and C. Chesneau. "Markov-switching asset allocation: Do profitable strategies exist?" *Journal of Asset Management*, vol. 12, no. 5 (2011), pp. 310–321.
- Chaudhuri, S. E. and A. W. Lo. "Spectral portfolio theory." Available at SSRN 2788999 (2016), pp. 1–44.
- Chopra, V. K. and W. T. Ziemba. "The effect of errors in means, variances, and covariances on optimal portfolio choice." *Journal of Portfolio Management*, vol. 19, no. 2 (1993), pp. 6–11.
- Cui, X., J. Gao, X. Li, and D. Li. "Optimal multi-period mean–variance policy under no-shorting constraint." *European Journal of Operational Research*, vol. 234, no. 2 (2014), pp. 459–468.
- Dai, M., Z. Q. Xu, and X. Y. Zhou. "Continuous-time Markowitz's model with transaction costs." *SIAM Journal on Financial Mathematics*, vol. 1, no. 1 (2010a), pp. 96–125.

- Dantzig, G. B. and G. Infanger. “Multi-stage stochastic linear programs for portfolio optimization.” *Annals of Operations Research*, vol. 45, no. 1 (1993), pp. 59–76.
- DeMiguel, V., L. Garlappi, F. Nogales, and R. Uppal. “A generalized approach to portfolio optimization: Improving performance by constraining portfolio norms.” *Management Science*, vol. 55, no. 5 (2009a), pp. 798–812.
- DeMiguel, V., L. Garlappi, and R. Uppal. “Optimal versus naive diversification: How inefficient is the $1/N$ portfolio strategy?” *Review of Financial Studies*, vol. 22, no. 5 (2009b), pp. 1915–1953.
- Diamond, S. and S. Boyd. “CVXPY: A Python-embedded modeling language for convex optimization.” *Journal of Machine Learning Research*, vol. 17, no. 83 (2016), pp. 1–5.
- Dias, J. G., J. K. Vermunt, and S. Ramos. “Clustering financial time series: New insights from an extended hidden Markov model.” *European Journal of Operational Research*, vol. 243, no. 3 (2015), pp. 852–864.
- Dohi, T. and S. Osaki. “A note on portfolio optimization with path-dependent utility.” *Annals of Operations Research*, vol. 45, no. 1 (1993), pp. 77–90.
- Domahidi, A., E. Chu, and S. Boyd. “ECOS: An SOCP solver for embedded systems.” In *Proceedings of the 12th European Control Conference* (2013), pp. 3071–3076.
- Downing, C., A. Madhavan, A. Ulitsky, and A. Singh. “Portfolio construction and tail risk.” *Journal of Portfolio Management*, vol. 42, no. 1 (2015), pp. 85–102.
- Fabozzi, F. J., D. Huang, and G. Zhou. “Robust portfolios: contributions from operations research and finance.” *Annals of Operations Research*, vol. 176, no. 1 (2010), pp. 191–220.
- Fastrich, B., S. Paterlini, and P. Winker. “Constructing optimal sparse portfolios using regularization methods.” *Computational Management Science*, vol. 12, no. 3 (2015), pp. 417–434.
- Fiecas, M., J. Franke, R. von Sachs, and J. T. Kamgaing. “Shrinkage estimation for multivariate hidden Markov models.” *Journal of the American Statistical Association*, vol. 112, no. 517 (2017), pp. 424–435.
- Fleming, J., C. Kirby, and B. Ostdiek. “The economic value of volatility timing.” *Journal of Finance*, vol. 56, no. 1 (2001), pp. 329–352.
- Frühwirth-Schnatter, S. *Finite Mixture and Markov Switching Models*. Springer: New York (2006).

- Garlappi, L., R. Uppal, and T. Wang. "Portfolio selection with parameter and model uncertainty: A multi-prior approach." *Review of Financial Studies*, vol. 20, no. 1 (2006), pp. 41–81.
- Gärleanu, N. and L. H. Pedersen. "Dynamic trading with predictable returns and transaction costs." *Journal of Finance*, vol. 68, no. 6 (2013), pp. 2309–2340.
- Goltz, F., L. Martellini, and K. D. Simsek. "Optimal static allocation decisions in the presence of portfolio insurance." *Journal of Investment Management*, vol. 6, no. 2 (2008), pp. 37–56.
- Grinold, R. C. "A dynamic model of portfolio management." *Journal of Investment Management*, vol. 4, no. 2 (2006), pp. 5–22.
- Grinold, R. C. and R. N. Kahn. *Active Portfolio Management: A Quantitative Approach for Providing Superior Returns and Controlling Risk*. McGraw-Hill: New York, 2nd ed. (2000).
- Grossman, S. J. and Z. Zhou. "Optimal investment strategies for controlling drawdowns." *Mathematical Finance*, vol. 3, no. 3 (1993), pp. 241–276.
- Guidolin, M. and A. Timmermann. "Asset allocation under multivariate regime switching." *Journal of Economic Dynamics and Control*, vol. 31, no. 11 (2007), pp. 3503–3544.
- Gülpınar, N. and B. Rustem. "Worst-case robust decisions for multi-period mean–variance portfolio optimization." *European Journal of Operational Research*, vol. 183, no. 3 (2007), pp. 981–1000.
- Herzog, F., G. Dondi, and H. P. Geering. "Stochastic model predictive control and portfolio optimization." *International Journal of Theoretical and Applied Finance*, vol. 10, no. 2 (2007), pp. 203–233.
- Ho, M., Z. Sun, and J. Xin. "Weighted elastic net penalized mean–variance portfolio design and computation." *SIAM Journal on Financial Mathematics*, vol. 6, no. 1 (2015), pp. 1220–1244.
- Ibragimov, R., D. Jaffee, and J. Walden. "Diversification disasters." *Journal of Financial Economics*, vol. 99, no. 2 (2011), pp. 333–348.
- Ilmanen, A. "Do financial markets reward buying or selling insurance and lottery tickets?" *Financial Analysts Journal*, vol. 68, no. 5 (2012), pp. 26–36.
- Jagannathan, R. and T. Ma. "Risk reduction in large portfolios: Why imposing the wrong constraints helps." *Journal of Finance*, vol. 58, no. 4 (2003), pp. 1651–1683.
- Jorion, P. "International portfolio diversification with estimation risk." *Journal of Business*, vol. 58, no. 3 (1985), pp. 259–278.

- Kan, R. and G. Zhou. “Optimal portfolio choice with parameter uncertainty.” *Journal of Financial and Quantitative Analysis*, vol. 42, no. 3 (2007), pp. 621–656.
- Khreich, W., E. Granger, A. Miri, and R. Sabourin. “A survey of techniques for incremental learning of HMM parameters.” *Information Sciences*, vol. 197 (2012), pp. 105–130.
- Kinlaw, W., M. Kritzman, and D. Turkington. “The divergence of high- and low-frequency estimation: Causes and consequences.” *Journal of Portfolio Management*, vol. 40, no. 5 (2014), pp. 156–168.
- Kinlaw, W., M. Kritzman, and D. Turkington. “The divergence of high- and low-frequency estimation: Implications for performance measurement.” *Journal of Portfolio Management*, vol. 41, no. 3 (2015), pp. 14–21.
- Kolm, P., R. Tütüncü, and F. Fabozzi. “60 years of portfolio optimization: Practical challenges and current trends.” *European Journal of Operational Research*, vol. 234, no. 2 (2014), pp. 356–371.
- Kritzman, M. and Y. Li. “Skulls, financial turbulence, and risk management.” *Financial Analysts Journal*, vol. 66, no. 5 (2010), pp. 30–41.
- Kritzman, M., S. Page, and D. Turkington. “Regime shifts: Implications for dynamic strategies.” *Financial Analysts Journal*, vol. 68, no. 3 (2012), pp. 22–39.
- Ledoit, O. and M. Wolf. “Improved estimation of the covariance matrix of stock returns with an application to portfolio selection.” *Journal of Empirical Finance*, vol. 10, no. 5 (2003), pp. 603–621.
- Ledoit, O. and M. Wolf. “A well-conditioned estimator for large-dimensional covariance matrices.” *Journal of Multivariate Analysis*, vol. 88, no. 2 (2004), pp. 365–411.
- Leland, H. E. “Who should buy portfolio insurance?” *Journal of Finance*, vol. 35, no. 2 (1980), pp. 581–594.
- Li, J. “Sparse and stable portfolio selection with parameter uncertainty.” *Journal of Business & Economic Statistics*, vol. 33, no. 3 (2015b), pp. 381–392.
- Lim, A. E., J. G. Shanthikumar, and G. Y. Vahn. “Conditional value-at-risk in portfolio optimization: Coherent but fragile.” *Operations Research Letters*, vol. 39, no. 3 (2011), pp. 163–171.
- López de Prado, M. “Building diversified portfolios that outperform out of sample.” *Journal of Portfolio Management*, vol. 42, no. 4 (2016), pp. 59–69.

- Mandelbrot, B. "The variation of certain speculative prices." *Journal of Business*, vol. 36, no. 4 (1963), pp. 394–419.
- Markowitz, H. "Portfolio selection." *Journal of Finance*, vol. 7, no. 1 (1952), pp. 77–91.
- Markowitz, H. "Mean-variance approximations to expected utility." *European Journal of Operational Research*, vol. 234, no. 2 (2014), pp. 346–355.
- Mattingley, J. and S. Boyd. "CVXGEN: A code generator for embedded convex optimization." *Optimization and Engineering*, vol. 13, no. 1 (2012), pp. 1–27.
- Mei, X., V. DeMiguel, and F. J. Nogales. "Multiperiod portfolio optimization with multiple risky assets and general transaction costs." *Journal of Banking & Finance*, vol. 69 (2016), pp. 108–120.
- Meindl, P. J. and J. A. Primbs. "Dynamic hedging of single and multi-dimensional options with transaction costs: a generalized utility maximization approach." *Quantitative Finance*, vol. 8, no. 3 (2008), pp. 299–312.
- Merton, R. C. "Lifetime portfolio selection under uncertainty: The continuous-time case." *Review of Economics and Statistics*, vol. 51, no. 3 (1969), pp. 247–257.
- Merton, R. C. "Theory of rational option pricing." *Bell Journal of Economics and Management Science*, vol. 4, no. 1 (1973), pp. 141–183.
- Merton, R. C. "On estimating the expected return on the market: An exploratory investigation." *Journal of Financial Economics*, vol. 8, no. 4 (1980), pp. 323–361.
- Michaud, R. O. "The Markowitz optimization Enigma: Is 'optimized' optimal?" *Financial Analysts Journal*, vol. 45, no. 1 (1989), pp. 31–42.
- Moreira, A. and T. Muir. "Volatility-managed portfolios." *Journal of Finance*, vol. 72, no. 4 (2017), pp. 1611–1644.
- Mossin, J. "Optimal multiperiod portfolio policies." *Journal of Business*, vol. 41, no. 2 (1968), pp. 215–229.
- Mulvey, J. M. and B. Shetty. "Financial planning via multi-stage stochastic optimization." *Computers & Operations Research*, vol. 31, no. 1 (2004), pp. 1–20.
- Nystrup, P., B. W. Hansen, H. O. Larsen, H. Madsen, and E. Lindström. "Dynamic allocation or diversification: A regime-based approach to multiple assets." *Journal of Portfolio Management*, vol. 44, no. 2 (2017a), pp. 62–73.

- Nystrup, P., B. W. Hansen, H. Madsen, and E. Lindström. "Regime-based versus static asset allocation: Letting the data speak." *Journal of Portfolio Management*, vol. 42, no. 1 (2015a), pp. 103–109.
- Nystrup, P., H. Madsen, and E. Lindström. "Stylised facts of financial time series and hidden Markov models in continuous time." *Quantitative Finance*, vol. 15, no. 9 (2015b), pp. 1531–1541.
- Nystrup, P., H. Madsen, and E. Lindström. "Long memory of financial time series and hidden Markov models with time-varying parameters." *Journal of Forecasting*, vol. 36, no. 8 (2017b), pp. 989–1002.
- Nystrup, P., H. Madsen, and E. Lindström. "Dynamic portfolio optimization across hidden market regimes." *Quantitative Finance*, vol. 18, no. 1 (2018b), pp. 83–95.
- Pedersen, L. H. "When everyone runs for the exit." *International Journal of Central Banking*, vol. 5, no. 4 (2009), pp. 177–199.
- Pedersen, L. H. *Efficiently inefficient: how smart money invests and market prices are determined*. Princeton University Press: Princeton (2015).
- Pinar, M. Ç. "Robust scenario optimization based on downside-risk measure for multi-period portfolio selection." *OR Spectrum*, vol. 29, no. 2 (2007), pp. 295–309.
- Rockafellar, R. T. and S. Uryasev. "Optimization of conditional value-at-risk." *Journal of Risk*, vol. 2, no. 3 (2000), pp. 21–42.
- Rubinstein, M. and H. E. Leland. "Replicating options with positions in stock and cash." *Financial Analysts Journal*, vol. 37, no. 4 (1981), pp. 63–72.
- Rydén, T., T. Teräsvirta, and S. Åsbrink. "Stylized facts of daily return series and the hidden Markov model." *Journal of Applied Econometrics*, vol. 13, no. 3 (1998), pp. 217–244.
- Samuelson, P. A. "Lifetime portfolio selection by dynamic stochastic programming." *Review of Economics and Statistics*, vol. 51, no. 3 (1969), pp. 239–246.
- Scutellà, M. G. and R. Recchia. "Robust portfolio asset allocation and risk measures." *Annals of Operations Research*, vol. 204, no. 1 (2013), pp. 145–169.
- Sharpe, W. F. "Mutual fund performance." *Journal of Business*, vol. 39, no. 1 (1966), pp. 119–138.
- Sharpe, W. F. "The Sharpe ratio." *Journal of Portfolio Management*, vol. 21, no. 1 (1994), pp. 49–58.

- Smidl, V. and F. Gustafsson. "Bayesian estimation of forgetting factor in adaptive filtering and change detection." In *Proceedings of the 2012 IEEE Statistical Signal Processing Workshop* (2012), pp. 197–200.
- Stein, C. "Inadmissibility of the usual estimator for the mean of a multivariate normal distribution." In *Proceedings of the Third Berkeley Symposium on Mathematical Statistics and Probability*, vol. 1. University of California Press: Berkeley (1956), pp. 197–206.
- Stenger, B., V. Ramesh, N. Paragios, F. Coetzee, and J. M. Buhmann. "Topology free hidden Markov models: Application to background modeling." In *Proceedings of the Eighth IEEE International Conference on Computer Vision*, vol. 1 (2001), pp. 294–301.
- Stoyanov, S. V., S. T. Rachev, and F. J. Fabozzi. "Sensitivity of portfolio VaR and CVaR to portfolio return characteristics." *Annals of Operations Research*, vol. 205, no. 1 (2012), pp. 169–187.
- von Neumann, J. and O. Morgenstern. *Theory of Games and Economic Behavior*. Princeton University Press: Princeton, 3rd ed. (1953).
- Zenios, S. A. *Practical Financial Optimization: Decision Making for Financial Engineers*. Blackwell: Malden (2007).
- Zhou, G. and Y. Zhu. "Is the recent financial crisis really a "once-in-a-century" event?" *Financial Analysts Journal*, vol. 66, no. 1 (2010), pp. 24–27.

